

Volume 2 - July 2013 (7)

International Journal of Sciences



Dr. Abraham

The International Journal of Sciences (ijSciences) ISSN (2305-3925) is well reputed and publishing with collaboration of expert doctors in relevant field. It focuses on Medical and Biology Science, Chemistry, Food Science, Agricultural Science, Materials Science, Modern Applied Science problems and their solutions and other relevant subjects. ijSciences is an Open Access journal, providing best research resources to be downloaded for free, though, copyrights are still with publisher.

Alkhaer Publications

Huma Block, Allama Iqbal Town

Lahore, Pakistan

Cell# +92 333 6701307

www.ijSciences.com

Vision

Provide the Best Research Resources in Sciences

Values

Scientific Valued Research and Methodology

Mission

Proving a platform to focus on Medical and Biology Science, Chemistry, Food Science, Agricultural Science, Materials Science, Modern Applied Science problems and their solutions and on other relevant subjects

Editorial Board Members

- **Dr. Abraham** (Editor-in-Chief)
The University of Manchester, UK
- **Dr. James L. Codling**
Sr. Lect of Biology, Mississippi State University USA
- **Prof. Berry Riphil**
Chemistry Department, Princeton University USA
- **Dr. John Yudelson**
California State University Channel Islands USA
- **Prof. Abid Ali**
COMSATS University, Lahore, Pakistan
- **Dr. Aliza Roy**
Higher Institute of management of Gabes, France
- **Prof. P. Malyadri**
Principal Government Degree College, Osmania University, India
- **Dr. H.A. Tervide**
University of Tehran, Iran
- **Dr. Jazzy Rolph**
Sr. Prof. University of Hertfordshire UK
- **Chiara Garau, Ph.D**
University of Cagliari, Sardinia – Italy

Table of Contents

Sr. No.	Article Title	Corrs. Author	Pages
1	Novel Synthesis of Diketo-Acid Chondroitin-4-Sulfate as Coordination Biopolymer Precursor through Oxidation of Chondroitin-4-sulfate by Alkaline Permanganate	Adil A. Gobouri	1-11
2	Stability Evaluation of Anthocyanin Extracted from Processed Grape Residues	Edmar Clemente	12-18
3	Embryos and Lateral Buds Culture of Tapeinochilos Ananassae (Hassk). K. Schum.	Lilia Willadino	19-25
4	Influence of Anthropometry on the Kinematics of the Cervical Spine in Frontal Sled Tests	Christoph Dehner MD	26-36
5	Perception of Suitability of Landscape Features of the Lagos Lagoon for Tourism by its Users and Users of Lagos Coastal Tourism Venues	Uduma-Olugu, N.	37-46
6	A Dynamic Approach to Money Supply	Yougui Wang	47-53
7	Distortional Lifshitz Vectors and Helicity in Nematic Free Energy Density	Amelia Carolina Sparavigna	54-59
8	Modelling Monthly Rainfall Data of Port Harcourt, Nigeria by Seasonal Box-Jenkins Methods	Ette Harrison Etuk	60-67
9	Post-Harvest Conservation of Orange cv. Folha Murcha Treated with 1-MCP and Stored Under Refrigeration	Cassia Inês Lourenzi Franco Rosa	68-75
10	Burnout among Junior Athletes' in relation to their Perceived Progress Academically in School and in Sport	Frode Moen	76-84
11	Some Features of Liquid Crystalline Oxadiazoles	Amelia Carolina Sparavigna	85-88
12	Synchronization of Kuramoto oscillators on Knots	Amelia Carolina Sparavigna	89-95
13	Clique Complex Homology: A Combinatorial Invariant for Chordal Graphs	Allen D. Parks	96-100
14	An Evaluation Instrument for Interviewing Skills in Psychiatry	Wen-Ching Chen	101-104
15	The Association of Functional Single Nucleotide Polymorphisms of the RBP4 Gene with Gene Expression and Insulin Resistance Risk	Malgorzata Malodobra-Mazur	105-113

Novel Synthesis of Diketo-Acid Chondroitin-4-sulfate as Coordination Biopolymer Precursor through Oxidation of Chondroitin-4-sulfate by Alkaline Permanganate

Adil A. Gobouri¹, Ishaq A. Zaafarany², Refat M. Hassan³

¹ Chemistry Department, Faculty of Science, Taif University, Taif 21995, Saudi Arabia Kingdom.

² Chemistry Department, Faculty of Applied Sciences, Umm Al-Qura University, Makkah Al-Mukarramah 13401, Saudi Arabia Kingdom

³ Chemistry Department, Faculty of Science, Assiut University, Assiut 71516, Egypt

Abstract: Coordination biopolymer diketo-acid derivative of chondroitin-4-sulfate (DKA-CS) was prepared by the oxidation of CS with potassium permanganate in alkaline solution at pH's > 12. The chemical structure of the synthesized heterocyclic macromolecule (DKA-CS) has been characterized by elemental analysis and IR spectroscopy. The tendency of DKA-CS as a coordination biopolymer chelating agent for some metal ions has been examined. A tentative mechanism consistent with the experimental results for oxidation is suggested.

Introduction

Chondroitin-4-sulfate, whose repeating units composed of N-acetyl-D-galactosamine-4-sulfate with D-glucuronic acid is a water soluble anionic polyelectrolyte macromolecule [1].

A much work has been done on the kinetics of permanganate oxidation of polysaccharides (PS) that containing functional alcoholic groups by acidic [2-4] or alkaline permanganate [4-9]. The oxidation of pectates [2], carrageenans [3] and carboxymethyl cellulose [4] by acidic permanganate showed sigmoidal curves of S-shapes consisting of two stages for pseudo-first-order plots. The first stage was relatively slow involving the formation of Mn^{3+} and / or Mn^{4+} short lived intermediates, followed by an autoaccelerated period to give rise to the oxidation products at the second stage. One-electron transfer mechanism via free-radical intervention of inner-sphere nature was postulated in these redox systems. On the other hand, the kinetics of oxidation of alginates [5], pectates [6], carboxymethyl cellulose [7], methyl cellulose [8] and carrageenans [9] by permanganate ion in alkaline solutions of higher pH's was found to proceed through two distinct stages with respect to absorbance-time curves. The first stage was found to be relatively fast involving the formation of detectable transient coordination biopolymeric intermediates $[CS, Mn^{VI}O_4^{2-}]$ and / or $[CS, Mn^{VO}_4^{3-}]$ involving green manganate (VI) or

blue hypomanganate (V) short-lived species, followed by slow decomposition of these intermediates to give rise to the reaction product at the second stage. Inner-sphere mechanisms involving one- or two-electron transfer processes of non-free radical intervention were suggested in these redox reactions. Both spectrophotometric and kinetic evidences for formation of such intermediate complexes have been revealed.

Therefore, the present work of permanganate oxidation of chondroitin-4-sulfate as a natural polymer containing both primary and secondary alcoholic groups seems to be of great significant and merit an investigation in order to gain further information on the nature of the products as well as on the interaction of these macromolecule in aqueous alkaline solutions with a special sight on the influence of the nature of the functional groups on the mechanisms and kinetics in these redox systems. In addition, this work aims to synthesize keto-acid derivatives as coordination biopolymer precursors. This biopolymer could be used to encapsulate, protect and deliver bioactive or functional components such as minerals, peptides, proteins, enzymes, drugs, lipids or dietary fibers. It is also useful as precursors for synthesis of new biopolymers as selective biochelating agents for polyvalent cations through formation of their corresponding coordination biopolymeric complexes. These



complexes would be useful as conductors, selective cation sieves, semi-permeable membranes, biocatalysts and cation exchange resins.

Experimental

All materials used were of analytical grade. Doubly distilled water was redistilled from alkaline permanganate and degassed by bubbling through nitrogen, boiling and cooling under atmosphere [10].

Stock solutions of chondroitin-4-sulfate (ICN Biomedicals, Inc.) were prepared by stepwise addition of the reagent powder to doubly distilled water whilst rapidly stirring the solution to avoid the formation of aggregates which swell with difficulty.

A stock solution of KMnO_4 was prepared and standardized by the conventional methods described elsewhere [10,11]. Then, the stock solution was stored in a dark bottle away from light. All other reagents were prepared by dissolving the requisite amounts of the sample in doubly distilled water.

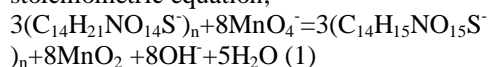
The ionic strength was controlled by addition of NaClO_4 as a non-complexing agent. The temperature was controlled within $\pm 0.05^\circ\text{C}$.

Polymerization test

The possibility of formation of free radicals was examined by adding acrylonitrile to the partially oxidized reaction mixture; no polymerization was observed indicating that the oxidation reaction probably does not proceed via a free-radical intervention mechanism.

Results and discussion

The experimental results indicated that one mole of CS was consumed 2.7 ± 0.1 mole of permanganate ion. Hence, such a result for oxidation of chondroitin-4-sulfate by potassium conforms to the following stoichiometric equation,



where $\text{C}_{14}\text{H}_{21}\text{NO}_{14}\text{S}^-$ and $\text{C}_{14}\text{H}_{15}\text{NO}_{15}\text{S}^-$ represent the chondroitin-4-sulfate and its corresponding keto-acid derivative, respectively.

Preparation of diketo-acid chondroitin-4-sulfate (DKA-CS)

A stoichiometric molar ratio of chondroitin-4-sulfate powder was dissolved in 250 cm^3 of deionized water whose pH was previously adjusted to $\text{pH} \geq 12$ using sodium hydroxide. This process was performed by stepwise addition of the powder CS to the solution while stirring rapidly and continuously to avoid the formation of aggregates. A 250 cm^3 solution containing the stoichiometric molar ratios of potassium permanganate and sodium fluoride were then added stepwise over 2 h to the CS solution. The reaction mixture was

stirred for 48 h at room temperature, the formed MnF_4 was filtered off, and the solution was concentrated to one-fifth of the original solution using a rotary evaporator. A portion of this concentrated solution was acidified using dilute acetic acid to a pH of ca. 5-6. The resultant solution dried under vacuum, and then subjected to elemental analysis and IR spectroscopy. The diketone were identified by 2,4-dinitrophenylhydrazine and hydroxylamine as described elsewhere [12-15].

Under our experimental conditions, the diketoacid chondroitin-4-sulfate was found to be in good agreement with the obtained results. This diketoderivative gave satisfactory elemental analysis and broad IR absorption bands at $1690\text{--}1650 \text{ cm}^{-1}$ (broad) that characterize the carbonyl group of α -diketone [16]. The disappearance of the absorption band of the OH group in the IR spectra indicated the complete oxidation of both OH groups in CS to the corresponding ketone. This product was also reacted with 2,4-dinitrophenylhydrazine and hydroxylamine to afford the corresponding bis-2,4-dinitrophenyl hydrazine and dioxime derivatives, which gave satisfactory elemental analysis and spectroscopic data as shown in Fig. 1. The yield was 95 %. It was found that the product has a high tendency to chelate with many metal cations such as Ag^+ , Ca^{2+} , Ni^{2+} , Pb^{2+} , Cd^{2+} , Ce^{4+} , etc. as shown in Scheme (I) and in Fig.1. The characteristics and geometrical configuration of these complexes are in progress in our laboratory

IR-spectra

The IR-spectra were scanned on a Pyc Unicam Sp 3100 spectrophotometer using the KBr disc technique ($4000\text{--}200 \text{ cm}^{-1}$).

The FTIR-spectra were scanned ANAL: Diketoacid chondroitin-4-sulfate (DKA-CS) $\text{C}_{14}\text{H}_{15}\text{NO}_{15}\text{S}$ FTIR: 3430 (OH of COOH group); 1795-1730 (broad) (C = O of -diketone); 1639 (C = O of COOH, γ_{as} OCO); 1418 (C = O of COOH, γ_{s} OCO) and 1338 cm^{-1} (C — O — C of CS) [12]

2,4-Dinitrophenyl hydrazone derivative

ANAL: $\text{C}_{26}\text{H}_{23}\text{N}_9\text{O}_{21}\text{S}$ (829): Calcd (Found) : C, 37.64 (37.45); H, 2.77 (2.66); N, 15.20 (15.10).

Dioxime derivative

ANAL: $\text{C}_{14}\text{H}_{17}\text{N}_3\text{O}_{15}\text{S}$ (499): Calcd (Found): C, 33.67 (33.62); H, 3.41 (3.39); N, 8.42 (8.40)

The most suitable reaction mechanism which may be suggested for oxidation in the present work involves a fast deprotonation of chondroitin-4-sulfate substrate by the alkali to form the corresponding alkoxide, followed by the attack of permanganate ion on the alkoxide to form a more reactive transient species prior to the formation of the green intermediate complex $[\text{CS-Mn}^{\text{VI}}\text{O}_4]^{2-}$ in the rate-determining step of the initial fast stage. Also,

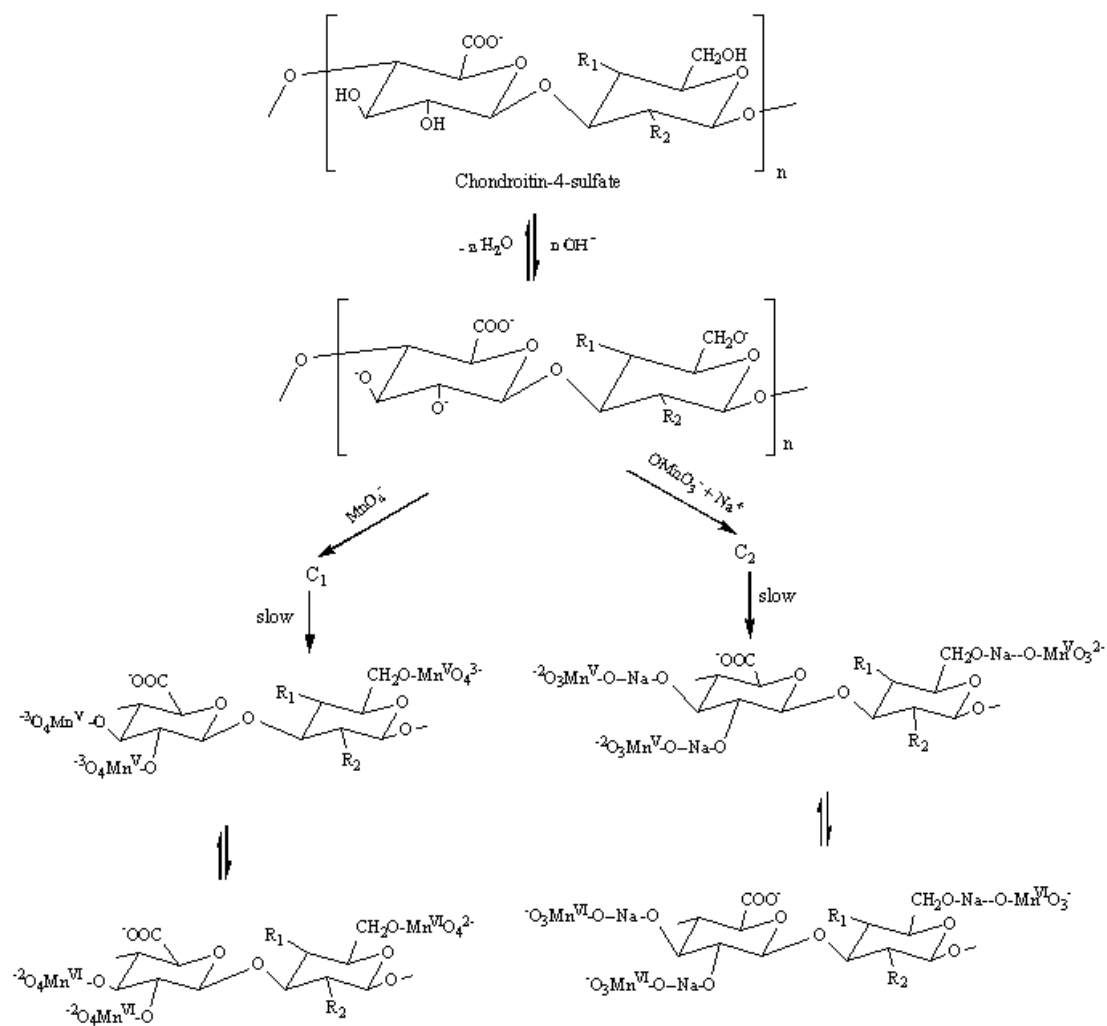
the formed $\text{Mn}^{\text{VI}}\text{O}_4^{2-}$ is capable to oxidize the formed alkoxide ion, but the reaction is of several orders of magnitude slower than permanganate oxidation owing to its lower reactivity [5-9, 17] and, hence, would not influence the kinetics of the initial stage reaction. The spectral changes during the progress of oxidation reaction for the formation of the coordination biopolymer complex are shown in Figs. 2 and 3, respectively. Again, the oxidation mechanisms for formation and decomposition for coordination biopolymer complex are illustrated in Schemes (I) and (II), respectively.

An alternative reaction mechanism based on the presence of two competitive reactions in the rate-determining step [7] may also be suggested. The first step corresponds to the removal of protons from the alcoholic group by alkali to give the reactive alkoxide form. This removal is followed by the attack of MnO_4^- to the alkoxide center which facilitated by the polarization of the Mn-O bond or NaMnO_4 forming the reactive transient species C_1 and C_2 prior to the formation of stable $[\text{CS}, \text{Mn}^{\text{VI}}\text{O}_4^{2-}]$ and/or $[\text{CS}, \text{Mn}^{\text{V}}\text{O}_4^{3-}]$ intermediate complexes. The presence of Na^+ cations may facilitate the oxidant attack since it reduces the net charge of the intermediate complexes formed. The proposal that alkoxide is formed prior to the attack of MnO_4^- ion fits some of the experimental facts such as the dependence of the formation rates of intermediates on $[\text{OH}^-]$.

References

- [1] H.Tsuge, M. Yonese, H. Kishimoto, Bulletin of the Chemical Society of Japan 52 (1979) 2846.
- [2] M.I. Abdel-Hamid, K.S.Khairou, R.M. Hassan, Eur. Polym. J. 39 (2003) 381.
- [3] R.M.Hassan, A.Fawzy, G.A.Ahmed, I.A. Zaafarany, B.S. Asghar, K.S. Khairou, J. Mol. Cat. 309 (2009) 95.
- [4] R. M. Hassan, D.A.Abdel-Kader, S.M. Ahmed, A.Fawzy, I.A. Zaafarany, B.H. Asghar, H.D. Takagi, Cat. Commun. 11 (2009) 184.
- [5] R. M. Hassan, J. Polym. Sci. 31 (1993) 51 ; 1147; A.M.Shaker, R.M.El-Khatib, L. A. E. Nassr, Carbohydr. Polym. 78 (2009) 710.
- [6] K. S. Khairou, R. M. Hassan, Eur. Polym. J. 36 (2000) 2021.
- [7] A. M. Shaker, J. Coll. Interf. Sci. 233 (2001) 197; 244, 254.
- [8] R. M. El-Khatib, Carbohydr. Polym. 47 (2002) 377; A. M. Shaker, R. M. El-Khatib, H. S. Mahran, J. Appl. Polym. Sci. 106 (2007) 2668.
- [9] R.M. Hassan, A. Fawzy, A. Alarifi, G.A. Ahmed, I.A.Zaafarany, H.D.Takagi, J. Mol. Cat. A 335 (2011) 38.
- [10] R. M.Hassan, M. A. Mousa, S. A. El-Shatoury, J. Chem. Soc., Dalton Trans. (1988) 601; R. M. Hassan, M. A. Mousa, M. H.Wahdan, J. Chem. Soc., Dalton Trans. (1988) 605; R. M. Hassan, Can. J. Chem. 69 (1991) 2018.
- [11] M. S. Manhas, F. Mohamed, Z. Khan, Coll. Surf. 295 (2007) 165; S.M.Z. Andrabi, M.A. Malik, Z. Khan, Coll. Surf. 58 (2007) 299; S.A.Khan, P.Kumar, K.Saleem, Z. Khan, Coll. Surf. 302 (2007) 102.
- [12] R. M. Silverstien, G. C. Bassler and T. C. Morrill, Spectrometric Identification of Organic Compounds, John Wiley; New York, 1981, pp. 121.
- [13] M. Hassan, M. A. Abdalla, M. F. El-Zohary, J. Appl. Polym. Sci., 47 (1993) 1649.
- [14] R. M. Hassan and M. A. Abdalla, J. Mater. Sci., 2 (1992) 609.
- [15] K. S. Khairou, R. M. Hassan and M. A. Shaker, J. Appl. Polym. Sci., 85 (2002) 1019.
- [16] P. C. S. Simon, Tables of Spectral Data for Structural Determination of Organic Compounds, Springer Verlag; Berlin, New York, 1983 (Translation).
- [17] D.G. Lee, C.F. Sebastin, Can. J. Chem. 59 (1981) 2776.

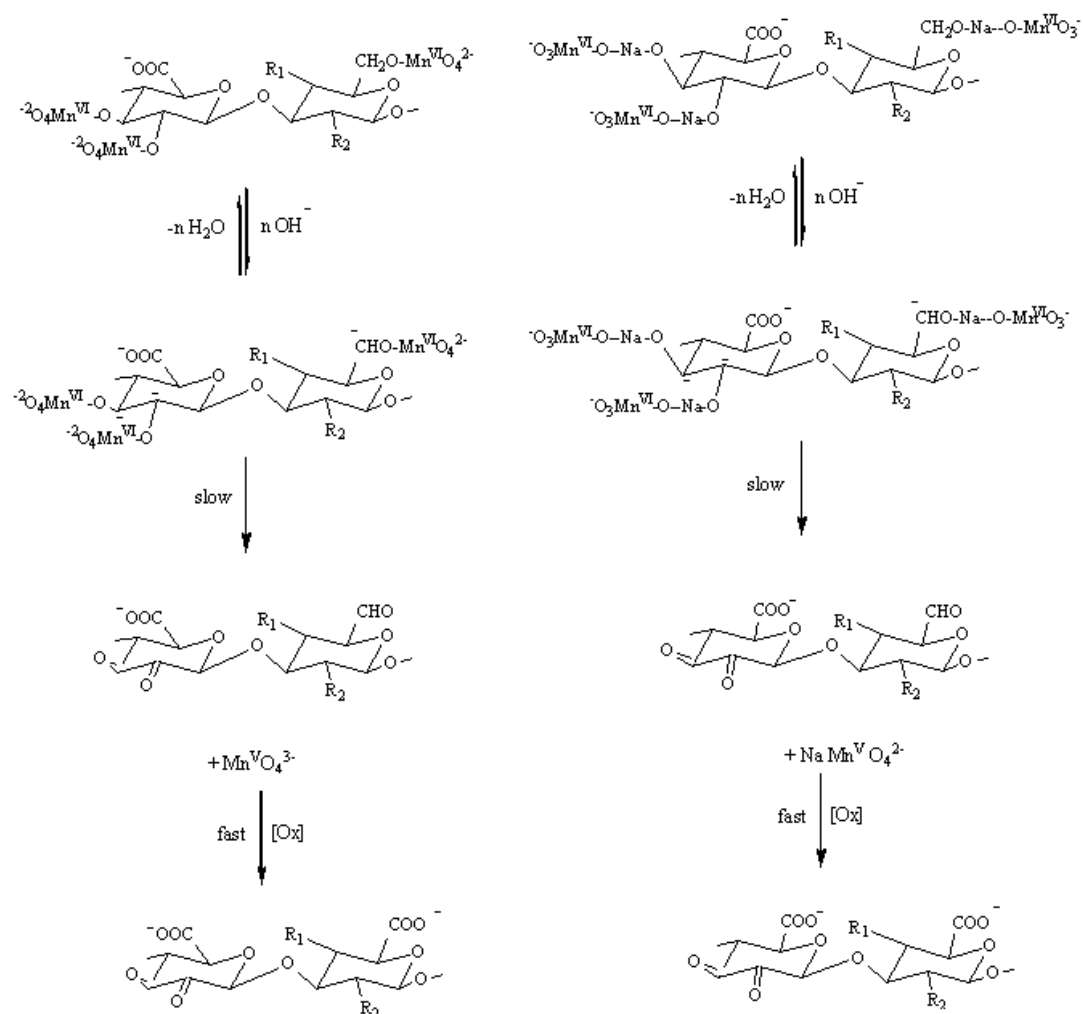
Formation



$\text{R}_1 = -\text{OSO}_3^-$ and $\text{R}_2 = -\text{NH}-\text{CO}-\text{CH}_3$

Scheme 1

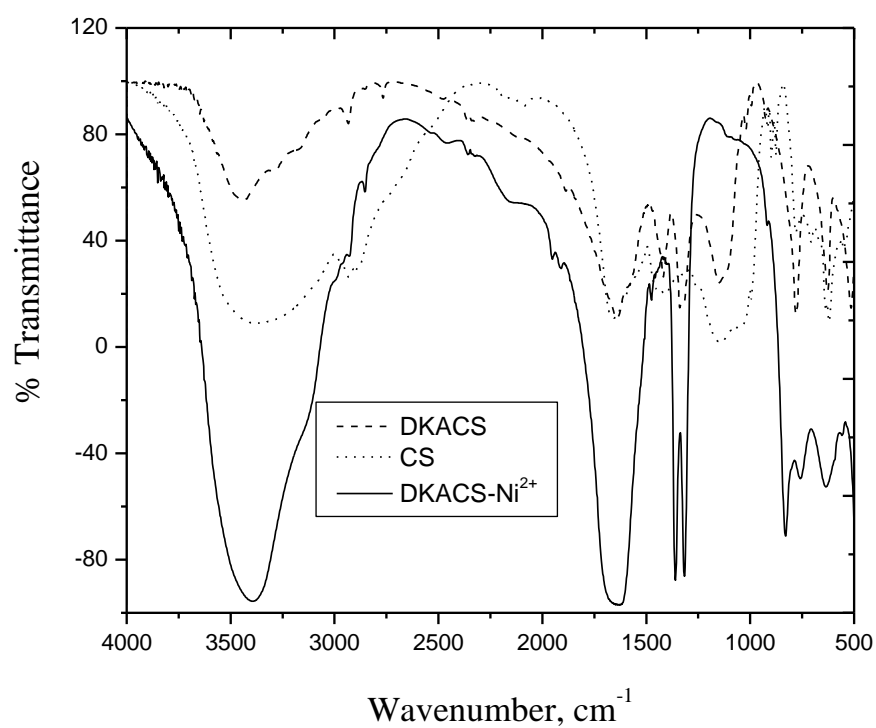
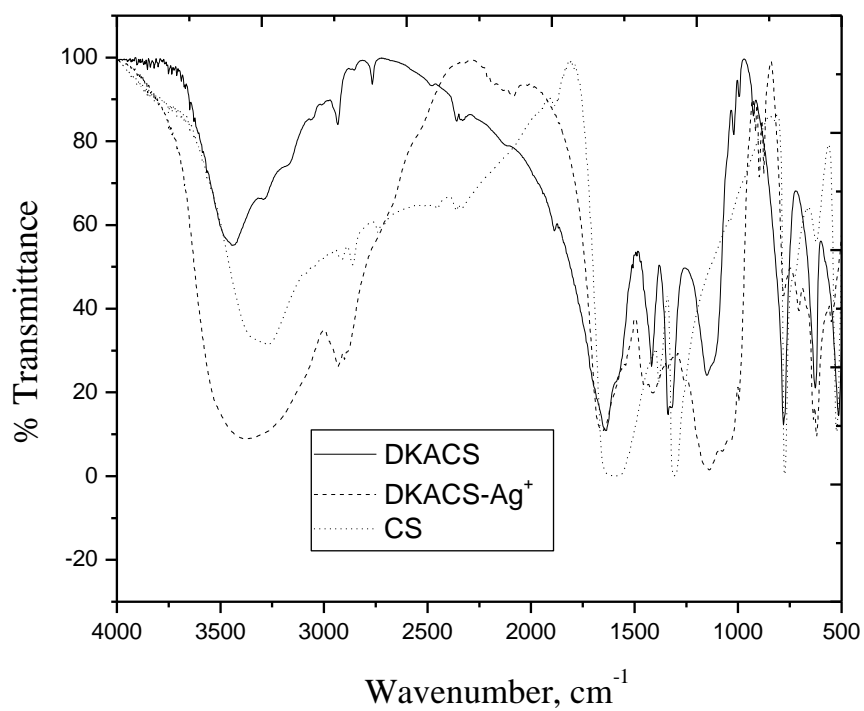
Decomposition



$\text{R}_1 = -\text{OSO}_3^-$ and $\text{R}_2 = -\text{NH}-\text{CO}-\text{CH}_3$

Scheme II





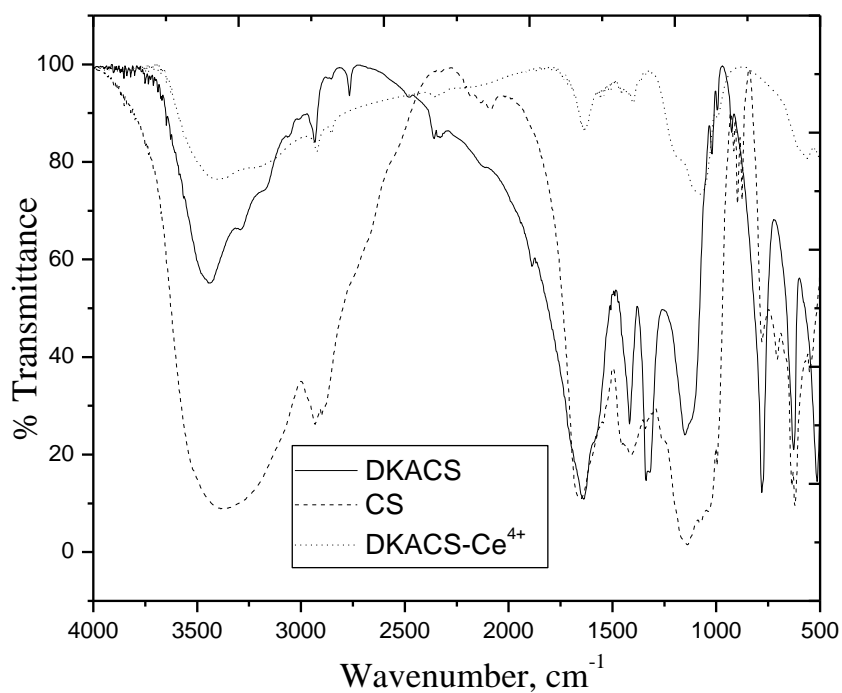


Figure 1. FTIR spectra of chondroitin-4-sulfate, its diketo-acid derivative (II) and metal complexes.

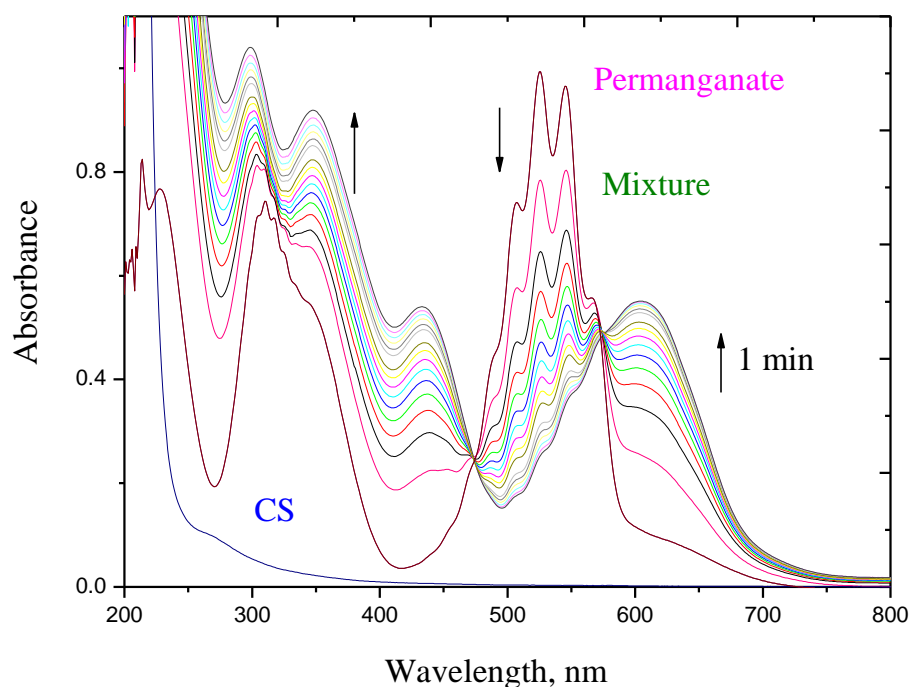


Figure 2. Spectral changes (200-800 nm) during the formation of the intermediate complex in the oxidation of chondroitin-4-sulfate by alkaline permanganate. $[\text{MnO}_4^-] = 4 \times 10^{-4}$, $[\text{CS}] = 5.5 \times 10^{-3}$, $[\text{OH}^-] = 0.05$ and $I = 0.1 \text{ mol dm}^{-3}$ at 25°C (scanning time intervals = 1 min).

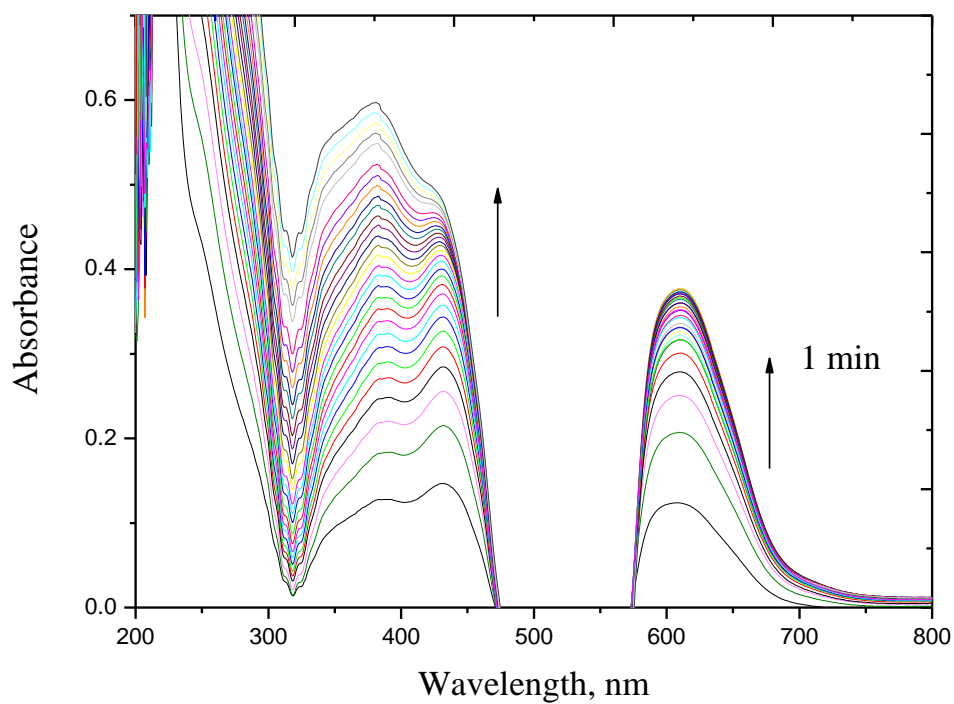
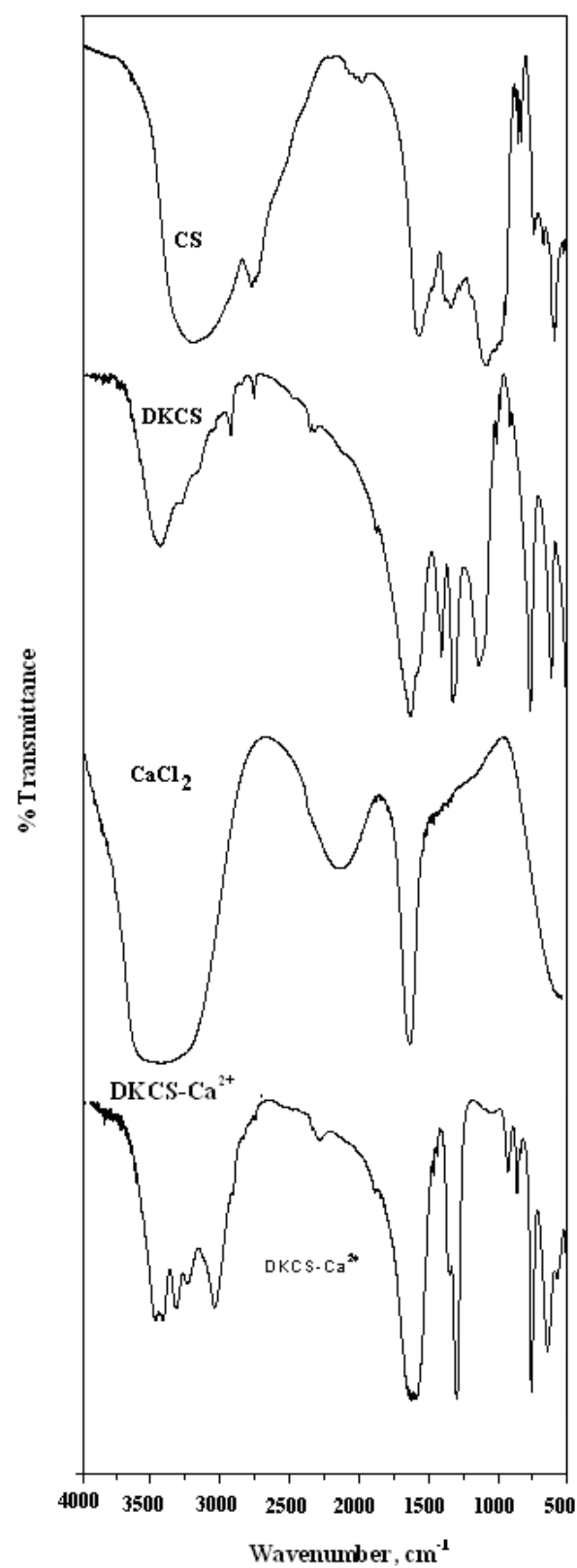
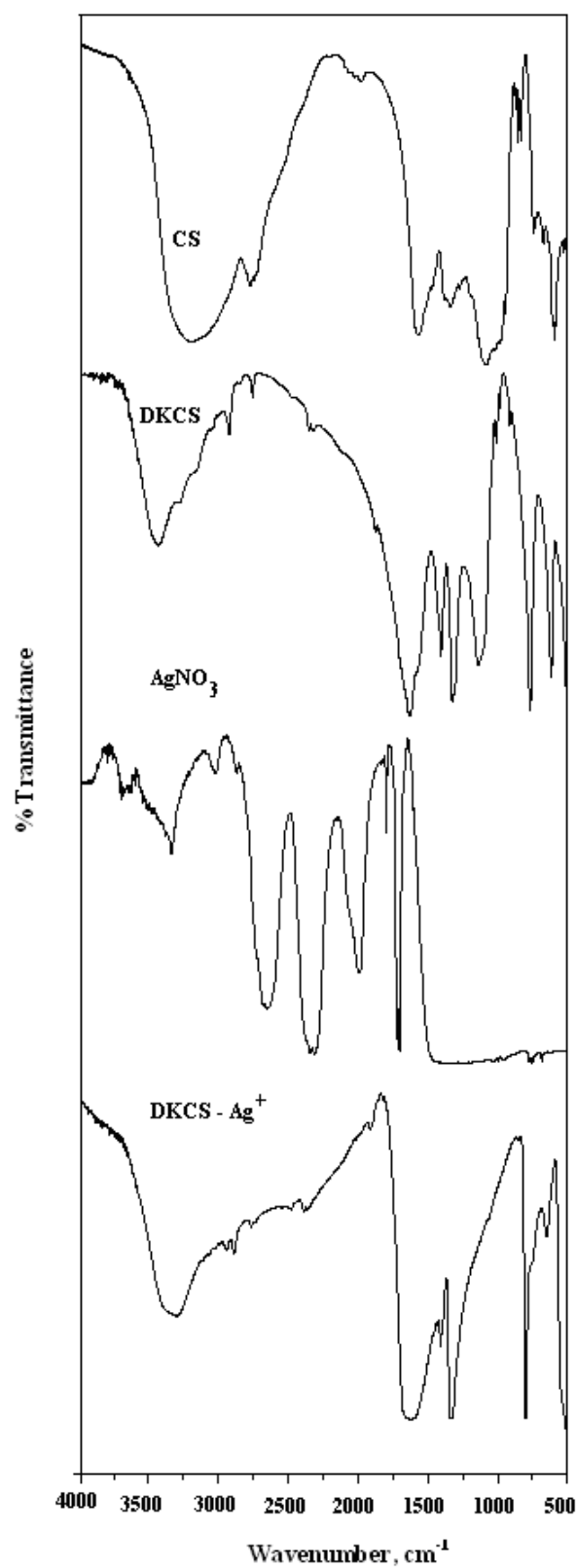
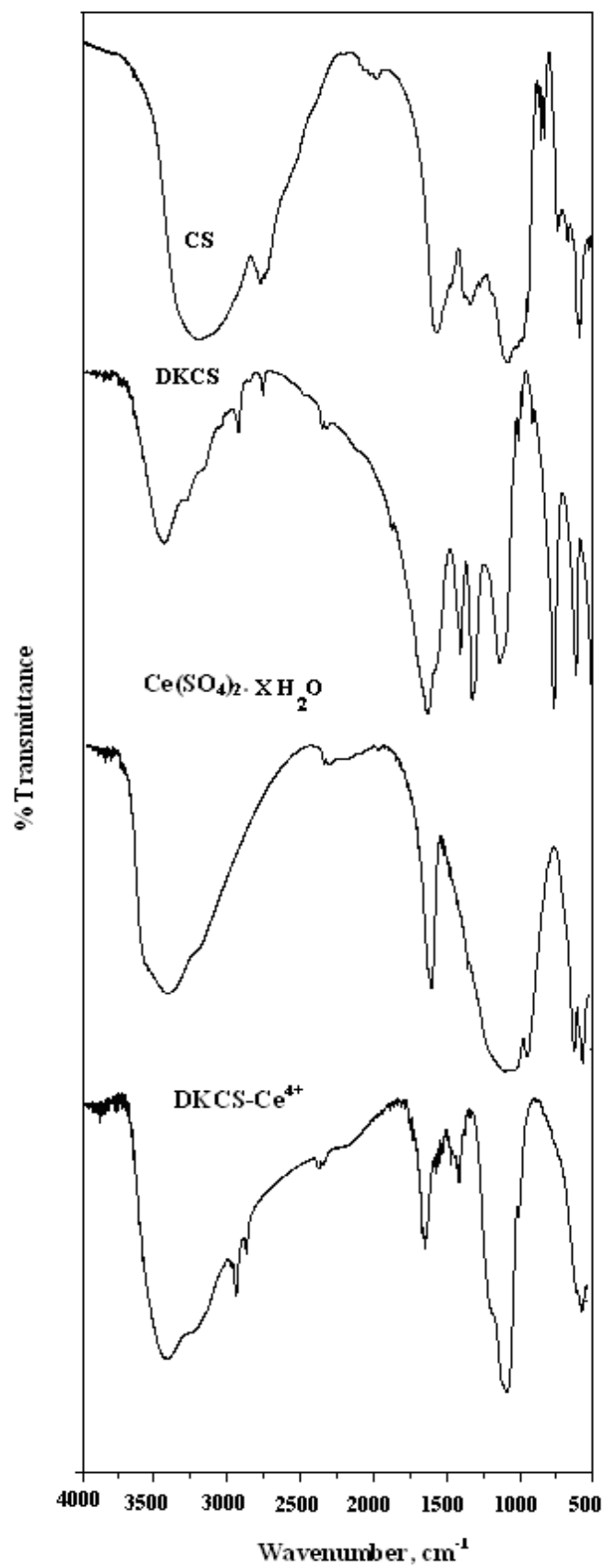


Figure 3. Spectral changes (200-800 nm) during the formation of the intermediate complex in the oxidation of chondroitin-4-sulfate by alkaline permanganate. $[\text{MnO}_4^-] = 4 \times 10^{-4}$, $[\text{CS}] = 5.5 \times 10^{-3}$, $[\text{OH}^-] = 0.05$ and $I = 0.1 \text{ mol dm}^{-3}$ at 25°C (scanning time intervals = 1 min). Ref. $[\text{MnO}_4^-] = 4 \times 10^{-4} \text{ mol dm}^{-3}$.





STABILITY EVALUATION OF ANTHOCYANIN EXTRACTED FROM PROCESSED GRAPE RESIDUES

Edmar Clemente¹, Dirseu Galli²

¹Laboratory of Food Biochemistry / UEM, State University of Maringá, Zip Code 87020-900, Maringá, Paraná, Brazil

²Laboratory of Agrochemistry and Environment / DQI, State University of Maringá - UEM, Zip Code 87020-900, Maringá, Paraná, Brazil

Abstract: Anthocyanins are extremely important phenolic compounds due to their antioxidant potential. They are used as natural colorants in food industry, but upon the industrial processes, they show low stability. Grape and grape-made products are a source of several phenolic compounds and the residues proceeding from wine making may display a large amount of these compounds. The aim of this work was to evaluate the stability of anthocyanins extracted from grape residues industrially processed for wine making. For the evaluation, the residues of grapes Bordô and Isabel, which were extracted with ethanol 70% acidified to pH 2.0, were used. For stability analysis, the application of organic compounds co-pigments, such as caffeic, ferulic and p-coumaric acids at 0.5; 0.8; 1:1 (p/v) concentrations, was evaluated. The acid that showed higher stability was p-coumaric acid at a 1:1 (p/v) concentration, with 84.37% of retention time and half-life of 1,634 days. The use of these organic acids as stabilizers in solution increased anthocyanins useful lifetime.

Keywords: *Vitis labrusca* L. - Anthocyanins - Co-pigments - Organic Acids

Introduction

Anthocyanins are natural pigmented phenolic compounds responsible for blue, purple and red colors in flowers, fruits, leaves and stems. These compounds have an antioxidant potential, acting as singlet oxygen reducers in lipidic oxidation reactions and metal chelation, a large amount of properties, such as pharmacological, anti-allergenic, anti-arteriogenic, anti-inflammatory, anti-microbial, anti-thrombotic and cardioprotective and vasodilator effects (PUUPPONEN-PIMIÄ et al., 2001; MANACH et al., 2005). Most substances responsible for coloring belong to the flavonoids class. The classification of the flavonoid type present in a plant extract is based initially on the study of solubility and coloring reaction properties. Grape is a source of several phenolic compounds in high concentrations and the byproducts and residues proceeding from wine making processes, mostly, may maintain reasonable amounts of these compounds.

Free anthocyanins are rarely found in plants and they occur together with glycosylated sugars that stabilize the molecule. Sugars that are usually linked to anthocyanins are glucose, galactose, rhamnose and arabinose. R1 and R2 groups vary according to Figure 1, where it can be noticed that R3 and R4 groups are usually hydroxyls or glycolic (mostly, glycoside). In nature, anthocyanins occur as monoglycoside (glucose linked to position 3) or

diglycoside (glucose linked to positions 1 and 3) (FRANCIS, 2000).

Figure 1. Basic structure of an anthocyanin (FRANCIS, 2000).

Anthocyanin sugars are acylated by p-coumaric, ferulic, caffeic, p-hydroxybenzoic, sinapinic, malonic, acetic, succinic and malic acids. Copigmentation reaction may be the main molecular interaction mechanism involved in color and astringency variations during wine production and aging (MAZZA, 1995). The increase in stability occurs because the pigment competes with water and interacts with anthocyanin, making complexes with colorful forms and modifying the pigment nature (GRIS et al., 2007). The phenolic acids of cinnamic series are found in grape combined with tartaric acids as monoesters. In Figure 2, it can be observed the representation of cinnamic acid, from which the phenolic acids of this series derive, being them ferulic, p-coumaric and caffeic acids.

Figure 2. Cinnamic acids structure (BALASUNDRAM, SUNDRAM and SAMMAN, 2006).

If we consider anthocyanin coloration only as a function of pH, we are led to believe that plants should not be colored, once the natural pH in plants, in most cases, is between neutral and slightly acid. In this pH scope, most anthocyanins are not colored.



However, it is observed that anthocyanins are always associated with colored parts in plants, pointing out that these substances must be stabilized by uncommon physicochemical factors. The presence of compounds named co-pigments may be one of the aforesaid factors. Non-anthocyanic flavonoids, alkaloids, amino acids and nucleotides may act as co-pigments and even anthocyanin itself may act co-pigmented to another anthocyanin. There may be three basic anthocyanin stabilizing mechanisms: with or without intramolecular co-pigmentation, intermolecular co-pigmentation and self-association together with anthocyanidin, flavonoid or aromatic acid and sugar molecules. Anthocyanin solutions that are much diluted show an increase in coloration, when co-pigmented with rutin, but this increase in absorbance is slowly reduced as anthocyanin concentration increases. The lowest anthocyanin availability for co-pigmentation with rutin may be associated with kation flavilium by means of anthocyanin self-association, when they are present in higher concentrations.

Anthocyanin extraction is the first step to determine its content in any kind of plant tissue and residues. Anthocyanins are located in the vacuoles of hypodermic cells, close to the surface and the extraction procedure usually involves the use of acid solvents that denature the cellular tissue membrane and dissolve the pigments, simultaneously (WROLSTAD; GIUSTI, 2001).

The aim of this work was to evaluate the stability of anthocyanins extracted from agroindustrial residues of grape used in wine making processes, varieties Bordô and Isabel, upon the application of co-pigments, such as caffeic, p-coumaric and ferulic acids.

EXPERIMENTAL STEP

Sampling

The residue of industrially processed grapes (*Vitis labrusca* L.), varieties Isabel (80%) and Bordô (20%) was collected in Cooperativa Agroindustrial dos Viticultores de Marialva (COAVITTI), in the municipality of Marialva, located in the north of Paraná state (latitude 23°29'06" S and 51°29'31"W). The material collection was carried out in January 2011, after a separation process in the wine making fermentation tank. The residue was pressed, in order to take off the wine excess, in a mechanical press and afterwards it was put in dark-colored (black) plastic bags with 0.5mm density and stored at -18°C for further analyses.

Extract preparation

Extract obtention was carried out from 100g of grape residue sample, homogenized with 200 mL of

extracting solution (70 mL of ethanol 70% and 30 mL of HCl 0.1%, pH 2.0), for two minutes in a blender, and left to rest for twelve hours at 4°C in a beaker covered with parafilm and aluminum foil for protection against light incidence. Afterwards, a filtration was made, transferring the content to a 250mL volumetric flask and completing it with an extracting solution (Ju and Howard, 2003).

An aliquot of 2.0mL was taken from the stock solution at 4±0.5°C to a volumetric flask of 25mL, completing the volume with extracting solution and leaving it at room temperature and in the dark for two hours. The extracting solution was used as blank. The extract absorbance reading was made in an UV-Vis spectrometer (Hitachi, mod. 2001) at 535nm. To determine the concentration of anthocyanin (total anthocyanin mg/100 g) the expressions from Equations 1 and 2, which provides the simplified calculation for its determination, were used (VANNI, KWIATKOWSKI, CLEMENTE, 2009).

$$FD = VEB / VA \times VS \quad (1)$$

$$AT \text{ (mg / 100g)} = A \times FD / E^{1\%}_{1cm} \quad (2)$$

Where:

FD = Dilution factor

VEB = Gross extract volume (250 mL)

VA = Volume of the extraction aliquot used for the dilution in extracting solution (2 mL).

VS = Volume of the solution used for the extract dilution (25 mL)

AT = Total Anthocyanin (mg) in 100g of sample.

A = Diluted extract absorbance in the maximum absorption wave length.

$E^{1\%}_{1cm} = 98.20$; Molar absorptivity coefficient for a mixture of purified anthocyanins from the processed grape extract

Evaluation of degradation parameters

The calculations of degradation speed constant (K), half-life ($t^{1/2}$) and percentage of color retention (%R) (GRIS et al., 2004) are used to analyze the anthocyanin pigments degradation as a function of time. Pigment degradation speed and ($t^{1/2}$) can be calculated according to Equations 3 and 4, respectively (VANINI; KWIATKOWSKI; CLEMENTE, 2009).

$$k.t = -2.303 \times \log At_x / At_0 \quad (3)$$

$$t^{1/2} = 0.693 / k \quad (4)$$

Where:

At_x = Absorbance in relation to the final time of the experiment,

At_0 = Absorbance in time zero, initial time of the experiment,

K = Speed Constant (hs^{-1}),

t = Time (days, hours, minutes, seconds),

$t^{1/2}$ = half-life time.

The percentage of color retention (%R), related to time, can be calculated by the absorbance readings, using Equation 5 (VANINI, KWIATKOWSKI, CLEMENTE, 2009).

$$\%R = At_x / At_0 \times 100 \quad (5)$$

Where:

%R = Percentage of color retention,

At_x = Absorbance as a function of the experiment final time,

At_0 = Absorbance in time zero, initial time of the experiment.

Results and Discussion

The stability of anthocyanins extracted from grape residues of wine making, added with p-coumaric acid, at 25°C and with absence of light can be seen on Figure 3. The increase in stability can be observed in all concentrations, when compared to the control treatment. It occurs due to the fact that the co-pigment competes with water and interacts with anthocyanins, creating complexes with colored forms and modifying the co-pigment nature. It can also be observe that the increase in absorbance (hyperchromatic effect) with higher intensity on concentration 1.0:1.0 (p/v), and with lower intensity in the control.

Figure 3. Anthocyanin stability, in the processed grape extract, added with p-coumaric acid, at a 25°C, with absence of light. A = Control; B = 0.5:1.0; C = 0.8:1.0; D = 1.0:1.0 (p/v) p-coumaric acid:anthocyanin extract.

The presence of caffeic acid in the molecule increases anthocyanin stability and the existence of interaction between the pelargonidin chromophore and caffeil groups of anthocyanins extracted from petals of *Pharbits nil*, cultivars purple-red (Dangles, Saito and

Brouillard, 1993). An increase in absorbance values (hyperchromatic effect) as well as a bathochromatic displacement, usually between 5 and 20 nm or more, in the maximum absorption length, with treatments with caffeic acid.

Figure 4. Anthocyanin stability in processed grape extract with caffeic acid, at 25°C, with absence of light. A = Control; B = 0.5:1.0; C = 0.8:1.0; D = 1.0:1.0, caffeic acid:anthocyanin extract (p/v).

The pigment/co-pigment complex created is dependent on both concentrations as the co-pigment/anthocyanin relation increases. It can be observed that there was an increase in absorbance values on the first day, with a hyperchromatic effect. It occurs due to the absorption coefficient that increases the colored molecules concentrations on the maximum absorption wave lengths, in treatments with and without caffeic acid (Figure 4). After the seventh day, there was a decrease in absorbance values in relation to the control. It can be explained by a local reduction on the chromophore flavilium polarity, caused by its involvement with the co-pigment, by means of a hydrophobic association. After this period, the samples showed constant absorbance linearity upon the addition of caffeic acid and the experiment lasted until day 400.

As for the experiment with caffeic acid addition, the concentration 0.5:1.0 (p/v) showed higher color retention (83.62%) and half-life time was 1,552 days, being observed that upon the addition of caffeic acid, the absorbance values were higher than the control (Figure 4). Darias-Martins et al. (2001) reported that after adding an amount of caffeic acid to wine, there was an increase of 60% in the absorbance values after 90 days. It shows that caffeic acid provides higher stability, increasing the concentration of anthocyanins. Tests T2 and T3 showed lower color retention.

Figure 5. Anthocyanin stability in processed grape extract with ferulic acid, at 25°C, with absence of light. A = Control; B = 0.5:1.0; C = 0.8:1.0; D = 1.0:1.0, ferulic acid:

As for co-pigmentation with ferulic acid, the control treatment showed higher absorbance values, when compared to the others, with retention time of 81,06% and half-life time of 1,322 days. The treatment with the same acid at a 0.5:1.0 concentration showed a retention time of 19.48% and half-life time of 169 days. Upon the addition of ferulic acid, at a concentration of 0.5:1.0 (p/v) there was slow anthocyanin degradation, thus having a bathochromatic effect (Figure 5). The retention time was 11.44% and half-life time was 129 days upon the addition of ferulic acid at a concentration of 0.8:1.0 (p/v) and there was slow anthocyanin degradation,

thus having a bathochromic effect. Upon the addition of ferulic acid at 1.0:1.0 (p/v) there was also higher anthocyanin degradation, when compared with the control treatment. The retention time was 22.84% and half-life time was 161 days. Regarding the other acids used in this study, ferulic acid showed the lowest retention time and the lowest half-life time, in days.

In Table 1, the retention time numbers and half-life values for anthocyanin extract of processed grape residues are displayed.

Table 1. Retention time and half-life of anthocyanin extracted from grape residues (varieties Bordo and Isabel) of wine making.

Treatment T9 had the best color retention time in anthocyanin extract of processed grape residues, with 84.37% of color retention and half-life time of 1,634 days, indicating that the addition of p-coumaric acid at a 1.0:1.0 (p/v) concentration provides higher stability.

Conclusions

Out of the used acids, the one which least degraded the anthocyanins and kept the best stability in the extract of processed grape residues were p-coumaric and caffeic acids. Thus, it is possible to extract anthocyanins and, upon the addition of organic acids, increase its half-life time, in order to avoid fast anthocyanin degradation.

Acknowledgement

To COAVITTI - Cooperativa Agroindustrial dos Viticultores de Marialva, Paraná, Brasil, for providing the samples.

Reference

1. BALASUNDRAM, N.; SUNDRAM, K.; SAMMAN, S. Phenolic compounds in plants and agri-industrial by-products: antioxidant activity, occurrence, and potential uses. *Food Chemistry*, v.99, p.191-203, 2006.
2. COSTA, C.T.; HORTON, D.; MARGOLIS, S.A. Review. Analysis of anthocyanins in food by liquid chromatography, liquid chromatography-mass spectrometry and capillary electrophoresis. *Journal of Chromatography A*, Amsterdam, v.881, p.403-410, 2000.
3. DARÍAS-MARTÍN, J. Enhancement of red wine colour by pre-fermentation addition of copigments. *Food Chemistry*, Great Britain, v.73, p.217-220, 2001.
4. DANGLES, O.; SAITO, N.; BROUILLARD, R. Anthocyanin intramolecular copigment effect. *Phytochemistry*, London, v. 34, n. 1, p. 119-124, 1993.
5. FRANCIS, F. J. Anthocyanins and betalains: composition and applications. *Cereal Foods World*, v. 45, p. 208-213, 2000.
6. GRIS, E.F.; FERREIRA, E.A.; FALÇÃO, L.D.; BORDIGNON - LUIZ, M.T. Caffeic acid copigmentation of anthocyanins from Cabernet Sauvignon grape extracts in model systems, *Food Chemistry*, v.100, p. 1289 -1296, 2007.
7. JU, Z.Y.; HOWARD, L.R. Effects of Solvent and Temperature on Pressurized Liquid Extraction of Anthocyanins and Total Phenolics from Dried Red Grape Skin. *Journal of Agricultural and Food Chemistry*, v.51, n.18, p.5207-5213, 2003.
8. MANACH, C.; MAZUR, A.; SCALBERT, A. Polyphenols and prevention of cardiovascular diseases. *Current Opinion in Lipidology*, v.16, n.1, p.77-84, 2005.
9. MATEUS, N.; PROENÇA, S.; RIBEIRO, P.; MACHADO, J. M.; DE FREITAS, V. Grape and wine polyphenolic composition of red *Vitis vinifera* varieties concerning vineyard altitude. *Ciência e Tecnologia de Alimentos*, v.3, n.2, p.102-110, 2001.
10. MAZZA, G. Anthocyanins in grapes and grape products. *Critical Review of Food Science and Nutrition*, Madison, v. 35, p. 341-371, 1995.
11. PUUPPONEN -PIMIÄ, R. et al. Antimicrobial properties of phenolic compounds from berries. *Journal of applied Microbiology*, v. 90, n. 4, p.494-507, 2001.
12. VANINI, L.S.; HIRATA, T.A.; KWIATKOWSKI, A.; CLEMENTE, E. Extraction and stability of anthocyanins from the Benitaka grape cultivar (*Vitis vinifera* L.) *Brazilian Journal Food Technology*. v.12, n.3, p.213-219, jul/set, 2009.
13. WORSLETT, D.R.E. GIUSTI, M.M. Characterization and measurement of anthocyanins by uv-visible spectroscopy. *Current Protocols in Food Analytical Chemistry*. New York, John Wiley & Sons, 2001.

Table 1. Retention time and half-life of anthocyanin extracted from grape residues (varieties Bordo and Isabel) of wine making.

Treatments	Added Concentration (p/v)	Retention (R%)	Time	Half-life time (t $\frac{1}{2}$) in days
C1	0.0:0.0	81.06		1.322
T1	0.5:1.0	83.62		1.555
T2	0.8:1.0	67.00		718
T3	1.0:1.0	68.31		727
T4	0.5:1.0	19.48		169
T5	0.8:1.0	11.74		129
T6	1.0:1.0	22.84		191
T7	0.5:1.0	62.50		592
T8	0.8:1.0	74.24		906
T9	1.0:1.0	84.37		1.634

C1- control; treatments T1; T2; T3 - caffeic acid; T4; T5; T6 - ferulic acid; T7; T8; T9 - p-coumaric acid.

Figure 1. Basic structure of an anthocyanin (FRANCIS, 2000).

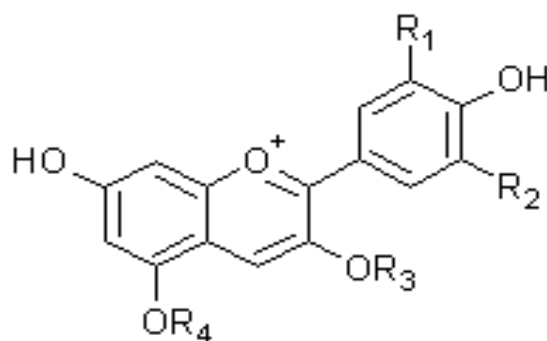


Figure 2. Cinnamic acids structure (BALASUNDRAM, SUNDRAM and SAMMAN, 2006).

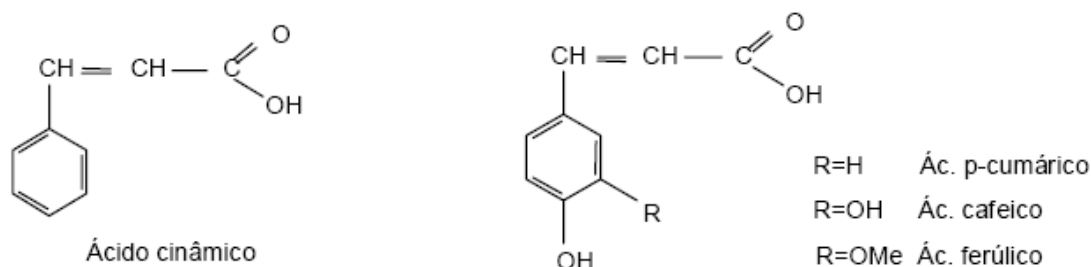


Figure 3. Anthocyanin stability, in the processed grape extract, added with p-coumaric acid, at a 25°C, with absence of light. A = Control; B = 0.5:1.0; C = 0.8:1.0; D = 1.0:1.0 (p/v) p-coumaric acid:anthocyanin extract.

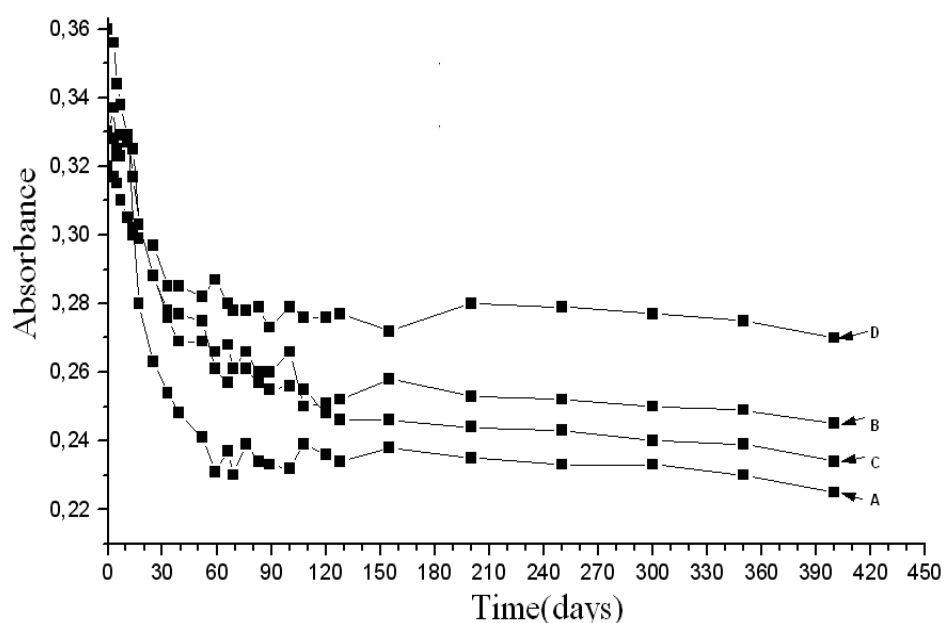


Figure 4. Anthocyanin stability in processed grape extract with caffeic acid, at 25°C, with absence of light. A = Control; B = 0.5:1.0; C = 0.8:1.0; D = 1.0:1.0, caffeic acid:anthocyanin extract (p/v).

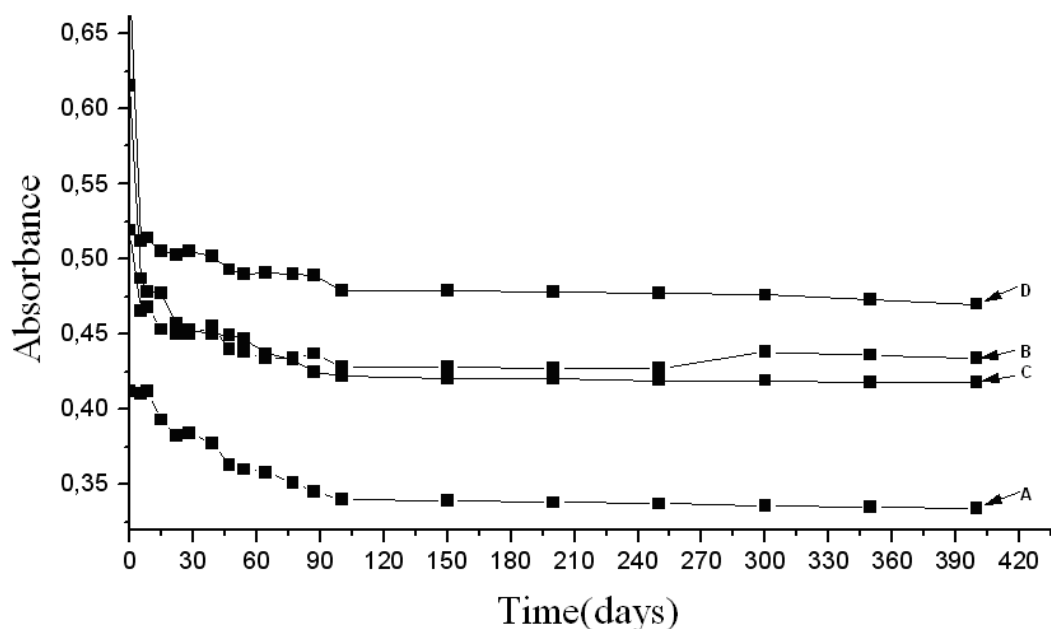
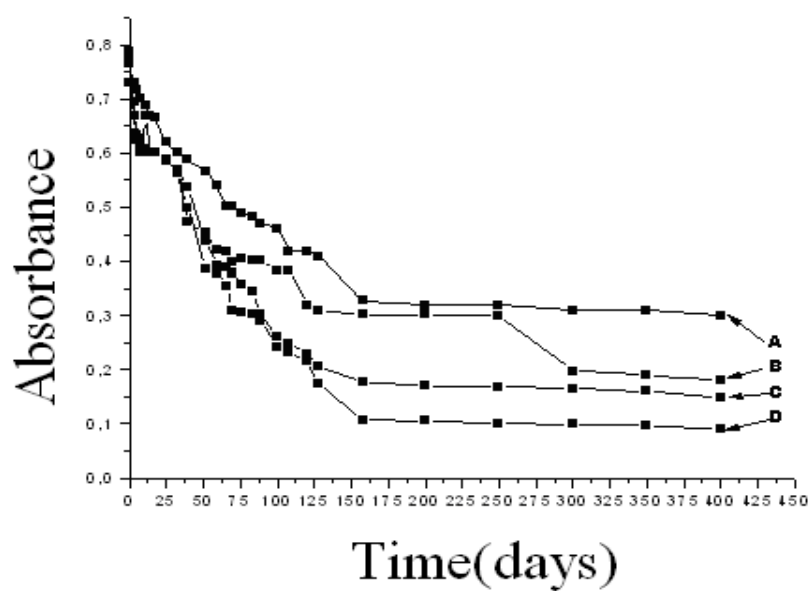



Figure 5. Anthocyanin stability in processed grape extract with ferulic acid, at 25°C, with absence of light. A = Control; B = 0.5:1.0; C = 0.8:1.0; D = 1.0:1.0, ferulic acid:anthocyanin extract (p/v).



Embryos and Lateral Buds Culture of *Tapeinochilos Ananassae* (Hassk). K. Schum.

Lilia Willadino², Nise de Fátima Coutinho Souto¹, Cláudia Ulisses², Ana Lúcia Figueiredo Porto³, Terezinha Camara⁴,
Marina Medeiros de Araújo Silva⁵

¹Projetos Técnicos Ltda - Projotec, Rua Irene Gomes Matos, 176, Pina, CEP 51011-530, Recife-PE, Brasil.

²Universidade Federal Rural de Pernambuco, Depto. de Biologia, Rua Dom Manoel de Medeiros, s/n, CEP 52071-900, Recife-PE, Brasil. E-mail: willadino.lilia@gmail.com

³Universidade Federal Rural de Pernambuco, Depto. de Morfologia e Anatomia Animal, Rua Dom Manoel de Medeiros, s/n, CEP 52071-900, Recife-PE, Brasil.

⁴Universidade Federal Rural de Pernambuco, Depto. de Química, Rua Dom Manoel de Medeiros, s/n, CEP 52071-900, Recife-PE, Brasil.

⁵Universidade Federal de Pernambuco, Depto. de Botânica, Av. Professor Luiz Freire, 1235, CEP 50670-901, Recife-PE, Brasil.

Abstract: Zygotic embryos and lateral buds of *Tapeinochilos ananassae* were inoculated into full or half-strength MS medium ($\frac{1}{2}$ MS) containing three antioxidants: ascorbic acid, activated charcoal, and PVP at concentrations of 0.25; 3.0 and 0.5 g.L⁻¹ respectively. The $\frac{1}{2}$ MS medium supplemented with 3.0 g.L⁻¹ activated charcoal resulted in the best embryo establishment and plant development. The lateral buds showed no significant development, an intense phenolic oxidation and high microbial contamination (mainly bacterial). Enzymatic analysis of oxidized lateral buds showed a decline in peroxidase activity and an increase in polyphenoloxidase activity.

Key-words tropical flowers, embryo culture, peroxidase, polyphenoloxidase

Cultura de embriões e gemas laterais de *Tapeinochilos ananassae* (Hassk). K. Schum.

Resumo: Embriões zigóticos e gemas laterais de *Tapeinochilos ananassae* foram inoculados em meio MS ou $\frac{1}{2}$ MS suplementado com três tipos de antioxidantes: ácido ascórbico, carvão ativado e PVP, nas concentrações 0,25; 3,0 e 0,5 g.L⁻¹, respectivamente. O meio $\frac{1}{2}$ MS suplementado com 3,0 g.L⁻¹ de carvão ativado propiciou o melhor estabelecimento dos embriões e o melhor desenvolvimento das plantas. As gemas laterais não apresentaram desenvolvimento significativo e sim uma intensa oxidação fenólica e elevada contaminação microbiana (sobretudo bacteriana). Análises enzimáticas das gemas laterais oxidadas mostraram um decréscimo da atividade da peroxidase e aumento na atividade da polifenoloxidase.

Palavras chave Flores tropicais, cultura de embriões, peroxidase, polifenoloxidase

Introduction

Tapeinochilos ananassae Hassk. K. Schum. (Costaceae) is a tropical flower with high commercial acceptance on the international market due to the brilliant red inflorescence and the spiral form of the stem. The species is a rhizomatous herbaceous perennial, with vegetative stems and leaves arranged in spiral. The inflorescences – located beneath the foliage, emerging directly from the rizome – are formed by rigid bracts rounded texture (Ferrero, 2001).

The low viability of the seeds makes vegetative

propagation its principal form of commercial reproduction, but can facilitate the spread of pests and illnesses among the planting stock (Paiva & Loges, 2005).

The tissue culture techniques can offer important tools to solve problems that limit the growth of this important ornamental culture. In vitro propagation (micropropagation) has been widely applied to produce, in a short time and at any time of the year, a large scale of high quality plantlets, ensuring varietal authenticity (Oliveira et al., 2011). Zygotic embryos and buds have been widely used as explant sources to



Lilia Willadino (Correspondence)



willadino.lilia@gmail.com

initiate in vitro cultures because their juvenile state and totipotency (Grattapaglia & Machado, 1998; Bona et al., 2012). Explant establishment is a crucial step for in vitro culture, but there are serious problems that can occur during this process, including microbial contamination and phenolic oxidation (García-González et al., 2010).

As there is a notable absence of published information about the in vitro culture of *T. ananassae*, the present work evaluated the establishment of different explants types as well as biochemical markers involved in oxidative processes.

Material and Methods

In vitro culture

Lateral buds and zygotic embryos were isolated and cultivated in complete MS (Murashige & Skoog, 1962) or half-strength medium ($\frac{1}{2}$ MS) supplemented with three types of antioxidants: citric acid, activated charcoal or polyvinylpyrrolidone (PVP). Eight different treatments were elaborated ($\frac{1}{2}$ MS; $\frac{1}{2}$ MS + 0.25 g.L⁻¹ acid citric; $\frac{1}{2}$ MS + 3.0 g.L⁻¹ activated charcoal; $\frac{1}{2}$ MS + 0.5 g.L⁻¹ PVP; MS; MS + 0.25 g.L⁻¹ acid citric; MS + 3.0 g.L⁻¹ activated charcoal; MS + 0.5 g.L⁻¹ PVP). 6.5 g.L⁻¹ of agar was added to nutritive media, the pH adjusted to 5.8, and autoclaving at 121 °C (1 atm. pressure) for 20 min. The plants were grown in 20 x 150 mm test tubes containing 10 mL of nutritive media. The cultures were maintained in a growth room at 28±1 °C.

During the first 8 days, the cultures remained in the dark followed by a photoperiodic regime of 16 h (50 μ mol.s.m⁻².s⁻¹). The explants were observed during 30 days to analyze plant development (shoot and root), undeveloped explants, and oxidation. The experimental design was completely randomized with 15 replicates for zygotic embryos and 20 for lateral buds per treatment.

The results obtained were submitted to the variance analysis (ANOVA) and statistical analysis was completed with Assistat-Statistical Assistance Software, version 7.5 beta. The z test was used to analyze proportions of plant, undeveloped explants,

and oxidation, with significance at $\alpha=5\%$. The homogeneity of the microbial contamination was evaluated using the Qui-square test (χ^2), with significant corrections at $\alpha=5\%$ (Vieira, 2003).

Histological analyses

Histological analyses were undertaken of the lateral buds when these failed to show regenerative structures. In order to verify the integrity of the bud tissue, samples were fixed in FAA 50 (Johansen, 1940), cut manually in transversal sections, cleared with 30% sodium hypochlorite, washed in distilled water, and then stained with Safrablau (Kraus & Arduin, 1997). The slides were examined and photographed under an optical microscope (Coleman).

Biochemical analyses

Peroxidase (POD) and polyphenoloxidase (PPO) enzyme activities of lateral buds inoculated into MS medium were evaluated after 7, 14, and 21 days of inoculation. Fresh tissue (0.05 g) was macerated in liquid nitrogen, and 2.5 mL of 0.1 M sodium phosphate buffer pH=6.5 at 0 to 4 °C was added. The extracts were centrifuged for 15 min at 8,000 rpm and the supernatant maintained at -20 °C until the analyses were performed. All analyses were carried out with three replicates: total soluble proteins (Bradford, 1976), peroxidase activity (Vieira & Fatibello-Filho, 1998) and polyphenoloxidase activity (Kar & Mishra, 1976). The data was submitted to polynomial regression analysis and expressed in U.min⁻¹.mg⁻¹ protein.g⁻¹ fresh weight.

Results and Discussion

Establishment of zygotic embryos

After 30 days, the zygotic embryos cultivated in $\frac{1}{2}$ MS supplemented with 3.0 g.L⁻¹ of activated charcoal demonstrated higher leaves and roots number than the others treatments (Table 1). The proportion of plant development in this treatment was 80% (p=80), and presented the lower levels of oxidation, 20% (p=20), and all embryos developed plants (non developed embryos p=0) (Table 2).

Table 1. Leaves and roots numbers and fresh weight of *Tapeinochilos ananassae* on the 30th day of zygotic embryos culture, in ½ MS and MS media with distinct concentration of acid citric, activates charcoal and PVP.

Tabela 1. Número de folhas, raízes e peso fresco de Tapeinochilos ananassae no 30º dia de cultivo de embriões zigóticos em meio ½ MS e MS com distintas concentrações de ácido cítrico, carvão ativado e PVP.

Treatments	Nº leaves	Nº roots	Fresh weight
½ MS	0,40 c	0,40 d	0,39 c
½ MS + 0.25 mg. L ⁻¹ acid citric	0,89 b	1,22 b	0,73 b
½ MS + 3.0 mg. L ⁻¹ activated charcoal	1,41 a	1,81 a	0,79 a
½ MS + 0.5 mg. L ⁻¹ PVP	0,91 b	1,05 b	0,74 ab
MS	0,51 c	-	0,43 c
MS + 0.25 mg. L ⁻¹ acid citric	0,98 b	0,80 c	0,78 a
MS + 3.0 mg. L ⁻¹ activated charcoal	0,74 b	0,80 c	0,73 b
MS + 0.5 mg. L ⁻¹ PVP	0,80 b	0,84 bc	0,75 ab

Means followed by the same letter do not differ by Tukey's test at 5% probability

Médias seguidas da mesma letra não apresentam diferença significativa pelo teste de Tukey a 5% de probabilidade

Table 2. Proportions of formation of plants, oxidation and non developed embryos in different culture media during in vitro establishment of zygotic embryos of *Tapeinochilos ananassae* (n= number of individuals; Z= standard reduced; p(%)= overall proporcion)

Tabela 2. Proporções de formação de plantas, oxidação e embriões não desenvolvidos em diferentes meios de cultura durante o estabelecimento in vitro de embriões zigóticos de Tapeinochilos ananassae (n= número de indivíduos; Z= padrão reduzido; p(%)= proporção geral)

Treatments	Formation of plants			Oxidation		Non developed embryos	
	N	p(%)	Z	p(%)	Z	p(%)	Z
½ MS	15	46.7	-0.512	40	0.105	6.7	1.433
½ MS + 0.25 acid citric (g.L ⁻¹)	14	57.1	1.702	42.9	0.692	0	3.393*
½ MS + 3.0 activated charcoal	15	80.0	6.695*	20	2.885*	0	3.465*
½ MS + 0.5 PVP	15	46.7	-0.512	46.7	1.599	6.7	1.433
MS	15	26.7	3.395*	20	2.885*	40	6.697*
MS + 0.25 acid citric	12	50	0.029	25	1.577	25	1.870
MS + 3.0 activated charcoal	15	46.7	-0.512	33.3	-0.105	13.3	-0.600
MS + 0.5 PVP	15	13.3	6.277*	60	4.589*	26.7	2.632*

* Significant values, considering Z values greater than 1.96 or less than -1.96 (α= 5%)

* *Valores significativos, considerando-se valores de Z superiores a 1,96 ou inferiores a -1,96 (α= 5%)*

The positive effects of activated charcoal are associated with its capacity to adsorb toxic substances, such as phenolic compounds and their degradation products that are liberated by plant tissue during in vitro culture (Cid & Teixeira, 2010). Activated charcoal at 2.5 g.L⁻¹ added in the culture medium increased the germination and the plant growth of *Piper hispidinervum* C. DC. (Guedes et al., 2006) and 2 mg.L⁻¹ could effectively induce large protocorms of *Cimbidium giganteum* (Hossain et al., 2010). Embryos of *Lychnophora pinaster* Mart.

(Souza et al., 2003) likewise better development in half strength MS medium. The reduced concentrations of nutrient in the tissue culture media represent considerable decrease in the osmotic potential (Paiva & Otoni, 2003) and, in particular reduced concentrations of metals such as iron, copper and zinc that are important to prevent the formation of the highly toxic hydroxyl radical via the metal-dependent Haber-Weiss or the Fenton reactions (Mittler, 2002) increasing the susceptibility of the explants to oxidations.

The addition of PVP to the culture media did not result in significant gains in terms of establishment of the zygotic embryos of *T. ananassae*. When PVP was associated with MS medium, a greater number of oxidized ($p=60$) and undeveloped ($p=26.7$) embryos were observed, as well as reduced numbers of plant formation ($p=13.3$). PVP (0.4 g.L^{-1}) did not control oxidation in *Syagrus oleraceae* MART. BECC (Melo et al., 2001). Conversely, both activated charcoal and PVP promote a higher establishment of *Lippia sidoides* Cham. zygotic embryos and their transformation into weel-formed plants eventually need different species to oxidant agents (Costa et al., 2007).

Anatomical aspects of lateral buds and their establishment

No development was observed in any of the treatments used to promote establishment of the lateral buds of *T. ananassae*. The explant showed organogenic potential, the stem apices was composed of undifferentiated cells indicating a potentially functional meristem, the internal tissue of the sheaths show less differentiation than the tissue of external sheath that had functional mature xylem and phloem. The epidermis was composed by only one layer of cells with a thin cuticle, as well as unicellular epidermal hairs (Figure 1A and B).

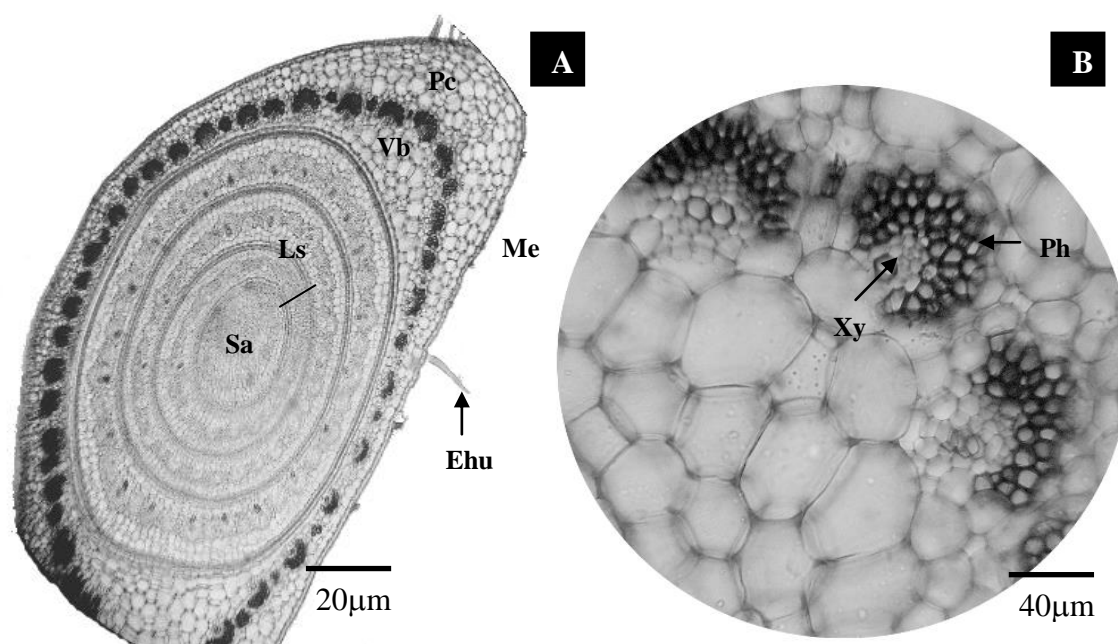


Figure 1. Transversal cut of lateral bud of *Tapeinochilos ananassae*. (A) Overview of the histological section showing stem apex (Sa), leaf sheath (Ls), parenchyma cells (Pc), monostratified epidermis (Me), vascular bundles (Vb) and epidermal hairs unicellular (Ehu); (B) phloem (Pl) and xylem (Xy)

Figura 1. Corte transversal da gema lateral de *Tapeinochilos ananassae*. (A) Seção histológica indicando o ápice caulinar (Ac), bainha foliar (Bf), células do parênquima (Cp), epiderme monoestratificada (Em), feixes vasculares (Fv) e pelos epidérmicos unicelulares (Peu); (B) floema (Fl) e xilema (Xi)

The cultures of lateral buds of *T. ananassae* demonstrated elevated phenolic oxidation levels and microbial contamination, negatively affecting explant development. The lateral buds showed total oxidation of the explants after the period of 20 to 30 days, regardless of the added antioxidant. According to Grattapaglia & Machado (1998) phenolic oxidation may be inherent of the tissues, reducing the effectiveness of any antioxidant used. Lateral buds of *Strelitzia reginae* also demonstrated high levels of oxidation that impeded explant development (North et al., 2010).

Lateral buds from basal branches demonstrated greater frequencies of contamination by fungi (36.2%

of all contaminations) and bacteria (42.5% of all contaminations) with χ^2 values of 18.06 and 29.17 respectively ($p<0.05$). Lateral buds recently formed presented 2.5% and 12.5% contamination for fungi and bacteria respectively. The lateral buds of basal branches generally have irregular and pilose surfaces associated with their less juvenile origin, which makes disinfection more difficult (Pasqual et al., 2010). During in vitro establishment of *Aniba rosaeodora* Ducke, there were lower levels of bacterial and fungal contamination when more recently formed buds were used (Handa et al., 2005).

The specific activity of peroxidase and polyphenoloxidase in lateral buds

During culture of lateral buds, peroxidase activity decreased 26.5% after 7 days, 51.2% after 14 days, and 58.8% after 21 days (Figure 2A). This decrease in peroxidase activity was coincident with the increase oxidation observed in the explants, these tissues did not also demonstrate any organogenic development during the 21 days of culture. In agreement with the results obtained in the present work, Andersen (1986), reported that the low POD activity may be related to the loss of morphogenic potential of *Rhododendron* cells culture, as well as the callus tissue of *Panax ginseng* (Bonfill et al., 2003) and *Hemerocallis* sp (Debiasi et al., 2007).

POD acts on the hydrogen peroxide and phenol (Lima et al., 1998), which are known to induce membranes, proteins and DNA damage. The loss or

decrease in activity of this enzyme can lead to the elevated production of toxic metabolites and subsequent cell program death (Jaleel et al., 2009). POD also plays a role in growth and differentiation, and their high activity could be correlated to the process of differentiation that occurs during shoot or root induction (Díaz-Vivancos et al., 2011) and somatic embryogenesis (Silva, 2010).

Polyphenoloxidase activity presented a discrete decrease after the seventh day, and then continued to fall until the 7th day. At 21 days the activity levels increased to almost three times than observed in recently excised buds (Figure 2B). The elevated PPO activity is directly correlated with quinone polymerization and the darkening of the explant tissue (Huang et al., 2002).

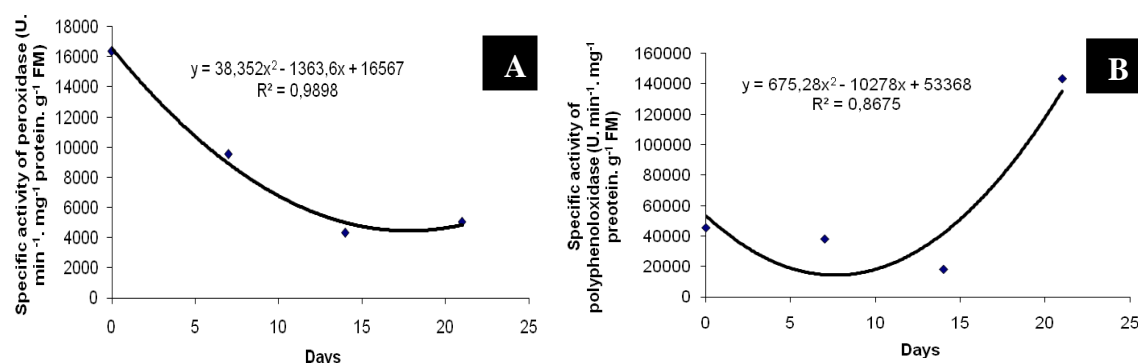


Figure 2. Specific activity of peroxidase (A) and polyphenoloxidase (B) (U.min⁻¹.mg⁻¹ de protein.gm⁻¹ of fresh material) in the lateral buds of *Tapeinochilos ananassae* cultivated in MS medium during 21 days

Figura 2. Atividade específica da peroxidase (A) e polifenoloxidase (B) (U.min⁻¹.mg⁻¹ de proteína.gm⁻¹ de matéria fresca) em gemas laterais de *Tapeinochilos ananassae* cultivadas em meio MS durante 21 dias

In *Tulipa gesneriana* L. cv. Apeldoorn, the elevated polyphenoloxidase activity was accompanied by an increasing degree of oxidation of the tissue (Van Rossum et al., 1997). Likewise, Virginia pine calli showed a lower PPO activity in healthy callus tissue showing low oxidation levels, but its activity was increased in callus under oxidative processes and dark tissue (Tang & Newton, 2004). We observed a gradual darkening of the bud tissue of *T. ananassae* originating in the basal region and extending over time to the entire explant. Darkening of newly formed bud tissue in various bamboo species extended to intact cells, suggesting that the autolysis of injured cells (resulting from the excision of the explants) could provoke autolysis of non-injured neighboring cells (Huang et al., 2002).

Conclusions

The zygotic embryos could be used successfully in the in vitro establishment of *Tapeinochilos ananassae*. The peroxidase and polyphenoloxidase can be used as biochemical markers of organogenesis and phenolic oxidation in lateral buds of *T. ananassae*.

Acknowledgements

The authors would like to thank Maria do Carmo F. Teixeira, Fazenda Mumbecas Flores Tropicais Ltda., Paulista, Pernambuco, Brazil, for supplying plants. E-mail: mariadocarmo@florestropicais.com.br

Literature Cited

- Andersen, W.C.A. A revised medium for shoot multiplication of *Rhododendron*. Journal American American Society Horticultural Science, v.109, p.343-347, 1986.
- Bona, C.M.; Santos, G.D.; Biasi, L.A. *Lavandula* calli induction, growth curve and cell suspension formation. Revista Brasileira de Ciências Agrárias, v.7, n.1, p.17-23, 2012. <http://www.agraria.pro.br/sistema/index.php?journal=agraria&page=article&op=view&path%5B%5D=agraria_v7i1a1121&path%5B%5D=1050> 23 Abr. 2012. doi: 10.5039/agraria.v7i1a1121
- Bonfill, M.; Cusidó, R.M.; Palazón, J.; Canut, E.; Piñol, T., Morales, T. Relationship between peroxidase activity and organogenesis in *Panax ginseng* calluses. Plant Cell, Tissue and Organ Culture, v.73, p.37-41, 2003. <www.springerlink.com/index/U8221N6453570410.pdf> 11 Nov. 2011. doi: 10.1023/A:1022615112745
- Bradford, M.M. A rapid and sensitive method for the quantization of microgram quantities of protein utilizing the principle of protein-dye binding. Analytical Biochemistry, v.72, p.248-254,

1976. <www.ciens.ucv.ve:8080/generador/sites/lab-bioq.../Bradford%201976.pdf> 16 Out. 2010.
- Cid, L.P.B.; Teixeira, J.B. Oxidação fenólica, vitrificação e variação somaclonal. In: Cid, L.P.B. (Ed.). Cultivo in vitro de plantas. Brasília- DF: Embrapa Informação Tecnológica, 2010. p. 51-66.
- Costa, A.S.; Arrigoni-Blank, M.F.; Blank, A.F.; Mendonça, A.B.; Amancio, V.F. Ledo, A.S. Estabelecimento de alecrim-pimenta in vitro. Horticultura Brasileira, v.25, p.68-72, 2007. <www.scielo.br/pdf/hb/v25n1/a13v25n1.pdf> 11 Nov. 2011.
- Debiasi, C.; Fráguas, C.B.; Lima, G.P.P. Estudo das poliaminas na morfogênese in vitro de *Heimerocallis* sp. Ciência Rural, v.37, n.4, p.1014-1020, 2007. <http://www.scielo.br/scielo.php?pid=S0103-84782007000400015&script=sci_arttext> 04 Fev. 2012. doi: 10.1590/S0103-84782007000400015
- Diáz-Vivancos, P.; Majourhat, K.; Fernández, J.A.; Hernández, J.A.; Piqueras, A. Study of the antioxidant enzymatic system during shoot development from cultured intercalary meristems of saffron. Plant Growth Regulation, v.65, p.119-126, 2011. <<http://www.springerlink.com/content/n01958g182430461/>> 03 Mar. 2012. doi: 10.1007/s10725-011-9581-2
- Ferrero, M. D. The genus *Tapeinochilos* from New Guinea: lifting the veil on the least know member of Costaceae. The Bulletin of Heliconia Society, Janeiro, p.5-10, 2001.
- García-González, R.; Quiroz, K.; Carrasco, B.; Caligari, P. Plant tissue culture: Current status, opportunities and challenges. Ciência e Investigación Agraria, v.37, n.3, p.5-30, 2010. <<http://www.scielo.cl/pdf/ciagr/v37n3/art01.pdf>> 18 Nov. 2011. doi: 10.4067/S0718-16202010000300001
- Guedes, R.S.; Schmitz, G.C.; Maciel, S.A.; Oliveira, J.P.; Pereira, J.E.S. Avaliação da germinação de sementes e do desenvolvimento inicial de plantas de pimenta longa in vitro. In: 46º Congresso Brasileiro de Olericultura, 2006, Goiânia. Anais... Goiânia: Horticultura Brasileira, 2006. suplemento, CD Rom, p.41-44.
- Grattapaglia, D.; Machado, M.A. Micropropagação. In: Torres, A.C.; Caldas, L.S.; Buso, J.A. (Eds.). Cultura de tecidos e transformação de plantas. Brasília: EMBRAPA-SPI/EMBRAPA-CNPq, 1998.
- Handa, L.; Sampaio, P.T.; Quisen, R.C. Cultura in vitro de embriões e de gemas de mudas de pau-rosa (*Aniba rosaedora* Ducke). Acta Amazonica, v.35, p.29-33, 2005. <http://www.scielo.br/scielo.php?script=sci_arttext&pid=S0044-59672005000100005&lng=en&nrm=iso> 12 Nov. 2011. doi: 10.1590/S0044-59672005000100005
- Hossain, M.M.; Sharma, M.; Silva, J.M.T.; Pathak, P. Seed germination and tissue culture of *Cymbidium giganteum* Wall. ex Lindl. **Scientia Horticulturae**, v.123, n.4, p.479-487, 2010. <<http://www.sciencedirect.com/science/article/pii/S030442380900466X>> doi: 10.1016/j.scienta.2009.10.009
- Huang, L.; Lee, Y.; Huang, B.; Kuo, C.; Shaw, J. High polyphenol oxidase activity and low titratable acidity in browning bamboo tissue culture. In Vitro Cell Development of Biology, v.38, p.358-365, 2002. <<http://www.springerlink.com/content/3025531862147404/>> 11 Nov. 2011. doi: 10.1079/IVP2002298
- Jaleel, C.A.; Riagh, K.; Gopi, R.; Manivannan, P.; Inès, J.; Al-Juburi, H.J.; Chang-Xing, Z.; Hong-Bo, S.; Panneerselvam, R. Antioxidant defense responses: physiological plasticity in higher plants under abiotic constraints. Acta Physiologiae Plantarum, v.31, p.427-436, 2009. <<http://www.springerlink.com/content/v450n230368957v5/fulltext.pdf>> 04 Dez. 2011. doi: 10.1007/s11738-009-0275-6
- Johansen, D.A. Plant Microtechnique. New York: McGraw Hill, 1940.
- Kar, M.; Mishra, D. (1976), Catalase, peroxidase, and polyphenoloxidase activities during rice leaf senescence. Plant Physiology, v.57, p.315-319, 1976. <<http://www.plantphysiol.org/content/57/2/315.full.pdf+html>> 23 Jul. 2010. doi: 10.1104/pp.57.2.315
- Kraus, J.E.E.; Arduin, M. Manual básico de métodos em morfologia vegetal. Rio de Janeiro: EDUR, 1977.
- Lima, G.P.P.; Broetto, F.; Brasil, O.G. Efeito da salinidade sobre o teor de proteínas e atividades da peroxidase e redutase de nitrato em calos de arroz. Acta Biologica Leopoldensia, v.20, p.357-363, 1998.
- Melo, B.; Pinto, J.E.B.P.; Luz, J.M.Q.; Peixoto, J.R.; Juliatti, F.C. Diferentes antioxidantes no controle da oxidação, germinação e desenvolvimento das plântulas na cultura in vitro de embriões da guarirôbeira [*Syagrus oleracea* (MART.) BECC.]. Ciência e Agrotecnologia, v.25, p.1301-1306, 2001. <www.editora.ufla.br/site_adm/upload/revista/25-6-2001_06.pdf> 21 Out. 2011.
- Mittler, R. Oxidative stress, antioxidants and stress tolerance. Trends in Plant Science, v.7, p.405-410, 2002. <<http://download.cell.com/trends/plant-science/pdf/PIIS1360138502023129.pdf>> 21 Out. 2011. doi: 10.1016/S1360-1385(02)02312-9
- Murashige, T.; Skoog, F. A revised medium for rapid growth and bioassays with tobacco tissue culture. Physiologia Plantarum, v.15, p.473-497, 1962. <<http://onlinelibrary.wiley.com/doi/10.1111/j.1399-3054.1962.tb08052.x/pdf>> 12 Set. 2011. doi: 10.1111/j.1399-3054.1962.tb08052.x
- North, J.J.; Ndakidemi, P.A.; Laubscher, C.P. The potential of developing na in vitro method for propagation Strelitziaceae. African Journal of Biotechnology, v.9, n.45, p.7583-7588, 2010. <<http://www.academicjournals.org/ajb/pdf/pdf2010/8Nov/North%20et%20al.pdf>> 18 Nov. 2011.
- Oliveira, J.R.G.; Morais, T.A.L.; Melo, N.F.; Yano-Melo, A.M. Acclimatization of *Tapeinochilos ananassae* plantlets in association with arbuscular mycorrhizal fungi. Pesquisa Agropecuária Brasileira, v.46, n.9, p.1099-1104, 2011. <<http://www.scielo.br/pdf/pab/v46n9/46n09a18.pdf>> 04 Fev. 2012. doi: 10.1590/S0100-204X2011000900018
- Paiva, W.O.; Loges, V. Costaceae. In: Terao, D.; Carvalho, A.; Barroso, A. (Eds.). Flores Tropicais. Brasília: EMBRAPA-STI, 2005.
- Paiva Neto, V.B.; Otoni, W.C. Carbon sources and their osmotic potential in plant tissue culture: does it matter? Scientia Horticulturae, v.97, p.193-202, 2003. <<http://www.sciencedirect.com/science/article/pii/S0304423802002315>> 15 Nov. 2011. doi: 10.1016/S0304-4238(02)00231-5
- Pasqual, M.; Dutra, L.F.; Araújo, A.G.; Pereira, A.R. Prevenção de contaminações microbianas na cultura de células, tecidos e órgãos de plantas. In: Scherwinski-Pereira, J.E. (Ed.). Contaminações microbianas na cultura de células, tecidos e órgãos de plantas. Brasília- DF: Embrapa Informação Tecnológica, 2010. p. 61-161.
- Silva, M.M.A. Embriogênese somática direta e indireta em cana-de-açúcar: busca de correlações com o estresse in vitro. Recife: Universidade Federal de Pernambuco, 2010. 74p. Dissertação Mestrado.
- Souza, A.V.; Pinto, J.E.B.P.; Bertolucci, S.K.V.; Corrêa, R.; Castro, E.M. Germinação de embriões e multiplicação in vitro de

Lychnophora pinaster Mart. Ciência e Agrotecnologia, Edição especial, p.1532-1538, 2003. <<http://www.sumarios.org/resumo/germina%C3%A7%C3%A3o-de-embri%C3%B5es-e-multiplica%C3%A7%C3%A3o-vitro-de-lychnophora-pinaster-mart>> 12 Nov. 2011.

Tang, W.; Newton, R.J. Increase of polyphenol oxidase and decrease of polyamines correlate with tissue browning in Virginia pine (*Pinus virginiana* Mill.). Plant Science, v.167, p.621-628, 2004. <<http://www.sciencedirect.com/science/article/pii/S016894520400216X>> 15 Nov. 2011. doi: 10.1016/j.plantsci.2004.05.024


Van Rossum, M.W.P.C.; Alberda, M.; Van Der Plas, L.H.W. Role

of oxidative damage in tulip bulb scale micropropagation. Plant Science, v.130, p.207-216, 1997. <<http://www.sciencedirect.com/science/article/pii/S016894529700215X>> 12 Nov. 2011. doi: 10.1016/S0168-9452(97)00215-X

Vieira, I.C.; Fatibello-Filho, O. Flow injection spectrophotometric determination of hydrogen peroxide using a crude extract of zucchini (*Cucurbita pepo*) as a source of peroxidase. Analyst, v.123, n.9, p.1809-1812, 1998. <<http://pubs.rsc.org/en/Content/ArticleLanding/1998/AN/a803478h>> 12 Nov. 2011. doi: 10.1039/A803478H

Vieira, S. Bioestatística: tópicos avançados. Rio de Janeiro: Editora da UFRJ, 2003.

Influence of Anthropometry on the Kinematics of the Cervical Spine in Frontal Sled Tests

Christoph Dehner MD¹, Wolfram Hell MD², Michael Kraus MD³, Götz Röderer MD¹, Michael Kramer MD¹

¹ Department for Trauma, Hand, Plastic and Reconstructive Surgery, University of Ulm, Albert-Einstein-Allee 23, 89081 Ulm, Germany

² Institute for Legal Medicine, Ludwig Maximilians University of München, Nussbaumstr. 26, 80336 München, Germany

³ Institute for Medical Rehabilitation Research, University of Ulm, Wuhrstr. 2/1, 88422 Bad Buchau, Germany

Abstract

Objective: The objective of this study was to investigate the influence of anthropometric factors on the kinematics of the cervical spine during in-vivo frontal collisions.

Methods: Therefore a frontal collision with a mean velocity change (ΔV) of 10.2 km/h was simulated in a sled test with ten healthy volunteers (seven men and three women). A high-speed camera was used to document motion data. Acceleration data were recorded using accelerometers. The study analyzed the association of anthropometric factors with defined kinematical characteristics.

Results: A smaller neck circumference led to an earlier peak of the dorsal horizontal head acceleration ($r=0.602$), an earlier beginning of the ventral head translation ($r=0.742$) and a greater maximal head flexion ($r=-0.717$). A smaller body weight led to a later beginning of the head flexion acceleration ($r=-0.713$) and a greater maximal head flexion ($r=-0.620$). With a smaller thorax circumference the beginning of the dorsal horizontal head acceleration ($r=0.623$), the peak of the head flexion acceleration ($r=0.756$) and the peak of the head extension acceleration ($r=0.679$) were reached earlier.

Conclusions: The main findings of the present study consist in the identification of relevant anthropometric parameters (neck and thorax circumference and body weight) on the cervical spine kinematics. Specific anthropometric factors increasing the risk of injury could not be identified. The head movement is mainly associated with the neck circumference and the body weight. The onset and occurrence of the acceleration parameter is mainly associated with the thorax circumference.

Keywords

frontal impact, anthropometric factors, head-neck kinematics, volunteer sled tests, whiplash

Introduction

The neck kinematics has been investigated in detail in numerous sled tests [1-4] mainly for rear-end collisions. These studies have shown that the kinematics of the cervical spine is dependent on various external influence factors, like the crash impulse, the acceleration and velocity change [5-7] and the seat and head restraint properties [1,8].

Also the influence of anthropometric factors was increasingly recognized. Epidemiological studies have found that women suffer whiplash more frequently than men [8,9]. A comprehensive study by Siegmund et al. [10] investigated the influence of individual anthropometric factors on the kinematical reaction and risk of injury during simulated rear collisions. They could show in a kinematics study that some kinematic parameters concerning the peak

amplitude and time-to-peak-amplitude of the head acceleration and head motion varied significantly with anthropometric parameters.

Although the accident mechanism operating during frontal collisions has been investigated in the last fifteen years in more detail [11-13], the influence of occupant anthropometry on the physical response of vehicle occupants in frontal collisions is mainly unknown. Links for the relevance of anthropometric influence parameters can be found in two former studies. Knox et al. [14] investigated indirectly the seat belt and air bag effect in high speed frontal crashes using mathematical dynamic modelling software. They found that that a properly timed air bag deployment reduced injury potential for all occupants of all sizes, but that the magnitude of this benefit was dependent on anthropometry. In another



Christoph Dehner (Correspondence)



christoph.dehner@uniklinik-ulm.de



0049 731-500-0

computer based model Armstrong et al. [15] found that the occupant posture was the most significant parameter affecting the overall risk of injury in frontal collisions.

As the first part of this study has investigated the muscle activity influence on the kinematics of the cervical spine [13], the second part of this study aimed to investigate the influence of anthropometric characteristics on the kinematics of the cervical spine during a frontal sled crash test. Ideally this information should serve as helpful hint in identifying possible anthropometric characteristics leading to an increased risk of injury during frontal collisions.

Methods

Subjects

The test procedure is analogous to the already for publication accepted article investigating the muscle activity influence on the kinematics of the cervical spine [13]. The work has been approved by the ethical committee of the University of Ulm. The subjects gave informed consent to participate in the study. Ten subjects (seven men, three women) aged 20 to 47 years (median: 35 years) without prior structural injuries to the spine participated in the study. Exclusion criteria were a history of whiplash injury of the cervical spine, neurological or psychiatric disease, functional impairments of the cervical spine or cervical spine pain.

Prior to the sled tests, subjects underwent clinical examination with determination of individual maximal cervical spine mobility. As anthropometric characteristics the head measurement (head circumference), the neck measurements (neck length and circumference) and the body measurements (thorax circumference, body height, seated height and body weight) were determined (see Table 1).

Experimental Design

For the frontal collision simulation we used a standard automobile seat (VW Passat, 1997 model, VW corporation, Wolfsburg, Germany) anchored to a target sled platform (see Figure 1). The seat sled was accelerated over a length of 20 meters towards the fixed iron barrier. Measurement of the sled acceleration was performed using a sensor (Endevco 2262, +/- 200g, uniaxial x-direction, CFC 60, Endevco Corporation, San Juan Capistrano, USA). The sled acceleration is characterized by a trapezoid impulse. The change of speed Δv was calculated by integration on the basis of the CFC180 filtered sled acceleration. The mean acceleration of the seat sled was 2.68 g (2.45-3.27 g), the mean duration of acceleration was 106 ms (100-112 ms) and the mean velocity change was 10.2 km/h (9.9-12.7 km/h).

An H-point dummy was used for seat adjustment and a 25° backrest angle was ensured before each test. After positioning the subjects on the test sled, head restraints were adjusted so that the upper edge of the head restraint was aligned with the vertex of the head of each subject (see Figure 1). A horizontal adjustment was not possible. The initial horizontal distance from the head to the head restraint ranged from 40 to 90 mm (median 60 mm). In addition, all subjects were secured with a three-point seat belt in passenger position. It is made up of a lap belt with buckle and a shoulder belt, which is adjusted to fit the subjects. The seat belt is equipped with a webbing-sensitive retractor that stops the belt from extending off the reel during severe deceleration. The subjects were then instructed to sit in the target sled without changing their initial position until the impact has been occurred and to stay in the target sled until the test has been fully completed.

Measurement Technique, Data Recording and Processing

The data mentioned below were recorded for all subjects from -800 ms to +800 ms, with "0" defining the time of the trigger signal, at the moment of the initial contact between the sled and the barrier. Data recording and processing according to SAE J211/1 (SAE 1995) was performed with Diadem® 8.0 (National Instruments Germany GmbH, Munich, Germany).

Motion Data

The experiments were recorded with a stationary LOCAM high speed camera (Visual Instrumentation Corporation, USA) and subsequent digitized with 100 images/s for the first 300 ms. The motion data were documented based on markings of the centre of gravity of the head, which is defined as the surface projection ca. 1.5 cm ventrally and cranially to the most cranial point of the external acoustic meatus [16,17], the Frankfort-plane (defined as the inferior margin of the osseous orbit and the upper margin of the external acoustic meatus) and the first thoracic vertebra. The target coordinates were all expressed in a sled-related coordinate system (x-axis (positive forwards), the y-axis (positive to the left) and the positive z-axis extends perpendicularly upwards). The data were further smoothed prior to further processing, using a third order spline which was least square error optimized. The relative horizontal head motion is calculated by the difference between the head and T1 motion in x-direction.

Accelerations

To measure the angular head acceleration a rotation rate sensor (Endevco 7302, up to 5000 rad/s², piezoresistive, CFC1000 (Endevco Corporation, San Juan Capistrano, USA)) was fixed in a position close to the projected centre of gravity of the head. The angular acceleration cannot be used in the form of

raw data, as individual values of more than 1300 rad/s² appeared as spikes in the curve. Moving average smoothing was applied across 20 values.

In order to measure the T1 acceleration, a two-axial linear accelerometer (Endevco 7264, +/- 200 g, CFC180 (Endevco Corporation, San Juan Capistrano, USA)) was mounted on a pliable metal plate, which was padded with tape, adjusted to the contour of the subject's back and attached directly to the skin above the spinal process of the first thoracic vertebra. The starting position of the T1 sensor above the spinal process of the first thoracic vertebral body defined the sensor-related coordinate system. The positive x-axis pointed in ventral direction, perpendicular to the body surface, and the positive z-axis, which was perpendicular to the x-axis pointed in cranial direction. Zero compensation was performed when the measurement was recorded, which reduced the gravity component to 0.

The measurement of the horizontal head acceleration was performed using a three-axial linear accelerometer MSC 123 sensor (+/- 100 g, CFC1000 (Micro-epsilon Messtechnik GmbH & Co. KG, Ortenburg, Germany)). The accelerometer was attached to the subject via a head harness with which the sensor could be positioned as close as possible to the projected centre of gravity of the head. Analogue to the motion data the anatomical head coordinate system was based on the Frankfort-plane. The relative acceleration between the head and T1 in x-direction was calculated from these accelerations. The maximal seat belt effect was defined by maximal negative peak of the thoracic acceleration.

Analysis

The analysis of the motion and acceleration curves was performed descriptively. Generally, the start of acceleration or motion was defined as the time at which 10% of the subsequent maximum/minimum was reached or the zero-crossing when a change of sign occurred. The following biomechanically relevant parameters of the motion and acceleration curves were ascertained chronologically and assigned to the kinematic phases (latency phase, translation phase, flexion phase, rebound phase) (see definition in Table 2 and 3).

The Spearman rank correlation coefficients (r) are used for the explorative analysis of the associations. If the coefficients are above +/-0.6, they are presented. Normally values under -0.5/-0.6 and above 0.5/0.6 are counted as statistical clearly recognizable correlation. Unfortunately standard guidelines in the literature don't exist. As the thresholds are floating and the number of cases investigated in this study is relatively small, we decided to choose the higher threshold with 0.6. No multivariate analysis is performed because of the small sample size. Thus,

the calculated significance values without Bonferroni adjustment should only be seen as an indication of associations.

Results

Analysis of the motion and acceleration parameters

The curve progression of the motion and acceleration parameters was reproducible for each individual subject (see Table 4 and 5, Figure 2). In the latency phase (0ms-44ms) the head remained in its initial position. The head flexion acceleration started after 31ms (21-46ms). In the translation phase (44ms-68ms) the ventral head translation began without a rotational component 44ms (25ms-64ms). The dorsal horizontal head acceleration started after 49ms (26-75ms). In the flexion phase (68ms-196ms) the isolated translational motion was followed by the initiation of ventral flexion of the head after a median of 68ms (60ms-80ms). The maximal braking effect of the seat belt occurred after a median of 90ms (81ms-99ms). Furthermore the head flexion acceleration reached its maximum (median: 177rad/s², 110-377rad/s²) after a median of 96ms (73ms-138ms) and the maximal dorsal horizontal head acceleration (median: 5.0g, 4.1-6.2g) after a median of 106ms (97ms-134ms). This was followed by the events of maximal head extension acceleration (median: 260rad/s², 231-425rad/s²) after a median of 149ms (144ms-164ms) and the minimum of dorsal horizontal head acceleration (median: 1.2g, 0.4-1.7g) after a median of 156ms (143ms-168ms). After a median of 196ms (175-233ms) the maximal ventral head translation was reached (median: 112mm, 62-132mm) during the rebound phase (196ms-300ms). Furthermore the head reached the maximal head flexion (median: 36.2°, 21.2-48.2°) after a median of 223ms (192-239ms).

Association between anthropometry and kinematics

Angular head movement

A smaller body weight ($r=-0,620$) and a smaller neck circumference ($r=-0,717$) led to a greater maximal head flexion (see Table 6).

Relative horizontal head movement

A smaller neck circumference ($r=0,742$) was associated with an earlier beginning of the ventral head movement (see Table 6). Concerning the movement amplitudes no association to the anthropometric data could be found.

Angular head acceleration

The smaller the body weight, the later the head flexion acceleration began ($r=-0,713$) (see Table 6). With a smaller body height ($r=0,622$) and a smaller thorax circumference ($r=0,756$) the maximal head flexion acceleration was reached earlier. With a

smaller thorax circumference also the maximal head extension acceleration ($r=0,679$) was reached earlier. Concerning the acceleration amplitudes no association to the anthropometric data could be found.

Relative horizontal head acceleration

A smaller thorax circumference led to an earlier beginning of the dorsal horizontal head acceleration ($r=0,623$) (see Table 6). With a smaller neck circumference the maximal dorsal horizontal head acceleration was reached earlier ($r=0,602$). Concerning the acceleration amplitudes no association to the anthropometric data could be found.

Discussion

The present study was conducted in order to elucidate the associations between anthropometric factors and kinematical characteristics of frontal collisions. Sled tests with human subjects have not, to date, been adequately employed in describing the kinematical processes occurring during frontal collisions. Previous studies have in most cases failed to provide an exact characterization of the biomechanical mechanisms [18,19]. It has simplifying been assumed that a hyperflexion movement of cervical spine occurs during crashes of this kind. Evidence that the kinematical reaction of the cervical spine is more complex than initially assumed has been provided by the study findings which are already accepted for publication [13].

In summary the kinematical analysis shows that a ventral translation movement begins at about 40ms, followed at about 70ms by a flexion movement. No significant dorsal translation or extension movement was observed. The study by Kumar et al. [12], which did not report movement data, documented the onset of head acceleration after 35.6ms with a mean sled acceleration of 1.4g. These data approximate findings of the present study regarding the onset of ventral head angle acceleration (31ms) and of dorsal horizontal acceleration of the head relative to T1 (49ms).

Unlike rear collisions the head-to-headrest distance is not associated with any effect on cervical spine kinematics [20,21]. Beside sled acceleration and change in velocity of the test sled, the restraint provided by the seat belt represents an important external parameter. For example, Siegmund et al. [22] found that maximum motion and acceleration values differed widely in relation to anchoring and tension of the seat belt. In their study, lax belt slack was associated with an increase in both ventral thorax movement and ventrally directed acceleration amplitudes.

Most correlations between the kinematics and the anthropometric factors have been found for the neck and thorax circumference and the body weight. Head circumference and neck length, however, were not found to affect cervical spine kinematics. By contrast, it was these characteristics that were shown to be the crucial parameters affecting cervical spine kinematics in rear-end collisions [10]. This difference could be explained by the different kinematic characteristics in frontal and rear-end collisions. As the kinematics in rear-end collisions are characterized by an initial extension and subsequent flexion of the head relative to the cervical spine the existing rotational movement plays an important role. Probably this rotational movement of the head relative to the cervical spine is getting greater, with a greater head circumference and neck length. In contrast to that these influence factors are less important in frontal collisions with an isolated flexion movement of the head.

Neck circumference correlates primarily with head movement. Smaller neck circumferences are associated with an earlier onset of ventral head translation relative to T1. This could be explained by the fact that a smaller neck circumference could be associated with less tissue resistance and therefore results in an earlier beginning of the relative movement and acceleration between the head and T1. Another possible explanation could be the fact that a smaller neck circumference leads to a better measurable differentiation between the head and T1 position in horizontal direction and therefore is simply a metrological phenomenon. Smaller neck circumferences are further associated with the development of a greater flexion amplitude. This may be explained by the fact that a smaller neck circumference could be associated with less muscle tissue, which in turn could lead to less active muscle resistance to the flexion movement. Furthermore a smaller body weight was associated with greater flexion amplitude but a later beginning of the head flexion acceleration. It is conceivable, that greater flexion amplitude could lead to a higher risk of injury, but this assumption couldn't be proved in this investigation.

Smaller thorax circumference is associated with the earlier onset of the dorsal horizontal acceleration and the occurrence of the maximal head flexion and extension acceleration. This means that, with smaller thorax circumferences, there is a more rapid change in the forces of acceleration operating on the body, resulting in a larger impulse. This may be explained by the fact that, with increasing thorax circumference – and probably an increasing body weight –, there is increasing delay in the onset of the maximal seat belt effect. Although this assumption is the most reasonable, it couldn't be directly proved in this investigation.

One limitation of the study is the small number of subjects, which makes it difficult to achieve statistically strong data. Up to now comparison studies of the influence of anthropometric parameters on cervical spine kinematics in frontal collisions have not been published in the literature. Hence, the findings of the present study should be considered pilot data requiring targeted evaluation in further kinematical studies. As further limitation the test setting represents only approximately the real crash situation. As the subjects are prepared for the upcoming crash event, cervical spine kinematics may be altered by pre-activated muscular influence. Concerning the risk of injury it is not possible to definitively determine which anthropometric factor is associated with an increased risk of injury, as multiple factors are involved in the kinematical response of the subjects.

The main findings of the present study consist in the identification of relevant anthropometric parameters (neck and thorax circumference and body weight). A smaller neck circumference and a smaller body weight are associated with greater flexion amplitude. A smaller thorax circumference is associated with an earlier onset of the dorsal horizontal acceleration, the head flexion acceleration and the head extension acceleration, which could be summarized in resulting in a larger impulse to the torso during the frontal impact. These parameters are distinct from those relevant in rear-end collisions (head circumference and neck length), which could be explained by the different kinematic characteristics in frontal and rear-end collisions.

Acknowledgements

The experiments comply with the current laws of Germany and were performed with approval of the local ethics board.

References

1. Watanabe Y, Ichikawa H, Kayama O, Ono K, Kaneoka K, Inami S (2000) Influence of seat characteristics on occupant motion in low-speed rear impacts. *Accid Anal Prev* 32 (2):243-250
2. Blouin JS, Descarreaux M, Belanger-Gravel A, Simoneau M, Teasdale N (2003) Attenuation of human neck muscle activity following repeated imposed trunk-forward linear acceleration. *Exp Brain Res* 150 (4):458-464
3. Kaneoka K, Ono K, Inami S, Hayashi K (1999) Motion analysis of cervical vertebrae during whiplash loading. *Spine* 24 (8):763-769
4. Mühlbauer M, Eichberger A, Geigl B, Steffan H (1999) Analysis of Kinematics and acceleration behavior of the head and neck in experimental rear-impact collisions. *Neuro-Orthopedics* 25 (1):1-17
5. Siegmund GP, Heinrichs BE, Chimich DD, DeMarco AL, Brault JR (2005) The effect of collision pulse properties on seven proposed whiplash injury criteria. *Accid Anal Prev* 37 (2):275-285
6. Bostrom O, Fredriksson R, Haland Y, Jakobsson L, Krafft M, Lovsund P, Muser MH, Svensson MY (2000) Comparison of car seats in low speed rear-end impacts using the BioRID dummy and the new neck injury criterion (NIC). *Accid Anal Prev* 32 (2):321-328
7. Brell E, Veidt M, Daniel W (2001) Influence of deceleration profiles on occupant velocity differential and injury potential. *Int J Crashworthiness* 6 (4):605-620
8. Jakobsson L, Lundell B, Norin H, Isaksson-Hellman I (2000) WHIPS--Volvo's Whiplash Protection Study. *Accid Anal Prev* 32 (2):307-319
9. Farmer CM, Wells JK, Werner JV (1999) Relationship of head restraint positioning to driver neck injury in rear-end crashes. *Accid Anal Prev* 31 (6):719-728
10. Siegmund GP, Heinrichs BE, Wheeler JB (1999) The influence of head restraint and occupant factors on peak head/neck kinematics in low-speed rear-end collisions. *Accid Anal Prev* 31 (4):393-407
11. Matsushita T, Sato TB, Hirabayashi K, Fujimura S, Asazuma T, Takatori T X-Ray study of the human neck motion due to head inertia loading. In: SAE technical paper series SoAE (ed) 37th Stapp Car Crash Conference, Fort Lauderdale, USA, 1994. pp 55-64
12. Kumar S, Narayan Y, Amell T (2003) Analysis of low velocity frontal impacts. *Clin Biomech (Bristol, Avon)* 18 (8):694-703
13. Dehner C, Schick S, Kraus M, Scola A, Hell W, Kramer M (2012) Muscle Activity Influence on the Kinematics of the Cervical Spine in Frontal Tests. *Traffic Injury Prevention* (accepted for publication). doi:DOI:10.1080/15389588.2012.734937
14. Knox JJ, Beilstein DJ, Charles SD, Aarseth GA, Rayar S, Treleven J (2006) Changes in head and neck position have a greater effect on elbow joint position sense in people with whiplash-associated disorders. *Clin J Pain* 22 (6):512-518
15. Armstrong B, McNair P, Taylor D (2008) Head and neck position sense. *Sports Med* 38 (2):101-117
16. Clauser CE, Mc Conville JT, Young JM (1969) Weight, volume, and centre of mass of segments of the human body. Technical Report AMRL-TR edn.,
17. Mc Conville JT, Churchill TD, Kaleps I, Clauser CE, Cuzzi J (1980) Anthropometric Relationships of Body and Body Segment Moments of Inertia., Technical Report AMRL-TR edn.,
18. Kullgren A, Krafft M, Nygren A, Tingvall C (2000) Neck injuries in frontal impacts: influence of crash pulse characteristics on injury risk. *Accid Anal Prev* 32 (2):197-205
19. Larder DR, Twiss MK, Mackay GM Neck injury to car occupants using seat belts. In: 29th Ann Proc Am Assoc Auto Med, Washington, USA, 1995. pp 153-165
20. Riemann BL, Myers JB, Lephart SM (2002) Sensorimotor system measurement techniques. *J Athl Train* 37 (1):85-98
21. Walz F (1994) Biomechanical aspects of injuries of the cervical vertebrae. *Orthopade* 23 (4):262-267
22. Siegmund GP, Chimich DD, Heinrichs BE, DeMarco AL, Brault JR (2005) Variations in occupant response with seat belt slack and anchor location during moderate frontal impacts. *Traffic Inj Prev* 6 (1):38-43

Figures



Fig. 1: Side view of test sled

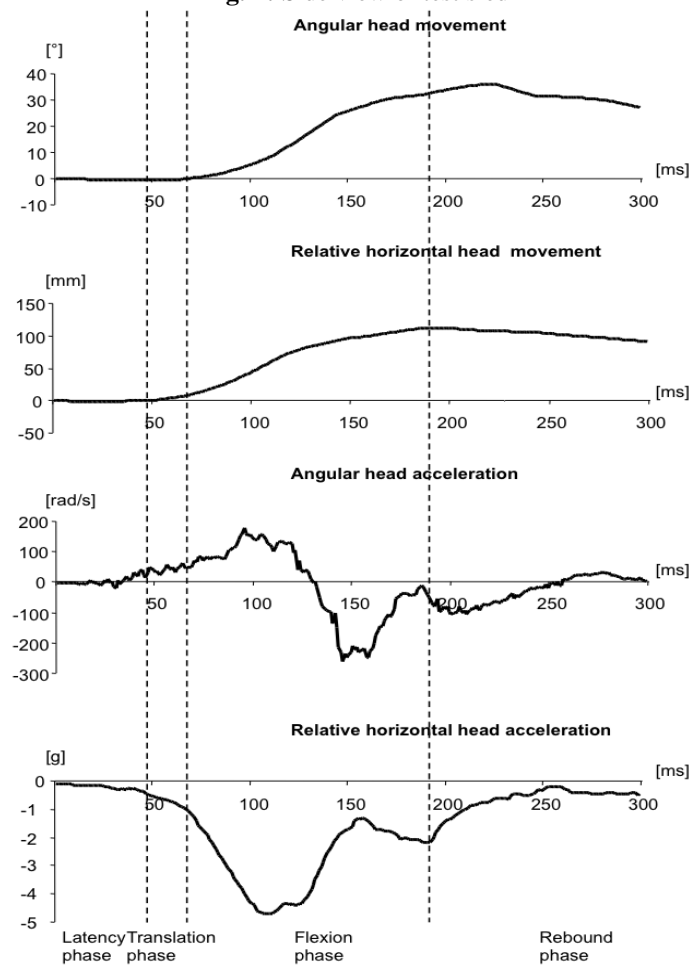


Fig. 2: Mean curves of the motion and acceleration parameters

Table 1: Subjects' anthropometric characteristics

Parameter	Definition	Median	Min	Max
Head measurement				
Head circumference [cm]	Head circumference 1cm parallel cranial to the Frankfurt plane *	58	53	61
Neck measurements				
Neck length [cm]	Distance between the Protuberantia occipitalis externa and C7 in 0° position	16	13	19
Neck circumference [cm]	Average neck circumference on the level of the Protuberantia occipitalis externa and C7	40	26	49
Body measurements				
Thorax circumference [cm]	Thorax circumference on the level of the inferior margin of the sternum	102	80	112
Body height [m]		1.80	1.70	1.91
Seated height [m]		0.92	0.82	1.05
Body weight [kg]		83.5	61.0	110.0

* Frankfurt plane (auriculo-orbital plane): a plane passing through the inferior margin of the left orbit and the upper margin of each ear canal)

Table 2: Definition of the motion phases

Motion phase	Parameter	Definition
Latency phase		
Start	Start of sled acceleration	Trigger signal at sled impact
End	Start of ventral translation	10% of the maximal head translation
Translation phase		
Start	Start of ventral translation	10% of the maximal head translation
End	Start of flexion	10% of the maximal head angle
Flexion phase		
Start	Start of flexion	10% of the maximal of head angle
End	Time of maximal ventral translation	Maximal head translation
Rebound phase		
Start	Time of maximal ventral translation	Maximal head translation
End	Time of maximal flexion	Maximal head angle

Table 3: Definition of the kinematic data and the seat belt effect and the time of occurrence

Parameter	Definition	Phase
Angular head movement		
Beginning of head flexion	10% of maximum	Flexion
Maximal head flexion	Maximum	Rebound
Relative horizontal head movement		
Beginning of ventral head translation	10% of maximum	Translation
Maximal ventral head translation	Maximum	Rebound
Angular head acceleration		
Beginning of head flexion acceleration	10% of maximum	Translation
Maximal head flexion acceleration	Maximal positive peak	Flexion
Beginning of head extension acceleration	Zero crossing	Flexion
Maximal head extension acceleration	Maximal negative peak	Flexion
Relative horizontal head acceleration		
Beginning of dorsal horizontal head acceleration	10% of maximum	Latency
Maximal dorsal horizontal head acceleration	Maximal negative peak	Flexion
Minimal dorsal horizontal head acceleration	Relative minimal negative peak	Flexion
Braking effect of the seat belt		
Maximal thoracic deceleration	Maximal negative peak	Flexion

Table 4: Time of occurrence of the motion and acceleration parameters in [ms]

Parameter	Median	Min	Max	Mean	SD
Angular head movement					
Beginning of head flexion	68	60	80	69	6
Time of maximal head flexion	223	192	239	212	19
Relative horizontal head movement					
Beginning of ventral head translation	44	25	64	43	12
Time of maximal ventral head translation	196	175	233	203	21
Angular head acceleration					
Beginning of head flexion acceleration	31	21	46	32	8
Time of maximal head flexion acceleration	96	73	138	102	21
Beginning of head extension acceleration	131	120	144	131	7
Time of maximal head extension acceleration	149	144	164	152	6
Relative horizontal head acceleration					
Beginning of dorsal horizontal head acceleration	49	26	75	53	16
Time of maximal dorsal horizontal head acceleration	106	97	134	108	10
Time of minimal dorsal horizontal head acceleration	156	143	168	158	7
Seat belt effect					
Time of maximal thoracic deceleration	90	81	99	90	10

The median value, minimum value (min), maximum value (max), mean value (mean) and the standard deviation (SD) are for each parameter presented.

Table 5: Amplitudes of the motion and acceleration parameters

Parameter	Median	Min	Max	Mean	SD
Angular head movement (°)					
Maximal head flexion	36.2	21.2	48.2	35.0	7.1
Relative horizontal head movement (mm)					
Maximal ventral head translation	112	62	132	110	20
Angular head acceleration (rad/s²)					
Maximal head flexion acceleration	177	110	367	207	69
Maximal head extension acceleration	260	231	425	308	82
Relative horizontal head acceleration (rad/s²)					
Maximal dorsal horizontal head acceleration	5.0	4.1	6.2	5.1	0.6
Minimal dorsal horizontal head acceleration	1.2	0.4	1.7	1.1	0.4


The median value, minimum value (min), maximum value (max), mean value (mean) and the standard deviation (SD) are for each parameter presented.

Table 6: Associations of anthropometry with the kinematic data

Parameter	Head circumference	Neck length	Neck circumference	Body height	Seated height	Body weight	Thorax circumference
Angular head movement (°)							
Maximal head flexion	o	o	-0,717	o	o	-0,620	o
Relative horizontal head movement (mm)							
Beginning of ventral head translation	o	o	0,742	o	o	o	o
Angular head acceleration (rad/s²)							
Beginning of head flexion acceleration	o	o	o	o	o	-0,713	o
Time of maximal head flexion acceleration	o	o	o	0,622	o	o	0,756
Time of maximal head extension acceleration	o	o	o	o	o	o	0,679
Relative horizontal head acceleration (rad/s²)							
Beginning of dorsal horizontal head acceleration	o	o	o	o	o	o	0,623
Time of maximal dorsal horizontal head acceleration	o	o	0,602	o	o	o	o

Spearman correlation coefficients $|r| > 0.6$ are presented.

PERCEPTION OF SUITABILITY OF LANDSCAPE FEATURES OF THE LAGOS LAGOON FOR TOURISM BY ITS USERS AND USERS OF LAGOS COASTAL TOURISM VENUES

Uduma-Olugu, N.¹; Okedele, O. S.¹; Adebamowo, M.¹;
Obiefuna, J. N.¹

¹ Department of Architecture, University of Lagos, Lagos

Abstract: The Lagos lagoon is a major geographical feature in Lagos Metropolis and is the largest of the network of lagoons that stretch from the Republic of Benin through to the Nigerian Niger Delta. Some parts of the Lagos lagoon waterfront has degenerated into a slum with non-distinctive housing, mainly shanties at various points, wood processing, sand dredging, markets and commercial fishing activities. Water-based tourism is a proven revenue earner globally, usually providing revenue for the government and a source of enjoyment, employment and recreation to the residents and visitors alike. The tourism potentials of the lagoon remain largely untapped. To determine the place of landscape features of the Lagos Lagoon in its suitability for tourism, the paper evaluates its landscape characteristics and compares the perception of users of water-based recreation destinations along the its waterfront with those of users of similar tourist attractions along the Lagos coast. The aim of the study is to answer questions of landscape perception and assessment of the area and to identify other factors which may be of relevance to its tourism development. Using structured questionnaires with pictures of the landscape features of the lagoon, field survey and interviews, the study identified the communities, problems, and factors influencing tourism at three venues on the lagoon waterfront and three water tourism venues along the Lagos coast. Results show that the landscape characteristics of the lagoon have a very significant effect on tourism in the area. It also identified the major factors influencing the tourism development of the Lagos Lagoon. The outcome of the research will be of benefit to property owners in the area, architects, landscape architects, tourists, visitors, industry practitioners and policy makers in determining appropriate facilities and land-use planning options in developing the natural resource.

Keywords: Landscape assessment and perception, tourism, water-based recreation, suitability and Lagos Lagoon

1.0 Introduction

Due to the location of Lagos State – with Badagry on the west, Lekki in the east, and Lagos Lagoon with an outlet to the sea, Lagos has been the gateway for European contact with the Nigerians on the coast from colonial times (Oshundeyi and Babarinde, 2003). Usually described as the state of aquatic splendor, Metropolitan Lagos is replete with ubiquitous creeks, bays, lagoons, coastlines and breath-taking scenic views; since it consists mostly of water, it therefore has a high capability to benefit from water tourism. There is however, insufficient emphasis on water as a tool for recreation and tourism in Lagos. Instead, water-based sites are largely neglected and they lie fallow and under-utilized (Uduma-Olugu & Oduwaye, 2010). The

existing developed waterfront sites in Lagos do not appear to have adequate infrastructure, nor do they present water-use in ways that are sufficiently appealing to tourists (Uduma-Olugu & Iyagba, 2009b; Uduma-Olugu & Onukwube, 2012).

A place's landscape characteristics determines its character and subsequently, its uses (Gnoth, 1997; Swaffield, 1999). The landscape features and characteristics of the Lagos Lagoon are key to determining the usage of the lagoon. Apart from water which is its main feature, its vegetation, land form, land cover, ecology, human settlement and general scenic quality are major assets in land use and management (Daniel & Boster, 1976). All these affect its usefulness for tourism or recreation. One of



the key indicators of a place's character, is its landscape – comprising not only of the landcover and landscape quality, but also of its very essence which can be captured when the landscape is assessed and evaluated, using pre-determined parameters (Swaffield, 1999). The uniqueness or otherwise of a place can influence tourism. Traditionally, water-based resources, either coastlines or lakes, are important tourism resources (Gunn, 2002). Globally, tourism has been identified as a major revenue source and continues to grow in popularity. In this blooming tourism industry, the Americans, Europeans and Asians are far ahead of Africa (UNWTO, 2011).

Lagoons are fragile ecosystems susceptible to pollution from municipal, industrial and agricultural runoff and the Lagos Lagoon specifically, is under intensified pressure from pollution (Nwankwo, 2004). Major sources of pollution in the lagoon have been identified as: the deposition of raw sewage, wood shaving, refuse and other domestic wastes, sand and gravel extraction, dredging, industrial waste, petroleum hydrocarbons and waste oil discharge among others (Nwilo, Peters & Badejo, 2009; Okoye *et al.*, 2010). With this level of pollution and misuse of the natural asset and landscape resources of the Lagos Lagoon, it is inhibited from benefiting from more laudable uses such as tourism and recreation. A great tourism potential continues to exist untapped in the Lagos Lagoon (Uluocha, 1999).

Tourism along the coast receives more attention and is better developed than on the lagoon as attested to the popularity of places like Bar Beach, Kuramo beach and Lekki/ Maiyegun Beach (Oshundeyi and Babarinde, 2003). Adejumo (2010) explored the economic impact of rural coastal beach tourism of Eleko beach. Some of the problems he identified as plaguing the water tourism industry include; lack of tourism product development, lack of government support, poor social capital, lack of financial resources and lack of human resources. Cultural issues were examined by Aina and Babatola (2010) in their study of its effect on a sustainable tourism development strategy for rural areas. Studies by Uduma-Olugu & Onukwube (2012) explored the potentials of tourism in some of these coastal tourism venues and highlighted the deficiencies in the provided facilities.

2.0 Landscape and Human Perception

The development of methods for systematically integrating aesthetic values in ecological and land-use decision making began in the mid-1960s.

Ndubuisi (2002) posits that K. Craik, L. Leopold, B. Linton, E. Shafer, J. Wohwill and E. Zube in the United States and K. Fines and his colleagues in Britain conducted pioneering studies in landscape perception and assessment during the late sixties. Zube's 1966 visual-assessment study on Nantucket Island and his 1968 resource-assessment study of the US Virgin Islands provided significant methodological directives for the assessment and integration of visual resources in ecological planning. Also notable in this period, was Linton's work which developed a framework in 1968 for describing and analyzing visual elements in large forested landscapes (Ndubuisi, 2002).

The landscape functions comprise the current and potential ability of the landscape to fulfil the human needs regarding the natural resources and the landscape experience. The degree of human impact and the visibility in the landscape can be measured by visual indicators as relief, vegetation, land use, structural elements or lines of sight. But characteristics such as harmony and scenic beauty that depend on the perceptual process the features of the landscape evoke in the human viewer should also be assessed (Daniel, 2001). The Scenic Beauty Model (SBME) which considers the relevance of physical features in evaluating a landscape (Daniel & Boster, 1976). Daniel *et al* (1976) updated by Daniel (2001) and Franco *et al.* (2003), posited that scenic beauty judgments depend jointly on the perceived properties of the landscape and the judgmental criteria of the observer.

Landscape assessment research has primarily focused on the visual properties of the land area under study. Consequently, the dimension most often measured is the scenic quality of a given area (Zube 1975). This variable also has been described as scenic beauty (Daniel and Boster, 1976) and landscape preference (Buhyoff and Wellman, 1978). Psychophysical landscape assessments typically represent the experiences of visitors to the area under study by means of color slides. Criticism has focused on whether human reactions to areas represented by photographs are valid indicators of reactions that would occur if people were to visit the areas and view them directly. However, when comparing between perceptual data gathered using color slide depictions of landscapes and data obtained at the actual sites where those slide photographs were taken, a very close relationship between the two has been established (Daniel and Boster, 1976; Malm *et al.*, 1981). Correlations between photo-based and direct on-site assessments have been found to be .80

or greater (Daniel, 1990). Landscape assessments utilizing psychophysical methodology have been obtained using Likert-type rating scales (Daniel and Boster, 1976), rank orders (Shafer and Brush, 1977) etc.

3.0 Methodology

A desktop study was done to identify the landscape resources in the area, and verified and upgraded by personal observation (via a field survey where the existing features were recorded). The motivation for selection of a destination were identified from the literature review is based on how the potential tourist perceives the location, as well as word-of-mouth and previous experience of the venue. These were covered by questions which dealt with facilities and factors as well as how a person feels at tourism venues. The various elements that constitute the landscape characteristics of the Lagos lagoon influence tourism differently and their effects were measured from the questionnaire in a table that listed them and used a likert scale to measure their level of influence.

The questionnaires consisted of a combination of types of questions, such as multiple choice, Likert

scale, and closed and open-ended questions, relating to respondents' perceptions. Preferences for five mapped landscape categories were compared with expert ratings of the same landscapes. The photo questionnaire presented 20 black and white photographs showing vegetation and landforms characteristic of the study site. Photographic sites were selected in consultation with botanical and landscape experts to represent a range of values related to dominant species and degree of human modification of landscape. A bigger, coloured version of the same pictures accompanied the questionnaires since the black and white pictures shown in the questionnaires were too small and insufficiently legible.

4.0 Findings

The study locations consisted of the three water-based recreational spots within the study area of the Lagos Lagoon (Unilag waterfront, Lekki Phase1 Club House – The Pavilion and Origin zoo and jetty, Ipakodo, Ikorodu) and three coastal water-based tourist destinations on the Lagos coast in close proximity to Lagos (Bar Beach, Alpha Beach and Maiyegun/Lekki Beach).

Table 4.1: Summary of Study Locations

Variable	Characteristics	Frequency	%	Total
Place	Bar Beach	132	31.3	422
	Lekki Phase1 Club House – The Pavilion	55	13.0	
	Alpha Beach	30	7.1	
	Maiyegun/Lekki Beach	27	6.4	
	Unilag Waterfront	137	32.5	
	Origin Zoo Jetty, Ikorodu	41	9.7	

Table 4.1 indicates the locations surveyed – the highest number of respondents came from Unilag waterfront – 32.5% (137) and the least from Maiyegun/Lekki Beach 6.4% (27).

Reliability Analysis of Demographic Variables

Table 4.2: Reliability Statistics

Cronbach's Alpha	Cronbach's Alpha Based on Standardized Items	N of Items
.848	.849	59

From Table 4.2, the test of reliability of questionnaire based on the standardized Cronbach's Alpha is obtained as 0.849 (84.9%). The result suggested that the instrument of evaluation (questionnaire) is highly reliable judging from the fact that 84.9% > 70%. Also that there is an internal consistency of the items in the instrument (questionnaire) used for data collection.

Table 4.3: ANOVA

	Sum of Squares	Df	Mean Square	F	Sig
Between People	590.954	105	5.628		
Within People					
Between Items	1474.834	58	25.428	18.445	.000
Residual	8395.641	6090	1.379		
Total	9870.475	6148	1.605		
Total	10461.428	6253	1.673		

Grand Mean = 3.32

From the ANOVA test, Since the P1-value = 0.000 < 0.05 significant level, the reliability of the instrument is significant. This further validates the adequacy of the instrument.

4.2 Socio-Economic Demographics of Respondents

Gender analysis of the respondents from Table 4.4 show that more males 65.4% (276) than females 34.6% (146) responded. The average age of respondents was 28.3 years, out of which the highest number of respondents were among the youth. The implication is that people that visit such destinations are mostly young and male. Respondents that fall under these age brackets are believed to have a lot of energy, dynamic and vibrant and are more likely to

be engaged in active rather than passive recreation. There was a high incidence of literate people among the respondents as graduates with BSc. Or MSc. had the highest number - 48.6% (205) while respondents with primary school education were the fewest -6.4% (27). This implies that more literate people appear to appreciate water-based tourism more than those with less education. The mean annual income of respondents was relatively high (N4,282,934), indicating that it is mostly middle income earners that visit the destinations.

Table 4.4: Summary of Socio-Demographic Variables

Variable	Characteristics	Frequency	%	Mean	Total
Gender	Male	276	65.4		
	Female	146	34.6		422
Age	(Below 16) Years	6	1.4	28.3 Yrs	
	(16---30) Years	284	67.3		
	(31---45) Years	112	26.5		
	(46---60) Years	20	4.7		422
Employment Status	Retired	8	1.9		
	Office Worker	192	45.5		
	Student	92	21.8		
	Site Worker	11	2.6		
	Business	98	23.2		
	Educator	2	.5		
	Unemployed	19	4.5		422
Marital Status	Married	171	40.5		
	Divorced/Separated	8	1.9		
	Widowed	3	.7		
	Unmarried	240	56.9		422
Educational Qualification	Primary school	27	6.4		
	Secondary school	57	13.5		
	Technical school /Polytechnic	49	11.6		
	Graduate (e.g. B.Sc., B.A)	205	48.6		
	Post Graduate (e.g. M.sc or PhD)	84	19.9		422
Average Annual Income	Low income - less than N500,000 per annum	85	25.4	N4,282,934	
	Middle income - N500,000 - N10,000,000 per annum	232	69.5		
	High income - more than N10,000,000 per annum	17	5.1		334
Place of Residence	Lagos Metropolis	280	66.4		

Nationality	Other town in Lagos State	71	16.8	422
	Other State in Nigeria	56	13.3	
	Outside Nigeria	15	3.6	
	Nigerian	414	98.1	
	European	5	1.2	422
	North American	1	.2	
	Middle East	1	.2	
	Other African Countries	1	.2	

The lowest percent was the group that earn more than N10,000,000 per annum – 5.1% (17). This is not surprising as most of such people are likely to travel out of the country than visit the local water tourism venues. Most of the respondents live in Lagos metropolis 66.4% (280), the tourists – coming from outside Lagos State and other countries made up the balance. This result was expected as the area does not

seem to have a high traffic of tourists which is what necessitated the study in the first place. The Nationality of the respondents was also not surprising as 98.1% were Nigerians. This shows that international tourism is not high at the venues; rather, domestic tourism is what is obtainable at some level on the Lagoon.

4.3 Ranking of Respondents' Perception of the Landscape characteristics of the Lagos Lagoon

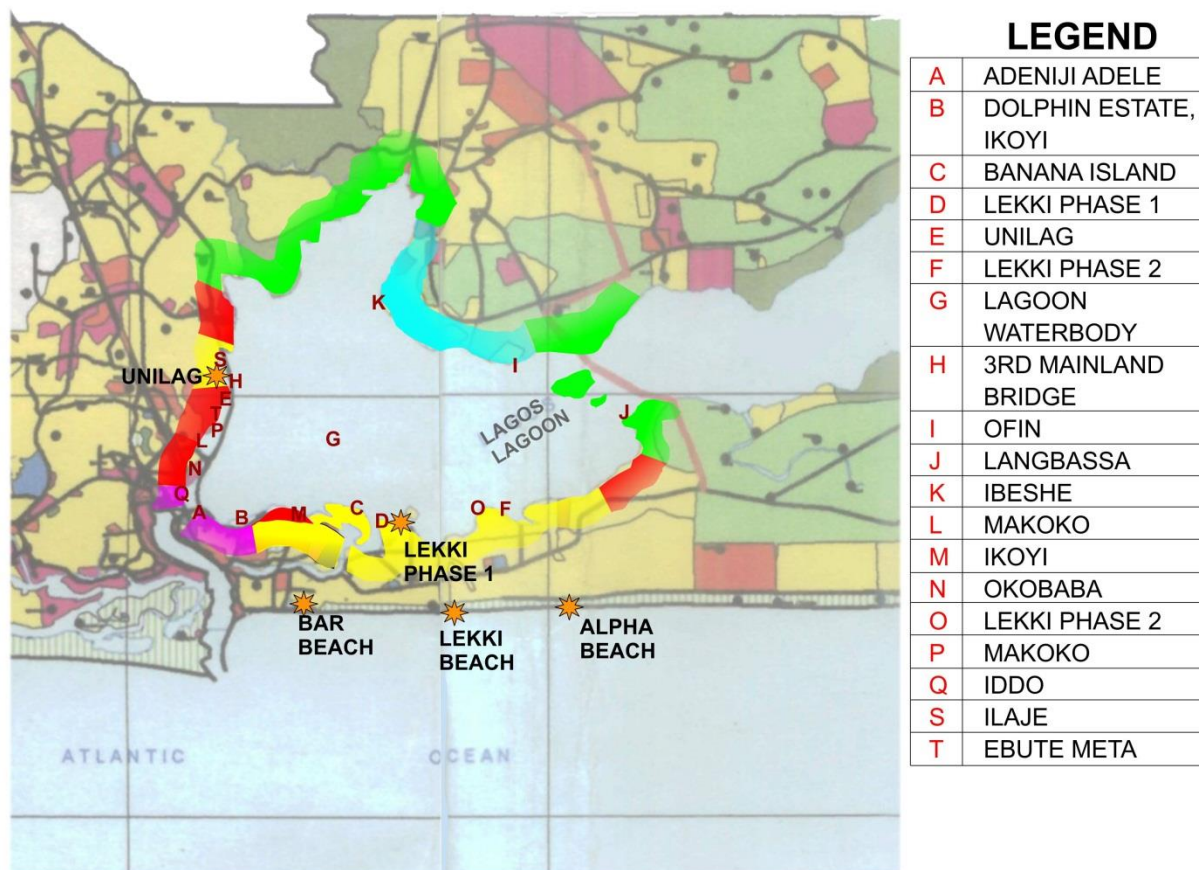


Figure 4.1: Showing areas where the pictures were taken along the Lagos Lagoon Waterfront



A { }

B{ }

C { }

D{ }

E { }

Figure 4.2: Totally Urban Pictures

Table 4.5: Ranking Of Landscape Perception of the Lagos Lagoon: Totally Urban

Picture	LB	%	A	%	FB	%	B	%	EB	%	Total	Scale Mean	Response Mean	%
Ranking of Picture: A	23	6.5	71	20.1	83	23.4	116	32.8	61	17.2	354	3.0	3.3	66
Ranking of Picture: B	33	9.3	76	21.5	96	27.2	110	31.2	38	10.8	353	3.0	3.1	62
Ranking of Picture: C	26	7.4	53	15.1	84	23.9	101	28.8	87	24.8	351	3.0	3.5	70
Ranking of Picture: D	28	8.0	68	19.3	97	27.6	107	30.4	52	14.8	352	3.0	3.2	64
Ranking of Picture: E	35	9.9	68	19.2	95	26.8	100	28.2	57	16.1	355	3.0	3.2	64
Total	145	8.2	336	19.04	455	25.78	534	30.28	295	16.7		3.0	3.3	66

Ranking of Landscape Perception of the Lagos Lagoon: LB (Least Beautiful), a (Average), FB (Fairly Beautiful), B (Beautiful), EB (Extremely Beautiful)

Table 4.5 shows the ranking of the totally urban aspects. In the first set of pictures (Figure 4.2) comprising shots of totally urban aspects of the lagoon. Results show that they were all considered

beautiful with picture C (showing a high-rise luxury building) having the highest score of 70. Picture C also had the highest score in the entire 20 pictures ranked by the respondents.



F { }

G{ }

H { }

I{ }

J{ }

Figure 4.3: Landscape Elements Pictures

Table 4.6: Ranking Of Landscape Perception of the Lagos Lagoon: Landscape Elements

Picture	LB	%	A	%	FB	%	B	%	EB	%	Total	Scale Mean	Response Mean	%
Ranking of Picture: F	29	8.1	68	19.0	114	31.8	82	22.9	65	18.2	358	3.0	3.2	64
Ranking of Picture: G	36	10.2	81	22.9	82	23.2	98	27.8	56	15.9	353	3.0	3.0	64
Ranking of Picture: H	45	12.8	97	27.6	66	18.8	103	29.3	41	11.6	352	3.0	3.0	60
Ranking of Picture: I	49	13.9	69	16.5	90	25.5	107	30.3	38	10.8	353	3.0	3.0	60
Ranking of Picture: J	54	15.3	78	22.2	84	23.9	104	29.5	32	9.1	352	3.0	2.9	58
Total	213	12.06	393	22.24	436	24.64	494	27.96	232	13.12		3.0	3.1	62

Ranking of Landscape Perception of the Lagos Lagoon: LB (Least Beautiful), a (Average), FB (Fairly Beautiful), B (Beautiful), EB (Extremely Beautiful)

In the second set of pictures (Figure 4.3) comprising shots of different landscape elements of the lagoon,

results show that they were considered beautiful except for picture J which had a score of 2.9.



Figure 4.4: Open Spaces Pictures

Table 4.7: Ranking Of Landscape Perception of the Lagos Lagoon: Open Spaces

Picture	LB	%	A	%	FB	%	B	%	EB	%	Total	Scale Mean	Response Mean	%
Ranking of Picture: K	63	17.2	85	23.2	81	22.1	98	26.7	40	10.9	367	3.0	2.9	58
Ranking of Picture: L	63	17.1	89	24.1	64	17.3	109	29.5	44	11.9	369	3.0	3.0	60
Ranking of Picture: M	59	16.0	82	22.3	81	22.0	115	31.3	31	8.4	368	3.0	2.9	58
Ranking of Picture: N	51	14.1	81	22.4	79	21.9	121	33.5	29	8.0	361	3.0	3.0	60

Ranking of Picture: O	52	14.4	65	18.0	93	25.8	98	27.1	53	14.7	361	3.0	3.1	62
Total	288	15.76	402	22	398	21.82	541	29.62	197	10.78		3.0	3.0	60

Ranking of Landscape Perception of the Lagos Lagoon: LB (Least Beautiful), a (Average), FB (Fairly Beautiful), B (Beautiful), EB (Extremely Beautiful)

In the third set of pictures (Figure 4.4) comprising shots of open spaces around the lagoon, the scores were generally low. Results showed that they were considered beautiful except for Pictures K (showing

fishing circles) and picture M (showing mixed vegetation) which jointly had the lowest score of 58, as the least liked pictures in the group.



Figure 4.5: Human and Social activities Pictures

Table 4.8: Ranking Of Landscape Perception of the Lagos Lagoon: Human and Social Activities

Picture	LB	%	A	%	FB	%	B	%	EB	%	Total	Scale Mean	Response Mean	%
Ranking of Picture: P	79	22.4	72	20.4	69	19.5	95	28.9	38	10.8	353	3.0	2.8	56
Ranking of Picture: Q	58	16.4	79	22.4	81	22.9	97	27.5	38	10.8	353	3.0	2.9	58
Ranking of Picture: R	64	18.5	91	26.3	65	18.8	89	25.7	37	10.7	346	3.0	2.8	56
Ranking of Picture: S	103	29.5	73	20.9	79	22.6	68	19.5	26	7.4	349	3.0	2.5	50
Ranking of Picture: T	68	19.6	52	15.0	88	25.4	79	22.8	60	17.3	347	3.0	3.0	60
Total	372	21.28	367	21	382	21.84	428	24.48	199	11.4		3.0	2.8	56

Ranking of Landscape Perception of the Lagos Lagoon: LB (Least Beautiful), a (Average), FB (Fairly Beautiful), B (Beautiful), EB (Extremely Beautiful)

The pictures (Figure 4.5) comprising shots of human and social activities around the lagoon had the lowest scores in the entire group of pictures. The picture with the lowest score in this group was picture S

(showing slum housing on stilts) which was least liked pictures in the group and also among the entire 20 pictures ranked by the respondents.

4.4. Factors most significant in determining the impact of landscape characteristics of the Lagos lagoon waterfront on tourism

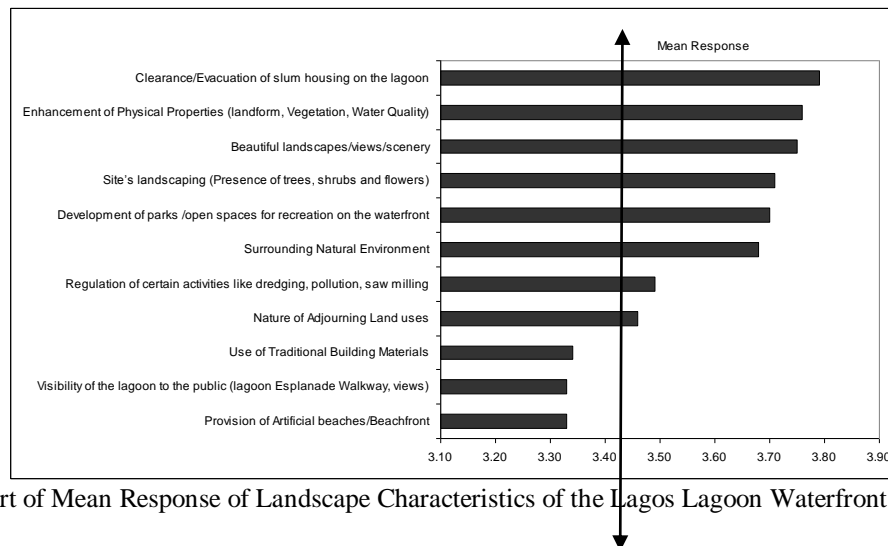


Figure 4.6: Chart of Mean Response of Landscape Characteristics of the Lagos Lagoon Waterfront on Tourism

Figure 4.6 shows the six factors considered important regarding the effect of the landscape characteristics. The landscape factor considered most significant is the clearance of the slum housing and similar blights on the shores of the lagoon. Handling the problem areas along the lagoon shores will help in influencing its acceptability for tourism. The issue of enhancing the physical properties of the lagoon needs to be addressed also as the water is coloured, smelly and polluted (Nwankwo, 2004; Onyema, 2009) as this was the second most important factor. This makes it unsuitable for most water tourism activities as visitors cannot swim in it, nor have direct access to it for hygienic reasons. The fifth factor considered relevant by the respondents, is the development of parks and open spaces for recreation along the waterfront. Currently, there are very few recreational open spaces or parks directly abutting the shores of the lagoon. Such places would afford the general public an opportunity to directly interact with the lagoon.

5. DISCUSSIONS/CONCLUSION

The results indicate that tourists and users of water-based recreational showed a preference of well developed parts of the Lagos Lagoon waterfront over the more natural landscape which is in line with previous findings globally (Thayer, 1989; Nassauer, 1995). The perception of the Lagos Lagoon as a tourism resource was generally low as most responded negatively to the use of the Lagoon for tourism, preferring rather the option of its use for urban agriculture and urban residential waterfront development. To a large extent it indicates that much work needs to be done in bringing the standards of the facilities and infrastructures of the lagoon to more

acceptable levels as well as the enlightenment of the public about the benefits and components of tourism to make it more acceptable. One of the very important outcome of the research is the opinion of the respondents that the most important factor that is a deterrent to tourism use of the lagoon especially as regards its landscape, is the existence of the slums and similar blights along the lagoonal shores. These, along with the issue of water pollution, ranked highest as critically impacting the tourism potential of the Lagos Lagoon. This was also reiterated by the choice of the slum as the worst picture among the twenty pictures shown to the respondents to rank.

REFERENCES

- Adejumo, O. T., (2010). Eleko rural beach initiative: Maximizing economic benefit of domestic tourism destination in littoral Lagos community. *Urban and Regional Planning Review*, 2 (1&2), 91-98.
- Aina, O. C. & Babatola O. (2010). Cultural Tourism: A sustainable development strategy for Nigeria's rural area. *Journal of Geography, Environment and Planning*. Pp.66-72.
- Buhyoff, G. J., & Wellman, J. D. (1978). Landscape architect's interpretation of people's landscape for visual landscape dimensions. *Journal of Environmental Management* 6: 255- 262.
- Daniel T. C., & Boster, R. S. (1976). Measuring landscape aesthetics: The scenic beauty estimation method. *USDA Forest Service*, Research Paper RM- 167. Ft. Collins, CO: USDA Forest Service, Rocky Mountain Forest and Range Experiment Station.
- Daniel, T. C. (2001). Whither scenic beauty? Visual landscape quality assessment in the 21st century. *Landscape and Urban Planning*, 54(1-4), 267-281.
- Franco, D., Franco D., Mannino, I & Zanetto, G. (2003). The impact of agroforestry networks on scenic beauty estimation; The role of a landscape ecological network on a socio-cultural process. *Landscape and Urban Planning*, 62, 119-138.
- Gnoth, J. (1997). Tourism motivation and expectation formation.

- Annals of Tourism Research*, 24 (2), 283-304.
- Gunn, C. A. (2002). *Tourism planning*. New York: Routledge.
- Malm, W. C., Kelley, K., Molenar, J. & Daniel, T. C. (1981). Human perception of visual air quality (uniform haze). *Atmospheric Environment* 15:1875- 1890.
- Nassauer, J. I. (1995). Messy ecosystems, orderly frames. *Landscape Journal*, 14(2), 161-169.
- Ndubuisi, F. (2002). *Ecological planning: A historical and comparative synthesis*. Baltimore and London: John Hopkins University Press.
- Nwankwo, D. I. (2004). *The microalgae: Our indispensable allies in aquatic monitoring and biodiversity sustainability*. University of Lagos Press. Inaugural lecture series.44pp.
- Nwilo, P. C., Peters, K. O. & Badejo, O. T. (2009). Development of a Lagos Lagoon information System. *Environmental Review*, 3 (2), 403-408.
- Okoye, C. O., Onwuka S. U., & Obiakor, M. O. (2010). Pollution survey in the Lagos Lagoon and its environmental consequences: A review. *Tropical Built Environment*, 1 (1), 41-54.
- Oshundeyi, O. A., & Babarinde, O. T. (2003). Tourism in Lagos State. In Ajetunmobi, R. (Ed), *The Evolution and development of Lagos State*, Lagos: A-Triad Associates. pp 260-285.
- Shafer, E. L., & Brush, R. O. (1977). How to measure preferences for photographs of natural landscapes. *Landscape Planning* 4:237- 256.
- Swaffield, S. (1999). A framework for landscape assessment. *Landscape Review*, 5(1), 45-51.
- Thayer, R. L. (1989). The experience of sustainable landscapes. *Landscape Journal*, 8:101-110.
- Uduma-Olugu, N. & Oduwaye, L. (2010). The regeneration of Lagos lagoon waterfront for recreation and tourism. REAL CORP 2010, 15th International Conference Proceedings held at Vienna 18th – 20th May, 2010. pp 759-764.
- Uduma-Olugu, N. & Onukwube, H. N. (2012). Exploring the coastal tourism potentials of Lagos. *Journal of Sustainable Development*, 5(7), 156-165.
- Uduma-Olugu, N., & Iyagba, R. (2009b). Comparative analysis of factors affecting water tourism patronage and potentials within the built environment in Nigeria and Ghana. *International Journal of Culture and Tourism Research*, 2(1), 91-105.
- Uluocha, N. O. (1999). Mapping for integrated management of tourism resources in Lagos State. In Balogun, O. Y. and Soneye, A. S. O. (Eds), *Cartography in the service of government*, Lagos: The Nigerian Cartographic Association. pp 71-82.
- United Nations World Tourism Organisation (2011). *Compendium of Tourism statistics 2005 - 2009*. Retrieved February 3, 2012, from, <http://www.e-unwto.org>.
- Zube, E.H., Brush, R.O. & Fabos, J. Gy. (Eds), (1975). *Landscape Assessment: Values, Perceptions and Resources*. Dowden, Hutchinson and Ross, Stroudsburg, PA, 367 pp.

A Dynamic Approach to Money Supply

Yougui Wang¹✉, Guobin Zhou¹, Wanting Xiong¹

¹ School of Systems Science, Beijing Normal University, Beijing 100875, P.R. China

Abstract: In this paper, we present the mechanism of money supply from a dynamic perspective, in which the behaviors of the sectors involved in the process of money creation and the interplay among them are taken into account. Specially, we introduce households' withdrawals of deposit and firms' repayments to loan, which are ignored in the conventional statement of money creation process. By deriving and analyzing the equilibrium solution to the dynamic equations which characterize the process, we can discuss the corresponding influence of each sector on the money supply.

Introduction

Money is the blood of economy. A healthy money supply channel is an indispensable part to the maintaining and flourishing of the economy. To revive the economy from the devastating financial crisis, many countries turn to remedies that amplify the supply of money, which are also known as "quantitative easing" policy measures. The effect, however, is debatable. Actually, the process of money supply is systematic and complex, in which both banks and non-bank sectors play a role.

There are extensive literatures on the mechanism of money supply. C. A. Phillips argues that if banks do not retain excess reserves and the public only hold the demand deposits, no currency and no time deposits, the increase of reserves will lead to the increase of loans as well as the demand deposits [1]. The change in demand deposits is determined by the change in reserves and the inverse of required reserves ratio--the "textbook money multiplier". However, in reality, the banks do retain excess reserves to provide enhanced liquidity and the public hold their wealth not only in the form of demand deposit but also in the form of currencies. P. Samuelson takes both facts into consideration, measuring them with "excess reserves ratio" and "cash leakage ratio". Then the money multiplier will be formulated as the inverse of the sum of required reserves ratio, excess reserves ratio and currency leakage ratio [2].

P. Cagan analyzes the ratio of currency to the money supply, which fluctuated dramatically during 1875-1955 in America [3]. Then he proposes six decisive factors of the ratio. J. Ahrensdoerf and S. Kanesathasan have performed an empirical analysis to test the effects of changes in currency, reserve ratios on the money supply. They also distinguish between the contribution of monetary authorities on the changes in the money supply and that of the private sector [4]. R. L. Teigen highlights the role of banking system in determining the money supply. He derives an aggregate money-supply function to segregate the exogenous and endogenous determinants on the money stock [5].

M. Friedman and A. Schwartz have performed a comprehensive study on this issue [6]. They develop a more detailed money multiplier model based on three proximate determinants, which are dependent on three sectors. It is also pointed out that the three factors have linkages with each other. Each one of them is jointly determined by the three sectors, rather than by a single sector respectively. P. Cagan carries out a deep and systematic research on the determinants and effects of the changes in the stock of money with the 1875-1960 data of America [7]. J. Jordan extends the analysis with a more complicated model by taking the differences between the member banks and the nonmember banks,



Yougui Wang (Correspondence)

ygwang@bnu.edu.cn

+86-10-58802732

as well as the fact that different kinds of deposits are subject to different reserve requirements [8].

Different from the model proposed in [6], K.Brunner and A.Meltzer create two money supply functions based on linear hypothesis and nonlinear hypothesis respectively. It uses statistical methods to have a regression which shows the multipliers of all the determinants of money stock, rather than for a single monetary base [9]. Compared with F-S's conceptual money multiplier, this method provides an empirical insight.

Some reformulations of money multiplier are made. C.Bourne proposes a process-oriented formulation of money multiplier with the case of Jamaica, which shows that in a small, open economy, the money market is demand centered [10]. A.W.A.McClean analyzes the properties of Bourne's model and acknowledges that the money multiplier analysis should be replaced to better accommodate the fact [11]. P.He,L.X.Huang, and R.Wright develop a new theory of money and banking based on the old story, then derives a money multiplier in a microfounded version [12]. M.Berardi presents an alternative and dynamic approach with the consideration of heterogeneous agents and their interactions [13].

It should be mentioned that economists have achieved fruitful results in understanding the mechanisms of the process of money supply. However, the quasi-static view adopted by the majority of the above works fails to capture the dynamics flows of the process as well as the explicit roles of different economic sectors. This paper, instead, provides a dynamic approach to understand the process of money supply and the determinants of money multiplier by analyzing both the money stocks and the in-and-out flows of the economy which are created and driven by the economic behaviors of different sectors including central and commercial banks, households and firms. With the established stock-flow relations, we not only present a dynamic analysis of the money creation process but also specifically compare and illustrate on the

consequences of the sectors' behaviors in extreme cases such as debt crises.

A CONVENTIONAL APPROACH TO MONEY SUPPLY

In the conventional statement of money supply, three sectors participated in this process: central bank, commercial banks and non-bank public.

The central bank issues monetary base to public, then the public retains a part in the form of currencies, saving the rest. Commercial banks hand over a part of the deposits as required reserves to the central bank. Then they lend the rest excess reserves to public. Public repeats. Eventually, money supply will be a multiple of monetary base, which is the "money multiplier". The traditional model describes a quasi-static process, which cannot reflect the change of money supply in a dynamic view.

The base model can be depicted as follows. Monetary base MB is composed of currencies C and reserves R . The reserves can be further divided into required reserves RR and excess reserves ER . That is

$$MB = C + RR + ER \quad (1)$$

These three components can be described respectively in terms of deposits D . As a result, Equation (1) can be rewritten as

$$MB = (c + r + e) \times D, \quad (2)$$

where c is currency-deposit ratio, r is the required reserves ratio, and e is the excess reserves ratio.

Money supply M is composed of currencies and deposits, that is

$$M = C + D. \quad (3)$$

Substituting (2) into (3), we have the money multiplier

$$m = \frac{M}{MB} = \frac{1 + c}{c + r + e}. \quad (4)$$

The conventional one mainly describes the money supply process conceptually without modelling the behavior of each sector. Regarding it as a quasi-static result, it derives a money supply within a money multiplier framework. Actually, this orthodox money multiplier is a poor description of money creation process.

AN ALTERNATIVE APPROACH TO MONEY SUPPLY

Money creation is a systematic and dynamic process. Generally, the following four sectors are involved in this process: the central bank, commercial banks, households and firms. The last two are sometimes combined into one sector which is called “non-bank public” as given above. Each of them plays a key but different role.

The central bank issues the monetary base, and takes up the required reserves from commercial banks. Households save their money to commercial banks, and withdraw them when they need money. Their savings are called deposits. Firms can borrow money from commercial banks, and repay them when the loan is due. It follows that the commercial banks play a core role in the money creation process. They accept deposits from households and hold reserves required by the central bank or as a buffer for abrupt withdrawals. They also make loans to firms and get the matured ones back.

The money creation starts as central bank issues monetary base, or high-powered money, to households.

Households hold a part as currencies for their need in transactions, then save the rest to commercial banks, through which the high-powered money is transformed to be reserves. Commercial banks accept deposits from households, and then hand over a portion to the central bank as required reserves. With the excess reserves, they can loan some to firms once they face demand of borrowing. Simultaneously, an equivalent amount of deposits are created by banks and held by firms. So this is the vital action in the process of money creation.

However, this is not a complete story of money creation. Actually, besides saving and borrowing, households can withdraw money from banks when they have a demand for currency, firms must repay the loans at their due time. These behaviors operate in the opposite direction as saving and borrowing do and exert an apparent influence on money supply. The introduction of these two behaviors is one practical improvement for the conventional money creation process.

The mechanism mentioned above is an exhaustive description of the process of money creation, which can be illustrated as the following chart.

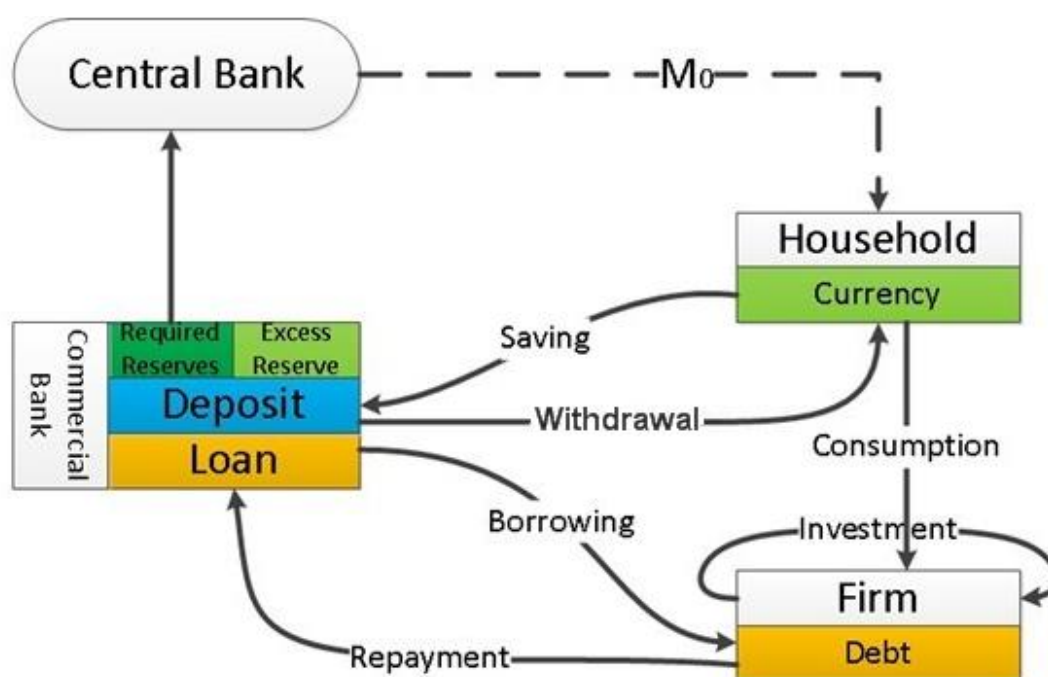


Figure 1: A schematic illustration of money creation process

The Model and Dynamic Equations

To describe mathematically the process mentioned above, we should integrate three stock variables: amount of currency $C(t)$, deposits $D(t)$, and outstanding loans $L(t)$. We also introduce four flow variables: saving flow $S(t)$, withdrawal $W(t)$, borrowing of firms $I(t)$, and repayment $R(t)$, each of which has a tight linkage with corresponding stock variable, specifying the behavior of corresponding sector.

At time t , households save money to commercial banks. The saving flow $S(t)$ is a portion (c_1) of the currencies $C(t)$ held by them, which is given by

$$S(t) = c_1 \cdot C(t). \quad (5)$$

Meanwhile, households may have withdrawals when they need money. The withdrawal flow $W(t)$ is a portion (c_2) of the deposits $D(t)$, which has the following form

$$W(t) = c_2 \cdot D(t). \quad (6)$$

When commercial banks face a demand for loans from firms, they will draw on excess reserves to make loans.

The loans to firms $I(t)$ is a ratio (c_3) of the excess

reserves $ER(t)$, which takes the form of

$$I(t) = c_3 \cdot ER(t). \quad (7)$$

The excess reserves $ER(t)$ is the remaining of the deposits $D(t)$ after delivering the required reserves

$r \cdot D(t)$ and subtracting total outstanding loans $L(t)$,

i.e.,

$$ER(t) = D(t) - r \cdot D(t) - L(t), \quad (8)$$

where r is the required reserves ratio. When firms repay the loans to commercial banks, the repayments

$R(t)$ is assumed to be a portion (c_4) of the loans

$L(t)$, which can be written as

$$R(t) = c_4 \cdot L(t). \quad (9)$$

Since the saving is the inflow of the currencies, but the withdrawal is the outflow, the change in currencies at time t is the difference between them, which can be expressed as

$$\frac{dC}{dt} = W(t) - S(t). \quad (10)$$

The behavior of firms mainly determines the change in outstanding loans, which is the difference between borrowing and repayments:

$$\frac{dL}{dt} = I(t) - R(t). \quad (11)$$

In contrast to these two variables, the change in deposits stems from both households and firms. The saving and withdrawal contribute to deposits in the opposite direction as to the currencies. On the other side, the loans turn out deposits of firms and repayments annihilate them. Thus the difference between borrowing and repayments also makes up additional part of the change in deposits. So we have

$$\frac{dD}{dt} = S(t) - W(t) + I(t) - R(t). \quad (12)$$

The above model presents the behavior of all sectors involved in the money creation system. From the model developed above, we can recognize that each sector plays a different role. These sectors exert influences on the money supply all the time. We should take a dynamic and systemic perspective to analyze it. Integrating (5)-(12) results in the following system of equations:

$$\begin{cases} \frac{dC}{dt} = c_2 D(t) - c_1 C(t) \\ \frac{dD}{dt} = c_1 C(t) + [c_3(1-r) - c_2]D(t) - (c_3 + c_4)L(t) \\ \frac{dL}{dt} = (1-r)c_3 D(t) - (c_3 + c_4)L(t) \end{cases} \quad (13)$$

Each variable is changing. The change of a stock variable causes the change of a flow variable, and vice versa. They are all interconnected by the interactions of the sectors.

The Equilibrium Solution

Starting from the initial condition of $C(0) = M_0$, the system will eventually move to an equilibrium state, where there is no more change in any stock variable over time, that is

$$\begin{cases} \frac{dC}{dt} = c_2 D(t) - c_1 C(t) = 0 \\ \frac{dD}{dt} = c_1 C(t) + [c_3(1-r) - c_2]D(t) - (c_3 + c_4)L(t) = 0 \\ \frac{dL}{dt} = (1-r)c_3 D(t) - (c_3 + c_4)L(t) = 0 \end{cases} \quad (14)$$

The set of equations confirms that when the system falls into a steady state, the quantity of loans must equal to the quantity of repayments, and the level of Solving the equations in (14) yields the result:

saving flow must equal to that of withdrawal. This is also an equilibrium state of the behaviors of all sectors.

$$\begin{cases} \frac{C(t)}{D(t)} = \frac{c_2}{c_1} \\ \frac{L(t)}{D(t)} = \frac{c_3(1-r)}{(c_3 + c_4)} \end{cases} \quad (15)$$

When the system comes to the equilibrium state, there is a proportional relationship between C , D and L . From (10) and (11), we have

$$M_0 = C(t) + D(t) - L(t). \quad (16)$$

Then from (15) and (16) we can obtain

$$\begin{cases} D = \frac{M_0}{1 + \frac{c_2}{c_1} - \frac{c_3(1-r)}{(c_3+c_4)}} \\ C = \frac{c_2}{c_1} \frac{M_0}{1 + \frac{c_2}{c_1} - \frac{c_3(1-r)}{(c_3+c_4)}} \\ L = \frac{c_3(1-r)}{(c_3+c_4)} \frac{M_0}{1 + \frac{c_2}{c_1} - \frac{c_3(1-r)}{(c_3+c_4)}} \end{cases} \quad (17)$$

This set of results is capable of demonstrating the intrinsic interactions of all sectors involved in the money supply. Currencies, held by households, are also determined by commercial banks, firms, even the

$$M = C + D = \frac{M_0}{1 - \frac{c_1}{(c_1+c_2)} \times \frac{c_3(1-r)}{(c_3+c_4)}} \quad (18)$$

Suppose that households retain all currencies first without saving at all, c_1 will be zero, then the money supply just stays at the level of monetary base without any expansion. In an extreme situation like bank run, it is possible that households withdraw all deposits and save none. Then the money creation will stop. An increase in c_1 , other things being equal, means a reduction of currency leakage, would turn more monetary base into the deposit and create more money.

This principle also suits the commercial banks. If banks make no loans, the money supply is also just the monetary base. When banks make more loans, that is, a rise in c_3 , other things being equal, the money supply will also be larger. So households' saving and commercial banks' lending can be regarded as playing a core role to some extent in the process of money creation.

Different from the movement mentioned above, when households withdraw more money for their demands,

central bank. Deposits and total loans, held by commercial banks and firms respectively, are also determined by other three sectors.

Using a generalized definition, the money supply is

which means a rise in c_2 , currency leakage will be more, then money circulated in the creation process will decrease, which will reduce the total money supply. When firms have more repayments, the same story goes. It is a way of money annihilation. Both of them should be worth to note. They may not cease the process, but actually exert heavy influences on the money creation.

Conclusion

In this paper, we discussed a miniature economy consisting of four sectors: central bank, commercial banks, firms and households. By considering the behaviors and interplays of the four sectors, we presented a stock-flow interpretation of the process of money supply in a dynamic model within a continuous time framework. With the help of the model, we then illustrate on the mechanism of money creation process and the determinants of the money multiplier based on the behaviors of the economic sectors. Specifically, when households hold less currency and save more to commercial banks, the money supply will be more, i.e. the money multiplier will be larger. When commercial

banks make more loans, a similar story repeats. More withdrawals will increase the currency leakage, thus reducing the money supply, or the money multiplier, while firms' repayments will do the same.

A new contribution should be noted that we innovatively include households' withdrawals and firms' repayments into the story of money supply, which are long neglected in the conventional theories.


References

1. Phillips, C. A. 1920. *Bank Credit*. New York :Macmillan.
2. Samuelson, P. 1997. *Economic:TheOirginal 1948 Edition*. Irwin:McGraw-Hill.
3. Cagan, P. 1958. "The Demand for Currency Relative to the Total Money Supply," *Journal of Political Economy*, 66(4):303-328.
4. Ahrensdoxf, J. and S. Kanesathasan. 1960. "Variations in the Money Multiplier and Their Implications for Central Banking," *Staff Papers-International Monetary Fund*, 8(1):126-149.
5. Teigen, R. L. 1964. "Demand and Supply Functions for Money in the United States: Some Structural Estimates," *Econometrica*, 32(4): 476-509.
6. Friedman, M. and A. Schwartz.1963. *A Monetary History of the U.S.1867-1960*. Princeton, N.J :Princeton Univ. Press.
7. Cagan, P. 1965.*Determinants and Effects of Changes in the Stock of Money,1875-1960*. New York:Columbia Univ. Press.
8. Jordan, J. 1969. "Elements of Money Stock Determination," *Federal Reserve Bank of St.Louis Review*, 1969(10):10-19.
9. Brunner, K. and H. Meltzer. 1964. " Some Further Investigations of Demand and Supply Functions for Money," *The Journal of Finance*, 19(2): 240-283.
10. Bourne, C. 1976. "The Determination of Jamaica Money Stock: 1961-1971," *Social and Economic Studies*, 25(4):367-385.
11. McClean, A. W. A. 1985. "A Further Comment On Conventional Money Multiplier," *Social and Economic Studies*, 34(3):259-264.
12. He, P., L. X .Huang, and R. Wright. 2005. "Money and Banking In Search Equilibrium," *International Economic*

Review, 46(2): 637-670.

13. Berardi, M. 2007. " Beyond the Static Money Multiplier In Search of a Dynamic Theory of Money," in *Artificial Markets Modeling*, A. Consiglio, ed. Berlin, Heidelberg : Springer, pp. 3-16.

Distortional Lifshitz Vectors and Helicity in Nematic Free Energy Density

Amelia Carolina Sparavigna¹ 

¹ Department of Applied Science and Technology, Politecnico di Torino, Torino, Italy

Abstract: Here we discuss the free energy of nematic liquid crystals using two vectors and the helicity, with the aim of having a compact form of its density. The two vectors are due to the splay and bend distortions of the director field. They have a polar nature, whereas the helicity is a pseudoscalar.

1. Introduction

The free energy density of the bulk of nematics is a well-known object, fundamental for continuous theories of liquid crystals [1]. Here we propose an elementary approach to the free energy density mainly based on the role of scalars and pseudoscalars. Let us remember that pseudoscalars have odd parity upon spatial inversion, whereas scalars have even parity.

We will see that we can use two vectors, coming from the splay and bend distortion of the director field, vectors that we can define as distortional Lifshitz vectors. It is better to use the adjective “distortional” because Lifshitz vectors are specific vectors of the relativistic gravitational field. These distortional vectors have a polar nature. In addition them we need a pseudoscalar, the helicity, to write the nematic free energy density. The helicity squared gives rise to the twist contribution. Note that the distortional vectors that we will use do not depend on a polar or axial nature of the director field of nematic

liquid crystals. Even if this choice does not influence the final result, we will see that the director behaves like a vector potential.

2. The free energy of nematics

Let us consider the bulk free energy as discussed in the book by Landau and Lifshitz [2]. The free energy of a nematic liquid crystal can have only scalar terms of the director field \vec{n} and its derivatives. The true scalars can be obtained from the following product of derivatives:

$$\frac{\partial n_k}{\partial x_i} \frac{\partial n_l}{\partial x_m} \quad (1)$$

where x_i are the coordinates of the frame. Moreover:

$$\frac{\partial}{\partial x_i} \vec{n}^2 = 2n_k \frac{\partial n_k}{\partial x_i} = 0 \quad (2)$$

because $\vec{n}^2 = 1$. After contraction of indices or multiplying by \vec{n} , we find the invariants:

$$[(\vec{n} \cdot \nabla) \vec{n}]^2 ; \frac{\partial n_k}{\partial x_i} \frac{\partial n_k}{\partial x_i} ; (\nabla \cdot \vec{n})^2 ; \frac{\partial n_k}{\partial x_i} \frac{\partial n_i}{\partial x_k} \quad (3)$$

The last two terms differ by a divergence. Since the divergence goes into a surface term, we do not consider among the bulk terms. Therefore we can keep only the divergence squared $(\nabla \cdot \vec{n})^2$. The second term is the sum of the divergence squared and

$(\vec{n} \cdot \nabla \times \vec{n})^2$. Another possible contribution is $(\vec{n} \cdot \nabla \times \vec{n})(\nabla \cdot \vec{n})$, and we have also that $[(\vec{n} \cdot \nabla) \vec{n}]^2 = [\vec{n} \times \nabla \times \vec{n}]^2$. Therefore the free energy density is given by Landau and Lifshitz as:

$$F = F_o + b\vec{n} \cdot \nabla \times \vec{n} + \frac{a_1}{2} (\nabla \cdot \vec{n})^2 + \frac{a_2}{2} (\vec{n} \cdot \nabla \times \vec{n})^2 + \frac{a_3}{2} [\vec{n} \times \nabla \times \vec{n}]^2 + a_{12} (\vec{n} \cdot \nabla \times \vec{n})(\nabla \cdot \vec{n}) \quad (4)$$

The first term is a contribution that does not depend

on the director field. As [2] is telling, $(\vec{n} \cdot \nabla \times \vec{n})$ is



a pseudovector. The second term in (4) must have a coefficient b which is a pseudoscalar. As a consequence, this term exists in cholesteric nematic. The last term is equal to zero, because in nematics we

$$F = F_o + \frac{a_1}{2} (\nabla \cdot \vec{n})^2 + \frac{a_2}{2} (\vec{n} \cdot \nabla \times \vec{n})^2 + \frac{a_3}{2} [\vec{n} \times \nabla \times \vec{n}]^2 \quad (5)$$

In his book [3], S.A. Pikin is starting the discussion of free energy density from the order parameter tensorial field, which is given by:

$$Q_{ik}(\vec{r}) = Q(\vec{r}) \left(n_i(\vec{r}) n_k(\vec{r}) - \frac{1}{3} \delta_{ik} \right) \quad (6)$$

In the isotropic phase $Q = 0$. The orientation order parameter Q , which is a function of temperature, far from phase transition points is not subjected to strong thermal fluctuations. For this reason, Q can be viewed as a constant which is characterizing the features of the anisotropic medium at a fixed temperature. At the same time, the director \vec{n} is subjected to appreciable thermal fluctuations and changes relatively easily under the action of external fields [3]. This circumstance is one and the most important reason for the instabilities of the orientational structures, appearing in the liquid crystal both as a result of temperature changes and under external action.

Under the condition that function $\vec{n}(\vec{r})$ is slowly varying along the bulk, i.e., the derivatives of this function with respect to the coordinates are small, the

$$\nabla \times \vec{n} \quad ; \quad \vec{n} \nabla \cdot \vec{n} \quad ; \quad [\vec{n} \times \nabla \times \vec{n}] = -(\vec{n} \cdot \nabla) \vec{n} \quad (7)$$

Additional scalar invariants are:

$$(\nabla \times \vec{n})^2 \quad ; \quad (\vec{n} \cdot \nabla \times \vec{n}) \nabla \cdot \vec{n} \quad ; \quad [\vec{n} \times \nabla \times \vec{n}]^2 \quad ; \quad (\vec{n} \cdot \nabla \times \vec{n})^2 \quad (8)$$

Since the combination $(\vec{n} \cdot \nabla \times \vec{n}) \nabla \cdot \vec{n}$ is odd with respect to \vec{n} and a pseudoscalar, we do not use it. Moreover, as a result of the relation (see Appendix A):

$$(\nabla \times \vec{n})^2 = (\vec{n} \cdot \nabla \times \vec{n})^2 + (\vec{n} \times \nabla \times \vec{n})^2 \quad (9)$$

We have again:

$$F = F_o + \frac{a_1}{2} (\nabla \cdot \vec{n})^2 + \frac{a_2}{2} (\vec{n} \cdot \nabla \times \vec{n})^2 + \frac{a_3}{2} [\vec{n} \times \nabla \times \vec{n}]^2 \quad (10)$$

It is a combination of these three terms that can be used to represent an arbitrary deformation in a nematic liquid crystal. The coefficients of this combination are the elastic constant of splay, twist and bend respectively. It is often the case that all these three constants are of the same order of

require the symmetry $\vec{n} \rightarrow -\vec{n}$. The nematic bulk free energy density is:

orientational free energy density F of the deformed nematic can be expanded in powers of the derivatives of function $\vec{n}(\vec{r})$. Such an expansion of a scalar quantity must contain scalar combinations of the vector $\vec{n}(\vec{r})$ and its derivatives. As previously told, \vec{n} is a unit vector, which can enter only in even combinations due to the equivalence $\vec{n} \rightarrow -\vec{n}$. In addition, the total derivatives that make a contribution to the surface energy and not to the volume energy of the body must be dropped in the expression of F .

$\nabla \cdot \vec{n}$ is odd in \vec{n} , moreover it is a surface term, and $\vec{n} \cdot \nabla \times \vec{n}$ is a pseudoscalar. We use these terms as squared, $(\nabla \cdot \vec{n})^2$ and $(\vec{n} \cdot \nabla \times \vec{n})^2$, as well as the scalar products of the vectors formed by the vector \vec{n} and its first derivatives. There are three such independent vectors:

magnitude: the combination is commonly approximated to have $K = a_1 = a_2 = a_3$. This approximation is commonly referred to as the one-constant approximation and is used predominantly because the free energy density simplifies to the compact form:

$$F = F_o + \frac{K}{2} [(\nabla \cdot \vec{n})^2 + (\nabla \times \vec{n})^2] \quad (11)$$

For computation, this form is quite easy but it is mixing the distortional contributions.

We could imagine the uniform state as energetically favored, but this state is unstable relative to spatial modulations of the director. The presence of a

$$F_{chol} = \frac{K_2}{2} (q + \vec{n} \cdot \nabla \times \vec{n})^2 \quad (12)$$

in the free energy density. Let us note that q has the dimensions of a wave number. Pikin is remarking that this expression contains the pseudoscalar $(\vec{n} \cdot \nabla \times \vec{n})$ which is giving the helical structure.

In Eq.4, the term appears as $b\vec{n} \cdot \nabla \times \vec{n}$, requiring b as a pseudoscalar, according to the chiral nature of molecules. In (12), we have the contribution $K_2 q \vec{n} \cdot \nabla \times \vec{n}$: since K_2 is a scalar, this means that q is a pseudoscalar (the microscopic origin of the chiral term had been discussed in Ref.4).

As we have seen, the free energy density is assumed as a true scalar. Or, as it is told in [5], the contributions to the free energy density “of course, have to be true invariant scalar”. Let me open a discussion on the densities, as proposed by Dalton Schnack, in his paper published in the Lectures Notes in Physics [6]. In this paper, it is told that since the volume is a scalar triple product, that is, the scalar product of a vector by a surface vector, according to a parity transformation it is more properly described as a pseudoscalar. As a consequence of the pseudoscalar nature of the volume, the mass density and the pressure, the ratio of the internal energy and volume, behave like pseudoscalars. That is, these quantities have an odd parity. The reference is concluding telling that the resulting expressions that we are using must have a consistent parity. The volume discussed in [6] is of course the oriented volume, which averages out to zero. However, we can use the modulus of the oriented volume and therefore assume the energy density like a scalar.

After this general review of the bulk free energy density, let us try to obtain its terms using two vectors that we can define as the distortional Lifshitz vectors, and the helicity. In fact, the distortional vectors are contained in some Lifshitz invariants. Therefore, before discussing these vectors, let us shortly review the Lifshitz invariants and their role in the appearance on modulated structures.

3. Lifshitz invariants and modulated structures

According to Lifshitz [7], near a phase transition point, the system may be unstable with respect to distortions of the appropriate order parameter. This

macroscopic inhomogeneity of the director in the cholesteric liquid crystals at distances that are large compared to molecular dimensions is related with the existence of an invariant of the form:

instability may develop if the irreducible representation allows a quadratic anti-symmetric combination, linear both in the order parameter components and in their gradients. Therefore the contributions to the free-energy density of terms in the derivatives of the order parameter are governing the appearance of spatially modulated structure in magnetic materials and liquid crystals. And in fact, it is possible to see the same invariant in the free energy, the Lifshitz invariant, as the responsible of undulated patterns.

A specific formulation by vectors of the Lifshitz invariants was first proposed for some magnetic structures characterized by a modulation of the spin arrangements [8,9]. Within a continuum approximation of magnetic properties, the interactions responsible for these modulations are expressed by inhomogeneous invariants. These contributions to the free magnetic energy, involving first derivatives of magnetization with respect to spatial coordinates, are defined as the inhomogeneous Dzyaloshinskii-Moriya interactions [10,11]. These interactions are linear with respect to the first spatial derivatives of the magnetization \vec{M} in an anti-symmetric mathematical form.

The structure of the Lifshitz invariant is, in the case of the inhomogeneous Dzyaloshinskii-Moriya interaction, a product of three vectors. The three vectors are: a vector \vec{D} representing an internal or external field, a vector \vec{M} representing the local order parameter, and ∇ operating on the order parameter components. The product has the following form:

$$F_L = \vec{D} \cdot [\vec{M}(\nabla \cdot \vec{M}) - (\vec{M} \cdot \nabla)\vec{M}] \quad (13)$$

We used the Dzyaloshinskii-Moriya interactions in 1996, to study the field-induced phase transition of BiFeO₃ [12]. An antiferromagnetic vector \vec{L} characterizes the BiFeO₃ spin structure. A Landau-Ginzburg energy density of the spin structure was given in Ref.12, using the following vector:

$$\vec{A} = \vec{L}(\nabla \cdot \vec{L}) - (\vec{L} \cdot \nabla)\vec{L} \quad (14)$$

One term of the free energy density is the Lifshitz invariant given as:

$$F_L = -\bar{\alpha} \vec{P}_S \cdot \vec{A} \quad (15)$$

In (15), $\bar{\alpha}$ is the inhomogeneous relativistic constant and \vec{P}_S the spontaneous polarization.

In Ref.12, we investigated the influence of an electric field on the spatially modulated spin structure (SDW state), using the analogy with nematic liquid crystals to study magnetic materials.

4. The flexoelectric vectors in nematics

Let us consider a nematic liquid crystal and assume the order parameter described by the director field \vec{n} , which is giving the local mean orientation of the molecules. Vector \vec{A} in Eq.14 can then be written in the following form:

$$\vec{P} = e_S \vec{n} (\nabla \cdot \vec{n}) - e_B (\vec{n} \cdot \nabla) \vec{n} = e_S \vec{n} \operatorname{div} \vec{n} + e_B \vec{n} \times \operatorname{rot} \vec{n} \quad (17)$$

The two terms in the polarization vector are due to the splay and the bend contribution.

The coupling of the flexoelectric polarization \vec{P} with an external electric field results in the appearance of a periodic distortion, as the term shown by Eq.(15) in the free energy density of BiFeO₃, where we have the coupling of vector \vec{A} with a spontaneous polarization.

In the flexoelectricity, the polarization is induced by a not uniform deformation. If we consider the flexoelectric coupling, the electric field \vec{E} is a polar

$$\vec{A} = \vec{n} \operatorname{div} \vec{n} + \vec{n} \times \operatorname{rot} \vec{n} = \vec{n} \nabla \cdot \vec{n} + \vec{n} \times \nabla \times \vec{n} \quad (18)$$

Let us note that assuming \vec{n} a vector, \vec{A} is a vector. Behaving \vec{n} like a pseudovector \vec{A} is a vector. Let us consider the first term in \vec{A} : the divergence of a pseudovector is a pseudoscalar, which multiplied by the pseudovector, gives a vector (the gradient operator transforms like a polar vector). The second term is the cross product of a pseudovector and a vector, therefore it is a vector. The fact that the Lifshitz vector is a true vector is in agreement with its appearance in the polarization of the flexoelectric effect, which is coupled with the electric field. The scalar product of the electric field, a true vector, and

$$\vec{n} \cdot \vec{A} = \vec{n} \cdot (\vec{n} \nabla \cdot \vec{n} + \vec{n} \times \nabla \times \vec{n}) = \vec{n} \cdot \vec{n} \nabla \cdot \vec{n} + \vec{n} \cdot (\vec{n} \times \nabla \times \vec{n}) = \nabla \cdot \vec{n} \quad (20)$$

This term does not appears because it does not satisfy symmetry $\vec{n} \rightarrow -\vec{n}$. The term squared is a correction of the free energy density.

Let us consider:

$$\vec{n} \times \vec{A} = \vec{n} \times (\vec{n} \nabla \cdot \vec{n} + \vec{n} \times \nabla \times \vec{n}) = \vec{n} \times \vec{n} \nabla \cdot \vec{n} + \vec{n} \times (\vec{n} \times \nabla \times \vec{n}) = \vec{n} \times (\vec{n} \times \nabla \times \vec{n}) \quad (21)$$

$$\vec{A} = \vec{n} (\nabla \cdot \vec{n}) - (\vec{n} \cdot \nabla) \vec{n} = \vec{n} \operatorname{div} \vec{n} + \vec{n} \times \operatorname{rot} \vec{n} \quad (16)$$

This vector is well known in the physics of liquid crystals. It is encountered in the structure of the flexoelectric contribution to the free energy which is

$f_{flexo} = -\vec{P} \cdot \vec{E}$. Flexoelectricity is a property of liquid crystals similar to the piezoelectric effect [13]. A distortion of the director field can induce a macroscopic polarization within the material [11,13].

The polarization vector \vec{P} , a polar vector, in the flexoelectric term is then described with a distortion in the nematic director field:

vector, the polarization is a polar vector, and then the additional term in the free energy density is a scalar.

\vec{A} has the nature of a vector, independently of the choice of \vec{n} as a vector or a pseudovector.

5. The distortional Lifshitz vectors and the free energy density

As we have previously discussed, the Lifshitz invariant can be defined using the vector:

\vec{A} vector gives a scalar term for the bulk free energy density. Therefore, let us consider some scalars that we can have after this vector:

$$\vec{A} \cdot \vec{A} = (\vec{n} \nabla \cdot \vec{n})^2 + (\vec{n} \times \nabla \times \vec{n})^2 \quad (19)$$

because $\vec{n} \cdot (\vec{n} \times \nabla \times \vec{n})$ is equal to zero for the properties of the cross product. The two terms are the splay and the bend contributions to the free energy. Let us try:

Again this term does not appear because of the required symmetry $\vec{n} \rightarrow -\vec{n}$. The term squared:

$$\begin{aligned} (\vec{n} \times \vec{A})^2 &= (\vec{n}(\vec{n} \cdot \nabla \times \vec{n}) - \nabla \times \vec{n}(\vec{n} \cdot \vec{n}))^2 = (\vec{n}(\vec{n} \cdot \nabla \times \vec{n}) - \nabla \times \vec{n})^2 = \\ &= (\vec{n} \cdot \nabla \times \vec{n})^2 - 2\vec{n}(\vec{n} \cdot \nabla \times \vec{n}) \cdot \nabla \times \vec{n} + (\nabla \times \vec{n})^2 = -(\vec{n} \cdot \nabla \times \vec{n})^2 + (\nabla \times \vec{n})^2 \end{aligned} \quad (22)$$

We have that: $(\nabla \times \vec{n})^2 = (\vec{n} \cdot \nabla \times \vec{n})^2 + (\vec{n} \times \nabla \times \vec{n})^2$ (see Appendix A), and then:

$$(\vec{n} \times \vec{A})^2 = -(\vec{n} \cdot \nabla \times \vec{n})^2 + (\nabla \times \vec{n})^2 = -(\vec{n} \cdot \nabla \times \vec{n})^2 + (\vec{n} \cdot \nabla \times \vec{n})^2 + (\vec{n} \times \nabla \times \vec{n})^2 = (\vec{n} \times \nabla \times \vec{n})^2 \quad (23)$$

From the previous equation, we see that we can obtain only two terms of the free energy density:

$$F = F_o + \frac{a_1}{2} (\nabla \cdot \vec{n})^2 + \frac{a_2}{2} (\vec{n} \cdot \nabla \times \vec{n})^2 + \frac{a_3}{2} [\vec{n} \times \nabla \times \vec{n}]^2 \quad (24)$$

Splitting \vec{A} vector in two vectors:

$$\vec{A} = \vec{A}_1 + \vec{A}_3 \quad ; \quad \vec{A}_1 = \vec{n} \nabla \cdot \vec{n} \quad ; \quad \vec{A}_3 = \vec{n} \times \nabla \times \vec{n} \quad (25)$$

We see that $\vec{A}_1 \cdot \vec{A}_3 = 0$ and $\vec{A} \cdot \vec{A} = \vec{A}_1^2 + \vec{A}_3^2$.

These are the two distortional Lifshitz vectors, which are polar orthogonal vectors, able to provide two terms of the free energy (splay and bend), but not the twist term $(\vec{n} \cdot \nabla \times \vec{n})^2$. In fact, this is a helicity term, which has a pseudoscalar nature, squared to be consistent with the true scalar nature of the free energy density.

Let us therefore define \vec{A}_1, \vec{A}_3 as the distortion vectors in general and add to them a pseudoscalar to obtain all the contributions of the bulk free energy.

6. The helicity density

In studying fluids, the helicity density is defined as:

$$h = \vec{v} \cdot \nabla \times \vec{v} \quad (26)$$

where \vec{v} is the velocity. The helicity density is a pseudoscalar, having the same form of $(\vec{n} \cdot \nabla \times \vec{n})$, that we have squared in the free energy density. And this is the pseudoscalar, that we are not able to obtain using the Lifshitz vectors. The pseudo nature of this term is forbidding its creation from the two orthogonal Lifshitz vectors. In particle physics, the helicity is the projection of the spin onto the direction of momentum. For massless particles, such as the photon, the particle appears to spin in the same direction along its axis of motion regardless of point of view of the observer. That is, the helicity is a relativistic invariant.

In electromagnetism, the magnetic helicity density is given by:

$$h = \vec{A} \cdot \nabla \times \vec{A} \quad (27)$$

Polar vector \vec{A} is the vector potential. It is a vector field and its curl is the magnetic field: $\vec{B} = \nabla \times \vec{A}$. If a vector field admits a vector potential \vec{A} , then the equality $\nabla \cdot (\nabla \times \vec{A}) = 0$ implies that \vec{B} must be a solenoid vector field. The vector potential is not unique: if \vec{A} is a vector potential, so is

$$\vec{A} + \nabla f \quad (28)$$

In (28), f is any continuously differentiable scalar function. This follows from the fact that the curl of the gradient is zero. This non-uniqueness leads to a degree of freedom in the formulation of electrodynamics which implies the choice of a gauge. In the case of the nematic liquid crystals, the director \vec{n} behaves like \vec{A} . And imposing \vec{n} as a unit vector, we are fixing the gauge. The free energy density of a nematic can be written in the following form:

$$F = F_o + \frac{a_1}{2} A_1^2 + \frac{a_3}{2} A_3^2 + \frac{a_2}{2} h^2 \quad (29)$$

Here I used a helicity different from the conserved quantity in nematic liquid crystal flows, which is given in Ref.14. In the case of a cholesteric:

$$F = F_o + bh + \frac{a_1}{2} A_1^2 + \frac{a_3}{2} A_3^2 + \frac{a_2}{2} h^2 \quad (30)$$

Equation (29) is a quite compact form of linear combinations of scalars. This form of the free energy density has been obtained using the triplet

$(\vec{A}_1, \vec{A}_3, h)$, of two polar vectors and a pseudoscalar. A motivation for the use of such a triplet is to increase the analogy of the distortional energy density with field theories. Second-order elasticity and surface terms are under investigation to obtain some similar results from terms already proposed in [15].

Appendix A


Let us show that: $(\nabla \times \vec{n})^2 = (\vec{n} \cdot \nabla \times \vec{n})^2 + (\vec{n} \times \nabla \times \vec{n})^2$. Let us use: $(\nabla \times \vec{n})_x = R_x$, $(\nabla \times \vec{n})_y = R_y$ and $(\nabla \times \vec{n})_z = R_z$. We have:

$$\begin{aligned} (\vec{n} \cdot \nabla \times \vec{n})^2 + (\vec{n} \times \nabla \times \vec{n})^2 &= (n_x R_x + n_y R_y + n_z R_z)^2 + \\ &+ (n_y R_z - n_z R_y)^2 + (n_x R_z - n_z R_x)^2 + (n_x R_y - n_y R_x)^2 = \\ &= n_x^2 R_x^2 + n_y^2 R_y^2 + n_z^2 R_z^2 + 2n_x n_y R_x R_y + 2n_x n_z R_x R_z + 2n_y n_z R_y R_z + \\ &+ n_y^2 R_z^2 + n_z^2 R_y^2 - 2n_y n_z R_y R_z + n_x^2 R_z^2 + n_z^2 R_x^2 - 2n_x n_z R_x R_z + n_x^2 R_y^2 + n_y^2 R_x^2 - 2n_x n_y R_x R_y = \\ &= n_x^2 R_x^2 + n_y^2 R_y^2 + n_z^2 R_z^2 + n_y^2 R_z^2 + n_z^2 R_y^2 + n_x^2 R_z^2 + n_z^2 R_x^2 + n_x^2 R_y^2 + n_y^2 R_x^2 = \\ &= n_x^2 R_x^2 + n_y^2 R_x^2 + n_z^2 R_x^2 + n_x^2 R_y^2 + n_y^2 R_y^2 + n_z^2 R_y^2 + n_x^2 R_z^2 + n_y^2 R_z^2 + n_z^2 R_z^2 = R_x^2 + R_y^2 + R_z^2 \\ &= (\nabla \times \vec{n})^2 \end{aligned}$$

References

- [1] G. Barbero and L.R. Evangelista, An Elementary Course on the Continuum Theory for Nematic Liquid Crystals, World Scientific, 2001.
- [2] L.D. Landau and E.M. Lifshitz, *Statistical Physics*, Pergamon Press, Oxford, 1980.
- [3] S.A. Pikin, *Structural Transformations In Liquid Crystals*, Gordon and Breach Science Publishers, 1991
- [4] A. B. Harris, Randall D. Kamien, T. C. Lubensky, Phys. Rev. Lett. 78, 1476–1479 (1997), Microscopic Origin of Cholesteric Pitch, <http://arxiv.org/pdf/cond-mat/9607084v3.pdf>
- [5] Mark Warner, Eugene Michael Terentjev, Liquid Crystal Elastomers, Oxford University Press, 31/mag/2007
- [6] Dalton Schnack, Review of Scalars, vectors, tensors and dyads, Lectures Notes in Physics, Springer, 780, 2009, pp.5-18.
- [7] E.M. Lifschitz, On the theory of second-order phase transitions. Zh. Eksp. Teor. Fiz. 1941, 11, 255-269.
- [8] I.E. Dzyaloshinskii, Theory of helicoidal structures in antiferromagnets .1. Nonmetals, Sov. Phys. JETP 1964, 19, 960.
- [9] T. Moriya, Anisotropic Superexchange Interaction and Weak Ferromagnetism, Phys. Rev. 1960, 120, 91.
- [10] A.N. Bogdanov, U.K. Röbber, M. Wolf, and K.-H. Müller, Magnetic structures and reorientation transitions in noncentrosymmetric uniaxial antiferromagnets, arXiv:cond-mat/0206291, 2002.
- [11] A. Sparavigna, Role of Lifshitz Invariants in Liquid Crystals, Materials, 2009, 2(2), 674-698.
- [12] A.Sparavigna, A.Strigazzi, A.K.Zvezdin, Phys. Rev. B 1994, 50, 2953.
- [13] R.B. Meyer, Piezoelectric effects in liquid crystals, Physical Review Letters, Vol. 22(18), 1969, 918-921.
- [14] François Gay-Balmaz, Cesare Tronci, The helicity and vorticity of liquid crystal flows, arXiv, 2010, <http://arxiv.org/abs/1006.2984>
- [15] G. Barbero, A. Sparavigna, A. Strigazzi, The structure of the distortion free-energy density in nematics: second- order elasticity and surface terms, Nuovo Cimento, 12D, 1990, 1259-1272.

Modelling Monthly Rainfall Data of Port Harcourt, Nigeria by Seasonal Box-Jenkins Methods

Ette Harrison Etuk¹, Imoh Udo Moffat², Benjamin Ele Chims³

¹ Department of Mathematics/Computer Science, Rivers State University of Science and Technology, Nigeria

² Department of Mathematics, Statistics and Computer Science, University of Uyo, Nigeria

³ Department of Mathematics and Statistics, Rivers State Polytechnic, Bori, Nigeria

Abstract: Brief review of literature of the well documented seasonal Box-Jenkins modelling is done. Rainfall is a seasonal phenomenon the world over. For illustrative purposes, monthly rainfall as measured in Port Harcourt, Nigeria, is modelled by a $(5, 1, 0) \times (0, 1, 1)_{12}$ seasonal ARIMA model. The time-plot shows no noticeable trend. The known and expected seasonality is clear from the plot. Seasonal (i.e. 12-point) differencing of the data is done, then a nonseasonal differencing is done of the seasonal differences. The correlogram of the resultant series reveals the expected 12-monthly seasonality, and the involvement of a seasonal moving average component in the first place and a nonseasonal autoregressive component of order 5. Hence the model mentioned above. The adequacy of the modelled has been established.

Keywords: Seasonal Time Series, ARIMA model, rainfall, Port Harcourt

1. Introduction

A time series is defined as a set of data collected sequentially in time. It has the property that neighbouring values are correlated and this tendency is called *autocorrelation*. A time series is said to be stationary if it has a constant mean and variance. Moreover the autocorrelation is a function of the lag separating the correlated values and is called the *autocorrelation function* (ACF).

A stationary time series $\{X_t\}$ is said to follow an *autoregressive moving average model of orders p and q* (designated ARMA(p, q)) if it satisfies the following difference equation

$$X_t - \alpha_1 X_{t-1} - \alpha_2 X_{t-2} - \dots - \alpha_p X_{t-p} = \varepsilon_t + \beta_1 \varepsilon_{t-1} + \beta_2 \varepsilon_{t-2} + \dots + \beta_q \varepsilon_{t-q} \quad (1)$$

Or

$$A(L)X_t = B(L)\varepsilon_t \quad (2)$$

where $\{\varepsilon_t\}$ is a sequence of random variables with zero mean and constant variance, called a *white noise process*, and the α_i 's and β_j 's constants; $A(L) = 1 - \alpha_1 L - \alpha_2 L^2 - \dots - \alpha_p L^p$ and $B(L) = 1 + \beta_1 L + \beta_2 L^2 + \dots + \beta_q L^q$ and L the backward shift operator defined by $L^k X_t = X_{t-k}$.

If $p = 0$, the model (1) becomes a *moving average model of order q* (designated MA(q)). If, however, $q = 0$ it becomes an *autoregressive process of order p*

(designated AR(p)). Besides stationarity, invertibility is another important necessity for a time series. It ensures the uniqueness of the model covariance structure and, therefore, allows for meaningful expression of current events in terms of the past history of the series [1].

An AR(p) model may be more specifically written as

$$X_t + \alpha_{p1} X_{t-1} + \alpha_{p2} X_{t-2} + \dots + \alpha_{pp} X_{t-p} = \varepsilon_t$$

The sequence of the last coefficients $\{\alpha_{ii}\}$ is called the *partial autocorrelation function* (PACF) of $\{X_t\}$. The ACF of an MA(q) model cuts off after lag q whereas that of an AR(p) model is a combination of sinusoidals dying off slowly. On the other hand the PACF of an MA(q) model dies off slowly whereas that of an AR(p) model cuts off after lag p. AR and MA models are known to exhibit some duality relationships.

Parametric parsimony consideration in model building entails the use of the mixed ARMA fit in preference to either the pure AR or the pure MA fit. Conditions for stationarity and invertibility for model (1) or (2) are that the equations $A(L) = 0$ and $B(L) = 0$ should have roots outside the unit circle respectively.

Often, in practice, a time series is non-stationary. Box and Jenkins [1] proposed that differencing of appropriate order could make a non-stationary series $\{X_t\}$ to become stationary. Let degree of differencing



necessary for stationarity be d . Such a series $\{X_t\}$ may be modeled as

$$A(L)\nabla^d X_t = B(L)\varepsilon_t \quad (3)$$

where $\nabla = 1 - L$ and in which case $A(L)\nabla^d = 0$ shall have unit roots d times. Then differencing to degree d renders the series stationary. The model (3) is said to be an *autoregressive integrated moving average model of orders p , d and q* and designated ARIMA(p , d , q).

2. Seasonal ARIMA Models

A time series is said to be seasonal of order d if there exists a tendency for the series to show periodic behaviour after every time interval d . The time series $\{X_t\}$ is said to follow a multiplicative $(p, d, q) \times (P, D, Q)_s$ seasonal ARIMA model if

$$A(L)\Phi(L^s)\nabla^d\nabla_s^D X_t = B(L)\Theta(B^s)\varepsilon_t \quad (4)$$

where Φ and Θ are polynomials of order P and Q respectively. That is,

$$\Phi(L^s) = 1 + \phi_1 L^s + \dots + \phi_P L^{sP} \quad (5)$$

$$\Theta(L^s) = 1 + \theta_1 L^s + \dots + \theta_Q L^{sQ} \quad (6)$$

where the ϕ_i and the θ_j are constants such that the zeros of the equations (5) and (6) are all outside the unit circle for stationarity or invertibility respectively. Equation (5) represents the autoregressive operator whereas (6) represents the moving average operator. Here $\nabla_s = 1 - L^s$.

Existence of a seasonal nature is often evident from the time plot. Moreover for a seasonal series the ACF or correlogram exhibits a spike at the seasonal lag. Box and Jenkins[1] and Madsen [2] and Etuk[3] are a few authors that have written extensively on such models. A knowledge of the theoretical properties of the models provides basis for their identification and estimation.

The purpose of this paper is to fit a seasonal ARIMA model to the Port Harcourt monthly rainfall totals. Osarumwense[4] has modelled the quarterly rainfall data as a $(0, 0, 0) \times (2, 1, 0)_4$ seasonal ARIMA model. Olofintoye and Sule[5] fitted the trend line $y = 0.3903x - 587.5125$ which is indicative of a positive trend for rainfall. A few other researchers who have published research results on Port Harcourt rainfall are Chiadikobi et al.[6], Dike and Nwachukwu[7] and Salako[8].

3. Materials and Methods

The data for this work are monthly rainfall totals from 1990 to 2006 obtainable from the meteorological centre of Port Harcourt International

Airport.

3.1. Determination of the orders d , D , P , q and Q :

Seasonal differencing is necessary to get rid of the seasonal trend. If there is secular trend non-seasonal differencing will be necessary to remove it. In order for the model not to be too complicated it has been advised that orders of differencing d and D should add up to at most 2 (i.e. $d + D < 3$). The involvement of a seasonal AR component is suggestive if the ACF of the differenced series has a positive spike at the seasonal lag; if, however, it has a negative spike at the seasonal lag then a seasonal MA term is suggestive.

As already mentioned above, an AR(p) model has a PACF which truncates at lag p and an MA(q) has an ACF which truncates at lag q . In practice $\pm 2/\sqrt{n}$ where n is the sample size are the non-significance limits for both functions.

3.2. Model Estimation

The fact that items of a white noise process are involved in an ARIMA model entails a nonlinear iterative process in the estimation of the parameters. An optimization criterion like least error sum of squares, maximum likelihood or maximum entropy is used. An initial estimate is usually chosen. Each iterative step is expected to be an improvement of the last one until the estimate converges to an optimal one. However, for pure AR and pure MA models linear optimization techniques exist (See for example, Box and Jenkins[1], Oyetunji[9]. There are efforts to propose and adopt linear methods to estimate ARMA models (See for example, Etuk[10, 11]. We shall use Eviews software which employs the least squares approach involving nonlinear iterative techniques.

3.3. Diagnostic Checking

The estimated model should be tested for goodness-of-fit. This shall be done by some analysis of the residuals of the model. Should the model be correct, the residuals would be uncorrelated and would follow a normal distribution with mean zero and constant variance. The autocorrelations of the residuals should not be significantly different from zero.

4. Results and Discussion

The time plot of the original series RAINFALL in Figure 1 shows seasonality as expected but no secular trend. Seasonal (i.e. 12-month) differencing of the series produces a series SDRAINFALL with seasonality (see Figure 2). Non-seasonal differencing of SDRAINFALL yields a series DSDRAINFALL with seasonality (See Figure 3). Its ACF in Figure 4 has a negative spike at lag 12 revealing a seasonality of lag 12 and a seasonal MA component of order one

to the model. The PACF shows spikes at the first five lags suggesting a non-seasonal AR component of order five. We therefore propose the seasonal model

$$X_t + \alpha_1 X_{t-1} + \alpha_2 X_{t-2} + \alpha_3 X_{t-3} + \alpha_4 X_{t-4} + \alpha_5 X_{t-5} = \varepsilon_t + \beta_{12} \varepsilon_{t-12} \quad (7)$$

where $X = \text{DSDRAIN FALL}$. The estimation of the model is summarized in Table 1. The fitted model is given by

$$X_t + 0.84X_{t-1} + 0.67X_{t-2} + 0.62X_{t-3} + 0.45X_{t-4} + 0.23X_{t-5} = \varepsilon_t - 0.89\varepsilon_{t-12}$$

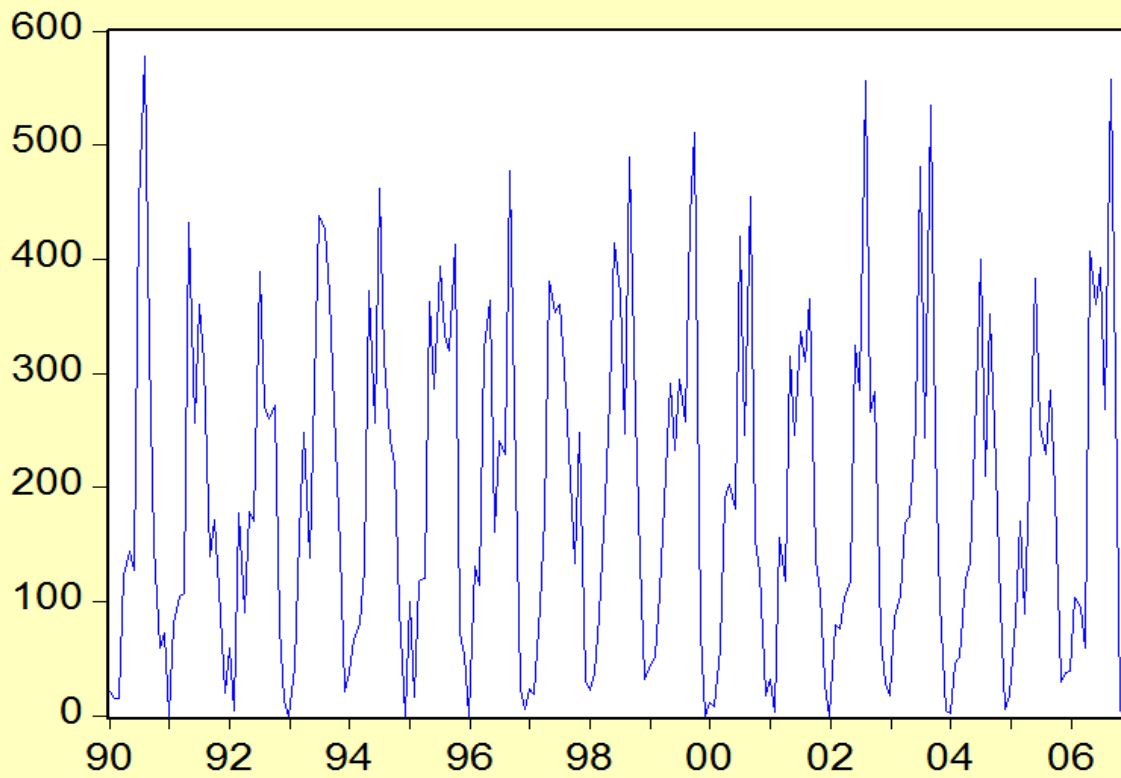
All coefficients are significantly different from zero, each being larger than twice its standard error. As high as 72% of the variation in DSDRAIN FALL is explained by the model. In Figure 5, the fitted model agrees closely with the actual data. In Figure 6, the correlogram of the residuals indicates model adequacy since virtually all the autocorrelations are non-significant.

5. Conclusion

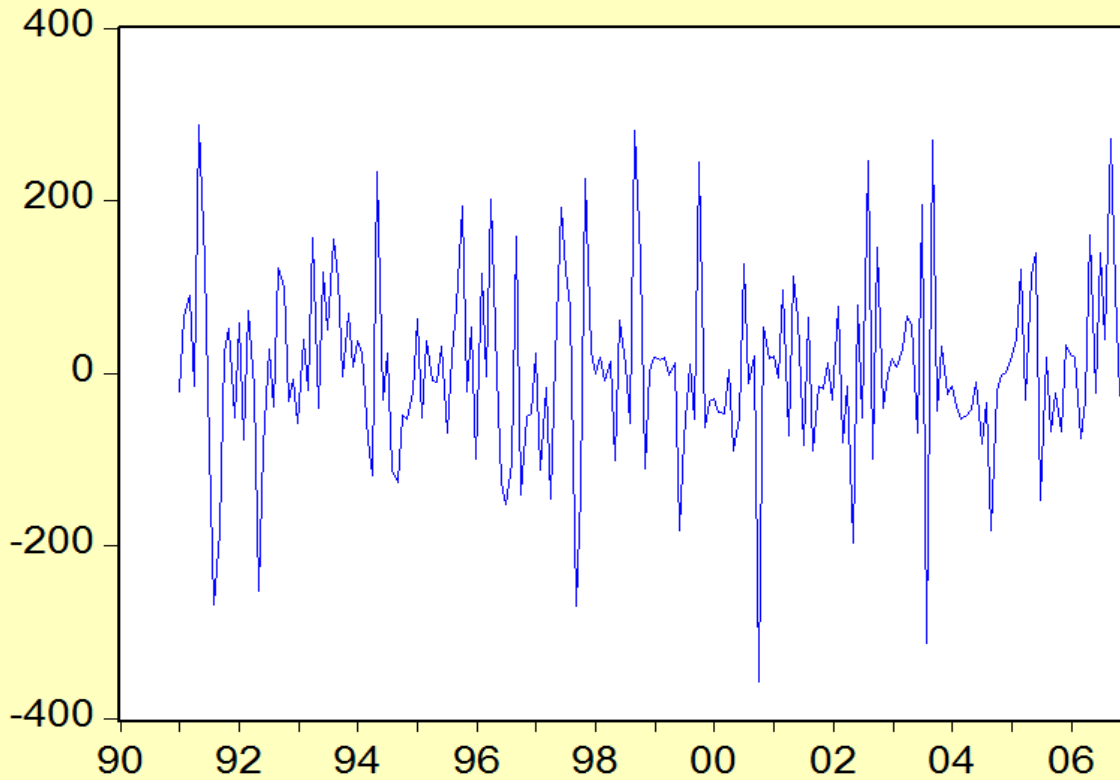
The literature of seasonal Box-Jenkins modelling is briefly reviewed. A $(5, 1, 0) \times (0, 1, 1)_{12}$ seasonal autoregressive integrated moving average model is fitted to rainfall data in Port Harcourt. The model has been shown to be adequate.

References

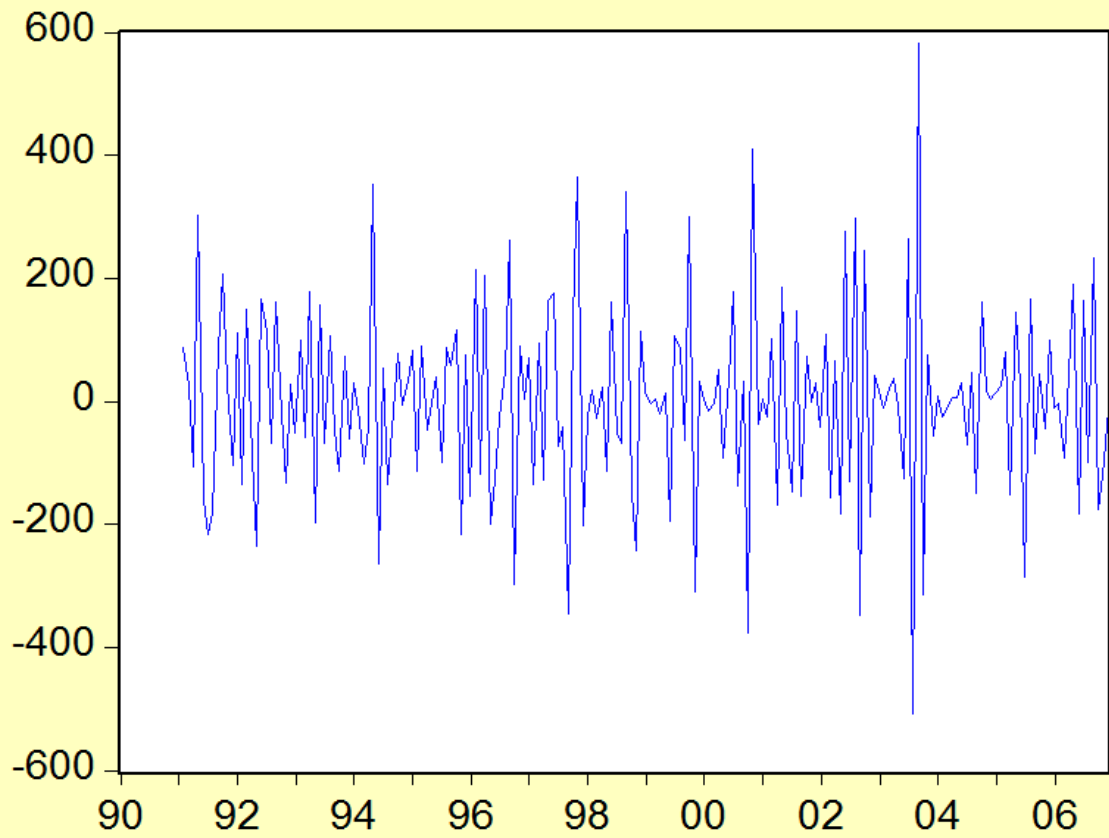
- [1] Box, G. E. P. and Jenkins, G. M. (1976). "Time Series Analysis, Forecasting and Control", *Holden-Day*, San Francisco.
- [2] Madsen, H. (2008). "Time Series Analysis", *Chapman & Hall/CRC*, London.
- [3] Etuk, E. H. (2013). A Seasonal Time Series for Nigerian Monthly Air Traffic Data. *International of Review and Research in Applied Sciences*, 14, 3, pp. 596 – 602.
- [4] Osarumwense, O.I. (2013). Applicability of Box Jenkins SARIMA Model in Rainfall Forecasting: A Case Study of Port-Harcourt South South Nigeria. *Canadian Journal on Computing in Mathematics, Natural Sciences, Engineering and Medicine*, 4, 1, pp. 1-4-.
- [5] Olofinloye, O. O. And Sule, B. F. (2010). Impact of Global Warming on the Rainfall and Temperature in the Niger Delta of Nigeria. *USEP-Journal of Research Information in Civil Engineering*, 7, 2, pp. 33 – 48.
- [6] Chiadikobi, K. C., Omoboriowo, A. O., Chiaganam, O. I., Opatola, A. O. And Oyeibanji, O. (2011). Flood Risk Assessment of Port Harcourt, Rivers State, Nigeria. *Advances in Applied Research*, 2, 6: pp. 287 – 298.
- [7] Dike, B. U. And Nwachukwu, B. A. (2003). Analysis of Nigerian Hydrometeorological Data. *Nigerian Journal of Technology*, 22, 1, pp. 29 – 38.
- [8] Salako, F. K. (2007). Rainfall seasonality in the Niger Delta Belt, Nigeria. *Journal of Geography and Regional*, 52, 2, pp. 51 – 60.
- [9] Oyetunji, O. B. (1985). "Inverse Autocorrelations and Moving Average Time Series Modelling". *Journal of Official Statistics*, 1, pp. 315 – 322.
- [10] Etuk, E. H. (1987). *On the Selection of Autoregressive Moving Average Models*. An unpublished Ph. D. Thesis, Department of Statistics, University of Ibadan, Nigeria.
- [11] Etuk, E. H. (1998). "An Autoregressive Integrated Moving Average (ARIMA) Model: A Case Study". *Discovery and Innovation*, 10, 1 & 2, pp. 23 – 26.



— FIGURE 1: RAINFALL



— FIGURE 2: SDRAINFALL



— FIGURE 3: DSDRAINFALL

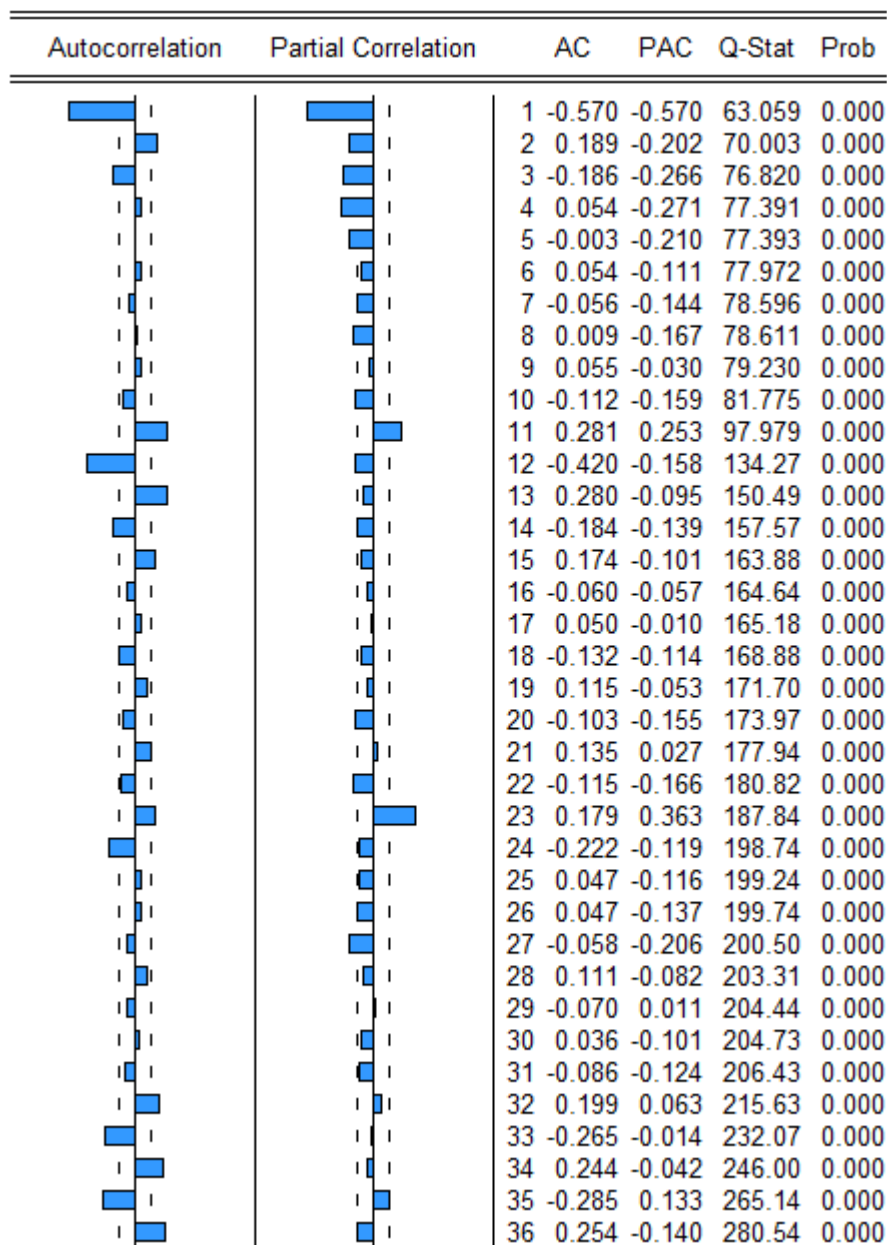
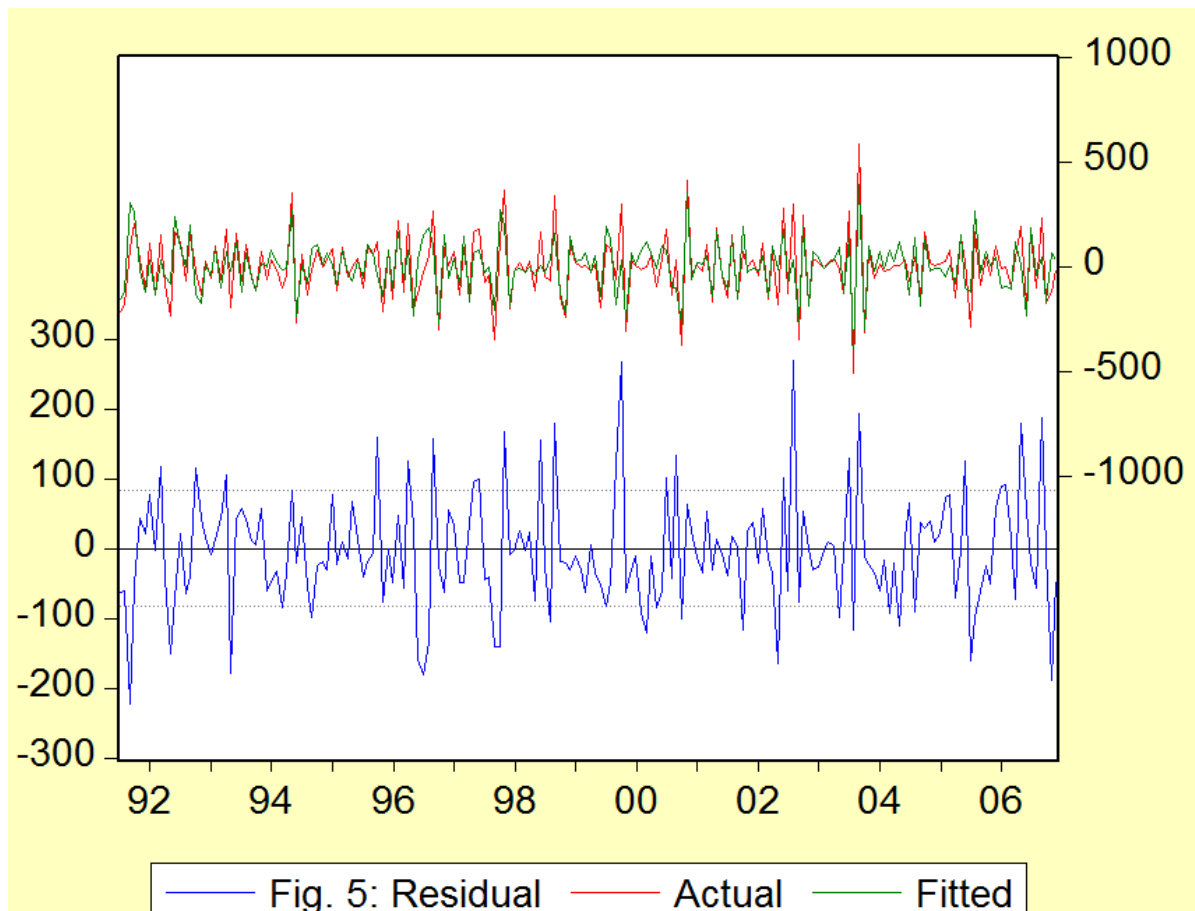


FIGURE 4: CORRELOGRAM OF DSDRAINFALL

Dependent Variable: DSDRAINFALL
Method: Least Squares
Date: 03/05/12 Time: 20:51
Sample(adjusted): 1991:07 2006:12
Included observations: 186 after adjusting endpoints
Convergence achieved after 19 iterations
Backcast: 1990:07 1991:06

Variable	Coefficient	Std. Error	t-Statistic	Prob.
AR(1)	-0.839691	0.057295	-14.65545	0.0000
AR(2)	-0.671853	0.070072	-9.587996	0.0000
AR(3)	-0.622000	0.073157	-8.502286	0.0000
AR(4)	-0.449151	0.069994	-6.417028	0.0000
AR(5)	-0.229516	0.058884	-3.897737	0.0001
MA(12)	-0.885785	0.000120	-7376.413	0.0000
R-squared	0.715492	Mean dependent var	-0.897849	
Adjusted R-squared	0.707589	S.D. dependent var	153.9822	
S.E. of regression	83.26588	Akaike info criterion	11.71368	
Sum squared resid	1247977.	Schwarz criterion	11.81774	
Log likelihood	-1083.372	F-statistic	90.53437	
Durbin-Watson stat	2.122132	Prob(F-statistic)	0.000000	
Inverted AR Roots	.34+.73i -.73	.34-.73i	-.39+.57i -.39-.57i	
Inverted MA Roots	.99 .49+.86i -.49+.86i	.86+.49i .00-.99i -.86-.49i	.86-.49i -.00+.99i -.86+.49i	.49-.86i -.49-.86i -.99



Date: 03/31/12 Time: 15:45
Sample: 1991:07 2006:12
Included observations: 186
Q-statistic probabilities adjusted for 6 ARMA term(s)

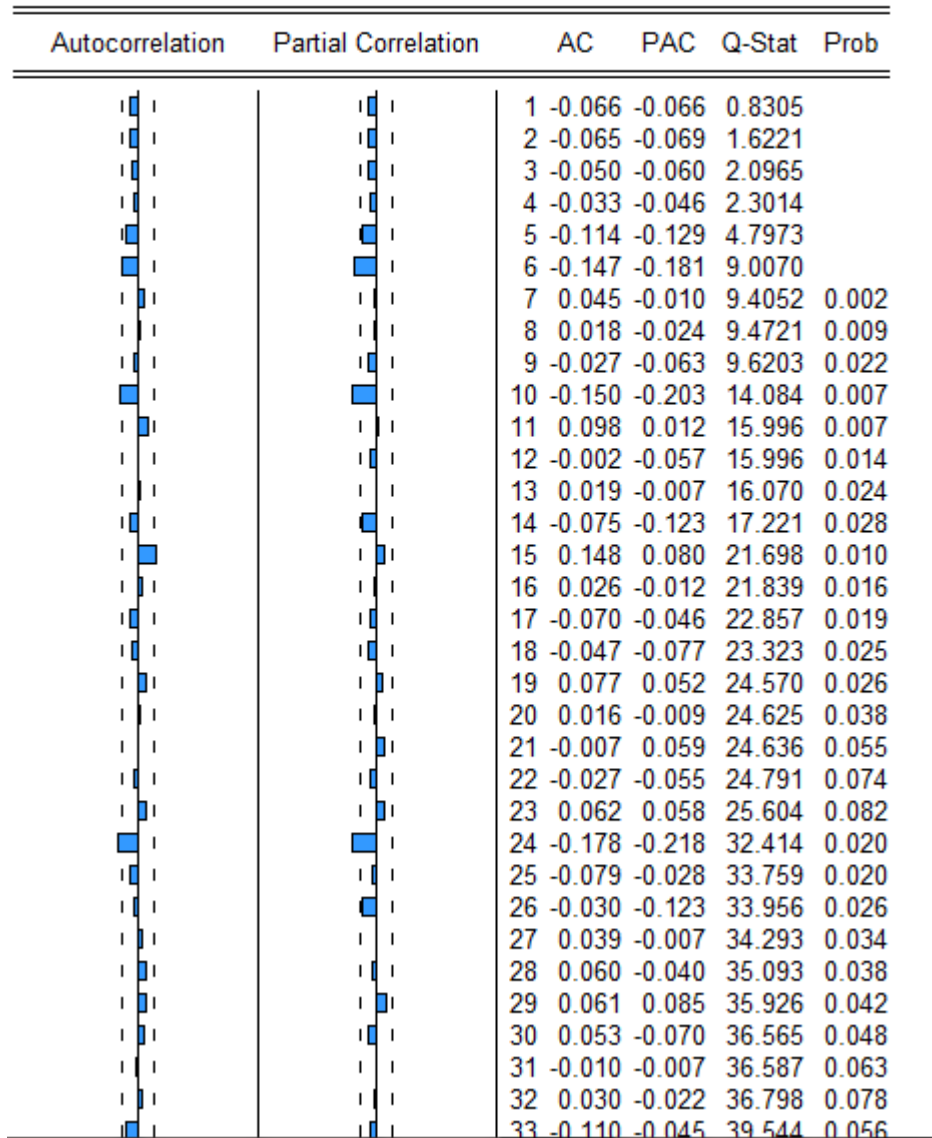


FIGURE 6: CORRELOGRAM OF RESIDUALS

POST-HARVEST CONSERVATION OF ORANGE cv. FOLHA MURCHA TREATED WITH 1-MCP AND STORED UNDER REFRIGERATION

Cassia Inês Lourenzi Franco Rosa¹, Edmar Clemente², Auri
Brackmann³

¹ Engenheira Agrônoma, Doutora, Universidade Estadual do Centro Oeste. Rua Simeão Camargo Varela de Sá, 03 - Cx. Postal 3010 - CEP 85040-080 - Guarapuava – Paraná

² Químico, Doutor, Universidade Estadual de Maringá

³ Engenheiro Agrônomo, Doutor, Universidade Federal de Santa Maria

Abstract: This study aimed to evaluate the postharvest quality of oranges cv. Folha Murcha, treated with 1-MCP and stored for 60 days at 7, 14 and 25 °C. The analysis performed every 15 days were: weight loss, percentage of juice, content of soluble solids (SS), titratable acidity (TA), ratio (SS/TA), and content of vitamin C, phenolic compounds and total carotenoids. Results showed: 1-MCP did not provide greater postharvest conservation for fruits analyzed; the application of 1-MCP did not changed the chemical characteristics as SS, TA, vitamin C, carotenoids and phenolic compounds; and the shorter the period between harvesting and cooling, the better was the preservation of fruits.

Keywords: *Citrus sinensis* L., ethylene, low temperature.

1. Introduction

Oranges are the main Citrus species cultivated in Brazil, where domestic production is focused on the export of their orange juice; because of the constant dissemination about its nutritional qualities, demand for this product is in full expansion. In Paraná State, the citrus industry is sustained mainly by the production of mandarin and orange (SCHÄFER and DORNELLES, 2000).

Oranges are classified as non-climacteric fruits, i.e., are not able to complete the ripening off the mother plant, given their low and constant rate of respiration and ethylene production. However, despite the low production, ethylene also interferes in the fruit ripening and can often affect the qualitative aspects of the product (CHITARRA and CHITARRA, 2005).

The effects of ethylene on the ripening of fruits in general make necessary to adopt some techniques, especially those of post-harvest, which can preserve them for longer time. One of the most recent examples is the use of 1-methylcyclopropene (1-MCP), a product in the form of gas that has characteristically the fact of linking to ethylene receptor, and therefore preventing its action (GIRARDI et al, 2007). The application of 1-MCP in horticultural products has obtained positive results for several fruits and vegetables, but studies

on its effect on non-climacteric fruits, such as oranges, are scarce.

Given the importance of citrus in the State of Paraná and the scarcity of studies on the product 1-MCP on citrus fruits and more specifically oranges, studies addressing to this issue become relevant. In this context, the present study aimed to evaluate the conservation and post-harvest quality of oranges cv. Folha Murcha, through the use of 1-MCP and cooling for 60 days of storage.

2. Material and Methods

The fruits of cv. Folha Murcha were collected in 2008/2009 and 2009/2010 seasons in the experimental orchard of Cocamar Cooperativa Agroindustrial, located in Paranavai County, Northwest Paraná (23 ° 4 '22 "S, 52 ° 27' 54" W); fruits were harvested in December in both seasons. In the first year (2008/2009), soon after harvesting, fruits were transported to the Laboratory of Food Biochemistry, State University at Maringá - UEM, and in the next harvesting (2009 / 2010), the fruits were transported to the Center for Post-harvest Research, Federal University at Santa Maria (UFSM-NPP), Santa Maria, State of Rio Grande do Sul.

After the reception in the laboratory, fruits were sanitized and divided into parcels. The 1-MCP applied is the commercial product SmartFreshTM from Rohm and Hass Co., in the form of watered



powder containing 0.14% of active ingredient. Four doses were used: T1: 0; T2: 0.1; T3: 0.5 and T4: 1.0 $\mu\text{L L}^{-1}$, and the amount of product required for each concentration was calculated according to the volume of boxes and the concentration of ingredient present in the commercial product. The product in the form of powder was placed in 20 mL flasks which were tightly sealed with rubber strips and later water Milli-Q was added at room temperature via syringe and then flasks were shaken vigorously until to completely dissolved product.

The sealed flasks were placed inside the boxes with the fruits previously packed and then the flasks were opened and the boxes immediately closed, remaining this way for 12 hours. The fruits from control treatment (no application of 1-MCP) also remained for 12 hours inside a box identical to those used for other treatments. After this period, the fruits harvested in 2008/2009 were stored at temperatures of 7 and 21 °C and those harvested in the 2009/2010 stored at temperatures of 7, 14 and 21 °C. Analyses were performed at 0, 15, 30, 45 and 60 days of storage.

After taking the weight of fruits, juice extraction was performed with subsequent filtering and mixing for evaluation, which showed:

- The content of total soluble solids (SS), obtained by refractometry, from the juice extracted from each sample and the results expressed in ° Brix.
- Titratable acidity (TA), determined by potentiometric titration with NaOH 0.1 M, from a solution containing 10 mL of orange juice diluted with 100 mL of distilled water until pH reaches 8.1. The pH was determined by a pHmeter Digimed ®. Values were expressed in meq 100 mL⁻¹.

- The ratio soluble solids/titratable acidity was calculated by the relation soluble solids and acidity,

in which the factor is multiplied by 100, resulting in percentage.

- The content of vitamin C was obtained by titration of ascorbic acid in solution of 2,6-dichlorobenzeneindophenol, expressed in milligrams of ascorbic acid per 100 mL of juice; the extraction of the samples was performed with a solution of oxalic acid at 1%.

- Total carotenoids were obtained with a spectrophotometer at 663nm for chlorophyll, at 646 nm for chlorophyll b and at 470 nm for carotenoids. Phenolic compounds were obtained by the method of Follin-Ciocauteau according to Bucic-Kojic et al. (2007).

- The mass loss of fruits was determined by the difference between initial mass and mass after storage, using a semi-analytical balance.

- The juice yield was determined by the relation between the mass of orange juice and the total fruit mass.

The experimental design was completely randomized in a 2x4 factorial design (storage temperature x doses of 1-MCP) for fruits from 2008/2009 season with four replicates per treatment and five fruits per plot; and in a 3x4 factorial design (storage temperature x doses of 1 - MCP) for fruits from 2009/2010 season, with four replicates and eight fruits per plot. Data were subjected to analysis of variance (test F) and the means were studied by regression method ($P \leq 0.05$), utilizing the statistical program SISVAR (FERREIRA, 2008), and data in percentages were previously transformed in arc.sen

$$\sqrt{x/100}$$

3. Results and Discussion

In relation to SS, Table 1 shows there was significant interaction between treatment for 30 days of storage and temperatures at 7 and 21 °C, for 45 days of storage and temperature of 7 °C and for 60 days of storage and temperature of 21 °C. In other conditions of storage, there was no significant interaction between treatments.

Table 1. Content of total soluble solids (°Brix) in fruits of cv. Folha Murcha, stored for 60 days at temperatures of 7, 14 and 21 °C.

Stored time	Tratament 1-MCP ($\mu\text{L L}^{-1}$)	TOTAL SOLUBLE SOLIDS (°Brix)				
		2008/2009		2009/2010		
		7 °C	21 °C	7 °C	14 °C	21 °C
INICIAL		9,28±0,29	9,28±0,29	8,73±0,21	8,73±0,21	8,73±0,21
15 DAYS	0,0	8,98±0,46 ^{NS}	9,25±0,39 ^{NS}	8,50±0,12 ^{NS}	8,43±0,30 ^{NS}	8,20±0,41 ^{NS}
	0,1	9,20±0,41 ^{NS}	9,40±0,47 ^{NS}	8,98±0,17 ^{NS}	8,65±0,06 ^{NS}	8,33±0,15 ^{NS}
	0,5	9,18±0,37 ^{NS}	9,20±0,27 ^{NS}	8,65±0,55 ^{NS}	8,48±0,09 ^{NS}	8,45±0,17 ^{NS}
	1,0	9,45±0,27 ^{NS}	9,65±0,42 ^{NS}	8,57±0,29 ^{NS}	8,43±0,30 ^{NS}	8,30±0,46 ^{NS}

30 DAYS	0,0	9,40±0,18*	9,65±0,52*	8,20±0,16*	9,00±0,29*	8,70±0,58*
	0,1	9,90±0,25*	9,83±0,32*	8,750±0,34*	9,20±0,59*	8,20±0,16*
	0,5	9,43±0,09*	9,26±0,51*	8,75±0,19*	8,80±0,29*	8,00±0,33*
	1,0	9,38±0,39*	8,25±0,58*	8,70±0,12*	8,47±0,25*	N/C
45 DAYS	0,0	9,40±0,18*	9,50±0,43 _{NS}	8,63±0,05 ^{NS}	8,75±0,30 ^{NS}	N/C
	0,1	9,90±0,25*	9,88±0,21 _{NS}	8,53±0,22 ^{NS}	8,85±0,41 ^{NS}	N/C
	0,5	9,43±0,09*	9,45±0,57 _{NS}	8,58±0,35 ^{NS}	8,68±0,40 ^{NS}	N/C
	1,0	9,38±0,37*	9,30±0,25 _{NS}	8,40±0,33 ^{NS}	N/C	N/C
60 DAYS	0,0	9,53±0,29 _{NS}	9,65±0,52*	7,08±0,19*	8,93±0,25 _{NS}	N/C
	0,1	10,03±0,61 _{NS}	9,83±0,32*	7,80±0,52*	9,20±0,16 _{NS}	N/C
	0,5	9,73±0,36 _{NS}	9,23±0,51*	7,40±0,29*	9,07±0,34 _{NS}	N/C
	1,0	9,40±0,48 _{NS}	8,25±0,58*	7,85±0,19*	N/C	N/C

^{NS} – Averages not presenting significant differences, in the same row, according to variance analysis (test F, $p \leq 0,05$).

* – Averages presenting significant difference, in the same row, according to variance analysis (teste F; $p \leq 0,05$).

N/C – No fruits for analysis.

In periods when there was interaction, the concentration of 0.1 µL of 1-MCP per liter (T2) showed the highest content of soluble solids, and in doses of 0.5 and 1.0 µL of 1-MCP per liter (T3 and T4, respectively), values were lower than the control (T1). The results from T3 and T4 differ from those found in pineapple by Selvarajah et al. (2001), who observed an increase in the levels of SS in fruits treated with 1-MCP. The findings in this study confirm those reported by Porat et al. (1999) who described no change in SS of oranges cv. Shamouti treated with 1-MCP.

The average values observed in this study were lower than those reported by Stenzel et al. (2005) who found levels from 11.3 to 13.1 °Brix in fruits of the same cultivar. However, one emphasizes that fruits in this experiment were harvested before complete ripeness, given that it was necessary to anticipate the harvest to accomplish the application of 1-MCP.

The content of SS is an important attribute in determining the fruit flavor, since it is indicative of

the amount of existing sugars, along with compounds that occur in smaller amounts, such as acids, vitamins, amino acids, etc. (KLUGE et al., 2002). Pereira et al. (2006) describe that minimum levels of SS in oranges and tangerines should stand around 9.0 to 10.0 °Brix. Thus, the average content of SS found for cv. Folha Murcha in this work is close to the standard value, with or no application of 1-MCP.

In relation to titratable acidity (TA), Table 2 shows there was significant interaction in the temperature of 7 °C only for fruits evaluated at 30 days of storage. At 21 °C, there was significant interaction at 15, 30 and 45 days, with a decrease in the values. According to Volpe et al. (2002), citric acid begins to accumulate in the fruit soon after its formation and quickly reaches the maximum, after which the content of this acid decreases. The decrease in concentration during maturation is partly due to increasing size of fruit by absorption of water and consequent dilution of the acid content and due to respiratory rate, which is temperature dependent.

Table 2. Titratable acidity (mg 100 mL⁻¹) in fruits of cv. Folha Murcha stored for 60 days at temperatures of 7, 14 and 21 °C.

Stored time	Tratament 1-MCP (μL L ⁻¹)	TITRATABLE ACIDITY (mg 100mL ⁻¹)				
		2008/2009		2009/2010		
		7 °C	21 °C	7 °C	14 °C	21 °C
INICIAL		0,62±0,09	0,62±0,09	0,56±0,01	0,56±0,01	0,56±0,01
15 DAYS	0,0	0,61±0,04 _{NS}	0,59±0,04*	0,59±0,04 ^{NS}	0,66±0,02*	0,59±0,03 _{NS}
	0,1	0,58±0,04 _{NS}	0,51±0,03*	0,58±0,05 ^{NS}	0,59±0,04*	0,60±0,04 _{NS}
	0,5	0,57±0,06 _{NS}	0,61±0,03*	0,55±0,04 ^{NS}	0,61±0,02*	0,60±0,05 _{NS}
	1,0	0,57±0,03 _{NS}	0,61±0,04*	0,56±0,01 ^{NS}	0,59±0,01*	0,61±0,09 _{NS}
30 DAYS	0,0	0,54±0,08*	0,61±0,06*	0,53±0,01*	0,58±0,02 _{NS}	0,56±0,04 _{NS}
	0,1	0,66±0,02*	0,53±0,03*	0,56±0,02*	0,59±0,04 _{NS}	0,53±0,01 _{NS}
	0,5	0,66±0,05*	0,57±0,02*	0,56±0,01*	0,56±0,02 _{NS}	0,51±0,02 _{NS}
	1,0	0,62±0,02*	0,57±0,02*	0,55±0,01*	0,54±0,02 _{NS}	N/C
45 DAYS	0,0	0,61±0,03 _{NS}	0,72±0,03*	0,55±0,003 ^{NS}	0,56±0,02 _{NS}	N/C
	0,1	0,64±0,08 _{NS}	0,61±0,03*	0,55±0,01 ^{NS}	0,57±0,03 _{NS}	N/C
	0,5	0,63±0,04 _{NS}	0,61±0,11*	0,55±0,02 ^{NS}	0,56±0,03 _{NS}	N/C
	1,0	0,62±0,05 _{NS}	0,57±0,04*	0,54±0,02 ^{NS}	N/C	N/C
60 DAYS	0,0	0,67±0,09 _{NS}	0,58±0,06 _{NS}	0,65±0,03 ^{NS}	0,51±0,05 _{NS}	N/C
	0,1	0,58±0,04 _{NS}	0,54±0,01 _{NS}	0,64±0,04 ^{NS}	0,57±0,04 _{NS}	N/C
	0,5	0,61±0,02 _{NS}	0,53±0,06 _{NS}	0,64±0,02 ^{NS}	0,57±0,01 _{NS}	N/C
	1,0	0,59±0,03 _{NS}	0,49±0,04 _{NS}	0,62±0,02 ^{NS}	N/C	N/C

^{NS} – Averages not presenting significant differences, in the same row, according to variance analysis (test F, p≤0,05).

* – Averages presenting significant difference, in the same row, according to variance analysis (teste F; p≤0,05).

^{N/C} – No fruits for analysis.

The average values of acidity in this work (Table 2) are low when compared to those of Nascimento et al. (2005) who found value of 1.10 mg of citric acid per 100 mL for cultivar Folha Murcha, in the County of Brotas, São Paulo State. According to Volpe et al. (2002), nutritional conditions and mainly temperature are the factors influencing the levels of citric acid, which may explain partly the difference among results found in different regions.

As occurred in SS, the TA content observed in this study was indifferent in relation to doses of 1-MCP, which confirms Porat et al. (1999) who found no significant differences between the control fruits

and the different doses of 1-MCP applied in oranges cv. Shamouti.

The ratio is calculated by the relation between SS and TA contents. It is one of the main indicators used to determine the maturity stage, which regulates the balance of sweetness/acidity (COUTO and CANNIATTI-BRAZACA, 2010). According to Viégas (1991), the ratio range can vary between 6 and 20, and the interval from 15 to 18 is preferred by consumers. But Sartori et al. (2002) regard as suitable for consumption fruits having a SS/TA ratio between 8.8 and 15.4. In Brazil, the preference is for juices with a ratio above 14. The evolution of

this content can be partly explained by the relationship graft bearer/canopy, age of plants, flowering and productivity, besides climate changing from year to year (VOLPE et al., 2002). For fruits of cv. Folha Murcha harvested in the 2008/2009 and stored at 7 °C there was no significant interaction for any period analyzed. However, under 21 °C there was interaction at 15, 30 and 45 days. For fruits stored at 7 °C, the ratio was between 14.4 and 17.8, while for fruits stored at 21 °C it was between 13.2 and 18.6. In the following season (2009/2010), the mean ratios were between 10.9 and 15.9 at temperature of 7 °C, between 14.9 and 17.8 at 14 °C and between 13.2 and 15.0 at 21 °C. Significant variation between treatments was observed only for 60 days at 7 °C and 14 °C. In other periods and temperatures, there was no significant difference between treatments.

The average ratios in the present study are high when compared to that of Nascimento et al. (2005), who found value of 7.6 for the same cultivar. Some authors consider the SS/TA as the main feature to indicate the point of commercial maturation for citrus (COUTO and CANNIATTI-BRAZACA, 2010). However, Santos et al. (2010) claim that the use of this parameter solely can lead to misinterpretations, since in their work with seedless citrus fruits, the ratio found was considered high; however, this happened due to low TA, although SS content was considered inadequate. The authors state that the impression is a fruit that pleases fully the consumer, due to the high ratio, but in reality the result is tasteless because of the imbalance in the relation SS/TA. Similar fact was observed in this study, with high values of ratio, however with soluble solids content close to the recommended.

In relation to ascorbic acid or vitamin C for fruits harvested in the 2008/2009 season, there was no significant interaction between treatments for any temperature and period analyzed. For fruits stored at 7 °C, the levels of vitamin C ranged between 47.9 and 70.8 mg 100 mL⁻¹, whereas for fruits stored at 21 °C, this levels were between 43.7 and 77.1 mg 100 mL⁻¹. The mean values of vitamin C for fruits of 2009/2010 season were between 31.9 and 48.9 mg 100 mL⁻¹ at temperature of 7 °C, between 32.0 and 65.6 mg 100 mL⁻¹ at 14 °C and between 31.9 to 72.1 mg 100 mL⁻¹ at 21 °C. It was also noted that for the fruits from this season, there was no significant difference between treatments of 15 days at 21 °C and 45 days at 14 °C, and no statistical difference in the other periods analyzed.

In this study, there was great variation in vitamin C content during storage at the three temperatures. The same oscillation was observed by Andrade et

al. (2002), who analyzed orange fruits at different maturation stages with a approximate range from 50 to 75 mg of ascorbic acid 100 mL⁻¹. The authors also noted that greener fruits presented lower content of vitamin C when compared to more mature fruits.

The determination of vitamin C is an important attribute of quality for citrus in general. It is a natural antioxidant involved in reactions taking place during the senescence of fruits as a way to repair oxidative damage in cells.

It should be noted that applications of 1-MCP showed no increase or decrease in the levels of vitamin C and data were adjusted into cubic equations, with oscillation between the values without, however, be possible to say that higher dose of 1-MCP increases or reduces the amount of ascorbic acid in the fruits. As observed in this work, Jomori et al. (2003) did not obtain significant differences in the levels of vitamin C in acid lime cv. Tahiti, when comparing treatments of 1-MCP; the authors explained this result to the fact that the action of products applied was restricted to the albedo and flavedo of fruits, not happening possibly a more internal dissemination of these products. This fact should also justify the insignificant results between treatments found in this study.

Another important compound in citrus is the carotenoids that make up one of the most important groups of natural pigments due to wide distribution, structural diversity and number of functions (RIBEIRO and SERAVALLI, 2004). These compounds are unique in the nature; they are present in various structures of plants, in a variety of animals, algae, fungi and bacteria and are responsible for the colors yellow, orange and red (MELÉNDEZ-MARTÍNEZ et al., 2007).

For fruits harvested in 2008/2009 and kept at 7 °C, the carotenoids content was between 0.386 and 0.601 mg 100 mL⁻¹, whereas for fruits stored at 21 °C, the total carotenoids stayed between 0.390 and 0.728 mg 100 mL⁻¹. Fruits stored at 7 °C and 21 °C showed significant differences among treatments in the periods of 30 and 60 days and no difference in the periods of 15 and 45 days. In the season 2009/2010, the values observed were between 0.309 and 0.870 mg 100 mL⁻¹ at the temperature of 7 °C, between 0.108 and 0.607 mg 100 mL⁻¹ at 14 °C and between 0.132 and 0.446 mg 100 mL⁻¹ at 21 °C. Significant variation between treatments was observed only for 15 days at temperature of 7 °C and for 30 days at 21 °C, and no statistical difference in the other periods analyzed.

Table 3. Content of total carotenoids (mg 100 mL⁻¹) in fruits of cv. Folha Murcha, stored for 60 days at temperatures of 7, 14 and 21 °C.

Stored time	Tratament 1-MCP (μL L ⁻¹)	TOTAL CAROTENOIDS TOTAIS (mg 100mL ⁻¹)				
		2008/2009		2009/2010		
		7 °C	21 °C	7 °C	14 °C	21 °C
INICIAL		0,58±0,05	0,58±0,05	0,29±0,04	0,29±0,04	0,29±0,04
15 DAYS	0,0	0,43±0,05 ^{NS}	0,51±0,11 ^{N/C}	0,57±0,08*	0,12±0,03 ^{NS}	0,21±0,22 ^{NS}
	0,1	0,50±0,21 ^{N/C}	0,49±0,16 ^{N/C}	0,44±0,09*	0,14±0,08 ^{N/C}	0,13±0,05 ^{NS}
	0,5	0,46±0,10 ^{N/C}	0,56±0,09 ^{N/C}	0,31±0,03*	0,12±0,04 ^{NS}	0,15±0,02 ^{NS}
	1,0	0,45±0,04 ^{N/C}	0,59±0,08 ^{N/C}	0,39±0,06*	0,11±0,07 ^{NS}	0,15±0,05 ^{NS}
30 DAYS	0,0	0,48±0,06*	0,73±0,08*	0,41±0,09 ^{N/C}	0,49±0,04 ^{NS}	0,29±0,08*
	0,1	0,39±0,04*	0,59±0,06*	0,44±0,04 ^{N/C}	0,47±0,07 ^{NS}	0,37±0,02*
	0,5	0,49±0,13*	0,57±0,04*	0,42±0,04 ^{N/C}	0,45±0,06 ^{NS}	0,45±0,04*
	1,0	0,59±0,03*	0,51±0,04*	0,44±0,04 ^{N/C}	0,42±0,07*	N/C
45 DAYS	0,0	0,39±0,05 ^{N/C}	0,73±0,08 ^{N/C}	0,81±0,09 ^{N/C}	0,51±0,08 ^{NS}	N/C
	0,1	0,42±0,12 ^{N/C}	0,59±0,06 ^{N/C}	0,87±0,07 ^{N/C}	0,45±0,06 ^{NS}	N/C
	0,5	0,43±0,03 ^{N/C}	0,57±0,04 ^{N/C}	0,81±0,11 ^{N/C}	0,48±0,06 ^{NS}	N/C
	1,0	0,44±0,02 ^{N/C}	0,51±0,04 ^{N/C}	0,79±0,09 ^{N/C}	N/C	N/C
60 DAYS	0,0	0,39±0,06*	0,57±0,03*	0,45±0,03 ^{N/C}	0,59±0,12 ^{NS}	N/C
	0,1	0,48±0,06*	0,58±0,04*	0,48±0,07 ^{N/C}	0,61±0,15 ^{NS}	N/C
	0,5	0,60±0,04*	0,53±0,06*	0,49±0,11 ^{N/C}	0,44±0,02 ^{NS}	N/C
	1,0	0,58±0,05*	0,39±0,11*	0,45±0,06 ^{N/C}	N/C	N/C

^{NS} – Averages not presenting significant differences, in the same row, according to variance analysis (test F, p≤0,05).

* – Averages presenting significant difference, in the same row, according to variance analysis (test F; p≤0,05).

^{N/C} – No fruits for analysis.

In relation to phenolic compounds, fruits of 2008/2009 season stored at 7 °C presented average values between 0.071 and 5.303 mg 100 mL⁻¹, whereas for fruits stored at 21 °C, phenolic compounds ranged from 0.075 to 11.579 mg 100 mL⁻¹. There was a significant influence of treatments only at 21 °C for all storage periods, whereas for fruits stored at 7 °C the significant influence of treatments was observed only in 45 days of storage.

Mean values of phenolic compounds in fruits of cv. Folha Murcha from 2009/2010 season were between 3.675 and 13.650 mg 100 mL⁻¹ at temperature of 7 °C, between 6.093 and 15.129 mg 100 mL⁻¹ at 14 °C and between 8.329 and 10.332 mg 100 mL⁻¹ at 21 °C. It was noted that there was significant difference between treatments of 15 days at temperature of 7 °C and 45 days at temperature of 14 °C, and no statistical difference in the remaining periods analyzed.

Results in this study differ from those found in the literature. Duzioni et al. (2010) observed values of phenolic compounds in the range of 648.6 for orange cv. 'Valencia' and 551.9 mg 100 mL⁻¹ for tangerine cv. Murcott. Melo (2008) obtained results

of total phenolic of 208.10 for orange cv. Pera and 146.30 g mL⁻¹ for orange cv. Cravo. Couto and Canniatti-Brazaca (2010) obtained results of 78.47 mg 100 mL⁻¹ for orange cv. Valencia and 21.47 mg 100 mL⁻¹ for tangerine cv. Murcott.

Morais et al. (2007), in a study with sapodilla, found variation in the content of phenolic compounds in fruits treated with 1-MCP. These authors observed that content of phenolic compounds remained higher in fruits that received the application of 1-MCP when compared to the control throughout the storage period. Sales (2002) reported similar results for bananas treated with 1-MCP, with a delay in the reduction of phenolic compounds in fruits treated when compared with the control treatment.

In relation to weight loss for fruits of the 2008/2009 season, the average values were between 5.5 and 21.8% for fruits kept at temperature of 7 °C and 5.2 to 38.1% for fruit stored at 21 °C. There was difference between treatments 15 and 60 days at temperature of 7 °C and 45 and 60 days at 21 °C, trending to increase mass loss with increasing levels of 1-MCP applied. Analyzing data over storage period, the weight loss had a tendency to

increase gradually, as Figure 1 shows.

For fruits from the season 2009/2010, the average values were between 3.5 and 20.9% for fruits kept at temperature of 7 °C, between 5.4 to 59.5% for fruits stored at 14 °C and 2.8 to 19.6% at 21 °C. There were significant differences between

treatments for 15 days, at temperatures of 14 and 21 °C and for 30 days at 21 °C; there was no statistical difference in the remaining periods analyzed. Most of the results found in this study showed that application of 1-MCP did not significantly affect fruit weight loss, and the mass loss observed was due to storage time (Figure 1).

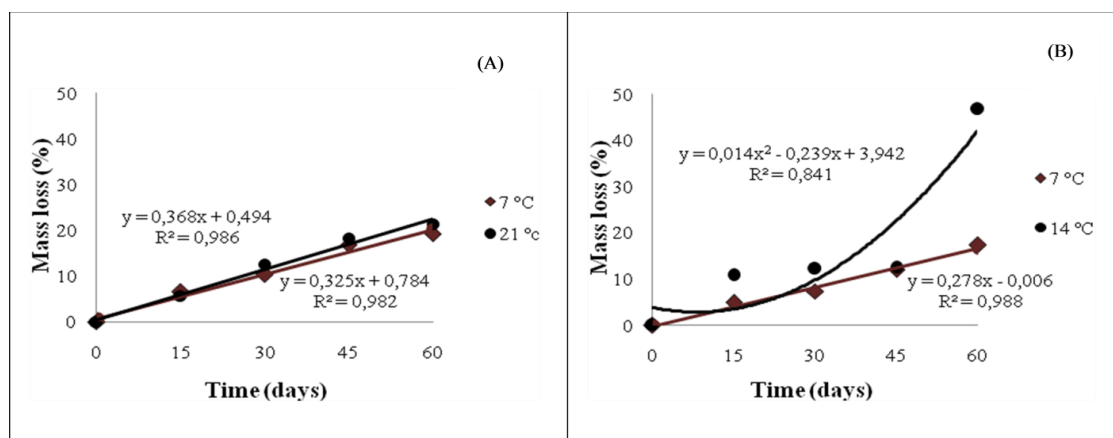


Figure 1. Weight loss along 60 days of storage for fruits of cv. Folha Murcha: (2008/2009) and (2009/2010).

Results in this study confirm those reported by Mendonça et al. (2003) who observed an increase of mass loss in lemon cv. Siciliano throughout the storage time. The authors reported the fact to transpiration as the main process involved in post-harvest losses of fresh matter. Malgarim et al (2007) found similar results in oranges cv. Navelina, with increasing mass loss during the storage period.

As to the influence of 1-MCP on the mass loss, some authors reported lower mass loss in fruits treated with 1-MCP, such as tangerines (LAAMIN et al., 2005), plums (VALERO et al. 2005), mango (LIMA et al., 2006, SILVA et al., 2004) and avocado (JEONG et al., 2002). These results differ from this present study, in which the application of 1-MCP showed no significant difference for most of the periods and temperatures analyzed.

As previously reported, in general, the application of 1-MCP did not significantly affect fruit weight loss, and the mass loss observed was due to storage time. Porat et al. (1999) also reported that mass loss in oranges treated with 1-MCP was not significant.

In relation to juice yield, fruits of the 2008/2009 season stored at 7 °C presented mean values from 49.3 to 60.6% and 53.4 to 65.4% for fruits stored at temperature of 21 °C. For fruits from this season, there was no significant difference between treatments. In the 2009/2010 season, the juice yield was between 35.4 and 48.6% for fruit kept at temperature of 7 °C, between 41.9 and 48.9% at temperature of 14 °C and between 46.1 and 48.5%

at 21 °C. As occurred in the 2008/2009 season, there was no significant variation between treatments for any temperature or period studied.

4. Conclusions

- The product 1-MCP does not provide longer post-harvest conservation of fruits.
- The application of 1-MCP did not cause a change in the chemical characteristics of fruits, such as SS, TA, vitamin C, carotenoids and phenolic compounds.
- The shorter the period between harvesting and cooling, the better was the conservation of fruits.

5. Acknowledgements

To CNPq for the first author scholarship, to Rohm and Haas Chemical® in Brazil for the supply of 1-MCP; and to Cocamar Cooperativa Agroindustrial for the fruits.

6. References

- ANDRADE, R.S.; DINIZ, M. C. T.; NEVES, E. A.; NÓBREGA, J. A. Determinação e distribuição de ácido ascórbico em três frutos tropicais. *Eclética Química*, São Paulo, v. 2, (n.especial), p. 1-8, 2002.
- COUTO, M. A. L.; CANNIATTI-BRAZACA, S. G. Quantificação de vitamina C e capacidade antioxidante de variedades cítricas. *Ciência e Tecnologia de Alimentos*, Campinas, v. 30, n. 1, p.15-19, maio 2010.
- DUZZIONI, A. G.; FRANCO, A. G.; SYLOS, C. M. de. Determinação da atividade antioxidante e de constituintes bioativos em frutas cítricas. *Alimentos e Nutrição*, Araraquara, v. 21, n. 4, p. 643-649, out./dez. 2010
- JEONG J.; HUBER D. J.; SARGENT S. A. Influence of 1-methylcyclopropene (1-MCP) on ripening and cell-wall matrix polysaccharides of avocado (*Persea americana*) fruit. *Postharvest Biology and Technology*, Amsterdam, v. 25, p.241-56, 2002.
- JIANG, Y.; JOYCE, D. C.; TERRY, L. A. 1-

methylcyclopropene treatment affects strawberry fruit decay. **Postharvest Biology and Technology**, Amsterdam, v. 23, n.3, p. 227-232, 2001.

KLUGE, R. A.; JACOMINO, A. P.; OJEDA, R. M.; BRACKMANN, A. Inibição do amadurecimento de abacate com 1-metilciclopropeno. **Pesquisa Agropecuária Brasileira**, Brasília, v. 37, n. 7, p. 895-901, 2002.

KLUGE, R. A.; JOMORI, M. L. L.; EDAGI, F. K.; JACOMINO, A. P.; DEL AGUILA, J. S. Danos de frio e qualidade de frutas cítricas tratadas termicamente e armazenadas sob refrigeração. **Revista Brasileira de Fruticultura**, Jaboticabal, SP, v.29, n.2, 2007, p. 233-238.

LAAMIM, M.; AIT-OUBAHOU, A.; BENICHO, M. Effect of 1-methylcyclopropene on the quality of clementine mandarin fruit at ambient temperature. **Journal of Food, Agriculture & Environment**, Helsinki, v.3, n.1, p.34-36, 2005.

LIMA, M. A. C. de; SILVA, A. L.; AZEVEDO, S. S. N.; SANTOS, P. de S. Tratamentos pós-colheita com 1-metilciclopropeno em manga 'Tommy Atkins': efeito de doses e número de aplicações. **Revista Brasileira de Fruticultura**, Jaboticabal, v.28, n.1, p.64-68, 2006.

MALGARIM, M. B.; CANTILLANO, R. F. F.; TREPTOW, R. O. Armazenamento refrigerado de laranjas cv. Navelina em diferentes concentrações de cera à base de carnaúba. **Acta Scientiarum Agronomy**, Maringá, v. 29, n. 1, p. 99-105, 2007.

MELÉNDEZ-MARTÍNEZ, A. J.; VICARIO, I. M.; HEREDIA, F. J. Pigmentos carotenoides: consideraciones estructurales y físico-química. **Archivos Latinoamericanos de Nutricion**, Caracas, v. 57, n. 2, 2007.

MENDONÇA, K.; JACOMINO, A. P.; MELHEM, J. X.; KLUGE, R. A. Concentração de etileno e tempo de exposição para o desverdecimento de Limão 'Siciliano'. **Brazilian Journal of Food Technology**, Campinas, v.6, n.2, p.179-183, 2003.

MORAIS, P. L. D. de; LIMA, L. C. de O.; ALVES, R. E.; ALVES, J. D.; ALVES, A. de P. Amadurecimento de sapoti (*Manilkara zapota* L.) submetido ao 1- metilciclopropeno. **Revista Brasileira de Fruticultura**, Jaboticabal, v.28, n. 3, p. 369-373, 2007.

MULLINS, E. D.; McCOLLUM, T. G.; McDONALD, R. E. Consequences on ethylene metabolism of inactivating the ethylene receptor sites in diseased non-climacteric fruit. **Postharvest Biology and Technology**, Amsterdam, v.19, p. 155-164, 2000.

NASCIMENTO, L. M. do et al. Laranja charmute de brotas: promissora variedade tardia. **Revista Laranja**, Cordeirópolis, v.26, n.1, p.69-75, 2005.

PORAT, R.; WEISS, B.; COHEN, L.; DAUS, A.; GOREN, R.; DROBY, S. Effects of ethylene and 1-methylcyclopropene on the postharvest qualities of 'Shamouti' oranges. **Postharvest Biology and Technology**, Amsterdam, v.15, p.155-163, 1999.

RIBEIRO, E. A.; SERAVALLI, E. A. G. **Química de Alimentos**. São Paulo: Edgard Blücher Ltda, p.179-181, 2004.

SANTOS, D. dos; MATARAZZO, P. H. M.; SILVA, D. F. P. da; SIQUEIRA, D. L. de; SANTOS, D. C. M. dos; LUCENA, C. C. de. Caracterização físico-química de frutos cítricos apirênicos produzidos em Viçosa, Minas Gerais. **Revista Ceres**, Viçosa, v. 57, n.3, p. 393-400, 2010.

SARTORI, I. A.; KOLLER, O. C.; SCHWARZ, S. F.; BENDER, R. J.; SCHAFER, G. Maturação de frutos de seis cultivares de laranjas-doces na depressão central do rio grande do sul. **Revista Brasileira de Fruticultura**, Jaboticabal, SP, v. 24, n. 2, p. 364-369, 2002.

SELVARAJAH, S.; BAUCHOT, A. D.; JONH, P. Internal browning in cold-stored

pineapples is suppressed by a postharvest application of 1-methylcyclopropene. **Postharvest Biology and Technology**, Amsterdam, v. 23, p. 167-170, 2001.

SILVA, S. M.; SANTOS, E. C.; SANTOS, A. F. dos; SILVEIRA, I. R. B. S.; MENDONÇA, R. M. N. Influence of 1-methylcyclopropene on postharvest conservation of exotic mango cultivars. **Acta Horticulturae**, Brugg, n.645, p.565-572, 2004.

STENZEL, N. M. C.; NEVES, C. S. V. J.; GONSALEZ, M. G. N.; SCHOLS, M. B. S.; GOMES, J. C. Desenvolvimento

vegetativo, produção e qualidade dos frutos de laranja 'Folha Murcha' sobre seis porta-enxertos no Norte do Paraná. **Ciência Rural**, Santa Maria, v.35, n.6, p.1281-1286, 2005.

VALERO D., MARTINEZ-ROMERO D., VALVERDE J. M., GUILLEN F., CASTILLO S., SERRANO M. Could the 1-MCP treatment effectiveness in plum be affected by packaging? **Postharvest Biology and Technology**, Amsterdam, v.34, n.3 p.295-303, 2004.

VIÉGAS, F. C. P. A industrialização dos produtos cítricos. In: RODRIGUEZ, O.; VIÉGAS,

F.; POMPEU JÚNIOR, J.; AMARO, A. A. (Ed.). **Citricultura brasileira**, Campinas, v.2, p. 898-922, 1991.

VOLPE, C. A.; SCHOFFEL, E. R.; BARBOSA, J. C. Influência da soma térmica e da chuva durante o desenvolvimento de laranjas 'Valência' e 'Natal' na relação entre sólidos solúveis e acidez e no índice tecnológico do suco. **Revista Brasileira de Fruticultura**, Jaboticabal-SP, v.24, n.2, p.436-441, 2002.

Burnout among Junior Athletes' in relation to their Perceived Progress Academically in School and in Sport^[1]

Frode Moen¹ 

^[1] Running head: BURNOUT AMONG NORWEGIAN JUNIOR ATHLETES

¹ Department of Education, Norwegian University of Science and Technology, Granliveien 14, 7024 Trondheim
Phone: +47 72 56 81 76, Mobile: +47 932 48 750

Abstract: This article looks at whether lower levels of perceived satisfaction with own progress academically in school and in sport, were associated with higher levels of Athlete Burnout among junior athletes attending different high schools specialized for sports. In order to explore this, we investigated junior athletes' perceptions of their own feeling regarding the different dimensions of Athlete Burnout, and how these perceptions related to their own satisfaction with their progress academically in school and in sport during the last year. The Athlete Burnout Questionnaire (ABQ) measures three dimensions of Athlete Burnout, Accomplishments, Exhaustion and Devaluation. Our hypothesis was partly confirmed as the results revealed that lower levels of perceived satisfaction with progress academically in school were associated with higher Athlete Burnout. This result applies for the dimensions Exhaustion and Devaluation as well as the sum of Athlete Burnout. The athletes who reported to be very dissatisfied with their progress academically reported that they frequently felt exhausted and devaluated their sports. However, only the dimension Accomplishments was associated with Athlete Burnout when satisfaction with own progress in school was analysed.

Keywords: Athlete Burnout, junior athletes, sport schools.

Introduction

Athlete burnout is found to be a considerable concern in sport due to the potential negative consequences burnout has for athletes' performances and welfare (Coakley, 1992; Cresswell & Eklund, 2005; Goodger, Gorely, Lavalley & Harwood, 2007; Gould, Udry, Tuffey & Loehr, 1996; Silva, 1990). Burnout in sport is manifested by a shift in an athlete from a passionate and self-determined engagement in the sporting activity, to low or no motivation at all (Ryan & Solky, 1996). Thus, burnout is viewed as an experiential state from the subjective point of view, ranging from low to high levels, and lack of motivation is the most common consequence from high levels of burnout (Goodger, et al., 2007). Interestingly, the number of athletes who are suffering from burnout is discussed to be on the rise, and this tendency is discussed to be a possible result of an increasing amount of competitive and training stress (Gould & Dieffenbach, 2002). However, is this completely true?

Athlete burnout appears to be a complex interaction of multiple stressors, inadequate recovery and frustration from unfulfilled expectations (Goodger, et al., 2007; Gustafsson, Hassmén, Kenttä and Johansson, 2008). In particular, young athletes who

are undertaking high school education at specialized sport schools are exposed to several stressors as most of them have ambitions both academically in school subjects and in their sports. Possible unfulfilled expectations academically or within sports, might soon become a contributor for higher levels of burnout (Gustafsson, 2007; Gustafsson, Kenttä, Hassmén & Lundqvist, 2007). As a result, athletes might drop out of their sport due to the burnout experience. It is well documented that unfulfilled expectations within sports might lead to burnout (Goodger, et al., 2007; Gould & Dieffenbach, 2002). However, it would be interesting to investigate how different levels of athletes' satisfaction with their progress both academically in school and in their sports contribute to Athlete Burnout. This study aims to investigate this question.

Theoretical background

The definition of athlete burnout has derived from the predominant conceptualization of burnout employed in the human service and organizational psychology literatures (e.g., Maslach & Goldberg, 1998; Maslach, Jackson & Leiter, 1996; Maslach, Schaufeli & Leiter, 2001). Based on this framework athlete burnout is viewed as a multidimensional construct that consists of three central dimensions:



Frode Moen (Correspondence)



frmoe@online.no

1) Emotional and physical exhaustion, 2) Reduced sense of accomplishment, and 3) Sport devaluation (Raedeke & Smith, 2009).

Emotional and physical exhaustion is characterized by feelings of emotional and physical fatigue stemming from the emotional, mental and physical demands associated with performance, training and competitions. The exhaustion dimension consists of both an emotional and a physical component. The physical component is associated with the intensity and duration in training and competitions, whereas the emotional component is associated with the psychosocial stressors that an athlete experiences.

In principle, training and competitions are meant to challenge an athlete's homeostatic balance in order to elicit bodily adaption and performance development (Main & Landers, 2012). However, when stress responses from psychosocial and physical demands are overloaded, the process of adaptation might be challenged. Since the earliest accounts of burnout there has been nearly unanimous agreement that burnout is a reaction to an overload of stress, where exhaustion is the result from the chronic demands made on an athlete's resources (Cherniss, 1980; Cordes & Dougherty, 1993; MacNeil, 1981). The emotional and physical exhaustion dimension is the most widely accepted dimension in burnout (Raedeke & Smith, 2009).

Reduced sense of accomplishment is characterized by an athlete's feeling of inefficacy and a general tendency to evaluate him or herself negatively in terms of his or her sport performances and accomplishments. The dimension is related to an athlete's perception of his or her skills and abilities. An athlete who is experiencing this state is unable to achieve personal goals or performs below his or her own and other's expectation. This dimension is concerned about an athlete's subjective perception of own performance and accomplishments within sports. This dimension is debated among researchers and scholars (Cox, Tisserand & Taris, 2005; Schaufeli & Taris, 2005). However, for an athlete in sport performance is the central concern, as he or she continually is being evaluated by him- or herself, or by others. Therefore, it appears important to address this dimension associated with the burnout syndrome among athletes in sport (Raedeke & Smith, 2009). Reduced sense of accomplishments might be a major stressor for athletes.

Sport devaluation is defined as a negative, detached attitude toward the sport, reflected by a lack of concern about the sport itself and the performance quality. This is the most accepted dimension in burnout measurements following exhaustion. According to Raedeke (1997) this dimension is

concerned with an athlete's feeling of reduced value related to the personal effort that he or she has, or is willing to invest in order to reach his or her goals within sport. While exhaustion depicts the ability to expand effort, devaluation represents the willingness to expand effort.

Thus, the degree of athlete burnout is in general viewed as an experiential state seen from an athlete's subjective point of view. In a 25-year review of the burnout literature Schaufeli and Buunk (2003) outlined five categories of symptoms associated with the construct: affective symptoms as depressed mood, cognitive symptoms as feeling helpless, physical symptoms as feeling exhausted or ill, behavioral symptoms as impaired performance, and motivational symptoms as the lack of enthusiasm and engagement in the sport. These symptoms are also found in sport as well as the implications to the athletes' performances (Goodger, et al., 2007). Athlete burnout is obviously a syndrome that coaches in sport should pay attention to because of the negative consequences that come from burnout.

Junior athletes who are studying at specialized sport schools are exposed to several stressors in their environment; in particular they are exposed to demands both academically as well as in their sports. It is found that athletes' favor their sports at high school compared to their school subjects (Bishop, 2008). Research also shows that students combining high school with their sports outperform students who are not participating in sports academically (Stegman, 2000; Whitley, 1999; Zaugg, 1998). Interestingly, research also shows that athletes have higher general self-concept than their student peers who are not participating in sports (Brooks, 2007). This is explained by the impact their sports have on their general self-concept because of the importance of psychological centrality on a person's self (Rosenberg, 1968). Research also claims that burnout is a possible result of an increasing amount of competitive and training stress for an athlete (Gould & Dieffenbach, 2002). Based on this research there is reason to believe that athletes who are studying at specialized high schools for sports and are experiencing low level of satisfaction with their progress in sport, should be in danger of experiencing burnout. Compared to their satisfaction with progress in school, sport should have a more significant impact on an athlete's level of burnout. Therefore, an interesting question to investigate is how different levels of perceived satisfaction with own progress academically in school and in sport are associated with athlete burnout. Hypothesis 1: Lower levels of satisfaction with progress academically in school and in sport are associated with higher burnout among Norwegian junior elite athletes, whereas

higher levels of satisfaction are associated with lower burnout.

Method

Participants in the present study were 114 high school athletes who voluntarily participated in an online questionnaire that measured psychological variables concerning their thoughts, feelings and actions within sport at their schools. They were all students at different high schools for sports in the middle Norway region. The athletes were from age 16 to 20, with an average age of 17. The athletes were competing in sports such as football, volleyball, handball, ice hockey, biathlon, cross country skiing, ski jumping, nordic combined, alpine skiing, ice skating, shooting, orienteering, track and field, and bicycling.

The Athlete Burnout Questionnaire

The first author translated the 15 item Athlete Burnout Questionnaire into Norwegian using a double Translation-Back-Translation technique (Raedeke & Smith, 2009). The stem for each question was: "How often do you feel this way?" Athletes were requested to rate the extent to which the items refer to their participation motives on a five-point Likert scale anchored by (1) "Almost Never" and (5) "Almost Always". The ABQ has three five-item subscales assessing three key dimensions of burnout: (1) Reduced sense of accomplishment, (2) Emotional and physical exhaustion, and (3) Devaluation of sport participation. Examples of items covering the different dimensions are respectively; "*It seems that no matter what I do, I don't perform as well as I should*"; "*I feel so tired from my training that I have trouble finding energy to do other things*", and "*The effort I spend participating in my sport would be better spent doing other things*". A total summed score for the ABQ is achieved by averaging all three subscale scores.

Perceived satisfaction with progress in sport and academically in school

Performances in sport are often measured as results in different competitions. However, such measurements are contaminated by different variables such as random chance and opponent's outstanding performance (Courneya & Chelladurai, 1991). The use of athletes' satisfaction with their own performances is a way to avoid this pitfall (Chelladurai & Riemer, 1997). However, it might be difficult to separate these two variables because of the athletes' affective reactions regarding their actual performance (Chelladurai & Riemer, 1998). In this study we chose to use athletes' satisfaction with their own progress in sport during the last year

as an outcome variable. This was done to avoid short-term affective reactions regarding results in competitions, and to include experienced progress in daily training sessions.

The athletes in this study were asked to consider how satisfied they were with their own progress academically in school and in sport during the last year on a 7-point scale. The levels of perceived satisfaction with progress in sport are ranging from: Level 1) Extremely dissatisfied, Level 2) Very dissatisfied, Level 3) Dissatisfied, Level 4) Either...or, Level 5) Satisfied, Level 6) Very satisfied, Level 7) Extremely satisfied.

Data Analysis

To explore the impact of perceived satisfaction with progress academically in school and in sport, and Athlete burnout (ABQ), analyses was conducted by means of descriptive statistics and one-way between groups analysis of variance (ANOVA) using the SPSS 20 software. ANOVA was employed to investigate whether the means between the different groups (levels of athletes' perceived satisfaction 1-7) were equal or not. In general, when conducting ANOVA the observed variance in a particular variable is partitioned into components attributable to different sources of variation. ANOVA conducts a statistical test of whether or not the means of several groups are all equal, and therefore generalizes the t-test to more than two groups (Pallant, 2010; Gall, Gall & Borg, 2007). Since ANOVA is useful when comparing three or more means, this analytic approach was chosen to explore our research questions.

Results

Table 1 shows correlations between the study variables as well as the number of items for each dimension of the ABQ and the sum of ABQ, statistical means of the sum score, standard deviations, and the Cronbach's alphas.

Table 1
Correlations between the variables and descriptive statistics

Variable	1	2	3	4
<i>ABQ</i>				
1. Accomplishments	-	.41**	.44**	.72**
2. Exhaustion		-	.72**	.87**
3. Devaluation			-	.89**
4. ABQ sum				-
Number of items	5	5	5	15
Mean	11.93	11.33	10.76	34.03
Standard deviation	4.08	4.61	4.94	11.32
Cronbach's alpha	.80	.89	.85	.91

Note. **Correlations are significant at $p < .001$, $N=114$.

The zero order correlations between the study variables vary from moderate to strong. All variables had satisfactory Cronbach's alphas. The mean values of the sum scores of the different dimensions were not high, indicating that these athletes in general almost never or rarely experience reduced accomplishments, exhaustion or devaluation. The strongest correlation is found between Exhaustion and Devaluation, with a coefficient of .72.

Table 2 shows the means and standard deviations of the different dimensions of the ABQ and the sum of ABQ, sorted by the different levels of athletes' satisfaction with their progress in school during the last year.

Table 2
The dimensions of ABQ and each level of satisfaction with progress academically in school

		N	Mean	SE
ABQ Accomplishments	very dissatisfied	6	15.50	4.14
	dissatisfied	15	13.13	3.20
	either..or	34	11.82	3.60
	satisfied	44	11.36	4.60
	very satisfied	12	11.67	4.05
	extremely satisfied	3	9.33	1.15
ABQ Exhaustion	very dissatisfied	6	20.00	5.55
	dissatisfied	15	13.53	4.31
	either..or	34	9.79	3.36
	satisfied	44	11.11	4.52
	very satisfied	12	10.25	2.73
	extremely satisfied	3	8.00	1.73
ABQ Devaluation	very dissatisfied	6	21.50	2.88
	dissatisfied	15	12.07	5.05
	either..or	34	9.53	3.74
	satisfied	44	9.89	4.63
	very satisfied	12	11.08	3.68
	extremely satisfied	3	8.33	0.58
ABQ Sum	very dissatisfied	6	57.00	10.95
	dissatisfied	15	38.73	9.76
	either..or	34	31.15	7.75
	satisfied	44	32.36	11.61
	very satisfied	12	33.00	7.64
	extremely satisfied	3	25.67	3.06

Note. No athletes reported that they were extremely dissatisfied with their progress academically in school.

In general, the mean values of the sum scores of the different dimensions at the different levels of perceived satisfaction academically are not high. However, the athletes who are very dissatisfied with their progress academically report high scores on the dimension Exhaustion and Devaluation (Mean=20.00 and 21.50, respectively), and the sum score of Athlete Burnout (Mean=57.00). In fact,

these results are indicating that these athletes frequently experience exhaustion and devaluation.

Table 3 shows the means and standard deviations of the different dimensions of the ABQ and the sum of ABQ, sorted by the different levels of athletes' satisfaction with their progress in sport during the last year.

Table 3

The dimensions of ABQ and each level of satisfaction with progress in sport

		N	Mean	SE
ABQ Accomplishments	extremely dissatisfied	3	13.67	4.51
	very dissatisfied	5	13.20	4.21
	dissatisfied	15	15.53	3.85
	either..or	16	14.88	3.88
	satisfied	38	11.53	3.61
	very satisfied	24	9.75	2.51
	extremely satisfied	13	8.46	2.60
ABQ Exhaustion	extremely dissatisfied	3	11.00	3.61
	very dissatisfied	5	9.40	3.65
	dissatisfied	15	12.87	4.32
	either..or	16	12.06	5.81
	satisfied	38	11.55	5.08
	very satisfied	24	10.79	4.20
	extremely satisfied	13	9.85	2.82
ABQ Devaluation	extremely dissatisfied	3	8.67	1.53
	very dissatisfied	5	11.60	5.27
	dissatisfied	15	12.87	5.26
	either..or	16	11.63	5.94
	satisfied	38	10.68	5.25
	very satisfied	24	9.08	2.90
	extremely satisfied	13	10.77	5.36
ABQ Sum	extremely dissatisfied	3	33.33	3.06
	very dissatisfied	5	34.20	9.01
	dissatisfied	15	41.27	10.48
	either..or	16	38.56	12.99
	satisfied	38	33.76	12.25
	very satisfied	24	29.63	8.20
	extremely satisfied	13	29.08	9.48

In general, the mean values of the sum scores of the different dimensions at the different levels of perceived satisfaction in sport are not high. The results indicate that the athletes in general, across the different levels of perceived satisfaction, almost never or rarely experience reduced accomplishments, exhaustion or devaluation.

lower scores on the different dimensions of the ABQ and the sum of ABQ. However, this trend does not apply consequently. Accordingly, there seems to be a trend that lower levels of athlete satisfaction within sport is associated with higher scores on Accomplishments and the sum of ABQ. However, this trend does not seem to apply to the other dimensions (Exhaustion and Devaluation).

According to the scores in Table 2 and 3 the majority of the athletes are satisfied or either or, with their own progress academically in school (68,4 %, N= 44 and 34, respectively), and satisfied or very satisfied with their own progress in sport (54,4 %, N= 38 and 24, respectively). There seems to be a trend that higher satisfaction with own progress academically in school is associated with

The ANOVA analysis was conducted to explore possible significant differences between the groups in their mean scores on the different dimensions of the ABQ and the sum of ABQ. The groups were based on their level of satisfaction with progress academically in school and in sport (as in Table 2 and 3). The results are presented in Table 4 and 5.

Table 4
Summary of ANOVA where school performance is the factor

		Sum of Squares	df	Mean Square	F
ABQ Accomplishments	Between Groups	133.75	5	26.75	1.65
	Within Groups	1747.69	108	16.18	
	Total	1881.44	113		
ABQ Exhaustion	Between Groups	653.36	5	130.67	8.06**
	Within Groups	1751.97	108	16.22	
	Total	2405.33	113		
ABQ Devaluation	Between Groups	821.69	5	164.34	9.19**
	Within Groups	1930.92	108	17.88	
	Total	2752.61	113		
ABQ	Between Groups	4124.86	5	824.98	8.60**
	Within Groups	10366.05	108	95.99	
	Total	14490.92	113		

**p < 0.01

Table 5
Summary of ANOVA where sport performance is the factor

		Sum of Squares	df	Mean Square	F
ABQ Accomplishments	Between Groups		5	104.55	8.92**
	Within Groups		108	11.72	
	Total		113		
ABQ Exhaustion	Between Groups		5	16.74	0.78
	Within Groups		108	21.51	
	Total		113		
ABQ Devaluation	Between Groups		5	27.15	1.72
	Within Groups		108	24.20	
	Total		113		
ABQ	Between Groups		5	317.20	2.70*
	Within Groups		108	117.64	
	Total		113		

* p < 0.05, ** p < 0.01

The results of the analysis indicate that there are statistically significant differences at the $p < .001$ level between the mean scores on all of the dimensions of ABQ and satisfaction with progress academically in school, except from the dimension Accomplishments. Accordingly, statistically significant differences were found at the $p < .001$ level between the mean scores on the dimension

Accomplishments and the sum of ABQ, and satisfaction with progress in sport. In order to gain a clearer picture of which groups that differ, multiple comparisons post-hoc tests were conducted. The Tukey HSD test was chosen to explore which levels of satisfaction with progress within school and sport that differed from each other. The results of the post-hoc tests are presented in Table 6 and 7.

Table 6
Tukey HSD Comparison of Athlete burnout and perceived level of satisfaction academically in school

Dimension	Comparisons	Mean Difference	SE	95% CI	
				Lower Bound	Upper Bound
ABQ Exhaustion	Level 2 vs. Level 3	6.47*	1.95	0.82	12.11
	Level 2 vs. Level 4	10.21**	1.78	5.03	15.38
	Level 2 vs. Level 5	8.89**	1.76	3.80	13.97
	Level 2 vs. Level 6	9.75**	2.01	3.91	15.59
	Level 2 vs. Level 7	12.00**	2.85	3.74	20.26
	Level 3 vs. Level 4	3.74*	1.25	0.12	7.36
ABQ Devaluation	Level 2 vs. Level 3	9.43**	2.04	3.50	15.36
	Level 2 vs. Level 4	11.97**	1.87	6.54	17.40
	Level 2 vs. Level 5	11.61**	1.84	6.27	16.95
	Level 2 vs. Level 6	10.42**	2.11	4.28	16.55
	Level 2 vs. Level 7	13.17**	2.99	4.49	21.84
ABQ	Level 2 vs. Level 3	18.27**	4.54	4.54	32.00
	Level 2 vs. Level 4	25.85**	4.34	13.27	38.44
	Level 2 vs. Level 5	24.64**	4.26	12.27	37.00
	Level 2 vs. Level 6	24.00**	4.90	9.79	38.21
	Level 2 vs. Level 7	31.33**	6.93	11.23	51.43

* $p < 0.05$, ** $p < 0.01$

Table 6 shows that there are significant differences among several of the levels of satisfaction with progress academically in school at the $p < .01$ level and the $p < .05$ level. In general, the results indicate that the lower levels differ significantly from the higher levels (level 2 vs. level 3,4,5,6 and 7 for the

two dimensions and the sum of ABQ, and level 3 vs. level 4 for exhaustion). A trend is that the lower levels of perceived satisfaction have a mean value that is significantly higher than the higher levels (indicating higher levels of burnout).

Table 7
Tukey HSD Comparison of Athlete burnout and perceived level of satisfaction with progress in sport

Dimension	Comparisons	Mean Difference	SE	95% CI	
				Lower Bound	Upper Bound
ABQ Accomplishments	Level 3 vs. Level 5	4.01**	1.04	0.87	7.14
	Level 3 vs. Level 6	5.78**	1.13	2.40	9.17
	Level 3 vs. Level 7	7.07**	1.30	3.17	10.97
	Level 4 vs. Level 5	3.34*	1.02	0.28	6.42
	Level 4 vs. Level 6	5.13**	1.11	1.80	8.45
	Level 4 vs. Level 7	6.41**	1.28	2.57	10.26
ABQ	Level 3 vs. Level 6	11.64*	3.57	0.91	22.37

* $p < 0.05$, ** $p < 0.01$

Table 7 shows that there are significant differences among several of the levels of satisfaction with progress in sport at the $p < .01$ level and the $p < .05$ level. In general, the results indicate that the lower levels differ significantly from the higher levels (level 3 vs. level 5, 6 and 7, and level 4 vs. level 5, 6 and 7 for the dimension Accomplishments, and level 3 vs. level 6 for the sum of ABQ). A trend is that the lower levels of perceived satisfaction have a mean value that is significantly higher than the

higher levels. However, this trend is not true for the athletes who are extremely and very dissatisfied with their progress in sport.

Discussion

It is claimed that possible unfulfilled expectations academically or within sports might become a contributor for higher levels of Athlete Burnout (Gustafsson, 2007; Goodger, et al., 2007). The main purpose of this study was to explore how different

levels of perceived satisfaction with own progress academically in school and in sport are associated with Athlete Burnout (ABQ). In order to explore this question, we investigated junior athletes' perceptions of items that are measuring the different dimensions of Athlete Burnout, and how these perceptions relate to their own satisfaction with their progress academically in school and in sport during the last year.

Our hypothesis was that lower levels of satisfaction with progress academically in school and in sport were associated with higher levels of burnout among Norwegian junior elite athletes, whereas higher levels of satisfaction are associated with lower levels of burnout. Our hypothesis was partly confirmed as the results revealed that lower levels of perceived satisfaction with own progress academically in school and in sport were associated with higher Athlete Burnout than higher levels of perceived satisfaction with own progress (see Table 6 and 7). This result applies for the two dimensions Exhaustion and Devaluation of Athlete Burnout, and the sum score of Athlete Burnout, when perceived satisfaction with progress academically was the factor (see Table 4). Interestingly, the athletes who were very dissatisfied with their progress academically reported an alarming high level of Athlete Burnout (see Table 2). When perceived satisfaction with progress in sports was the factor (see Table 5), only the dimension Accomplishments applied this result. However, the trend was not so clear when perceived satisfaction with progress in sport was the factor. Interestingly, the general mean scores on Athlete Burnout were not alarming high at neither level when perceived satisfaction with progress in sport was taken into account (see Table 3).

The results in this study indicate that the impact from perceived satisfaction with own progress in sport on Athlete Burnout is less than the impact from perceived satisfaction with own progress academically in school. There is a trend that lower levels of perceived satisfaction with own progress academically significantly differ from higher levels of perceived satisfaction on Athlete Burnout scores. Interestingly, the mean scores for junior athletes who are very dissatisfied with their perceived progress academically show that these athletes frequently feel emotional and physical exhausted, and frequently devalue their sports. This is an important finding that both coaches and theoreticians should notice. A possible explanation to this finding can be found in theories concerning psychological centrality (Rosenberg, 1968; Skaalvik & Skaalvik, 2005). Areas that are psychologically central to a person is claimed to determine the affect this area has on his or her self.

Thus, academic performance in school seems to be an important area for young athletes in these specialized high schools for sports and a highly dissatisfaction with own progress within the academic area seems to be an important contributor to Athlete Burnout. As a consequence, it seems to be important that both coaches and athletes favour athletes' academic work as well as their sports at specialized high schools for sports.

Research also shows that sport is an area that has significant impact on an athlete's general self-concept (Brooks, 2007). Thus, it was expected that dissatisfaction with own perceived progress in sport should contribute to significant higher levels of Athlete Burnout than higher levels of satisfaction with own progress. However, this was not the case which was a surprise. Only the dimension Accomplishments applied such a trend. However, this is not a result that supports the expectation in this study. An athlete's feeling of accomplishment should reflect this athlete's perceived satisfaction with own progress in sport at different levels. They are more or less the same measure. Since these junior athletes study at specialised high schools in sports, one should expect that sport is an area that is psychological central among the athletes and in their environment. A possible explanation to this result might be that sport is a volunteer activity, and that the athletes have the opportunity to end their careers if they want, while school is not a volunteer activity. Especially in Norway, it seems to be a culture pressure to finish higher education and achieve academically results in different school subjects (Skaalvik & Skaalvik, 2005). Thus, these results indicate that the athletes' and the environment's academic expectations might be a greater stressor than their expectations in sport. However, in order to fully understand these results further research is needed.

Conclusion

This main finding in this study indicates that frustration from unfulfilled expectations academically in school among junior athletes attending high school education at specialised schools for sport might be a contributor for higher levels of Athlete Burnout. These results might indicate that to fully meet the psychosocial and physical demands associated with training and competitions, an athlete must be satisfied with his or her perceived progress academically in school. Accordingly, when academically progress is not satisfactorily, an athlete might start to develop a detached attitude toward the sport that is reflected by a lack of concern about the sport itself and his or her performance quality.

However, the present study has several limitations. Sample size may have influenced the results.

Studies with larger number of participants are therefore called for in future research, as well as a more solid and causal design. Moreover, one should note that the collected data is constituted by self-reporting measures and one do not know to which extent these self-reports accurately reflect the variables under study.

References

- Bishop, J. (2008). *Examining our 'sports obsessed' culture*. Eastern Mennonite University. Retrieved from <http://www.emu.edu/news/index.php/1622/>
- Brooks, D. T. (2007). *The effects of athletic participation on the student's self-concept*. (Unpublished doctoral dissertation). The Graduate College University of Wisconsin: Stout, WI.
- Cherniss, C. (1980). *Professional burnout in human service organizations*. New York: Praeger.
- Chelladurai, P., & Riemer H. A. (1997). A classification of facets athlete satisfaction. *Journal of sport management*, 11, 13–159.
- Chelladurai, P., & Riemer, H. A. (1998). Measurement of leadership in sports. In J. L. Duda (Ed.), *Advances in sport and exercise psychology measurement* (pp. 227–253). Morgantown, WV: Fitness Information Technology.
- Coakley, J. (1992). Burnout among adolescent athletes: A personal failure or social problem? *Sociology of Sport Journal*, 9, 271–285.
- Cordes, C. L., & Dougherty, T. W. (1993). A review and an integration of research on job burnout. *Academy of Management Review*, 18, 621–656.
- Courneya, K. S., & Chelladurai, P. (1991). A model of performance measures in baseball. *Journal of Sport Psychology*, 13, 16–25.
- Cox, T., Tisserand, M., & Taris, T. (2005). Editorial: the conceptualization and measurement of burnout: questions and directions. *Work & Stress*, 19, 187–191.
- Cresswell, S. L., & Eklund, R. C. (2005). Motivation and burnout among top amateur rugby players. *Medicine and Science in Sports and Exercise*, 37, 469–477.
- Gall, M. D., Gall, J. P., & Borg, W. R. (2007). *Educational research: an introduction*. Boston: Allyn and Bacon.
- Goodger, K., Gorely, T., Harwood, C., & Lavallee, D. (2007). Burnout in sport: A systematic review. *The Sport Psychologist*, 21, 127–151.
- Gould, D., & Dieffenbach, K. (2002). Overtraining, underrecovery, and burnout in sport. In M. Kellman (Ed.), *Enhancing recovery: Preventing underperformance in athletes*. Champaign, IL: Human Kinetics.
- Gould, D., Udry, E., Tuffey, S., & Loehr, J. (1996). Burnout in competitive junior tennis players: I. A quantitative psychological assessment. *The Sport Psychologist*, 10, 322–340.
- Gustafsson, H. (2007). Prevalence of burnout in competitive adolescent athletes. *The Sport Psychologist*, 21, 21–37.
- Gustafsson, H., Hassmén, P., Kenttä, G., & Johansson, M. (2008). A qualitative analysis of burnout in elite Swedish athletes. *Psychology of Sport and Exercise*, 9, 800–816. <http://dx.doi.org/10.1016/j.psychsport.2007.11.004>.
- Gustafsson, H., Kenttä, G., Hassmén, P., & Lundqvist, C. (2007). Prevalence of burnout in competitive adolescent athletes. *The Sport Psychologist*, 21, 21–37.
- Main, L. C., Landers, G. J. (2012). Overtraining or Burnout: A Training and Psycho-Behavioral Case Study. *International Journal of Sports Science & Coaching*, 7, 23–31.
- Maslach, C., & Goldberg, J. (1998). Prevention of burnout: New perspectives. *Applied and Preventive Psychology*, 7, 63–74.
- Maslach, C., Jackson, S. E., & Leiter, M. P. (1997). Maslach Burnout Inventory, In C. P. Zalaquett, & R. J. Wood (Eds.), *Evaluating stress: A book of resources* (pp. 191–218). London: The Scarecrow Press.
- Maslach, C., Schaufeli, W. B., & Leiter, M. P. (2001). Job burnout. *Annual Review of Psychology*, 52, 397–422.
- Maslach, C., Jackson, S. E., & Leiter, M. P. (1996). *Maslach burnout inventory manual* (3rd ed.). Palo Alto, CA: Consulting Psychologists Press.
- MacNeill, D. K. (1981). The relationship of occupational stress to Burnout. In J. W. Jones (Ed.), *The Burnout Syndrome* (pp. 68–88). Park Ridge, Ill.: London House Press.
- Pallant, J. (2010). *SPSS survival manual a step by step guide to data analysis using the SPSS program* (4th ed.). Maidenhead: Open University Press.
- Raedeke, T. D. (1997). Is athlete burnout more than stress? A commitment perspective. *Journal of Sport & Exercise Psychology*, 19, 396–417.
- Raedeke, T.D., & Smith, A.L. (2009). *The Athlete burnout questionnaire manual*. Morgantown, WV: Fitness Information Technology.
- Rosenberg, M. (1968). Psychological selectivity in self-esteem formation. In C. Gordon & K. J. Gergen (Eds.), *The Self in social Interaction*. (pp. 339–346). New York: Wiley.
- Ryan, R. M., & Solky, J. A. (1996). What is supportive about social support? On the psychological needs for autonomy and relatedness. In G. R. Pierce, B. R. Sarason, & I. G. Sarason (Eds.), *Handbook of social support and the family* (pp. 249–267). New York: Plenum Press.
- Schaufeli, W.B., & Buunk, B.P. (2003). Burnout: An overview of 25 years of research and theorizing. In M.J. Schabracq, J. A.M. Winnubst, & C.L. Cooper (Eds.), *The handbook of work and health psychology* (2nd ed., pp. 383–425). New York: John Wiley & Sons.
- Schaufeli, W.B., & Taris, T.W. (2005). Commentary. The conceptualization and measurement of burnout: Common ground and worlds apart. *Work and Stress*, 19, 356–362.
- Silva, J. M. (1990). An analysis of the training stress syndrome in competitive athletics. *Journal of Applied Sport Psychology*, 2, 5–20.
- Skaalvik, E. M. & Skaalvik, S. (2005). *Skolen som læringsarena. Selvoppfatning, motivasjon og læring*. Oslo: Universitetsforlaget.
- Stegman, M. (2000). Athletics and academics. *High School Magazine*, 7, 36–39.
- Whitley, R. (1999). Those 'dumb jocks' are at it again: A comparison of the education performances of athletes and non-athletes in North Carolina high schools from 1993 through 1996. *The High School*, 82, 223–233.
- Zaugg, H. (1998). Academic comparison of athletes and non-athletes in a rural high school. *NASSP Bulletin*, 82, 63–72.

Synchronization of Kuramoto oscillators on Knots

Amelia Carolina Sparavigna¹ 

¹ Department of Applied Science and Technology, Politecnico di Torino, Corso Duca degli Abruzzi 24, Torino, Italy

Abstract: A knot is a circle embedded in the space. Projecting a knot on a plane, we obtain a diagram which is known as the knot diagram. The vertices of the diagram, where the curved lines are crossed, can be considered as sites occupied by oscillators. The synchronization of these oscillators can be studied by means of a Kuramoto model. Here we propose to define some order parameters, of the complete knot diagram and of its regions, to study the synchronization of the system with regard to the different parts of it.

Keywords: Knots, Synchronization, Kuramoto model

Introduction

Networks of coupled systems have been used to model the collective dynamics of biological oscillators in self-organizing systems and in excitable media. Under certain conditions, the collective dynamics shows synchronization [1]. In fact, the importance of the synchronized behaviours in biology was already highlighted by A.T. Winfree [2] in 1967: in his paper, the author told that "the variety of biological rhythms leaves no doubt that autonomously periodic processes contribute to the coordination of life-processes."

To study the synchronized behaviour of coupled oscillators, a mathematical model, which is known as the Kuramoto model, had been developed. This model assumed the oscillators were nearly identical and that the phase of each oscillator was coupled to the collective behaviour [3,4]. Recently, some studies based on the Kuramoto model have been proposed for a modelling of neuronal synchronisation [5], after the discovery that the regions of the brain are coupled and exhibit synchronous activity [6]. As told in [5], neuronal synchronisation also plays a role in vision, movement, memory and epilepsy [7–13]. Thus, the Kuramoto model would provide a basis to modelling some phenomena of the brain.

In fact the Kuramoto model had been applied to many networks of coupled oscillators to study the collective dynamics. Studies have been performed either on regular networks, such as cubic lattices, or on random networks [3]. The small-world networks, which are intermediate of the local regular networks and the fully random networks, have been used too. The small-world networks are characterized by the fact that a high clustering, which is a characteristic of the regular networks is accompanied by a short path length, which is typically observed in random networks [14]. Phase synchronization on small-world networks emerges in the presence of even a tiny fraction of shortcuts,

indicating that the same synchronizability as that of a random network can be achieved [14].

Kuramoto oscillators and knots

Here we propose the study of the synchronization of Kuramoto oscillators placed on the graph created by the projection of a mathematical three-dimensional knot on a bidimensional plane. This projection is known as the knot diagram. An intuitive suggestion is provided by Wikipedia [15]: think of a knot casting a shadow on the wall to have the knot diagram. Here we are talking about mathematical knots which are the embedding of a closed line in the three-dimensional space: this line can be knotted or unknotted. From a more theoretical standpoint, a knot is a homeomorphism that maps a circle into three-dimensional space and cannot be reduced to the simple circle by a continuous deformation. The difference between the mathematical and the conventional notion of a knot is that mathematical knot is closed; the conventional knot has the ends to tie or untie. The branch of mathematics that studies knots is known as knot theory [16-19].

In the upper part of Fig.1, it is shown the so-called Jordan curve of a knot, a non-self-intersecting continuous loop in the plane representing the three-dimensional knot. A "trip code" can be created considering the intersections and labelling them [17]. In the case of the diagram in Fig.1, the trip code is ABCDEFBCGEHAFGHA. The labels are letters in alphabetic order (A,B,...,H). The label is put on the vertices the first time we meet it during the trip on the knot diagram. Each letter labelling the intersections is then appearing twice in the trip code. The starting label appears three times for the convenience of the reader. We can see from the figure that each vertex of the graph can be connected with two or four other sites, according to the curve. The knot diagram subdivides the space in several regions.



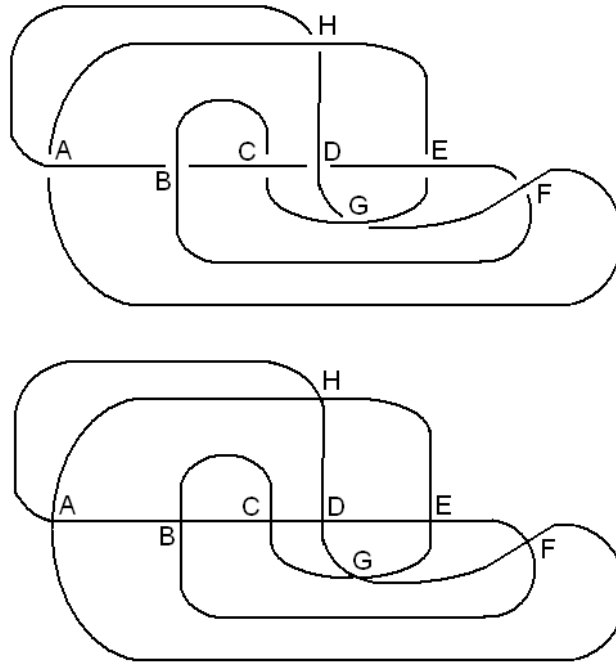


Fig.1 – The Jordan curve of a knot and the corresponding graph. The trip code is ABCDEFBCGEHAFGHA.

Let us study the synchronization on the knot, using then a Kuramoto approach. The Kuramoto model as it stands describes oscillators of nearly natural frequencies, connected together via coupling constants. Each vertex i of the knot diagram has an oscillator, the state of which is characterized by its phase φ_i . We write the set of equations of motion governing the dynamics of the N oscillator system:

$$\dot{\varphi}_i + \frac{K}{2k} \sum_{j \in \Lambda_i} \sin(\varphi_i - \varphi_j) = \omega_i \quad (1)$$

where Λ_i denotes the nodes connected to site i . For instance, let us consider site $i=G$: from the figure we see that it is connected with C, D, E and F. Then we have $\Lambda_i=C,D,E,F$, when we assume a coupling just to the nearest neighbour sites. K is the coupling strength, k the range of the local connection [14]. In our example $k=4$. ω_i is the intrinsic frequency of the i -th oscillator.

To evaluate the synchronization, an order parameter is defined [14]. Let us define it as:

$$m = \left\langle \left| \frac{1}{n} \sum_{j=1}^n e^{i\varphi_j} \right| \right\rangle \quad (2)$$

where n is the number of oscillators chosen for calculation. The bracket $\langle \rangle$ indicates the average over time. The average over different realizations of the intrinsic frequencies, as used in [14], is not considered in the proposed calculation.

To show an example of synchronization on a knot we look at the diagram in Fig.1, having oscillators on vertices with frequencies which are ranging from 1.20 to 0.85 s^{-1} , reducing by steps of 0.05 s^{-1} , following the alphabetic order of labels ($\omega_A = 1.20 s^{-1}$, $\omega_B = 1.15 s^{-1}$, ..., $\omega_H = 0.85 s^{-1}$).

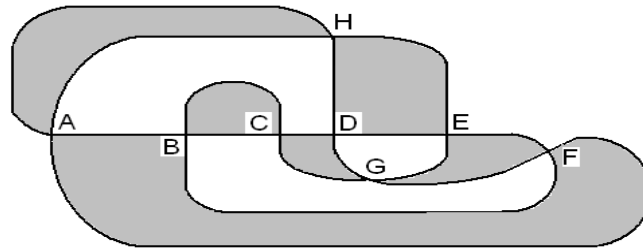


Fig.2 – The diagram corresponding to the knot in Figure 1 divides the plane in several regions. The grey ones are here used to study the synchronization.

Discussion and results

We can study the role of the coupling strength K in the frequency synchronization. It is interesting to compare the overall behaviour of the synchronization, that we obtain using all the sites in the evaluation of the order parameter, with the synchronization of each single region of the knot diagram. As we can see in Fig.2, the curve obtained by the projection of the knot on a plane, is a curve which divides the plane in several region.

In Fig.3, the red dotted curve is showing the behaviour of the order parameter obtained from Eq.2, when it is assumed index j ranging from 1 (corresponding to vertex A) to $n=8$ (corresponding to vertex H). The order parameter is then evaluated considering all the vertices of the knot. The other curves are referring to the synchronization of each of the grey regions in the

following way. Let us consider for instance region CDG: it is assumed in Eq.2 that j is ranging from 1 to 3, where 1 corresponds to C, 2 to D and 3 to G.

Let us note the different behaviour of the synchronization of regions AH and BC shown in Fig.3 (obtained from the Equation 2 of the order parameter, evaluated for $j=A,H$ and $j=B,C$, respectively). As we can see from the figure, BC is synchronized for lower values of the coupling strength K . The reason is that BC have two vertices occupied by oscillators with the lowest possible difference in frequency, connected each other by two edges. Moreover B and C are connected by the trip code with other vertices having close frequencies. AH is a region where the vertices have oscillators with the highest frequency difference and the trip code is connecting them with oscillators quite different too.

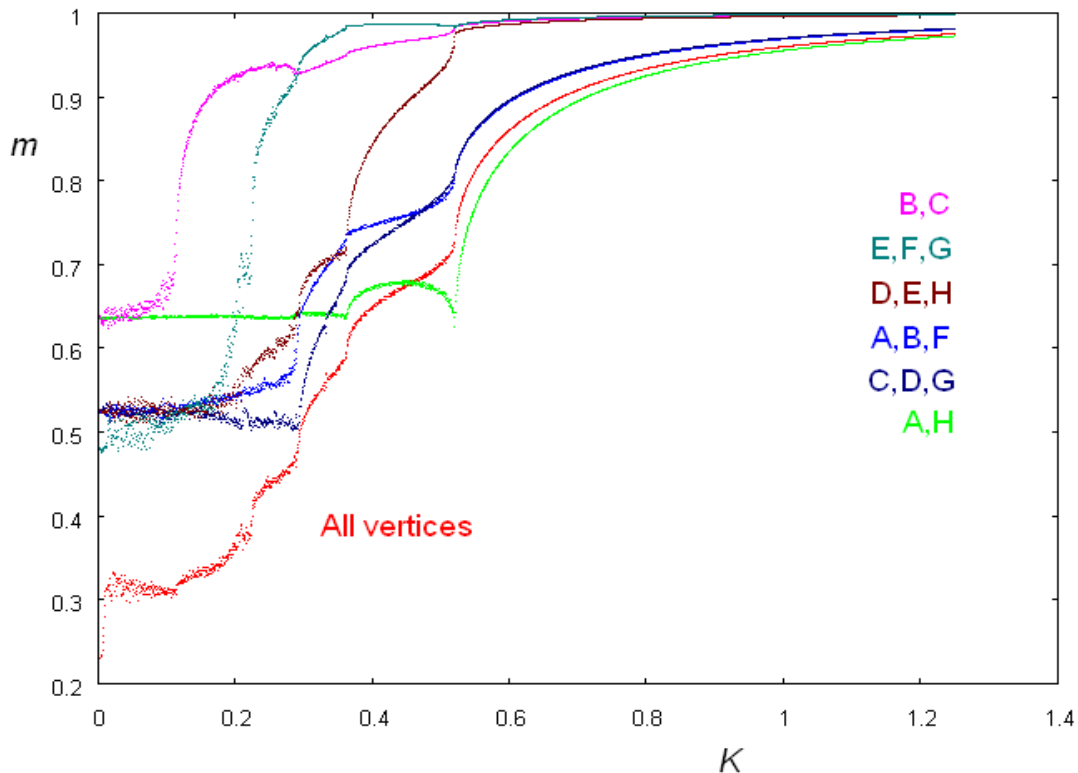


Fig.2 – Behaviour of the order parameter defined in Equation 2 (see text for explanation) as a function of the coupling strength K .

The use of knot diagrams to simulate the behaviour of real systems composed by several oscillators could be useful in studying the synchronization of the system. Adjusting the frequency values according to the labels and the trip code according with the connections among sites we can obtain some order parameters, suitable to analyse the behaviour of the system. A study and analysis of existing functional integrals and invariants defined on knots is under development to verify a connection with the proposed order parameter for oscillators.

References

- [1] D.J. Watts, S.H. Strogatz, Collective dynamics of 'small-world' networks, *Nature*, 393 (1998) 440-442.
- [2] A.T. Winfree, Biological rhythms and the behaviour of populations of coupled oscillators, *J. Theor. Biol.* 16 (1967) 15.
- [3] S.H. Strogatz, From Kuramoto to Crawford: Exploring the onset of synchronization in populations of coupled oscillators, *Physica D* 143 (2000) 1–20.
- [4] Y. Kuramoto, H. Arakai, *Chemical Oscillations, Waves and Turbulence*, Springer, Berlin, 1984.
- [5] D. Cumin, C.P. Unsworth, Generalising the Kuramoto model for the study of neuronal synchronisation in the brain, *Physica D* 226 (2007) 181–196.
- [6] M.V.L. Bennet, R.S. Zukin, Electrical coupling and neuronal synchronisation in the mammalian brain, *Neuron* 41 (2004) 495–511.
- [7] H. Sompolinsky, D. Golomb, D. Kleinfeld, Cooperative dynamics in visual processing, *Phys. Rev. A* 43 (1991) 6990–7011.
- [8] M. Cassidy, P. Mazzone, A. Oliviero, et al., Movement-related changes in synchronisation in the human basal ganglia, *Brain* 125 (2002) 1235–1246.
- [9] W. Klimesch, Memory processes, brain oscillations and EEG synchronisation, *Int. J. Psychophysiol.* 24 (1996) 61–100.
- [10] R.D. Traub, R.K. Wong, Cellular mechanisms of neural synchronisation in epilepsy, *Science* 216 (1982) 745–747.
- [11] F. Mormann, K. Lehnertz, P. David, C.E. Elger, Mean phase coherence as a measure for phase synchronization and its application to the EEG of epilepsy patients, *Physica D* 144 (2000) 358–369.
- [12] F.H. Lopes das Silva, P. Suffczynski, J. Parra, et al., Epilepsies as dynamic diseases of brain systems: Basic models and the search for EEG/Magnetoencephalography (MEG) signals of impending seizures, *Epilepsia* 42 (Suppl. 7) (2001) 3.
- [13] F.J. Varela, The preictal state: Dynamic neural changes preceding seizure onset, *Epilepsia* 42 (Suppl. 7) (2001) 3.
- [14] H. Hong and M. Y. Choi, Beom Jun Kim, Synchronization on small-world networks, *Phys. Rev. E*, 65 (2002) 026139-1-5.
- [15] Wikipedia, Knot Theory, http://en.wikipedia.org/wiki/Knot_diagram#Knot_diagrams
- [16] L.H. Kauffman, On knots, *Annals of Mathematical Studies*, Princeton University Press, 1987.
- [17] L.H. Kauffman, *Knots and Physics*, World Scientific, 2001.
- [18] A. Kawauchi, *A survey of knot theory*, Birkhäuser, 1996.
- [19] P.R. Cromwell, *Knots and links*, Cambridge University Press, 2004.

Some Features of Liquid Crystalline Oxadiazoles

Amelia Carolina Sparavigna¹ 

¹ Department of Applied Science and Technology, Politecnico di Torino, Corso Duca degli Abruzzi 24, Torino, Italy

Abstract: We propose a survey of some features of those oxadiazole compounds which are mesogenic, that is, which are displaying liquid crystalline properties induced by their rod- or disk-like molecules. We will see that they can have bend-shaped molecules too, creating biaxial phases, and other interesting peculiarities in the nematic and smectic phases. With large electric dipoles and luminescent properties, these materials are also very appealing for technological applications.

1. Introduction

Certain oxadiazoles are mesogenic compounds possessing the typical liquid crystalline nematic and smectic mesophases. Even the elusive biaxial nematic phase is displayed: this peculiar phase, theoretically proposed in 1970 by Freiser, can be observed in the mesophase of oxadiazoles with boomerang-shaped molecules [1-3]. Therefore, oxadiazoles are rather interesting for both experimental and theoretical researches. However, these compounds are relevant for applications too, in particular in the electroluminescent devices where they are the emissive materials [4].

Before starting a short survey of researches and results obtained with these compounds, let us discuss the basic structure of the oxadiazole molecule, because it is mainly the oxadiazole group that gives the shape to the final molecule in which it is inserted.

As generally told, the liquid crystal compounds are mesogenic due to their molecular rod-like or disk-like shape. However, the role of the molecular shape in the features of mesophases is more complex. If the rod-like structure of the molecule is bent for instance, the material can produce a spontaneous symmetry

breakdown, as in the case of the banana-shaped molecules studied by Niori et al.[5]. This experimental discovery by the Tokyo Technology group in 1996, of a ferroelectric behavior in a mesophase of a compound having achiral bend-core (banana) molecules, represented a revolution for the liquid crystals community. It is then not surprising the persistent interest for compounds where the shape of molecules is not simply rod-like or disk-like: oxadiazoles are among them.

The oxadiazole is an aromatic heterocyclic molecule, which structure is shown in the Figure 1. It has carbon, hydrogen, nitrogen and oxygen. In fact, it contains two nitrogen atoms (for instance, oxazole has one nitrogen atom). There are four possibilities to arrange nitrogen and oxygen, as the figure shows. Moreover, we have the possibility to substitute or di-substitute the hydrogen in the other two positions. An example is the 1,2,5-oxadiazole-3,4-diamine compound in the same figure. We can easily imagine how some longer threads attached to the oxadiazole, substituting diamine groups, can create a possible mesogenic compound with a bend-core shape. For this reason, the oxadiazole was used to build the boomerang-shaped molecules.

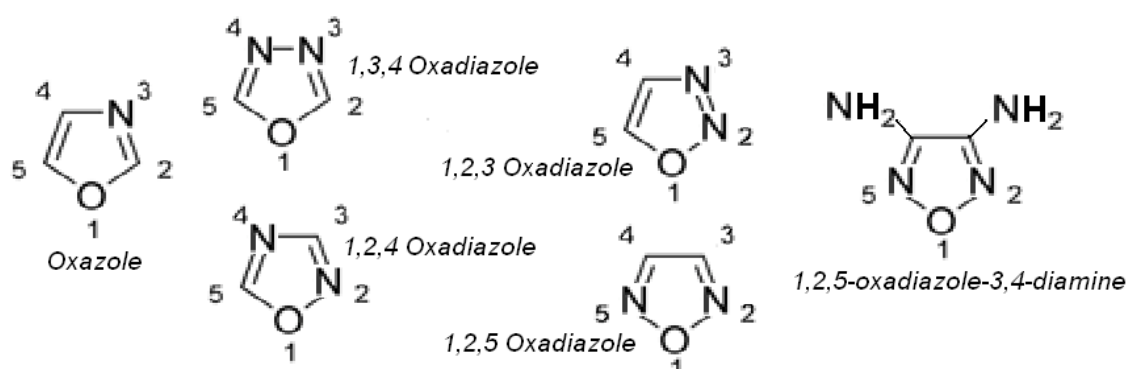


Figure 1 The four oxadiazoles in the middle, the oxazole on the left and an example of a substance with the 1,2,5-oxadiazole on the right.



Amelia Carolina Sparavigna (Correspondence)



d002040@polito.it

2. Symmetric compounds with 1,3,4-oxadiazoles with biaxial features.

References [1,2] show the boomerang molecules obtained with the 1,3,4-oxadiazole. These molecules have a biaxial molecular arrangement in the smectic A phase. But they have a biaxial nematic too. This is a mesophase different from the uniaxial nematic phase, where three distinct optical axes are present. The uniaxial phase has a single preferred axis, around which the system is rotationally symmetric $D_{\infty h}$. The symmetry group of a biaxial nematic is D_{2h} . This group can be represented by the geometry of a rectangular right parallelepiped. And in fact, a route to biaxiality in nematics is the development of molecules, which have the shape of parallelepipeds.

Numerical simulations [6] of transitions, from the ordinary nematic to the biaxial one, give the evolution of schlieren textures as they can be observed with the polarized light microscope. It results that the problem is more complex than what is commonly suggested, that it is the charge of disclinations which distinguishes the biaxial form from the uniaxial phase. To see beautiful images obtained with polarized microscope of such transition, let us look at Reference 7, where mesophases of 1,4"-*p*-terphenyl-bis-2,3,4-tri-dodecyloxy-benzal-imine are investigated. This is a calamitic compound with a biaxial nematic phase. An example of how the texture transition appears, when the nematic passes from uniaxial to biaxial symmetry, inspired from images in [7], is shown in the Figure 2.

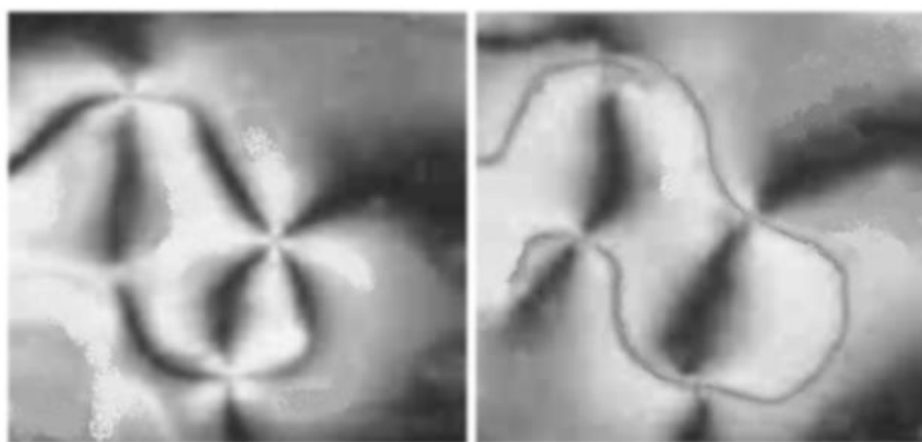


Figure 2 The image illustrates the transition from uniaxial (on the left) to biaxial (on the right) nematic phases as shown by the schlieren texture observed by means of the polarized light microscopy.

In spite of the fact that a biaxial nematic prefers to have a schlieren texture with disclinations of strength $1/2$, unambiguous results are given by H^2 -NMR investigations [1]. The resonance demonstrates that ODBP-Ph- C_7 and ODBP-Ph- C_{12} have a truly biaxial nematic (see Figure 3 for the molecular structure of such compounds). The researchers defined these molecules as boomerangs, because the angle at the

core of the molecule, which is the angle determined by the oxadiazole group, is approximately of 140° , greater than the typical value of 120° of banana mesogenic molecules. There are of course biaxial-shaped calamitic materials, but ODBP boomerangs have a large electric dipole ($\approx 4D$), which adds the possibility of strong intermolecular association.

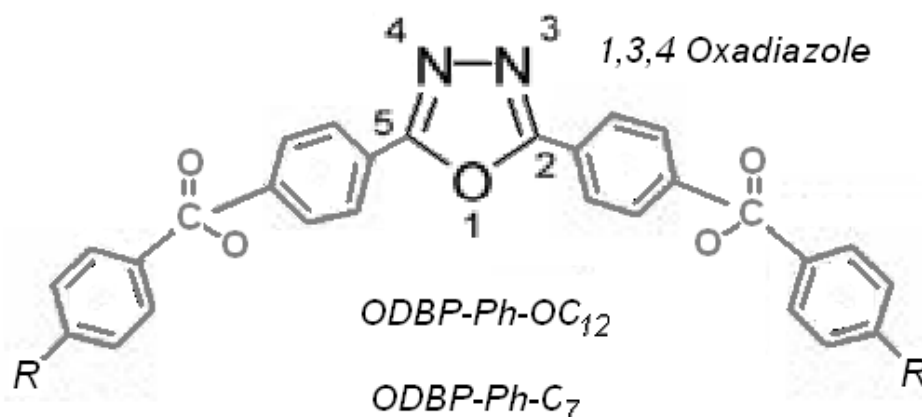


Figure 3 Boomerang molecules. *R* is the different fragment OC_{12} or C_7 .

3. The 2,5-disubstituted-1,3,4-oxadiazoles

Many compounds with 1,3,4 oxadiazoles have been prepared to study their luminescence property [4]. The compounds are generally chemically stable, sometimes with good electron-transport properties. The study on these materials allows the conclusions that the presence of mesophases is affected by both electronic and steric factors within terminal substituents [4]. Smectic and nematic, enantiotropic and monotropic phases were observed with polarized light microscope. Let us remember that an enantiotropic phase can be observed both heating and cooling the material, whereas a monotropic phase can be entered only during the heating or the cooling, not both.

In Reference 4, it is reported how a large molecular dipole can be obtained inserting a fluorine-substituent in oxadiazoles with 2,5-diphenyl-1,2,3-oxadiazole

(electron-deficient) and *p*-alkoxyphenyl (electron-rich) moieties. F atom, having a strong tendency to gain an electron, perturbs the charge distribution producing the dipole. The insertion of F atom is then stabilizing, whereas the insertion of electron-donor substituents destabilizes the mesophases. Liquid crystalline oxadiazole compounds with halogens (both 1,3,4-oxadiazoles and 1,2,4-oxadiazoles, see Figure 4) were investigated also in the Refs.[8-10].

The importance of oxadiazole compounds is due to the simultaneous presence of a bend-shape and of an electric dipole; this fact is very attractive in the framework of researches on materials with achiral molecules, which could display ferroelectric states. The fact that the dipolar nature of the oxadiazole core is influencing the mesomorphism was shown by molecular simulations too [11].

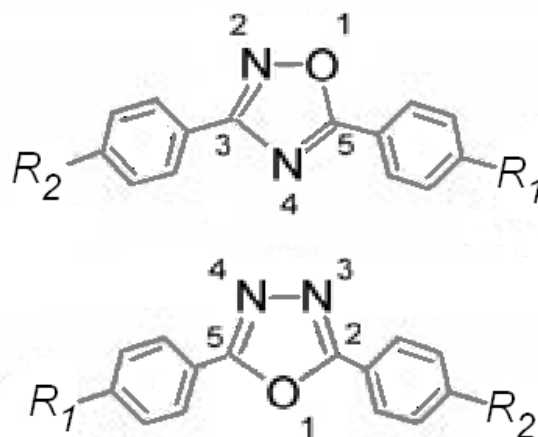


Figure 4 ODBPs structures with 1,3,4 and 1,2,4 oxadiazoles.
R₁ and R₂ are substituents with can be halogen atoms.

4. The 3,5-disubstituted-1,2,4 oxadiazoles with bend-shape

The Liquid Crystal Group of the Organic Intermediates and Dyes Institute in Moscow was the first group to study 3,5-disubstituted 1,2,4-oxadiazoles as fragments of liquid crystalline compounds [8-10]. Before their studies, these compounds were used only for pharmaceutical purposes. In Ref.12, several

asymmetric heterocyclic structures are proposed, leading to molecules with bend-shape and mesogenic properties (Figure 5). The 1,2,4-oxadiazole compounds display distinct aspects such as an asymmetrical distribution of electronic density, giving a dipole moment of ≈ 1.5 D. A distortion of the linearity of the molecule due to the bonding angles is observed and then the authors named the compounds as banana-shaped 1,2,4-oxadiazoles.

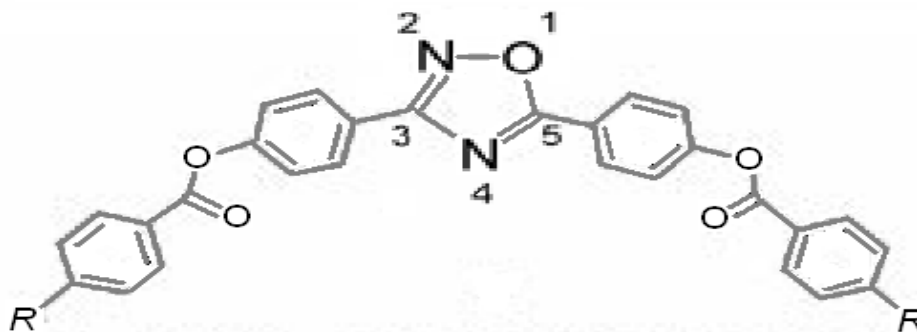


Figure 5 A banana-shaped compound from Ref.12.

5. Asymmetric oxadiazoles

The correlation between the existence of mesophases and the chemical structure of molecules is always important for the research in liquid crystals. When a family of asymmetric structures is under investigation, the variety of results is strongly enhanced. This is true for mesomorphic oxadiazole compounds too. Then, asymmetric oxadiazoles have been developed [8], because of their molecular structure with heterocycles and several possible substituents, providing a variety of smectic and nematic mesophases. The examples we can find in the references previously reported, show that not only the chemical structure of the substituents, but also their position with respect to the oxadiazole ring is relevant for the mesophases.

The optical microscope investigations show very interesting behavior of the smectic and the nematic phase of some of these oxadiazole compounds [13]. In particular the smectic phases have a toric texture that changes in a spherulitic nematic. Moreover, it is possible to observe a remarkable behavior in the nematic phase of 3,5-disubstituted-1,2,4-oxadiazoles, a texture transition driven by the temperature. We consider a “texture transition” as a change in the nematic texture observed by means of the polarized light microscope. The low temperature nematic has a texture with spherulitic domains. Figure 6 shows the transition between the smectic and the spherulitic

nematic of compound C of Ref.13 (here simply called ODBP). The figure shows the smectic (a) and the low-temperature (b) and the high-temperature (c) nematic phases.

Texture transitions have been previously observed inside the nematic phase of some mesomorphic thermotropic materials belonging to the families of the alkoxybenzoic and cyclohexane acids [14–16]. In some cases, peaks in DSC scanning and dielectric spectroscopy investigations accompany the evidence of the texture transition observed by polarized light microscopy. [17]. The Figure 6 in its upper part shows the smectic (a) and the two nematic phases (b) and (c) of the alkoxybenzoic acid HOBA.

Alkoxybenzoic and cyclohexane acids have mesophases because the mesogenic units are hydrogen-bonded dimers. The more common explanation for the presence of a texture transition in the nematic range is based on the existence of cybotactic clusters of such dimers, favoring a local smectic order in the nematic range [18]. Of course, the texture transition inside the nematic phase of oxadiazole compounds could be due to surface effects, but we suggest a possible existence of cybotactic clusters in these materials too. In Reference 2, the possibility of cybotactic cluster is also reported. Probably, this is a biaxial feature; however this fact needs to be studied by further investigations.

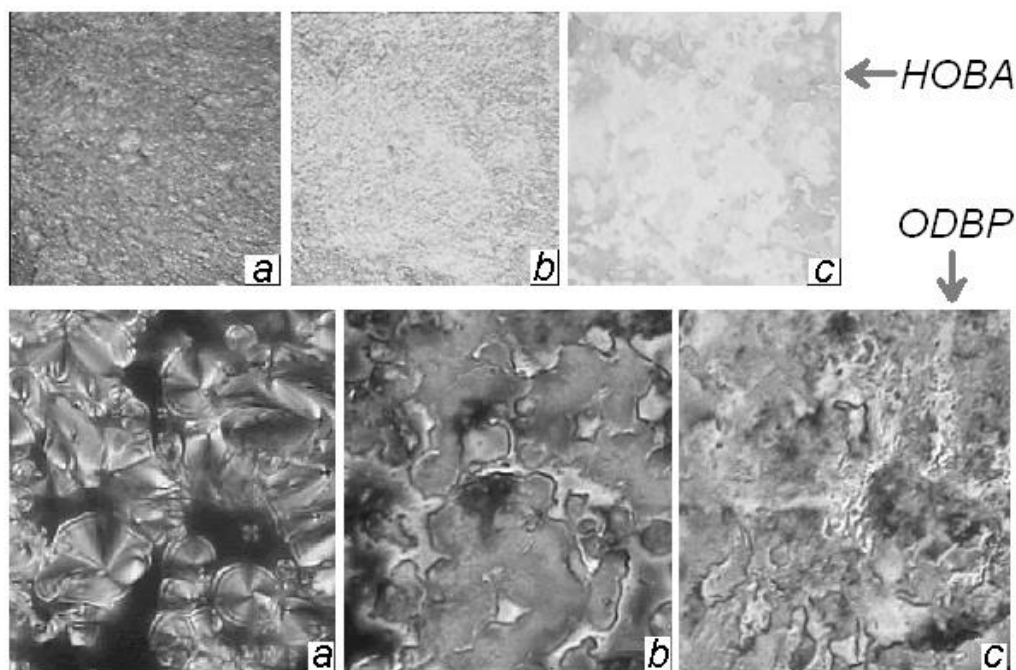


Figure 5 Smectic and nematic phases of HOBA [16] and ODBP (compound C in [13]). The smectic phase (a) turns in a nematic with smectic-like texture (b). This nematic transforms into an ordinary nematic (c) when subjected to further increase of temperature.

Hydrogen-bonded oxadiazoles have been also prepared and studied [19], to understand the role of an increased flexibility of molecules. One of the parameters of materials with bend-core molecules, relevant for mesomorphism, is the bend angle. If this angle is too small, the mesomorphism is usually suppressed. For large angles, we have the boomerang oxadiazoles, which display the biaxial phase, where molecules have 140 degrees for the bend angle. If the angle is greater, the behavior of the system is expected to be that of a calamitic material. The suggestion in [19] is therefore to use flexible linked dimers, to tune the value of the bend angle and check if and when a biaxial or a calamitic behavior is observed.

Asymmetric molecules containing metals and 1,3,4-oxadiazole and 1,3,4-thiadiazole heterocycles have been proposed too [20]. These materials are named as "metallomesogens" when are exhibiting thermotropic mesophases and are classified according to the bond formed between the metal and the organic molecule. The interest in synthesizing of metal-containing liquid crystals is due to some advantages in combining the properties of liquid crystal systems with those of transition metals, for applications in optical devices.

6. Oxadiazoles for electroluminescence

Organic compounds mostly behave like insulators. But organic compounds with proper structure and orientation of molecules can transport electric current upon certain conditions, competing then with the conventional materials used in electronics. Chains of polythiophenylenes for instance, have a charge transport comparable to poor metallic conductors.

In electronics, organic compounds can operate as rectifiers if they have a donor electron-rich part and an acceptor electron-poor part, linked by an insulating bridge. The lowest unoccupied molecular orbital (LUMO) of the acceptor and the highest occupied molecular orbital (HOMO) of the donor are used for transport of electrons. Some organic compounds with proper HOMO and LUMO orbitals can emit light when an electric current is passing through them. This is the electroluminescence. It is based on an electron transfer from LUMO and HOMO orbitals. The molecule in an excited state comes back to its ground state by an electron transfer from LUMO to HOMO orbital, accompanied by irradiation of energy difference in the form of light.

Materials that can simultaneously act as liquid crystals, charge transport agents and emitters are of interest for potential applications in organic light emitting diodes. In 1990, it was found that a compound with 1,3,4-oxadiazole is an excellent electron transport material in an organic electroluminescent diode [21]. After this report, the research to use various oxadiazole molecules to obtain high electroluminescence performances strongly increased. The researches on

polymer light-emitting diodes showed that the oxadiazole moieties possess a high potentiality for transport [22,23].

Discotic oxadiazoles, with columnar mesophases, were proposed too, for applications in organic electronics in Ref.24. Recently [25], star-shaped molecules consisting of a 1,3,4-oxadiazole core were synthesized. These molecules have columnar mesophases over a wide temperature range, where the mesophases exhibiting strong blue fluorescence. It is interesting to note that the researchers found that on cooling, one compound transforms into a transparent glass at room temperature, where the mesophase texture was retained. This glassy film is exhibiting blue luminescence, with an absolute quantum yield of 26%. The team observed that the length of the alkyl substituents inserted in the molecules has a significant effect on the absorption and fluorescence properties of the materials, due to the role of the alkyl substituents in controlling the nature of the molecular packing.

The introduction of oxadiazole moieties to polymer main chains and to mesogens in liquid crystalline compounds is then used to tune the electroluminescence efficiency and the transport properties. Electroluminescent polymers were also prepared, in which thiophene and oxadiazole moieties are connected alternately to form fully conjugated polymers. Likewise, liquid crystalline compounds containing oxadiazole moieties were reported to exhibit a high electron transport capability and a blue electroluminescence emission [22,26].

Another recent research is proposing new oxadiazole compounds containing silane, which have high morphological stability [27]. The researchers found that the disruption of the π -aromatic conjugation by introduction of Si atoms leads to a large band gap and high triplet energy. They identified among their new compounds the best host for FLRpic, to have a phosphorescent organic light emitting diode (PHOLED). Let us remember that in OLED, two modes of light emission have to be considered: fluorescence and phosphorescence. OLEDs using fluorescent materials are limited by the internal quantum efficiency, whereas in phosphorescent materials the internal quantum efficiency can reach up to 100%. Classical examples of phosphorescent emitting materials have green and red emitters. In order to attain blue emission, FLRpic, a prototypical blue-green emitter is used, where the heteroleptic iridium complex contains two fluoro-substituted phenylpyridine ligands and an anionic 2-picolinic acid [28].

7. Enantioselective segregation and drugs

To conclude, let us see another reason to investigate oxadiazoles. Studying the oxadiazoles which display

the biaxial nematic phase [29], Görtz and Goodby found that the achiral biaxial nematic phase can segregate into chiral domains of opposite handedness. In fact then, they observed a nematic phase which exhibited the properties of a conglomerate. The enantioselective segregation has been obtained in the smectic and nematics phases of other banana oxadiazoles, without introducing any chiral species, by a Japanese group [30]. This sort of segregation is rather important for drugs, because the stereoisomers of chiral drugs often exhibit pronounced differences in their properties, so pronounced that it is necessary to study each stereoisomer separately [31]. This is the reason why the pharmaceutical research has converged to use single enantiomers as substitutes for their racemates. And then, new developments in medicine could start from liquid crystals laboratories, with further investigations on boomerang or banana-oxadiazoles.

In Section 4 we have already observed the fact that 1,2,4-oxadiazoles are significant in terms of their pharmacological properties. For instance, the 1,2,4-oxadiazole systems is used in the Oxolamine which is a cough suppressant. Oxadiazoles are antibacterial, antimalarial, anti-inflammatory, antifungal and anticonvulsant (see for instance, [32] and [33]). Recently [34], some 2,5-substituted diphenyl-1,3,4-oxadiazoles have been studied for their biological activities of the $-N=C-O-$ grouping. According to the authors, the derivatives of 1,3,4-oxadiazole are versatile hydrophobic molecules with biological activities, with lesser or limited amount of toxicities. And therefore, the researchers consider them as most promising compounds in antidepressant, anticonvulsant and antianxiety activity with no neurotoxicity when compared with standard.

Let us conclude that, even if oxadiazole compounds have been explored largely in the past, several recent publications on their role in electronics and in the development of new drugs tell that new oxadiazoles are constantly produced for research purposes and investigated for future applications.

References

[1] L.A. Masden, T.J. Dingemans, M.Nakata and E.T. Samulski, Thermotropic biaxial nematic liquid crystals, *Phys. Rev. Lett.* 92, 145505 (4 pages), 2004.
 [2] T.J. Dingemans and E.T. Samulski, Non-linear boomerang-shaped liquid crystals derived from 2,5-bis(p-hydroxyphenyl)-1,3,4-oxadiazole, *Liquid Crystals* 27, 131-136, 2000.
 [3] M.J. Freiser, Ordered states of a nematic liquid, *Phys. Rev. Lett.* 24, 1041-1'43, 1970.
 [4] Jie Han, S. Sin-Yin Chui, Chi-Ming Che, Thermotropic liquid crystals based on extended 2,5-disubstituted-1,3,4-oxadiazoles: structure-property relationships, variable-temperature powder X-ray diffraction, and small-angle X-ray scattering studies, *Chem. Asian J.* 1, 814-825, 2006.
 [5] T. Niori, F. Sekine, J. Watanabe, T. Furukawa and H. Takezoe, Distinct ferroelectric smectic liquid crystals consisting of banana shaped achiral molecules, *J. Mater. Chem.*, 6, 1231-1233, 1996.
 [6] C. Chiccoli, I. Feruli, O. D. Lavrentovich, P. Pasini, S.V. Shiyonovskii and C. Zannoni, Topological defects in schlieren

textures of biaxial and uniaxial nematics, *Phys. Rev. E* 66, 030701 (4 pages), 2002.
 [7] S. Chandrasekhar, Geetha G. Nair, D. S. Shankar Rao, S. Krishna Prasad, K. Praefcke and D. Blunk, A thermotropic biaxial nematic liquid crystal, *Current Science*, 75(10), 1998, available at <http://www.iisc.ernet.in/currensci/nov251998/articles21.htm>
 [8] L.A. Karamysheva, S.I. Torgova, I.F. Agafonova and N.M. Shtikov, Dependence of mesomorphic properties of 3,5-disubstituted 1,2,4-oxadiazoles on geometric and electronic factors, *Mol. Cryst. Liq. Cryst.* 160, 217-225, 1995.
 [9] O. Francescangeli, L.A. Karamysheva, S.I. Torgova, A. Sparavigna and A. Strigazzi, X-ray investigation of new isomeric oxadiazoles, *Proceedings of SPIE* 3319, 139-144, 1998.
 [10] L.A. Karamysheva, I.F. Agafonova and S.I. Torgova, New heterocyclic analogs of BCH- and CBC-compounds, *Mol. Cryst. Liq. Cryst.* 332, 407-414, 1999.
 [11] J. Peláez and M.R. Wilson, Atomistic simulations of a thermotropic biaxial liquid crystal, *Phys. Rev. Lett.* 97, 267801 (4 pages), 2006.
 [12] S.I. Torgova, T.A. Geivandova, O. Francescangeli and A. Strigazzi, *Pramana*, Banana-shaped 1,2,4 oxadiazoles, 61(2), 239-248, 2003.
 [13] A. Sparavigna, A. Mello and B. Montrucchio, Fan-shaped, toric and spherulitic textures of mesomorphic oxadiazoles, *Phase Trans.* 80, 987-998, 2007.
 [14] A. Sparavigna, A. Mello and B. Montrucchio, Texture transitions in the liquid crystalline alkyloxybenzoic acid 6OBAC, *Phase Trans.* 79, 293-303, 2006; A. Sparavigna, A. Mello and B. Montrucchio, Texture transitions in binary mixtures of 6OBAC with compounds of its homologous series, *Phase Trans.* 80, 191-201, 2007.
 [15] M. Petrov, A. Braslau, A.M. Levelut and G. Durand, Surface induced transitions in the nematic phase of 4,n-octyloxybenzoic acid, *J. Phys. II (France)* 2, 1159-1194 (1992)
 [16] P. Simova and M. Petrov, On the electrical conductivity in the nematic phase of 4-n-alkyloxybenzoic acids HOBA, Ooba, and NOBA, *Phys. Stat. Sol. A* 80, K153-K156, 1983; M. Petrov and P. Simova, Depolarised Rayleigh scattering and textures in the nematic phase of some 4,n-alkyloxybenzoic acids, *J. Phys. D: Appl. Phys.* 18, 239-246, 1985.
 [17] L. Frunza, S. Frunza, A. Sparavigna, M. Petrov and S.I. Torgova, Dielectric and DSC investigations of 4-n-substituted benzoic and cyclohexane carboxylic acids .1. Textural changes in homologous 4-n-alkoxybenzoic acids, *Molecular Crystals and Liquid Crystals Science and Technology, Section C - Molecular Materials* 6(3), p.215-223, 1996.
 [18] A. De Vries, Evidence for the existence of more than one type of nematic phase, *Mol. Cryst. Liq. Cryst.* 10, 31-35, 1970.
 [19] P.J. Martin and D.W. Bruce, Hydrogen-bonded oxadiazole mesogens, *Liq. Cryst.* 34, 767-774, 2007.
 [20] M. Parra, S. Hernández and J. Alderete, Metallomesogens derived from chelating Schiff-bases containing 1,3,4-oxadiazole and 1,3,4-thiadiazole: synthesis, characterization and study of mesomorphic properties, *J. Chil. Chem. Soc.* 48, 57-60, 2003.
 [21] C. Adachi, T. Tsutsui and S. Saito, Blue light-emitting organic electroluminescent devices, *Appl. Phys. Lett.* 56, 799-781, 1990.
 [22] H. Mochizuki, T. Hasui, M. Kawamoto, T. Shiono, T. Ikeda, C. Adachi, Y. Taniguchi and Y. Shirota, Novel liquid-crystalline and amorphous materials containing oxadiazole and amine moieties for electroluminescent devices, *Chem. Commun.*, 1923-1924, 2000 (see references therein).
 [23] A.P. Kulkarni, C.J. Tonzola, A. Babel and S.A. Jenekhe, Electron transport materials for Organic Light-Emitting Diodes, *Chem. Mater.* 16, 4556-4573, 2004.
 [24] Y-D. Zhang, K.G. Jespersen, M. Kempe, J.A. Kornfield, S. Barlow, B. Kippelen and S.R. Marder, Columnar discotic liquid-crystalline oxadiazoles as electron-transport materials, *Langmuir* 19, 6534-6536, 2003.
 [25] D.D. Prabhu, N.S. Kumar, A.P. Sivasdas, S. Varghese and S.J. Das, Trigonal 1,3,4-oxadiazole-based blue emitting liquid crystals and gels, *Phys. Chem. B.* 116(43), 13071-80 (2012)
 [26] Rong Fan, D. Culjkovic, P. Piromreun, M.J. Turon, J.E. Langseth, G.G. Milliaras, Gu Shihai, L. Sukhomlinova and R.J. Twieg, Light-emitting diodes based on a liquid-crystalline oxadiazole derivative, *Proc. SPIE, Organic Light-Emitting Materials and Devices III*, Zakya H. Kafafi Ed. 3797, 170-177, 1999.

- [27] M.K. Leung, W-H. Yang, C-N. Chuang, J-H. Lee, C-F. Lin, M-K. Wei and Y-H. Liu, 1,3,4-oxadiazole containing silanes as novel hosts for blue phosphorescent Organic Light Emitting Diodes, *Org. Lett.*, 14 (19), 4986–4989, 2012.
- [28] V. Sivasubramaniam, F. Brodkorb, S. Hanning, H.P. Loeb, V. van Elsbergen, H. Boerner, U. Scherf, M. Kreyenschmidt, Fluorine cleavage of the light blue heteroleptic triplet emitter FIrpic, *Journal of Fluorine Chemistry* 130(7), 640–649, 2009
- [29] V. Görtz and J.W. Goodby, Enantioselective segregation in achiral nematic liquid crystals, *Chem Commun.* 3262-3264, 2005.
- [30] S-W. Choi, S. Kang, Y. Takanishi, K. Ishikawa, J. Watanabe and H. Takezoe, Intrinsic chiral domains enantioselectively segregated from twisted nematic cells of bent core mesogens, *Chirality* 19, 250-254, 2007.
- [31] V.M.L. Braga, S.J. Melo, R.M. Srivastava and E.P. da S. Falcão, Synthesis of new 1,2,4-oxadiazoles carrying (1S)-t-butyloxycarbonyl-1-amino-(2S)-methyl-1-butyl and (1S)-t-butyloxycarbonyl-1-amino-1-ethyl groups at C-5, *J. Braz. Chem. Soc.* 15, 603-607, 2004.
- [32] M.P. Hutt, E.F. Elslager and L.M. Werbel, 2-Phenyl-5-(trichloromethyl)-1,3,4-oxadiazoles, A new class of antimalarial substances, *Journal of Heterocyclic Chemistry* 7(3), 511–518, 1970
- [33] B. Silvestrini and C. Pozzatti, Pharmacological properties of 3-phenyl-5β diethylaminoethyl-1,2,4-oxadiazole, *Br J Pharmacol Chemother.* 16(3), 209–217, 1961.
- [34] P. Singh, P.K. Sharma, J.K. Sharma, A. Upadhyay and N. Kumar, Synthesis and evaluation of substituted diphenyl-1,3,4-oxadiazole derivatives for central nervous system depressant activity, *Organic and Medicinal Chemistry Letters* 2(1), Article 8, 10 Pages, 2012.

Clique Complex Homology: A Combinatorial Invariant for Chordal Graphs

Allen D. Parks¹ 

¹ Electromagnetic and Sensor Systems Department, 18444 Frontage Road Suite 327, Naval Surface Warfare Center Dahlgren Division, Dahlgren, VA 22448-5161, USA

Abstract: It is shown that a geometric realization of the clique complex of a connected chordal graph is homologically trivial and as a consequence of this it is always the case for any connected chordal graph G that $\sum_{k=1}^{\omega(G)} (-1)^{k-1} \eta_k(G) = 1$, where $\eta_k(G)$ is the number of cliques of order k in G and $\omega(G)$ is the clique number of G .

Keywords: algebraic graph theory; chordal graph; clique complex; hypergraph; homology; Mayer-Vietoris theorem; graph invariant; Euler-Poincaré formula

1. Introduction

In recent years much attention has been devoted to the study of chordal graphs. In addition to understanding their intrinsic properties from a graph theoretic perspective, a major motivation for this research has been their usefulness in such diverse applied domains as biology, relational database design, computer science, matrix manipulation, psychology, scheduling, and genetics, e.g., [1, 2]. Graph invariants have also been the subject of intense research because of their utility for determining class membership of graphs and recognizing non-isomorphic graphs, e.g., [3].

In this short paper a new combinatorial invariant for connected chordal graphs is found using the well-established relationship between a connected chordal graph G and its associated α -acyclic hypergraph $\mathcal{H}(G)$. The fact that $\mathcal{H}(G)$ is α -acyclic and that $\mathcal{H}(G)$ also generates the clique complex $\mathcal{C}(G)$ of G allows a straightforward application of the Mayer-Vietoris Theorem to show that a geometric realization \mathbb{K} of $\mathcal{C}(G)$ is homologically trivial. The combinatorial invariant for connected chordal graphs follows from the direct application of the Euler-Poincaré formula to \mathbb{K} .

The remainder of this paper is organized as follows: The relevant definitions and terminology are summarized in the next section. Required preliminary lemmas are provided in Section 3 and the main results are established in Section 4. A simple illustrative example is presented in Section 5. Closing remarks comprise the final section of this paper.

2. Definitions and Terminology

A graph G is a pair $(V(G), E(G))$, where $V(G)$ is a finite non-empty set of vertices and $E(G)$ is either a

set of doubleton subsets of $E(G)$ called edges or the empty set \emptyset . The order of G is the cardinality of $V(G)$ and the size of G is the cardinality of $E(G)$. Two vertices $u, v \in V(G)$ are adjacent when $e = \{u, v\} \in E(G)$ in which case e is said to join u and v . A u - v walk is an alternating sequence of vertices and edges beginning with u and ending with v such that every edge joins the vertices immediately preceding and following it. A u - v path is a u - v walk in which no vertex is repeated. In this case u is said to be connected to v . G is connected if its order is one or if every two vertices in G are connected. A u - v path for which $u = v$ and which contains at least three edges is a cycle. The length of a cycle is the number of edges contained within it and a chord of a cycle is an edge between nonconsecutive vertices in the cycle.

A graph is a chordal graph if every cycle of length at least four has a chord. A graph is complete if every two of its vertices are adjacent. A graph F is a subgraph of G if $V(F) \subseteq V(G)$ and $E(F) \subseteq E(G)$. A clique in G is either a vertex or a complete subgraph of G and is maximal if it is not a proper subgraph of another clique. The order of a clique is the cardinality of its vertex set and the clique number $\omega(G)$ of G is the maximum order among the maximal cliques of G .

A hypergraph \mathcal{H} is a pair $(\mathcal{N}, \mathcal{E})$, where \mathcal{N} is a finite set of vertices and \mathcal{E} is a set of hyperedges which are non-empty subsets of \mathcal{N} (it is hereafter assumed that \mathcal{H} is reduced, i.e., no hyperedge of \mathcal{H} is a subset of another hyperedge of \mathcal{H}). The hypergraph $\mathcal{H}(G)$ associated with graph G has $V(G)$ as its vertices and the hyperedges of $\mathcal{H}(G)$ are the sets of vertices in the maximal cliques of G . $\mathcal{H}(G)$ is connected if G is connected. A connected hypergraph is α -acyclic if it has the (nonempty) running intersection property, i.e., if there is an ordering $(\varepsilon_1, \varepsilon_2, \dots, \varepsilon_n)$ of its hyperedges so that for each $i, 2 \leq i \leq n$, there is a $j_i < i$ such that



Allen D. Parks (Correspondence)



allen.parks@navy.mil

$\emptyset \neq (\varepsilon_i \cap (\cup_{k < i} \varepsilon_k)) \subseteq \varepsilon_{j_i}$ (note the fact that each of these $n - 1$ intersections is non-empty implies connectedness) [4, 5].

The closure $Cl(S)$ of a finite set S is the family of nonempty subsets of S . The closure $Cl(\mathcal{H})$ of a hypergraph \mathcal{H} is the union of the closure of each of its hyperedges, i.e., $Cl(\mathcal{H}) = \cup_{\varepsilon \in \mathcal{H}} Cl(\varepsilon)$, and the closure $Cl(G)$ of a graph G is $Cl(G) = \cup_{\mathcal{V} \in \mathcal{M}} Cl(\mathcal{V})$, where \mathcal{V} is the set of vertices in a maximal clique of G and \mathcal{M} is the set of all such \mathcal{V} 's.

Let $\{a_0, a_1, \dots, a_k\}$ be a set of geometrically independent points in \mathbb{R}^n . The k -simplex (or simplex) σ^k spanned by $\{a_0, a_1, \dots, a_k\}$ is the set of points $x \in \mathbb{R}^n$ for which there exist non-negative real numbers $\lambda_0, \lambda_1, \dots, \lambda_k$ such that $x = \sum_{i=0}^k \lambda_i a_i$ and $\sum_{i=0}^k \lambda_i = 1$. In this case $\{a_0, a_1, \dots, a_k\}$ is the vertex set of σ^k . A face of σ^k is any simplex spanned by a non-empty subset of $\{a_0, a_1, \dots, a_k\}$. A finite geometric simplicial complex (or complex) \mathbb{K} is a finite union of simplices such that: (i) every face of a simplex of \mathbb{K} is in \mathbb{K} ; and (ii) the non-empty intersection of any two simplices of \mathbb{K} is a common face of each. The dimension $dim(\mathbb{K})$ of \mathbb{K} is the largest positive integer m such that \mathbb{K} contains an m -simplex. The vertex scheme of \mathbb{K} is the family of all vertex sets which span the simplices of \mathbb{K} . If $\{\mathbb{L}_i : i \in I\}$ is a collection of subcomplexes of \mathbb{K} , then $\cup_{i \in I} \mathbb{L}_i$ and $\cap_{i \in I} \mathbb{L}_i \neq \emptyset$ are also subcomplexes of \mathbb{K} .

A finite abstract simplicial complex (or abstract complex) is a finite collection S of finite non-empty sets such that if A is in S , then so is every non-empty subset of A . Thus, the vertex scheme of a complex is an abstract complex - as are finite unions of set closures and finite intersections of set closures. The abstract complex $Cl(G)$ is called the clique complex $\mathcal{C}(G)$ of graph G .

Two abstract complexes S and T are isomorphic if there is a bijection φ from the vertex set of S onto the vertex set of T such that $\{a_0, a_1, \dots, a_k\} \in S$ if, and only if, $\{\varphi(a_0), \varphi(a_1), \dots, \varphi(a_k)\} \in T$. Every abstract complex S is isomorphic to the vertex scheme of some geometric simplicial complex \mathbb{K} - in which case \mathbb{K} is the geometric realization of S and is uniquely determined (up to linear isomorphism). An isomorphism between S and the vertex scheme of \mathbb{K} is denoted $S \simeq \mathbb{K}$. An edge in S is a doubleton subset of vertices contained in S . A distinct pair of vertices u, v of S are path connected if there is an alternating sequence $u\{u, x_1\}x_1\{x_1, x_2\} \dots \{x_n, v\}v$ of vertices and edges of S . The abstract complex S is connected when either S has one vertex or all pairs of its vertices are path connected. If S is connected, then so is any geometric realization of S .

To each (simplicial) complex \mathbb{K} there corresponds a chain complex, i.e., abelian groups $\Gamma_p(\mathbb{K})$ and

homomorphisms $\partial_{p+1}: \Gamma_{p+1}(\mathbb{K}) \rightarrow \Gamma_p(\mathbb{K})$, $p \geq 0$. If \mathbb{K} is finite and $\xi_p(\mathbb{K})$ is the number of p -simplices in \mathbb{K} , then the rank of $\Gamma_p(\mathbb{K})$ is $\xi_p(\mathbb{K})$, i.e., $\Gamma_p(\mathbb{K})$ is isomorphic to (denoted " \cong ") the direct sum " \oplus " of $\xi_p(\mathbb{K})$ copies of the additive group of integers \mathbb{Z} . The p^{th} homology group of \mathbb{K} is the quotient group $H_p(\mathbb{K}) = \ker \partial_p / \text{im} \partial_{p+1}$ and its rank is the p^{th} Betti number $b_p(\mathbb{K})$. If \mathbb{K} is connected, then $H_0(\mathbb{K}) \cong \mathbb{Z}$ and \mathbb{K} is homologically trivial if it is connected and $H_p(\mathbb{K}) \cong 0$, $p \geq 1$, where 0 is the trivial group. The complex of a simplex is homologically trivial.

3. Preliminary Lemmas

Several lemmas are required to prove the main results found in the next section. The first three are well known and are repeated here for completeness. The fourth is lesser known and is due to D'Atri *et al.*

Lemma 3.1. [6] (Euler-Poincaré) If \mathbb{K} is a complex of finite dimension, then

$$\sum_{p=0}^{dim(\mathbb{K})} (-1)^p \xi_p(\mathbb{K}) = \sum_{p=0}^{dim(\mathbb{K})} (-1)^p b_p(\mathbb{K}).$$

Lemma 3.2. [7] (Mayer-Vietoris) Let \mathbb{K} be a complex with subcomplexes \mathbb{K}_0 and \mathbb{K}_1 such that $\mathbb{K} = \mathbb{K}_0 \cup \mathbb{K}_1$. Then there is an exact sequence

$$\dots \rightarrow H_p(\mathbb{K}_0 \cap \mathbb{K}_1) \rightarrow H_p(\mathbb{K}_0) \oplus H_p(\mathbb{K}_1) \rightarrow H_p(\mathbb{K}) \rightarrow H_{p-1}(\mathbb{K}_0 \cap \mathbb{K}_1) \rightarrow \dots$$

Lemma 3.3. [8] Let A be an abelian group, F be a free abelian group, and $\theta: A \rightarrow F$ be a surmorphism. Then $A \cong \ker \theta \oplus F$.

Lemma 3.4. [9] If G is a connected chordal graph, then $\mathcal{H}(G)$ is α -acyclic.

The closure operation Cl is also important for proving the main results. The following three lemmas provide the required key properties of Cl . Since the next lemma is straightforward, its proof has been omitted.

Lemma 3.5. Let $\{S_i : i \in I\}$ be a collection of non-empty finite sets. Then the following statements are true:

- (1) $A \subseteq B$ if, and only if, $Cl(A) \subseteq Cl(B)$;
- (2) $\cap_{i \in I} Cl(S_i) = Cl(\cap_{i \in I} S_i)$;
- (3) $\cup_{i \in I} Cl(S_i) \subseteq Cl(\cup_{i \in I} S_i)$;
- (4) $A \cap B \neq \emptyset$ if, and only if, $Cl(A) \cap Cl(B) \neq \emptyset$; and
- (5) $A \neq \emptyset$ if, and only if, $Cl(A) \neq \emptyset$.

Lemma 3.6. If the ordering of sets (S_1, S_2, \dots, S_n) has the running intersection property, then the ordering $(Cl(S_1), Cl(S_2), \dots, Cl(S_n))$ also has the running intersection property.

Proof. The proof results from use of the identity $S_i \cap (\cup_{k < i} S_k) = \cup_{k < i} (S_i \cap S_k)$ in the following

implication chain: $\emptyset \neq S_i \cap (\cup_{k < i} S_k) \subseteq S_{j_i} \Rightarrow \emptyset \neq \cup_{k < i} (S_i \cap S_k) \subseteq S_{j_i} \Rightarrow \emptyset \neq Cl(\cup_{k < i} (S_i \cap S_k)) \subseteq Cl(S_{j_i})$ (Lemma 3.5 (1),(5)) $\Rightarrow \emptyset \neq \cup_{k < i} (Cl(S_i \cap S_k)) \subseteq Cl(S_{j_i})$ (Lemma 3.5 (3)) $\Rightarrow \emptyset \neq \cup_{k < i} (Cl(S_i) \cap Cl(S_k)) \subseteq Cl(S_{j_i})$ (Lemma 3.5 (2)) $\Rightarrow \emptyset \neq Cl(S_i) \cap (\cup_{k < i} Cl(S_k)) \subseteq Cl(S_{j_i})$. Thus, the Cl operation preserves the running intersection property.

Lemma 3.7. *Let the ordering of sets (S_1, S_2, \dots, S_n) have the running intersection property. If $S' = S_i \cap (\cup_{k < i} S_k)$, then $Cl(S') = Cl(S_i) \cap (\cup_{k < i} Cl(S_k))$.*

Proof. Again use the identity $S' = S_i \cap (\cup_{k < i} S_k) = \cup_{k < i} (S_i \cap S_k)$ and let $A \neq \emptyset$. Application of Lemma 3.5 and the definition of Cl provides the following biconditional chain and completes the proof: $A \in Cl(S') \Leftrightarrow A \subseteq S' \Leftrightarrow A \subseteq S_i \cap S_k$ for some $k < i \Leftrightarrow A \in Cl(S_i \cap S_k)$ for some $k < i \Leftrightarrow A \in \cup_{k < i} Cl(S_i \cap S_k) \Leftrightarrow A \in \cup_{k < i} (Cl(S_i) \cap Cl(S_k)) \Leftrightarrow A \in Cl(S_i) \cap (\cup_{k < i} Cl(S_k))$.

4. Main Results

Lemma 4.1. *$Cl(\mathcal{H}(G))$ and $\mathcal{C}(G)$ are identical abstract complexes.*

Proof. By definition each hyperedge ε in $\mathcal{H}(G)$ is the vertex set \mathcal{V} of a maximal clique in G so that $Cl(\varepsilon) = Cl(\mathcal{V})$ (Lemma 3.5 (1)). Because of this one-to-one correspondence between hyperedges and maximal cliques, it must therefore be the case that $Cl(\mathcal{H}(G)) = \cup_{\varepsilon \in \mathcal{E}} Cl(\varepsilon) = \cup_{\mathcal{V} \in \mathcal{M}} Cl(\mathcal{V}) = Cl(G) \equiv \mathcal{C}(G)$.

Corollary 4.2. *$Cl(\mathcal{H}(G))$ and $\mathcal{C}(G)$ have the same geometric realizations.*

Proof. Let \mathbb{K} be the geometric realization of $Cl(\mathcal{H}(G))$ in which case $Cl(\mathcal{H}(G)) \simeq \mathbb{K}$. Since $\mathcal{C}(G) = Cl(\mathcal{H}(G))$ (Lemma 4.1), it must also be the case that $\mathcal{C}(G) \simeq \mathbb{K}$.

Lemma 4.3. *Let G be a connected chordal graph, $(\varepsilon_1, \varepsilon_2, \dots, \varepsilon_n)$ be an ordering of the hyperedges of $\mathcal{H}(G)$ which exhibit the running intersection property, and \mathbb{K} be a geometric realization of $\mathcal{C}(G)$. Then:*

- (1) *there is a subcomplex \mathbb{K}_i of a simplex in \mathbb{K} such that $Cl(\varepsilon_i) \simeq \mathbb{K}_i$;*
- (2) *the subcomplex \mathbb{L}_i of \mathbb{K} such that $\cup_{k < i} Cl(\varepsilon_k) \simeq \mathbb{L}_i$ is connected;*
- (3) *$\mathbb{K}_i \cap \mathbb{L}_i$ is the complex of a simplex of \mathbb{K} ; and*
- (4) *$\mathbb{K}_i \cup \mathbb{L}_i$ is a connected subcomplex of \mathbb{K} .*

Proof. Item (1) follows from Corollary 4.2; the one-to-one correspondence between maximal cliques in G and hyperedges in $\mathcal{H}(G)$; the fact that for each hyperedge ε_i there is a set \mathcal{V} of maximal clique vertices spanning a simplex in \mathbb{K} such that $\varepsilon_i = \mathcal{V} \Rightarrow$

$Cl(\varepsilon_i) = Cl(\mathcal{V})$ (Lemma 3.5 (1)); and that the abstract complexes $Cl(\varepsilon_i) = Cl(\mathcal{V})$ are therefore both isomorphic to the vertex scheme of the same simplex. Item (2) follows from an induction argument on $i \geq 2$ and the running intersection property's nonempty condition $\emptyset \neq (Cl(\varepsilon_i) \cap (\cup_{k < i} Cl(\varepsilon_k)))$, along with the one-to-one correspondence between hyperedges and vertex sets of maximal cliques. Item (3): Since \mathbb{K}_i and \mathbb{L}_i are subcomplexes of \mathbb{K} , then so is $\mathbb{K}_i \cap \mathbb{L}_i$. Because $\mathcal{H}(G)$ has the running intersection property, along with Lemma 4.1, Corollary 4.2, and Lemma 3.7, it follows that $\emptyset \neq (Cl(\varepsilon_i) \cap (\cup_{k < i} Cl(\varepsilon_k))) \simeq \mathbb{K}_i \cap \mathbb{L}_i$. But $(Cl(\varepsilon_i) \cap (\cup_{i < k} Cl(\varepsilon_k))) \subseteq Cl(\varepsilon_j)$ for some $j_i < i$ (Lemma 3.6). Since $Cl(\varepsilon_{j_i})$ is isomorphic to the vertex scheme for the complex of a simplex in \mathbb{K} , then $(Cl(\varepsilon_i) \cap (\cup_{i < k} Cl(\varepsilon_k)))$ is isomorphic to the vertex scheme of this complex of a simplex or to the complex of one of its faces. In either case, $\mathbb{K}_i \cap \mathbb{L}_i$ is a complex of a simplex of \mathbb{K} . Item (4): Since \mathbb{K}_i and \mathbb{L}_i are subcomplexes of \mathbb{K} , then so is $\mathbb{K}_i \cup \mathbb{L}_i$. Also, since \mathbb{K}_i and \mathbb{L}_i are connected (items (1) and (2)) and \mathbb{K}_i and \mathbb{L}_i have the complex of a simplex in common (item (3)), then $\mathbb{K}_i \cup \mathbb{L}_i$ must be connected.

Theorem 4.4. *If G is a connected chordal graph and \mathbb{K} is a geometric realization of $\mathcal{C}(G)$, then \mathbb{K} is homologically trivial.*

Proof. Since \mathbb{K} is a geometric realization of $\mathcal{C}(G)$, it is also a geometric realization of $Cl(\mathcal{H}(G))$ (Corollary 4.2) and since G is a connected chordal graph, then $\mathcal{H}(G)$ is an α -acyclic hypergraph (Lemma 3.4). Consequently, there is an ordering $(\varepsilon_1, \varepsilon_2, \dots, \varepsilon_n)$ of the hyperedges of $\mathcal{H}(G)$ which exhibit the running intersection property. Let \mathbb{K}_i and $\mathbb{L}_i, i \in \{2, 3, \dots, n\}$, be subcomplexes of \mathbb{K} such that

$$Cl(\varepsilon_i) \simeq \mathbb{K}_i \text{ and } \cup_{k < i} Cl(\varepsilon_k) \simeq \mathbb{L}_i,$$

in which case $\mathbb{K}_i \cap \mathbb{L}_i$ is the complex of a simplex (Lemma 4.3 (3)) and $\mathbb{K}_i \cup \mathbb{L}_i \equiv \mathbb{L}_{i+1}$ is a connected complex (Lemma 4.3 (4)). It follows that there is an associated exact sequence (Lemma 3.2)

$$\cdots \rightarrow H_p(\mathbb{K}_i \cap \mathbb{L}_i) \rightarrow H_p(\mathbb{K}_i) \oplus H_p(\mathbb{L}_i) \rightarrow H_p(\mathbb{L}_{i+1}) \rightarrow H_{p-1}(\mathbb{K}_i \cap \mathbb{L}_i) \rightarrow \cdots$$

Since \mathbb{K}_i and $\mathbb{K}_i \cap \mathbb{L}_i$ are complexes of simplices (Lemma 4.3 (1) and (3)), then for $p \geq 1$

$$H_p(\mathbb{K}_i) \cong H_p(\mathbb{K}_i \cap \mathbb{L}_i) \cong 0$$

and for $p = 0$

$$H_0(\mathbb{K}_i) \cong H_0(\mathbb{K}_i \cap \mathbb{L}_i) \cong \mathbb{Z}.$$

Substitution of these group isomorphisms into the above exact sequence induces the following two

relevant exact sequences:

$$0 \rightarrow H_p(\mathbb{L}_i) \rightarrow H_p(\mathbb{L}_{i+1}) \rightarrow 0 \quad (p \geq 2)$$

and

$$\begin{aligned} \cdots \rightarrow 0 \rightarrow H_1(\mathbb{L}_i) \rightarrow H_1(\mathbb{L}_{i+1}) &\xrightarrow{\delta} \mathbb{Z} \xrightarrow{\pi} \mathbb{Z} \oplus H_0(\mathbb{L}_i) \\ &\xrightarrow{\theta} H_0(\mathbb{L}_{i+1}) \rightarrow 0 \rightarrow \cdots \end{aligned}$$

Since $i \geq 2$ is arbitrary, the exactness of the first induced sequence provides the isomorphism chain

$$H_p(\mathbb{L}_2) \cong H_p(\mathbb{L}_3) \cong \cdots \cong H_p(\mathbb{L}_{n+1}) = H_p(\mathbb{K}) \quad (p \geq 2).$$

However, for $p \geq 2$, $H_p(\mathbb{L}_2) \cong 0$ (because \mathbb{L}_2 is the complex of a simplex) and it is concluded from the isomorphism chain that

$$H_p(\mathbb{K}) \cong 0 \quad (p \geq 2).$$

The exactness of the second induced sequence insures that θ is a surmorphism. Also, since \mathbb{L}_{i+1} is connected (Lemma 4.3 (4)), then $H_0(\mathbb{L}_{i+1}) \cong \mathbb{Z}$ and it is therefore a free abelian group. It follows from this, the fact that $\mathbb{Z} \oplus H_0(\mathbb{L}_i)$ is abelian, and Lemma 3.3 that

$$\mathbb{Z} \oplus H_0(\mathbb{L}_i) \cong \ker \theta \oplus H_0(\mathbb{L}_{i+1}) \cong \ker \theta \oplus \mathbb{Z}.$$

Using the fact that $H_0(\mathbb{L}_i) \cong \mathbb{Z}$ (because \mathbb{L}_i is a connected complex) and $\ker \theta = \text{im } \pi$ (from the exactness of the sequence) in the last expression yields

$$\mathbb{Z} \oplus \mathbb{Z} \cong \text{im } \pi \oplus \mathbb{Z}$$

which implies that $\text{im } \pi \cong \mathbb{Z}$. Thus, π is a monomorphism so that $\ker \pi = 0 = \text{im } \delta$ and exactness at \mathbb{Z} in the second sequence yields the exact sequence

$$0 \rightarrow H_1(\mathbb{L}_i) \rightarrow H_1(\mathbb{L}_{i+1}) \xrightarrow{\delta} 0$$

which reveals that

$$H_1(\mathbb{L}_i) \cong H_1(\mathbb{L}_{i+1}).$$

Since $i \geq 2$ is arbitrary, the following isomorphism chain holds:

$$H_1(\mathbb{L}_2) \cong H_1(\mathbb{L}_3) \cong \cdots \cong H_1(\mathbb{L}_{n+1}) = H_1(\mathbb{K}).$$

The closures of these hyperedges are

$$\begin{aligned} Cl(\varepsilon_1) = \\ \{ \{a, b, c, d\}, \{a, b, c\}, \{a, b, d\}, \{a, c, d\}, \{b, c, d\}, \{a, b\}, \{a, c\}, \{a, d\}, \{b, c\}, \{b, d\}, \{c, d\}, \{a\}, \{b\}, \{c\}, \{d\} \}, \end{aligned}$$

$$Cl(\varepsilon_2) = \{ \{b, c, e\}, \{b, c\}, \{b, e\}, \{c, e\}, \{b\}, \{c\}, \{e\} \},$$

and

$$Cl(\varepsilon_3) = \{ \{e, f\}, \{e\}, \{f\} \}$$

(these closures are easily seen to validate Lemma 3.6). Since $\mathcal{C}(G) = Cl(\mathcal{H}(G)) = Cl(\varepsilon_1) \cup Cl(\varepsilon_2) \cup Cl(\varepsilon_3)$, then the clique complex of G is the set

It can be concluded from this that since \mathbb{L}_2 is the complex of a simplex (because $Cl(\varepsilon_1) \cong \mathbb{L}_2$ and Lemma 4.3 (1)), then $H_1(\mathbb{L}_2) \cong 0$ and

$$H_1(\mathbb{K}) \cong 0.$$

Consequently, \mathbb{K} is homologically trivial since it is connected (Lemma 4.3 (4)) and $H_p(\mathbb{K}) \cong 0$, $p \geq 1$.

Theorem 4.5. *If G is a connected chordal graph and $\eta_k(G)$ is the number of cliques of order k in G , then*

$$\sum_{k=1}^{\omega(G)} (-1)^{k-1} \eta_k(G) = 1.$$

Proof. Let \mathbb{K} be a geometric realization of the clique complex of G . Since G is connected and chordal, then from Theorem 4.4, \mathbb{K} is homologically trivial. This implies that $b_0(\mathbb{K}) = 1$ and $b_p(\mathbb{K}) = 0$, $p \geq 1$, in which case Lemma 3.1 yields

$$\sum_{p=0}^{\dim(\mathbb{K})} (-1)^p \xi_p(\mathbb{K}) = 1.$$

The one-to-one correspondence between the $k-1$ dimensional simplices of \mathbb{K} and the cliques of order k in G implies $\xi_{k-1}(\mathbb{K}) = \eta_k(G)$ and $\dim(\mathbb{K}) = \omega(G) - 1$. The proof is completed by using these identities in the last expression and resuming over k , $1 \leq k \leq \omega(G)$.

5. Example

In order to illustrate the theory developed above, consider the connected chordal graph G , its associated hypergraph $\mathcal{H}(G)$, and a geometric realization of $\mathcal{C}(G) = Cl(\mathcal{H}(G))$ shown in Figure 1. By inspection it is seen that $\omega(G) = 4$; the hyperedges of $\mathcal{H}(G)$ are $\varepsilon_1 = \{a, b, c, d\}$, $\varepsilon_2 = \{b, c, e\}$, $\varepsilon_3 = \{e, f\}$; and $\mathcal{H}(G)$ is α -acyclic since the hyperedge ordering $(\varepsilon_1, \varepsilon_2, \varepsilon_3)$ exhibits the (nonempty) running intersection property, i.e.,

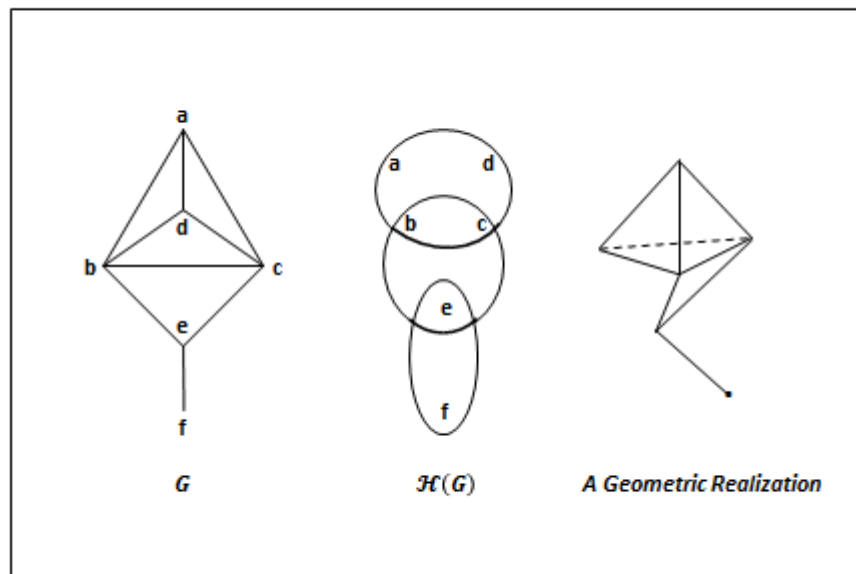
$$\begin{aligned} \varepsilon_3 \cap (\cup_{k < 3} \varepsilon_k) &= \varepsilon_3 \cap (\varepsilon_1 \cup \varepsilon_2) \\ &= \{e, f\} \cap \{a, b, c, d, e\} = \{e\} \subset \varepsilon_2 \end{aligned}$$

and

$$\begin{aligned} \varepsilon_2 \cap (\cup_{k < 2} \varepsilon_k) &= \varepsilon_2 \cap \varepsilon_1 = \{b, c, e\} \cap \{a, b, c, d\} \\ &= \{b, c\} \subset \varepsilon_1. \end{aligned}$$

$$\mathcal{C}(G) = \left\{ \{a, b, c, d\}, \{a, b, c\}, \{a, b, d\}, \{a, c, d\}, \{b, c, d\}, \{b, c, e\}, \{a, b\}, \{a, c\}, \{a, d\}, \{b, c\}, \{b, d\}, \{c, d\}, \{b, e\}, \{c, e\}, \{e, f\}, \{a\}, \{b\}, \{c\}, \{d\}, \{e\}, \{f\} \right\}.$$

Figure 1. A chordal graph G , its associated hypergraph $\mathcal{H}(G)$, and a geometric realization of $\mathcal{C}(G)$.



Theorem 4.4 is validated by observing that since it contains no “holes”, the geometric realization of $\mathcal{C}(G)$ in Figure 1 is homologically trivial (or somewhat more formally, there are no linear combinations of k -simplices in $\mathcal{C}(G)$ which form k -cycles that enclose “holes”). Theorem 4.5 is validated since by inspection it is easily determined that $\eta_1(G) = 6$, $\eta_2(G) = 9$, $\eta_3(G) = 5$, and $\eta_4(G) = 1$ in which case

$$\sum_{k=1}^4 (-1)^{k-1} \eta_k(G) = 6 - 9 + 5 - 1 = 1.$$

6. Concluding Remarks

It has been shown that any connected chordal graph has a clique complex that is isomorphic to the vertex scheme of (up to linear isomorphism) a unique homologically trivial geometric realization. As a consequence of this, the Euler-Poincaré formula provides a combinatorial invariant based simply upon the number of cliques in the graph and whose unit value holds for all connected chordal graphs. Accordingly, the contrapositive version of Theorem 4.5 serves to determine when a graph is not a connected chordal graph.

It is also interesting to note that since a tree is a connected chordal graph, then Theorem 4.5 subsumes the well-known fact that if a graph is a tree, then the difference between its order and its size is one (more specifically, if G is a tree, then $\omega(G) = 2$, $\eta_1(G)$ is its order, and $\eta_2(G) = \eta_1(G) - 1$ is its size so that

$$\sum_{k=1}^{\omega(G)} (-1)^{k-1} \eta_k(G) = \eta_1(G) - \eta_2(G) = \eta_1(G) - (\eta_1(G) - 1) = 1).$$

Acknowledgments

This work was supported by a grant from the Naval Surface Warfare Center Dahlgren Division’s In-house Laboratory Independent Research program.

References

1. McKee, T.; McMorris, F. *Topics in Intersection Graph Theory*; Society for Industrial and Applied Mathematics: Philadelphia, PA, USA, 1999.
2. Roberts, F. *Discrete Mathematical Models with Application to Social, Biological, and Environmental Problems*; Prentice-Hall, Inc.: Englewood Cliffs, NJ, USA, 1976.
3. Brigham, R.; Dutton, R. A compilation of relations between graph invariants. *Networks* **1985**, *15*, pp. 73-107.
4. Beeri, C.; Fagin, R.; Maier, D.; Yannakakis, M. On the Desirability of Acyclic Database Schemes. *Journal of the Association for Computing Machinery* **1983**, *30*, pp. 479-513.
5. Fagin, R. Degrees of Acyclicity for Hypergraphs and Relational Database Schemes. *Journal of the Association for Computing Machinery* **1983**, *30*, pp. 514-550.
6. Hocking, J.; Young, G. *Topology*; Addison-Wesley: Reading, MA, USA, 1961; p. 242.
7. Munkres, J. *Elements of Algebraic Topology*; Addison-Wesley: Reading, MA, USA, 1984; p. 142.
8. Rotman, J. *An Introduction to the Theory of Groups*; Allyn and Bacon, Boston, MA, USA, 1984; p. 254.
9. D’Atri, A.; Moscarini, M. On Hypergraph Acyclicity and Graph Chordality. *Information Processing Letters* **1988**, *29*, pp.271-274.

An Evaluation Instrument for Interviewing Skills in Psychiatry

Wen-Ching Chen¹, Miao-Chan Juan¹, Hsiang-Nan Lu¹,
Yueh-Yu Wu¹

¹Yuli Hospital, Department of Health, No.448, Chungwa Rd., Yuli Township, Hualien County 981, Taiwan

Abstract:

Background: Instruments to assess nurses' interviewing skills for in psychiatry are rare. In this study, we use such an instrument to identify and evaluate interviewing skills.

Methods: We designed a 6-month training program with 12 courses. The first 10 courses included didactic lectures combined with role-playing exercises to teach interviewing skills. We used an evaluation instrument that emphasized the six main elements of interviewing, including opening statements, conversation starters, empathetic statements, statements of the concrete effects of the patient's behavior, encouragement of the patient to discuss and identify conflict solutions that are mutually acceptable, and closing statements. In the last two courses, three examiners evaluated the nurses' interviewing skills.

Results: Four participants attended the training course two times, with an average score of 60.0. Two participants attended the course four, five or seven times, with average scores of 45.0, 52.5, and 72.5, respectively. One participant attended the course eight times and received a score of 82.5.

Conclusion: This study found that the more times the nurses engaged in the training course, the higher score their score in the assessment of interviewing skills. Because of this dose-response relationship, we suggest that this instrument is valuable for evaluating communication skills in difficult situations in psychiatric wards.

Keywords: Evaluation Instrument, Interviewing Skills, Psychiatry

Introduction

Interviewing skills are of paramount importance for nurses when caring for psychiatric patients, especially in difficult situations. For example, a dilemma may arise when a patient requests a discharge, but his mental status is not adequate to leave the hospital and return to his home or community. In addition, because of their poor insight into their disease, patients may refuse to

take medications in the ward. Communicative skills are necessary to persuade patients to cooperate.

Most studies seem to agree that the results of communication training are better when the skill can be practiced than when only didactic lectures are provided. Simulated patients and role-playing have frequently been used to train communication skills. However, a



Wen-Ching Chen (Correspondence)

oldchen@mail.ttyl.doh.gov.tw

recent review article indicated that using simulated patients is expensive and recommended that educators choose cheaper alternatives that are equally effective in improving interviewing skills. Nestel (2007) has offered guidelines to maximize the benefits of role-playing and Adkoli (2010) has used role-playing to teach conflict management.

A wide range of tools has been developed to evaluate interviewing skills (Swick et al. 2006). For example, an objective structured clinical examination (OSCE) is frequently used to evaluate communicative skills in medical care (White et al. 2009) and in psychiatry (Rimondini et al. 2010). However, instruments to assess interviewing skills for difficult situations are rare in psychiatric fields.

In this study, we used role-play in combination with didactic lectures. We then used a new instrument to evaluate nurses' interviewing skills to determine the effectiveness of the training course and the viability of the instrument.

Methods

This study was approved by the institutional review board of Yuli Hospital, which is located in mid-eastern Taiwan and provides highly rated long-term care and rehabilitation programs for approximately 2,600 chronic psychiatric patients. Fifteen new members of the nursing staff were included in this study, all of whom gave their informed consent to participate in the study.

From March 2009 to September 2009, we conducted a 6-month training program consisting of 12 courses. The first 10 courses included a didactic lecture combined with role-playing to teach interviewing skills for

difficult situations. In the last two courses, three heads of nursing and one senior nursing staff member acted as patients and were interviewed by the nurses who had attended the courses. The role-playing situations were decided by drawing lots. The possible situations included six vignettes (Appendix I), each describing a specific situation that may be encountered in a psychiatric ward, such as a patient smoking in his or her room. Three staff members evaluated the nurses' interviewing skills using an evaluation instrument (Appendix II) containing six main elements of interviewing: opening statements, conversation starters, empathetic statements, statements of the concrete effect of the patient's behavior, encouragement of the patient to discuss and identify conflict solutions that are mutually acceptable, and closing skills. For each element of interviewing, interviewers earned a score of 0 if they never used the skill, 1 if they used the skill once, and 2 if they used the skill twice or more. We averaged the scores for each element (0 – 2) to obtain the final score, which had a range of 0 – 12. For convenience in comparing the scores, we divided the total score by 12 and changed it to a 100 percentile score.

Results

Twelve out of 15 participants completed this study. All of the participants were female and between 23 and 35 years old. Three of the participants were married, their average education was approximately 15 years, and their average time working in this hospital was 16 months.

Table 1 shows that four participants attended the training course two times, with an average score of 60.0. Two participants attended four, five or seven times, with

average scores of 45.0, 52.5, and 72.5, respectively. One participant attended eight times with a score of 82.5.

Discussion

This study found that the more times the nurses engaged in the training course, the higher they scored in the assessment of interviewing skills. Because of this dose-response relationship, we suggest that this training course can effectively improve nurses' interviewing skills and that this instrument is viable for the evaluation of communication skills in difficult situations in psychiatric wards. The exception to this finding, that the scores of four members who attended only two times were better than the scores of the members who attended three, four or five times, is explained by the fact that these four members practiced interviewing skills more often in the ward. Thus, interviewing skills can also be improved by self-learning and practicing.

Because psychiatric patients are difficult to train and because they may suffer from negative feelings after participating in assessment exercises, this study used head nurses and senior nursing staff to role-play patients. However, the nursing staff may have experienced increased anxiety because they were interviewing the head nurses. Therefore, their scores might be underestimated.

Limitations

The main limitation of this study was the small sample size and its restriction to one hospital. Further research is necessary to evaluate the effectiveness of this instrument.

Conflict of Interest: nil.

References

- Adkoli, B. V. (2010). Using role play for teaching conflict management. *Medical Teacher*, 32, 90.
- Nestel, D. & Tierney, T. (2007). Role-play for medical students learning about communication: guidelines for maximising benefits. *Medical Education*, 7, 1-9.
- Rimondini, M., Del, Piccolo L., Goss, C., Mazzi, M., Paccaloni, M., and Zimmermann, C. (2010). The evaluation of training in patient-centred interviewing skills for psychiatric residents. *Psychological Medicine*, 40, 467-476.
- Swick, S., Hall, S., and Beresin, E. (2006). Assessing the ACGME Competencies in Psychiatry Training programs. *Academic Psychiatry*, 30, 330-351.
- White, C. B., Ross, P. T., and Gruppen, L. D. (2009). Remediating students' failed OSCE performances at one school: the effects of self-assessment, reflection, and feedback. *Academic Medicine*, 84, 651-654.

Table 1 Frequency distribution of attending times, number of nurses, and average scores

Attending times	2	3	4	5	7	8
Number of nurses	4	1	2	2	2	1
Average scores	60.0	40.0	45.0	52.5	72.5	82.5

Appendix I Six Vignettes

1. A patient always wants to smoke in the bedroom, but this behavior is against the law. How do you deal with him?
2. A patient says that this drug is a poison and does not want to take it. How do you deal with him?
3. A patient wants to go shopping, but you know that he has no money. How do you deal with him?
4. A patient says that he has completely recovered and needs to be discharged, but you know that he is not ready to be discharged yet. How do you deal with him?
5. A patient wants to become friends with you, but you know it is not appropriate. How do you deal with him?
6. A patient often commits theft in the ward, and you are his principle nurse. How do you deal with him?

Appendix II Evaluation Instrument for Interview

Remark: If the interviewer did not use the following skill, they received a score of 0; if they used once, 1; and if twice or more, 2 in each elements.

- a. Opening: saying hello to the interviewee, greeting him, introducing to him, welcoming him, and so on.
- b. Door openers: can use door openers such as “hmm, go on...”, “very interesting”, or nodding your head, saying “I see”, make eye contact with him, and so on.
- c. Empathetic statement: can respond to interviewee’s emotion and feeling, can use a tone that resonates with the interviewee’s feelings, and so on.
- d. Stating concrete effects: can state the tangible and concrete effects of the interviewee’s (patient’s) behavior on you.
- e. Determining solutions (the win-win method): can lead patient to determine the solutions that are acceptable to both the interviewer and interviewee involved in the conflict.
- f. Closing: can thank the interviewee, encourage him, and lift his spirit, and so on.

The Association of Functional Single Nucleotide Polymorphisms of the RBP4 Gene with Gene Expression and Insulin Resistance Risk

Malgorzata Malodobra-Mazur¹✉, Dorota Bednarska-Chabowska², Robert Olewinski³, Zygmunt Chmielecki⁴,
Rajmund Adamiec², Tadeusz Dobosz¹

¹ Department of Forensic Medicine, Molecular Technique Unit, Wrocław Medical University, Skłodowskiej-Curie 52, 50-369 Wrocław, Poland

² Department of Angiology, Hypertension and Diabetology, Wrocław Medical University, Borowska 213, 50-556 Wrocław, Poland

³ First Department and Clinic of General, Gastroenterological and Endocrinological Surgery, Wrocław Medical University, M. Curie-Skłodowskiej 66, 50-369 Wrocław, Poland

⁴ Provincial Specialist Hospital in Wrocław, Kamieńskiego 73 a, 51-124 Wrocław, Poland

Abstract:

Aims/Introduction: The RBP4 level has been found to correlate positively with risk of insulin resistance and type 2 diabetes. However, the exact mechanism linking RBP4 with metabolic disorders is not clear. In presented study the associations of two single nucleotide polymorphisms located in promoter region of the *RBP4* gene rs3758538 (-1265A>C) and rs3758539 (-803 G>A) with insulin resistance risk, *RBP4* mRNA level and biochemical parameters were analyzed.

Material and methods: Two polymorphisms were genotyped by multiplex minisequencing with the use of ABI PRISM® SNaPshot Multiplex Kit. *RBP4* gene expression analysis was done by Relative Real-Time PCR and normalized to β -actin and *GUS*- β genes. Insulin and cytokines were measured using commercial ELISA kits.

Results: IR patients were characterized by increased *RBP4* mRNA level in adipose tissue comparing to IS patients and control subjects, what correlated positively with insulin resistance. Polymorphism rs3758539 showed no differences in genotype frequencies between tested groups. The rs3758538 displayed higher number of C allele within type 2 diabetes patients. There was no relationship between genotype and *RBP4* gene expression level. Furthermore, no relationship of investigated SNPs with insulin resistant phenotype has been noticed.

Conclusions: Present results link the *RBP4* gene expression level with insulin resistance pathogenesis. However, there is lack of association between analyzed SNPs with insulin resistant phenotype, *RBP4* gene expression level and inflammatory state.

Keywords: RBP4, Insulin resistance, SNP

Introduction

Obesity is considered as the strongest risk factor for metabolic syndrome (MS), insulin resistance (IR) and type 2 diabetes mellitus (T2DM) [1,2]. In deed, numerous studies demonstrated that visceral adipose tissue correlated stronger with insulin resistance than subcutaneous adipose tissue [3,4]. Obesity leads to adipocytes hyperplasia and hypertrophy that impairs their metabolism and function [3,5]. On the other hand physical activity and body mass reduction

improve the whole body response to insulin and insulin sensitivity [6,7].

Apart from excess energy storage, the adipose tissue also functions as an active endocrine organ secreting into blood stream many important cytokines like leptin, adiponectin, resistin and recently discovered retinol binding protein 4 (RBP4). Furthermore, adipose tissue is implicated in generation of chronic low grade inflammatory state via secretion of many inflammatory cytokines like TNF- α (tumor necrosis factor-alpha), IL- 1, -6 and -10 (Interleukin 1,6,10) or



Malgorzata Malodobra-Mazur (Correspondence)



malgorzata.malodobra@am.wroc.pl



+48 71 784 15 95

MCP-1 (monocyte chemotactic protein-1). The levels of secreted inflammatory cytokines and adipocytokines are correlated with body mass index (BMI) [8,9], impairment of insulin action and insulin resistance [10].

The RBP4 is a principal retinol (Vitamin A) transporter and is secreted by adipose tissue and liver [11]. Increased circulating RBP4 level has been found in obese subjects. Interestingly, the increased RBP4 level correlated positively with risk of IR and type 2 diabetes [12]. According to Klöting et al. [13] the level of *RBP4* gene expression rate was higher in visceral comparing to subcutaneous adipose tissue, what positively correlated with BMI value. These findings link RBP4 with metabolic disorders; however, the exact mechanism linking RBP4 with metabolic disorders is not clear. There are several possible mechanisms implicating RBP4 with impairments in insulin sensitivity. It has been shown that circulating RBP4 level negatively correlated with GLUT4 level in adipose tissue [12,14], what might suggest influence on *SLC2A4* gene expression. RBP4 also seems to affect the phosphorylation of IRS-1 serine residues [15]. Furthermore numerous polymorphisms of the *RBP4* gene were associated with BMI, hypertriglyceridemia or risk of type 2 diabetes [16,17,18]. Kovacs et al. [19] displayed the relationship of six SNPs haplotypes with the *RBP4* gene mRNA level and increased risk of insulin resistance. Similar relationship of rare haplotypes has been seen by Hu et al. [20]. Additionally, they revealed associations with circulating RBP4 level and serum C-peptide level at fasting state and after OGTT.

In presented study the associations of *RBP4* gene expression with insulin resistance was assessed. Furthermore the mechanisms by which RBP4 might influence the insulin action were investigated. The *RBP4* gene expression level, the *SLC2A4* gene expression level and inflammatory cytokines were correlated. Two single nucleotide polymorphisms located in promoter region of the *RBP4* gene were genotyped and the genotype distribution was correlated with mRNA level, biochemical parameters and insulin resistance risk.

Material and Methods

The experimental protocols were approved by ethical review boards at Wroclaw Medical University.

Population characterization

130 unrelated diabetic patients (68 men and 62 women) and 98 healthy controls (39 men and 59 women) were genotyped. Type 2 diabetes patients were inpatients of the Department of Angiology,

Hypertension and Diabetology of Wroclaw Medical University. Adipose tissue biopsies both from type 2 diabetes patients and control subjects were taken during abdominal surgery performed in the First Department and Clinic of General, Gastroenterological and Endocrinological Surgery, Wroclaw Medical University and in the Regional Specialist Hospital, Kaminskiego Street in Wroclaw. The adipose tissue samples were collected from 15 patients with type 2 diabetes and from 24 control (without type 2 diabetes and insulin resistance) subjects. The aims of abdominal surgeries were mainly cholecystectomy, surgery of abdominal hernia or gastric surgery. The mean age of diabetic patients was 55 ± 7 years. The mean age of healthy subjects was similar and equaled 50 ± 10 years. Control subjects were selected based on fast glucose level below 100 mg/dl, lack of diabetes in family history, additionally for women no gestational diabetes in the past. All materials were taken after obtaining written consent. Diabetic patients were divided into two subgroups depending on the insulin sensitivity: *IS* – insulin sensitive and *IR* – insulin resistant.

BMI and insulin resistance ratios

BMI was calculated as weight in kilograms divided by square of height in meters [kg/m^2]. Insulin resistance ratios were calculated as follow [21]:

- 1) HOMA-IR [$(\text{glucose} [\text{mmol/l}] * \text{insulin} [\mu\text{U/ml}]) / 22.5$],
- 2) QUICKI [$1 / (\log \text{glucose} [\text{mg/dl}] + \log \text{insulin} [\mu\text{U/ml}])$].

Genotyping

The whole venous blood was taken on anticoagulant at fasten state both from healthy control and diabetic patients after obtaining written consent. The blood samples were centrifuged and plasma samples were taken for adipocytokines and insulin levels measurements. DNA was isolated with the use of EZNA Total DNA Kit (Omega Bio Tek.). Two polymorphisms were genotyped: rs3758538 (-1265A>C) and rs3758539 (-803 G>A). Amplified in multiplex PCR (QIAGEN® Multiplex PCR Kit, Qiagen), polymorphic fragments were genotyped by multiplex minisequencing (ABI PRISM® SNaPshot Multiplex Kit, Applied Biosystems) according to manufactured protocols. The minisequencing products were separated in capillary electrophoresis together with GeneScan™120LIZ® Size Standard (Applied Biosystems) on ABI PRISM 3130 Genetic Analyzer (Applied Biosystems) and analyzed with the use of GeneMapper ID v3.2 (Applied Biosystems).

Insulin, adipocytokines and inflammatory cytokines measurements

The concentrations of insulin and adiponectin were

measured using commercial kits: Human Adiponectin ELISA Kit (Millipore) and Human Insulin ELISA Kit (Millipore). IL-6 and TNF- α concentrations were measured using ELISA kits: PeliKine Human IL-6 ELISA Kit (Sanquin) and PeliKine Human TNF- α ELISA Kit (Sanquin) according to manufactured protocols.

Gene expression analysis

Visceral adipose tissue biopsies were taken during abdominal surgery. Samples were preserved in RNALater (Ambion) and stored at -70°C until analysis. RNA was isolated using TriPure Reagent (Roche). cDNA was synthesized with the use of High Capacity cDNA Reverse Transcription Kit (Applied Biosystems). The gene expression analysis was done by Relative Real-Time PCR using TaqMan Gene Expression Assay (Applied Biosystems) and normalized to β -actin and GUS - β genes as reference controls (housekeeping genes).

Adipocytes measurements

Adipose tissue biopsies taken from lean patients ($\text{BMI} < 25 \text{ kg/m}^2$) and from obese patients ($\text{BMI} > 30 \text{ kg/m}^2$) were fixed in 10% formalin and stained by hematoxylin-eosin (H&E). Adipocytes size was assessed by ImageJ and analyzed statistically by Student-T test.

Statistical analysis

Statistical analyses were done using STATISTICA software. Statistical significance was considered with $p < 0.05$. Differences between clinical features of tested groups were assessed by Student's *T*-Test. Association of SNPs with clinical parameters and *RBP4* gene expression level were done with use of one way variance analysis ANOVA. Correlation between gene expression and biochemical parameters were assessed by coefficient of correlation. Differences in SNP's frequencies were tested using χ^2 test. Hardy-Weinberg Equilibrium (HWE) was established by χ^2 test using following formula $p^2+2pq+q^2=1$. Linkage disequilibrium (LD) was assessed using formula $D=hf - p_i \times q_i$ (hf -haplotype frequencies, p_i , q_i - alleles frequencies). The gene expression level was analyzed using relative quantification delta-delta ($\Delta\Delta\text{Ct}$) model [22].

Results

Characterization of analyzed groups

The anthropometrical and biochemical characterizations of type 2 diabetes patients and healthy controls are presented in table 1. 67.5% of all diabetic patients were insulin resistant (*IR*), whilst 32.5% diabetic patients displayed proper insulin sensitivity (*IS*). The *IR* patients were characterized by

increased BMI value ($p=0.0203$) and fasting insulin level ($p=0.0000$) as well as insulin resistance ratios ($p=0.0000$ both for HOMA-IR and QUICKI) in comparison to *IS* patients. Furthermore insulin resistance positively correlated with BMI ($R=0.44$, $p=0.000$ (HOMA-IR) and $R=-0.53$, $p=0.000$ (QUICKI)). Furthermore, *IR* patients manifested higher hypertension and increased TG level. The glucose level did not show statistical difference between groups of patients with a slight increase in the *IR* group ($p=0.0538$).

Hardy- Weinberg Equilibrium and linkage disequilibrium analyses

Both genotyped SNPs did not show any divergences from Hardy-Weinberg Equilibrium. For both polymorphisms the p values were higher than 0.99 (χ^2). There was no linkage disequilibrium between two analyzed SNPs in the *RBP4* gene.

Adipocytes measurements

The adipocytes sizes differed significantly between investigated groups (lean: $\text{BMI} < 25 \text{ kg/m}^2$ and obese: $\text{BMI} > 35 \text{ kg/m}^2$) ($p=0.0000$). The histograms showed that obese subjects were characterized by increased adipocytes size, on the other hand histogram of lean subjects was shifted towards smaller cells (Figure 1).

Adipocytokines and inflammatory cytokines measurements analysis

There had been significant increase in IL-6 ($p=0.0157$) level but only slight increase in TNF- α level ($p=0.8859$) in type 2 diabetic patients with no differences between *IS* and *IR* groups. Furthermore IL-6 correlated positively with BMI values ($R=0.36$, $p=0.055$). However there was no correlation between IL-6 and insulin resistance ratios. On the other hand we observed strong negative correlation between TNF- α and QUICKI ($R=(-0.49)$, $p=0.046$), but there was no correlation with BMI. Adiponectin level was significantly lower in type 2 diabetes patients ($p=0.0293$) with no differences between *IS* and *IR* groups. More, the adiponectin showed slight negative correlation with BMI ($R=(-0.30)$, $p=0.0639$). There was however no correlation between adiponectin level and insulin resistance rate.

Genotype frequencies analysis

Genotype frequencies analysis showed slight differences in genotype distribution within investigated groups: the *IR*, *IS* and control subjects. The rs3758539 polymorphism showed no difference in genotype frequencies. The rs3758538 polymorphism displayed significantly higher number of C allele within type 2 diabetes patients. There was higher number of C/A and C/C genotype carriers

within type 2 diabetes patients ($p=0.0233$, CHI^2). However there was no statistical difference in genotype frequencies between *IR* and *IS* patients. The genotype and allele frequencies are presented in table 2.

Gene expression analysis

IR patients were characterized by increased *RBP4* mRNA level in adipose tissue comparing to *IS* patients and control subjects ($p=0.0277$ normalized to β -actin and $p=0.0105$ normalized to *GUS*- β , ANOVA) (figure 2). There was a slight positive correlation between *RBP4* gene mRNA level with HOMA-IR (*RBP4*_G $R=0.36$, $p=0.1$, *RBP4*_B $R=0.49$, $p=0.05$) and slight negative correlation with QUICKI (*RBP4*_G $R= (-0.20)$, *n.s.*, *RBP4*_B $R= (-0.37)$, $p=0.1$, figure 3). The *SLC2A4* gene expression level (encoding GLUT4) was slightly lower within type 2 diabetes patients, both in insulin resistant patients and in patients with proper insulin sensitivity comparing to healthy controls, however without statistically significance. Similar results have been obtained normalized to two housekeeping genes: β -actin and *GUS*- β (figure 3A). There was however no correlation between the *RBP4* and *SLC2A4* genes expression levels (figure 3B and 3C). Furthermore any associations between the expression of *RBP4* gene and adiponectin and inflammatory cytokines concentrations have been displayed.

Genotype association with the *RBP4* gene expression and insulin resistant phenotype

There was no relationship between genotypes of investigated SNPs and the *RBP4* gene expression levels. The level of *RBP4* gene mRNA did not differ depending on genotype. High level has been seen for *IR* patients and very low for *IS* patients and controls, but at the same level in carriers of all genotypes (figure 4a and b). Furthermore, no relationship of investigated SNPs with insulin resistant phenotype (BMI, HOMA-IR, QUICKI) has been noticed.

Discussion

The *RBP4* protein is considered as a principal retinol transporter [11]. It has been recently linked with increased risk for type 2 diabetes and insulin resistance [12]. It belongs to a family of adipocytokines secreted by adipose tissue. The level of secreted *RBP4* correlates positively with BMI and is secreted in higher level in obese when compared to lean subjects. It has been shown also that is highly expressed in visceral adipose tissue comparing to subcutaneous [14]. Obesity is accompanied by adipocytes hypertrophy and hyperplasia what favor insulin signaling impairment and induction of low grade inflammatory state by secretion of many cytokines like IL-6 or TNF- α [5]. Similarly, as it was

expected, we have shown significantly increase in adipocytes size within obese subjects. Obesity correlated positively with insulin resistance, what was confirmed by the correlation between BMI value and insulin resistance indexes: HOMA-IR and QUICKI. Furthermore obese subjects were characterized by increased IL-6 and TNF- α levels and lower adiponectin level that correlated either with BMI or with insulin resistant ratios. These data clearly suggest the role of obesity in insulin signaling impairment and insulin resistance pathogenesis. As the *RBP4* is one of cytokine secreted by adipose tissue, the possible mechanism mediating insulin resistance induction might involve *RBP4* protein.

Klötting et al. [14] showed increased *RBP4* gene expression level in visceral adipose tissue, the type of tissue considered as the more important in metabolic syndrome and type 2 diabetes developments. More, the level of *RBP4* gene expression positively correlated with BMI. Bajzová et al.[15] however demonstrated lower level of *RBP4* mRNA in visceral adipose tissue than in the subcutaneous adipose tissue. In our study we have focused on visceral adipose tissue and we demonstrated that the *RBP4* mRNA level was higher in type 2 diabetic patients suffering from insulin resistance. The *RBP4* gene expression level did not differ in diabetic patients with proper insulin sensitivity (assessed based on HOMA-IR and QUICKI) comparing to control subjects and was relatively low. Furthermore the *RBP4* gene expression rate correlated positively with insulin resistance (assessed by HOMA-IR and QUICKI). We demonstrated slight positive correlation with HOMA-IR and negative correlation with QUICKI what affirms the relationship of *RBP4* gene expression level with IR. Definitely, increasing number of subjects will allow obtaining strong statistically significant correlation. However there was no statistically significant correlation between *RBP4* gene expression level and inflammatory cytokines levels (IL-6 and TNF- α). This data might suggest that *RBP4* did not impair insulin sensitivity via mediating inflammatory state, but this need to be verified on larger cohort.

According to some authors the circulating *RBP4* level negatively correlated with GLUT4 level in adipose tissues [12,14]. To verify this statement we have checked for the *SLC2A4* gene expression rate in visceral adipose tissue and correlated it with the *RBP4* gene expression. The *SLC2A4* expression was lower in diabetic patients with insulin resistance comparing to controls and patients with proper insulin sensitivity, however, there was no correlation with the *RBP4* gene expression rate. It is likely that the circulating *RBP4* influence the GLUT4 content

on a protein level, but not on gene expression level.

Numerous studies demonstrated relationship between polymorphisms in the *RBP4* gene with increased risk for insulin resistance and type 2 diabetes [16,17,18]. Munkhtulga et al. [16] were the first that displayed the association of genetic variants in this gene with type 2 diabetes. In present study we were trying to evaluate the correlation of *RBP4* regulatory SNPs with *RBP4* gene expression, BMI and risk of insulin resistance. The both investigated SNPs were very well characterized in previous studies, where they displayed associations mainly with BMI [16], *RBP4* mRNA level [19], hypertriglyceridemia [18] and with increased risk of type 2 diabetes [17]. According to Munkhtulga et al. [16] A allele of rs3758539 correlated positively with higher BMI. On the other hand Van Hoek et al. [17] showed relationship of this SNP with type 2 diabetes risk. The bioinformatics analysis showed that the rs3758539 polymorphism is flanked by binding site for the MAZ and the R1/R2/Sp1 transcription factors when G allele is present. On the other hand when G allele is changed for the A allele the binding site is also changed for the c-Ets-2 transcription factor [19]. Thus the change of nucleotide in functional region might influence the gene expression. Despite the fact, in presented study we did not notice statistically significant relationship between genotypes of this SNP with *RBP4* gene expression. More, we did not show associations with any parameters like BMI, glucose and insulin levels or insulin resistance ratios. Furthermore there were no significant differences in genotype and allele frequencies between examined groups.

The rs3758358 displayed significant difference in genotype frequencies between tested groups. The C allele seems to occur in higher frequency in type 2 diabetes patients comparing to controls. However, there was no difference between *IS* and *IR* patients, what suggests that C allele might predispose to type 2 diabetes, but not seems to be implicated in insulin resistance pathogenesis. Statistical analysis for this polymorphic site revealed lack of association with insulin resistance ratios (neither with HOMA-IR nor with QUICKI). Furthermore we did not observed statistically significant relationship between clinical parameters characterizing metabolic disorders, although some studies provided that data [18]. Finally, we did not display changed *RBP4* gene expression profile depending on genotype. The reason for lack of association might be low size of analyzed study cohort or difference in the origin of analyzed population. The previous study was performed on Chinese [18], Japanese [16] and Holland [17] population.

Interesting approach was undertaken by Kovacs et al. [19] and Hu et al. [20] who displayed the relationship of rare haplotypes with increased risk of insulin resistance and with the *RBP4* gene mRNA and circulating RBP4 levels. In present study we did not demonstrated strong linkage disequilibrium value between two analyzed SNPs. Thus our results could not be analyzed in terms of haplotypes and statistic analysis could be irrelevant. In order to obtain more accurately results, present study should be performed on larger sample size and duplicated in distinct populations. However single locus analysis did not revealed statistically significant associations between analyzed SNPs in *RBP4* gene with insulin resistant phenotype, lipids deregulations and increased risk of insulin resistance and type 2 diabetes. Our results confirmed results presented by others [19,20], where single locus analysis also did not display mentioned associations.

Concluding, presented results implicate the RBP4 in insulin resistance pathogenesis. The level of *RBP4* mRNA in adipose tissue correlated positively with insulin resistant state. Furthermore, the *RBP4* gene expression level was highly expressed in *IR* patients comparing to *IS* patients and controls subjects. However, the mechanisms linking RBP4 with insulin resistance remain unsolved. We did not reveal any association of analyzed SNPs in the *RBP4* gene promoter region with insulin resistant phenotype as well as with the *RBP4* gene expression level. Similarly, there was no correlation between RBP4 and *SLC2A4* gene expressions rate or inflammatory cytokines. Further investigations on larger number of subjects need to be done to assess the relationship between RBP4 with insulin resistance pathogenesis.

Acknowledgements

The project was supported by Ministry of Science and Higher Education of Poland, Grant No: N N401 009436. No conflict of interest relevant to the article has been reported.

References

1. Karelis AD, St-Pierre DH, Conus F et al. Metabolic and body composition factors in subgroups of obesity: what do we know? *J Clin Endocrinol Metab* 2004; 89: 2569-2575.
2. Eckel RH, Alberti KG, Grundy SM et al. The metabolic syndrome. *Lancet* 2005; 365: 1415-1428.
3. Preis SR, Massaro JM, Robins SJ et al. Abdominal subcutaneous and visceral adipose tissue and insulin resistance in the Framingham heart study. *Nature* 2010; 18: 2191-2198.
4. Alvehus M, Burén J, Sjöström M et al. The human visceral fat depot has a unique inflammatory profile. *Obesity* 2010; 18: 879-883.
5. Gustafson B, Gogg S, Hedjazifar S et al. Inflammation and impaired adipogenesis in hypertrophic obesity in man. *Am J Physiol Endocrinol Metab* 2009; 297: 999-1003.
6. Paulson QX, Hong J, Holcomb VB et al. Effects of body weight and alcohol consumption on insulin sensitivity. *Nutr J* 2010; 22: 9-14.

7. Solomon TP, Sistrun SN, Krishnan RK et al. Exercise and diet enhance fat oxidation and reduce insulin resistance in older obese adults. *J Appl Physiol* 2008; 104: 1313-1319.
8. Fisher-Posovszky P, Wabitsch M, Zochberg Z. Endocrinology of adipose tissue – An update. *Horm. Metab. Res* 2007; 39: 314-321.
9. Rasouli N, Kern PA. Adipocytokines and the metabolic complications of obesity. *J Clin Endocrinol Metab* 93: 64-73.
10. Rabe K, Lehrke M, Parhofer KG, Broedl UC (2008) Adipokines and insulin resistance. *Mol. Med* 2008; 14: 741-751.
11. Esteve E, Ricart W, Fernandez-Real JM Adipocytiknes and insulin resistance. The possible role of lipocalin-2, reginol binding protein-4 and adiponectin. *Diabetes Care* 2009; 32: 362-367.
12. Graham TE, Yang Q, Blüher M, et al. Retinol Binding protein 4 and insulin resistance in lean, obese and diabetic subjects. *N Engl J Med* 2006; 354: 2552-2563.
13. Klöting N, Hraham TE, Berndt J et al. Serum retinol binding protein is more highly expressed in visceral than in subcutaneous adipose tissue and is a marker of intra-abdominal fat mass. *Cell Metab* 2007; 6: 79-87.
14. Bajzová M, Kováčiková, Vítková M et al. Retinol-binding protein 4 expression in visceral and subcutaneous fat in human obesity. *Physiol Res* 2008; 57: 927-934.
15. Ost A, Danielsson A, Lidén M et al. Retinol binding protein 4 attenuates insulin-induced phosphorylation of IRS and ERK1/2 in primary human adipocytes. *FASEB J* 2007; 21: 3693-3704.
16. Munkhtulga L, Nagashima S, Nakayama K et al. Regulatory SNP in the RBP4 gene modified the expression in adipocytes and associated with BMI. *Obesity* 2010; 18: 1006-1014.
17. Van Hoek M, Dehghan A, Zillikens MC et al. An RBP4 promoter polymorphism increases risk of type 2 diabetes. *Diabetologia* 2008; 51: 1423-1428.
18. Wu Y, Li H, Loos RJ et al. RBP4 variants are significantly associated with plasma RBP4 levels and hypertriglyceridemia risk in Chinese Hans. *J Lipid Res* 2009; 50: 1479-1486.
19. Kovacs P, Geyer M, Berndt J et al. Effects of genetic variation in the human retinol binding protein-4 gene (RBP4) on insulin resistance and fat depot-specific mRNA expression. *Diabetes* 2007; 56: 3095-3100.
20. Hu C, Jia W, Zhang R et al. Effect of RBP4 gene variants on circulating RBP4 concentration and type 2 diabetes in a Chinese population. *Diabet Med.* 2008; 25: 11-18.
21. Ruano M, Silvestre V, Castro R, et al. HOMA, QUICKI and MFfm to measure insulin resistance in morbid obesity. *Obes Surg* 2006; 16: 549-553.
22. Pfaffl M W. A new mathematical model for relative quantification in real-time RT-PCR. *Nucleic Acids Res* 2001; 29: 2002-2007.

Table 1. The anthropometrical and biochemical characterization of type 2 diabetic patients and healthy controls. Values represent mean±SD

Clinical feature	Type 2 Diabetic Patients [Mean±SD ^a]		Healthy control	P (T Student Test)		
	IR	IS		IR vs Control.	IS vs Control	IR vs IS
Age [year]	55±9	53±7	50±10	0.0015 ^b ,	n.s. ^{c,d}	
BMI [kg/m ²]	33±9	29±6	24±4	1.18E-12 ^b ,	0.00022 ^c	0.02039 ^d
Glucose [mg/dl]	160±50	135±54	93±13	8.14E-20 ^b ,	1.02E-10 ^c	0.05365 ^d
Insulin [μU/ml]	16±11	4,9±3,3	6,12±6,3	0.00011 ^b ,	n.s. ^c	2.1E-05 ^d
HOMA-IR	5,8±4,14	1,4±0,77	1,52±1,1	2.0E-06 ^b ,	n.s. ^c	2.1E-06 ^d
QUICKI	0,303±0,02	0,378±0,04	0,391±0,04	3.3E-18 ^b ,	n.s. ^c	1.2E-13 ^d
TG [mg/dl]	204±145	142±61	111±62	0.00862 ^b ,	n.s. ^c	0.05165 ^d
IL-6 [pg/ml]	26,7±44	18±8,4	22,6±23	0.01578 ^b	n.s. ^{c,d}	
TNF-α [pg/ml]	5,25±1,0	3,6±1,5	4,7±1,7		n.s. ^{b,c,d}	
Adiponectin [μg/ml]	5,35±2,2	5,3±3,8	8,0 ±3,6	0.02297 ^b	n.s. ^{c,d}	

^a Standard deviation

^b Comparison between IR and control group

^c Comparison between IS and control group

^d Comparison between IR and IS

n.s. non significant

Table 2. Allele and genotype frequencies of analyzed SNPs. The analysis was done with and without IR and IS classification.

RS ID	ALLELE FREQUENCIES				GENOTYPE FREQUENCIES						<i>P</i> ^{a,b,c} (<i>CHI</i> ²)
	T2DM		Control		T2DM		Control				
	IR	IS			IR	IS					
rs375	A	G	A	G	A/A	A/G	G/G	A/A	A/G	G/G	n.s. ^{a,b,c}
8539	0,18	0,82	0,15	0,85	0,01	0,33	0,66	0,01	0,29	0,70	
	A	G	A	G	A/A	A/G	G/G	A/A	A/G	G/G	
	0,16	0,84	0,20	0,80	0,02	0,29	0,69	0,04	0,33	0,63	
	A	C	A	C	A/A	A/C	C/C	A/A	A/C	C/C	0.0233 ^a
rs375	0,83	0,17	0,92	0,08	0,70	0,25	0,05	0,83	0,17	0,0	0.0293 ^b
8538	A	C	A	C	A/A	A/C	C/C	A/A	A/C	C/C	n.s. ^c
	0,84	0,16	0,85	0,15	0,69	0,29	0,02	0,79	0,12	0,09	

^a Analysis done with IR and IS classification

^b Analysis done without IR and IS classification

^c Analysis between IR and IS

n.s. not significant

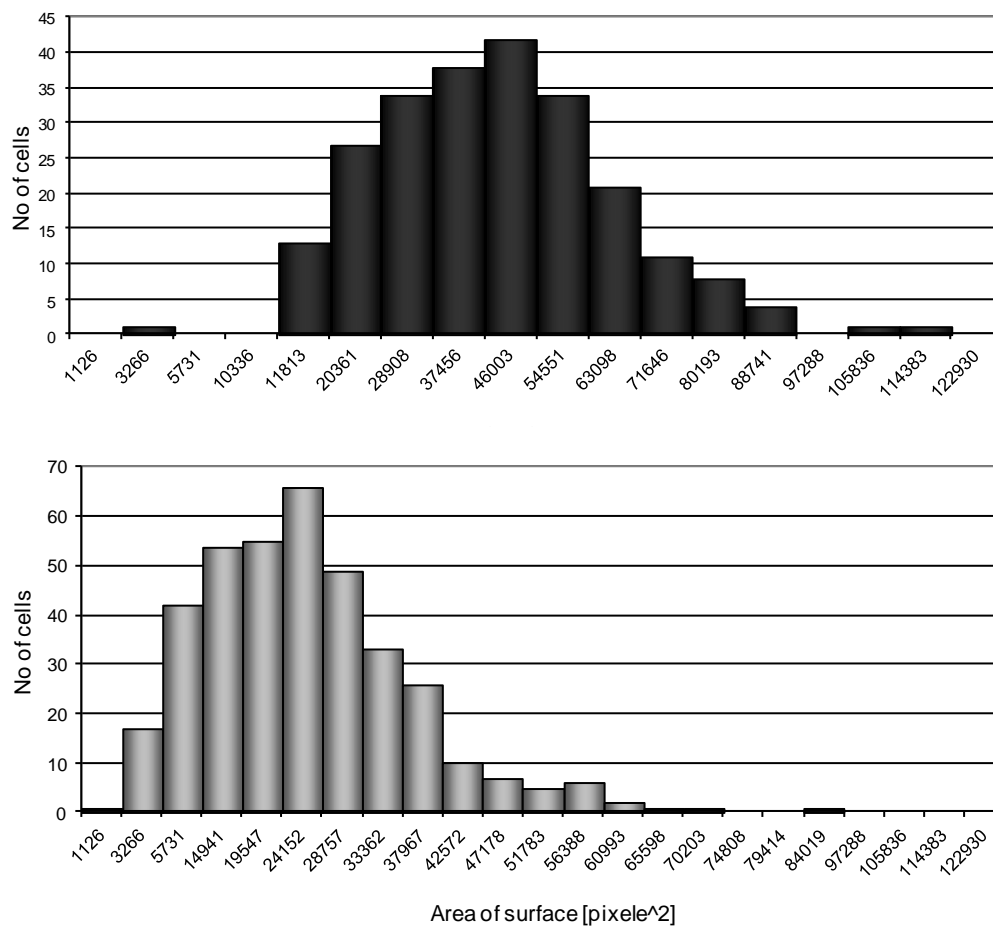


Figure 1. Comparison of adipocytes size: **A** – BMI > 35 kg/m² (obese), **B** – BMI < 25 kg/m² (lean).

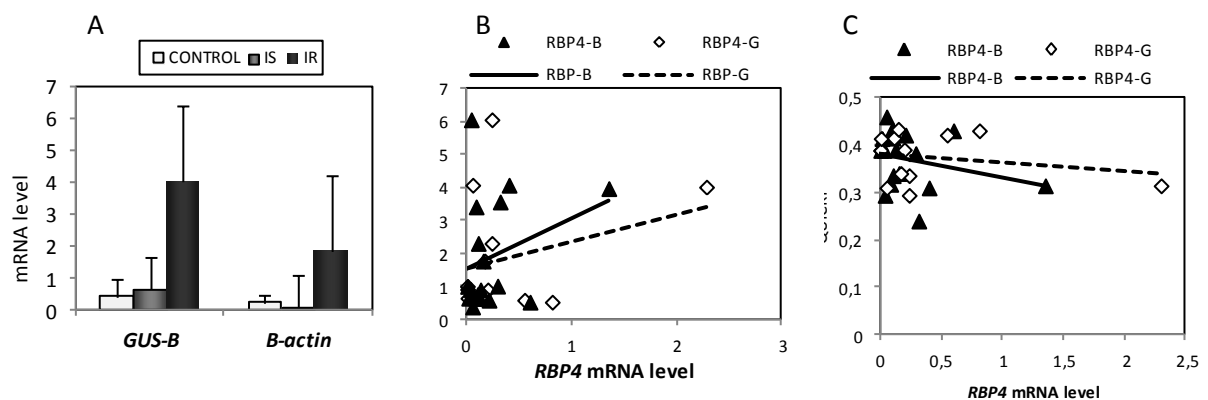


Figure 2. **A** – Comparison of the *RBP4* gene expression levels between examined groups normalized to *GUS-β* and *β-actin* (IS – insulin sensitive, IR – insulin resistant). Correlation between the *RBP4* mRNA level (normalized to *GUS-β* – RBP-G and to *β-actin* – RBP-B) and insulin resistance ratios: **B** – HOMA-IR, **C** – QUICKI, (* $p < 0.05$).

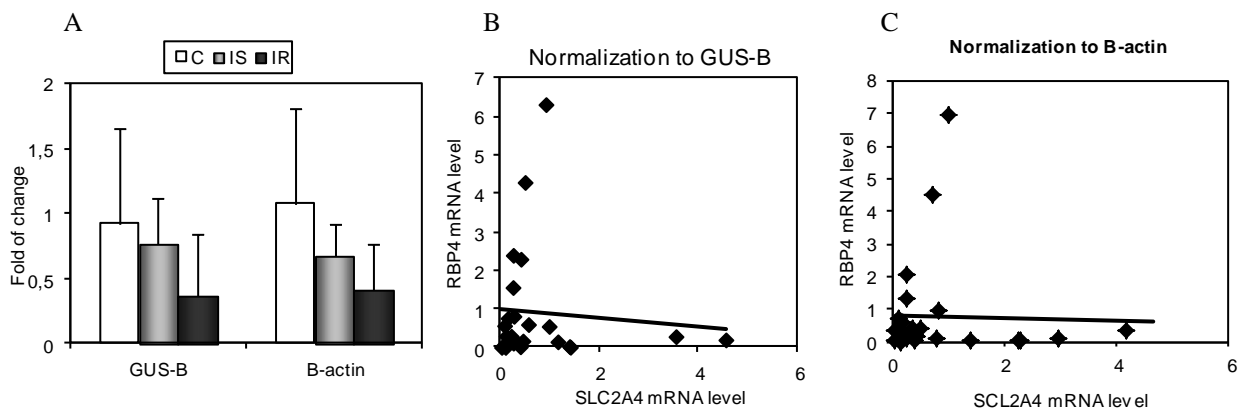


Figure 3. The *SCL2A4* gene expression rate in adipose tissue of tested groups (IS – insulin sensitive, IR – insulin resistant) (A), the correlation between *RBP4* and *SLC2A4* genes expressions rate normalized to *GUS-β* (B) and *β-actin* (C).

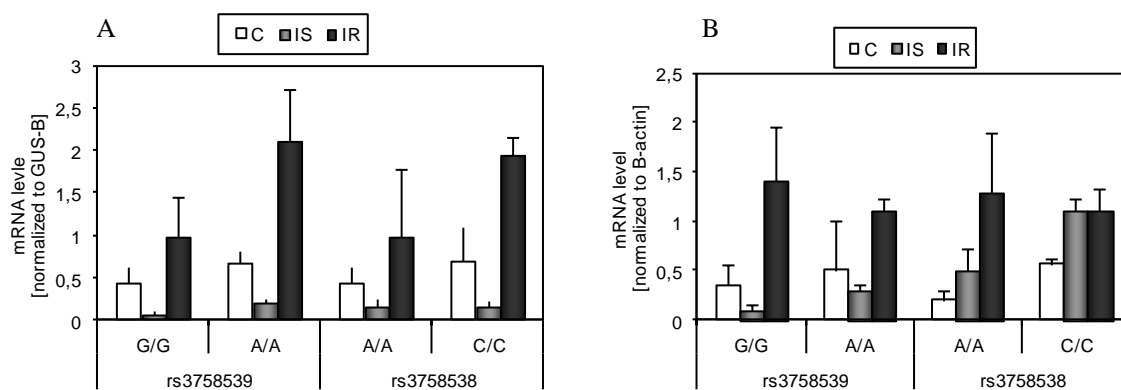


Figure 4. Comparison of the *RBP4* gene expression depending on genotype between tested groups: A – normalize to *GUS-β*, B – normalized to *β-actin*.